UC Irvine
UC Irvine Electronic Theses and Dissertations

Title
Aerosol chemistry of riparian shrub emissions and oxygenated terpenes

Permalink
https://escholarship.org/uc/item/6124q458

Author
Khalaj, Farzaneh

Publication Date
2022

Peer reviewed|Thesis/dissertation

UNIVERSITY OF CALIFORNIA,
IRVINE

Aerosol chemistry of riparian shrub emissions and oxygenated terpenes

DISSERTATION

submitted in partial satisfaction of the requirements
for the degree of

DOCTOR OF PHILOSOPHY

in Ecology and Evolutionary Biology

by

Farzaneh Khalaj

Dissertation Committee:
Assistant Professor Celia B. Faiola, Chair
Professor Sergey A. Nizkorodov
Professor Diane R. Campbell

2022

DEDICATION

To

my parents, family, and friends

in recognition of your love and kindness

TABLE OF CONTENTS

LIST OF FIGURES

LIST OF TABLES

ACKNOWLEDGEMENTS

Last but certainly not least, thank you to my family. I do thank your incredible support and pure love. You have kept me motivated during all stages of my life, especially during graduate school.

CURRICULUM VITAE

Farzaneh Khalaj

EDUCATION
2018-2022 Ph.D. University of California, Irvine, Ecology and Evolutionary Biology
2017 MS University of California, Irvine, Earth System Science

2016 MS University of Texas at Arlington, Civil and Environmental Engineering

RESEARCH INTEREST
Air dispersion modeling
Biogenic volatile organic compound emissions and secondary organic aerosol chemistry
Particle toxicity

FELLOWSHIPS
2019-2020 Ridge to Reef Fellowship, University of California Irvine
2016-2017 Jenkins Family Graduate Fellowship, Earth System Science Department, University of California, Irvine
2015-2016 Solid Waste Scholarship, Civil and Environmental Engineering Department, University of Texas at Arlington
2014-2015 Graduate Scholarship, Civil and Environmental Engineering Department, University of Texas at Arlington

TECHNICAL SKILLS
Software and Programs: AERMOD, AERMET, Igor Pro., LabView, SAP, SAFE, ETABS, STAAD Pro., AutoCAD, Microsoft Office, RStudio, MATLAB

MEMBERSHIPS
- Member of Air and Waste Management Association (AWMA)
- Member of American Geophysical Union (AGU)
- Member of American Association for Aerosol Research (AAAR)
- Member of Frontiers of Atmospheric Chemistry Seminar Series (FACSS)

TEACHING AND PROFESSIONAL EXPERIENCE
- Poster judge at Environmental Research Poster Symposium, University of California, Irvine
- Teaching assistant for Biology: Processes in Ecology and Evolution, University of California, Irvine
- Teaching assistant for Biology: From DNA to organisms, University of California, Irvine
- Teaching assistant for Biology: Organisms to ecosystems, University of California, Irvine
- Student assistant at 37th annual aerosol conference, AAAR
- Undergraduate mentor, University of California, Irvine
- Moderator at technology session in Climate Summit event, University of California, Irvine
- Student assistant at 10th International aerosol conference, AAAR, IAC
- Member of Cool Block Leader, a program by the City of Irvine

PEER-REVIEWED PUBLICATIONS
- **Khalaj**, F., Rivas-Ubach, A., Anderson, C., China, S., Mooney, K., Faiola, C., 2021, "Acyclic Terpenes Reduce Secondary Organic Aerosol Formation from Emissions of a Riparian Shrub". ACS Earth Space Chemistry

- **Khalaj**, F., Sattler, M., 2019, "Modeling of VOCs and criteria pollutants from multiple natural gas well pads in close proximity, for different terrain conditions: A Barnett Shale case study", Atmospheric Pollut
- Mehra, A., Krechmer, J.E., Lambe, A.T., Sarkar, C., **Khalaj, F.**, Guenther, A., Jayne, J., Coe, H., Worsnop, D.R., Faiola, C., Canagaratna, M.R., Williams, L., 2020. "Oligomer and highly oxygenated organic molecule formation from oxidation of oxygenated monoterpenes emitted by California sage plants". Atmospheric Chem. Phys
- Faiola, C. L., **Khalaj,** F., Buchholz, A., Kari, E., Ylisirniö, A., Kivimäenää, M., Holopainen, J. K., Yli-Juuti, T., Virtanen, A, 2019," Secodary organic aerosol production from healthy and aphid-stressed Scots pine emissions", Earth and Space Chemistry, Special Issue: New Advances in Organic Aerosol Chemistry

PRESENTATION

2022 Oral Presentation: "Secondary Organic Aerosol from Photooxidation of Oxygenated Terpenes," AAAR annual conference (virtual)

2021 Oral Presentation: "Acyclic Terpenes Reduced Secondary Organic Aerosol from Riparian Shrub," AAAR annual conference (virtual)

2020 Oral Presentation: "Effects of Aphid Herbivory on the Atmo-ecometabolome of a Riparian Shrub", AAAR annual conference (virtual)

2019 Poster presentation: "Healthy and Aphid-stressed Shrubby Plant (Baccharis salicifolia) Metabolomics Impact on Produced Biogenic Secondary Organic Aerosol", EMSL Integration meeting last week in Richland, WA, USA

2019 Poster presentation: "Healthy and Aphid-stressed Shrubby Plant (Baccharis salicifolia) Metabolomics Impact on Produced Biogenic Secondary Organic Aerosol", 37th Annual Aerosol Conference, Oregon Convention Center, Portland, Oregon, USA

2018 Poster presentation: "Secondary Organic Aerosol Production from Healthy and Aphid-Stressed Scots Pine Biogenic Volatile Organic Compound Emissions in Different Oxidant Systems" in the second annual Environmental Research Poster Symposium by the Department of Ecology and Evolutionary Biology, the Ridge to Reef Program, and the Humanities Commons

2018 Poster presentation: "Secondary Organic Aerosol Production from Healthy and Aphid-Stressed Scots Pine Biogenic Volatile Organic Compound Emissions in Different Oxidant Systems", 10th International Aerosol Conference, America's Center Convention Complex, St. Louis, Missouri, USA

2017   Oral Presentation: "Air Dispersion Modeling of Multiple Natural Gas Well Pads, in Different Terrain Types and Determination of Exponential Value in Inverse Distance Weighting Function," Air & Waste Management Association 110th Annual Conference. Pittsburgh, PA

ABSTRACT OF THE DISSERTATION

Aerosol chemistry of riparian shrub emissions and oxygenated terpenes

by

Farzaneh Khalaj

Doctor of Philosophy in Ecology and Evolutionary Biology

University of California, Irvine, 2022

Assistant Professor Celia B. Faiola, Chair

Biogenic volatile organic compounds (BVOCs) released primarily from vegetation are the major contributors to the total atmospheric volatile organic compounds (VOCs) globally. These BVOCs can play important ecological functions. In Chapter 1, I summarized the ecological roles of these important atmospheric volatiles at the organism and population, and community levels, their adaptive values, and their impacts at the climate level. In addition to the ecological processes, plant VOCs can influence atmospheric chemistry and physics. Many of these plant VOCs are highly reactive, and upon release into the atmosphere, they react with atmospheric radicals forming secondary organic aerosol (SOA). SOA can affect human health and impact Earth's radiative balance directly and indirectly by absorbing and scattering sunlight and influencing clouds' formation and properties, respectively. I investigated SOA formation from less-studied VOCs in the laboratory by generating SOA inside an oxidation flow reactor (OFR) using different VOCs as SOA precursors. In Chapter 2, I investigated SOA formation from a riparian shrub emission exposed to insect herbivory. The acyclic BOVCs, regardless of herbivory stress, reduced SOA potential formation. This result can have an important implication for SOA prediction in chemical transport models. In Chapter 3, I studied SOA from dominant BVOCs of a shrub species in California's coastal sage shrub ecosystem. SOA formation potential of most of these oxygenated

monoterpenes was higher than that of a common plant volatile, α-pinene, as a reference system. I also investigated the chemical composition of the SOA from these oxygenated terpenes and compared that with the SOA chemical composition formed from real plant emissions that were dominated by these compounds. I observed that the chemical composition of SOA from plant mixtures was similar to each other and equally different from SOA formed from single precursors. This result emphasized that SOA formed from single VOC standards does not capture the complexity of VOC emissions from real plants.

INTRODUCTION

Plants emit various atmospheric organic compounds (Dudareva et al., 2013), known as biogenic volatile organic compounds (BVOC)s. Plant BVOC emissions can affect many ecological processes such as plant-plant communication (Arimura et al., 2009; Baldwin et al., 2006a), plant-insect communication (Blande, 2017; Moreira et al., 2018a, 2018b), plant signaling (Dicke, 2004), and plant-pollinator communication (Schiestl and Johnson, 2013). Different mechanisms in a changing world, such as plant stresses, affect BVOC emissions, resulting in plant stress compounds. Plant stress compounds can contribute to a large portion of the plant's total emissions, and conditions such as insect herbivory, air pollution, and extreme weather are some examples of stressors (Faiola and Taipale, 2020; Holopainen et al., 2018; Niinemets et al., 2013). In addition to affecting ecology, BVOCs also can play an important role in atmospheric chemistry and physics due to their high reactivity. Upon release into the atmosphere, BVOCs react with oxidants and produce secondary organic aerosol (SOA). VOCs from both natural (derived from vegetation, BVOCs) and anthropogenic (from human activities) sources contribute to the SOA formation through processes of nucleation, condensation, or multiple chemical reactions of their oxidation products (Hallquist et al., 2009; Nozière et al., 2015). Plant BVOCs can impact the aerosol climate effects by changing particle composition (Faiola et al., 2015; Jimenez et al., 2009; Kiendler-Scharr et al., 2009b), hygroscopicity (Zhao et al., 2017), and optical properties (Lambe et al., 2013; Moise et al., 2015; Zhang et al., 2011). In general, increasing and modification of the BVOCs would consequently impact SOA.

Atmospheric aerosols have adverse health impacts on humans (Nel, 2005). In addition to human health, atmospheric aerosols can influence environmental health, both directly and indirectly. Atmospheric particles can effectively scatter or absorb solar and terrestrial radiation.

Therefore, they can affect the radiative energy balance in the atmosphere (Jacobson et al., 2000), and consequently, radiative forcing and visibility would be directly impacted by this effect. The properties of the particles determine the absorption or scattering effect. The other important significance of the atmospheric aerosol is that they can modify the abundance and properties of clouds and thus indirectly affect global climate (Andreae and Rosenfeld, 2008). A large fraction of fine atmospheric aerosol (20-90%) is organic compounds (Jimenez et al., 2009). A large portion of the global budget of organic aerosol is SOA, which is the atmospheric oxidation product of volatile organic compounds (VOC)s (Shrivastava et al., 2015).

The SOA formation mechanism in global climate and air quality models is highly variable (Kanakidou et al., 2005; Lee et al., 2016), and SOA formation consistently has been underestimated in current models compared with actual measurements and observations (Hodzic et al., 2010, 2009; Yang et al., 2018). The uncertainties in the inputs of these models arise from incomplete chemical knowledge of degradation pathways and significant variability in measured SOA yields (Fry et al., 2014; Marais et al., 2017; M. Donahue et al., 2005; Odum et al., 1996). Therefore, there is an excellent motivation for further investigations on SOAs from complex mixtures like actual plant emissions or SOAs from less-studied terpenes such as oxygenated monoterpenes to improve the data inputs of the models. This lack of knowledge could limit accurate understanding of the SOA effects on regional and global scales.

In my dissertation research, first, I review the ecological roles of plant BVOCs, as the major contributors to atmospheric VOCs. Then, I focus on the investigation of SOA formed from two different less-studied systems.

In Chapter 1, "Ecological roles of plant volatile organic compounds" , I summarized the most important ecological functions of plant volatiles at the organism, population, and community

levels and their evolution. I also provided the significance of plant BOVCs at the broader scale, at the climate level.

In Chapter 2, "Acyclic terpenes reduced secondary organic aerosol formation from emissions of a riparian shrub", I focused on SOA from actual plant emissions exposed to herbivory stress. The aerosol formation from complex mixtures of actual plant emissions has been done previously in many laboratory studies (Faiola et al., 2019, 2018, 2014; Hao et al., 2011; Joutsensaari et al., 2015, 2005; Kiendler-Scharr et al., 2012, 2009a, 2009b; Mehra et al., 2020; Mentel et al., 2009; VanReken et al., 2006; Yli-Pirilä et al., 2016; Ylisirniö et al., 2020; Zhao et al., 2017). However, our study was the first to evaluate the effects of insect herbivory on SOA formation from shrubs, which are the dominant vegetation type in many regions, such as chaparral and coastal sage scrub in California. Specifically, the project evaluated the effect of the aphid herbivory on SOA formation from BVOCs of *Baccharis salicifolia*. Additionally, I investigated the leaf-level metabolomic analysis to investigate the effect of the aphid herbivory on plant metabolism. I believe the project's outcome is critical for improving SOA production predictions in global climate models and regional transport models.

In Chapter 3, "Secondary organic aerosol from the photooxidation of oxygenated biogenic volatile organic compounds", I investigated the SOA from less-studied terpenes (oxygenated monoterpenes), such as camphor, borneol, bornyl acetate, and 1,8-cineole. BVOCs have been studied in laboratory scales for chemical characterization of their formed SOA (Griffin et al., 1999b; Ng et al., 2007, 2006a; Odum et al., 1996), and the output provided the basic input information for model predictions of SOA production. However, these experiments are not completely representative of all BVOCs. Therefore, it is essential to improve the models for better SOA predictions for this rapidly changing world, where the distribution of BVOC profiles, and

SOA sources, could be very different from now. For instance, it was reported that more than 80% of the BVOCs emission of common shrub species throughout the U.S. and Canada consisted of oxygenated monoterpenes (Mehra et al., 2020), specifically camphor and 1,8-cineole, but their SOA formation potential and chemical characteristics have not been studied well yet. I studied SOA from four different oxygenated monoterpenes and α-pinene (as the reference SOA) and provided the first measurement of the chemical composition of those SOAs from the high-resolution mass spectrometry analysis.

My dissertation seeks to investigate SOA formation potential and SOA properties of some less-studied compounds and mixtures to provide information for better SOA prediction via chemical transport models. In summary, to improve the knowledge of SOA impacts on global climate and air quality models, there should be more investigation about SOA formed from sources that have not been studied well yet. For instance, more projects should aim for SOA formation from less-studied terpenes, stressed plants, or a mixture of BVOCs.

CHAPTER 1

Ecological roles of plant volatile organic compounds

Plants produce a large diversity of secondary metabolites (Pichersky and Gang, 2000; Pichersky and Lewinsohn, 2011), including volatile organic compounds called biogenic volatile organic compounds (BVOCs). Table 1.1 summarizes the plant volatiles ecological functions and some corresponding examples (Yuan et al., 2009). At the organismal level, plant BVOCs can act as fast and efficient within-plant signaling for a defense mechanism. For instance, reaching further locations of the damaged plant itself, as was reported in lima bean (Heil and Bueno, 2007) and sagebrush (Karban et al., 2006), or signal from older leaves to younger leaves of the plant (Holopainen and Blande, 2013). Undamaged leaves of hybrid poplar exposed to BVOCs from herbivory-damaged leaves on the same stem had shown enhanced defensive responses to feeding by the gypsy moth (Frost et al., 2007). To protect plant tissues from oxidative damage, UV-B radiation, and heat damage, plants emit BVOCs for thermal tolerance and environmental stress adaptation (Dudareva et al., 2006; Holopainen, 2004; Holopainen and Gershenzon, 2010; Peñuelas and Llusià, 2004; Sharkey et al., 2008; Vickers et al., 2009a). For instance, plants exposed to emissions of certain BVOCs recovered more rapidly from being exposed to high temperatures than control plants (Copolovici et al., 2005; Sharkey and Singsaas, 1995; Vickers et al., 2009a). Regarding alleviating oxidative stresses, lower reactive oxygen species and consequently less cell damage and higher photosynthetic rates than control plants were reported for plants fumigated with certain BVOCs (Delfine et al., 2000; Loreto et al., 2001; Vickers et al., 2009b).

The emissions of plant BVOCs can provide a reproductive advantage by attracting pollinators and seed dispensers (Chen et al., 2009; Hossaert-McKey et al., 2010; Luft et al., 2003; Shuttleworth and Johnson, 2009). Pollinators use the floral scent to locate flowers, and as a reward,

5

plants provide sugar-rich nectar for pollinators (Chapurlat et al., 2019; Galen et al., 2011; Gervasi and Schiestl, 2017; Gross et al., 2016; Kantsa et al., 2019; Raguso, 2006). Pollinators prefer this reward above other flowering materials such as color (Wink, 2003). It was reported that floral scent was an important attractant in a specific pollination system with wasps (Shuttleworth and Johnson, 2009). Based on an innate plant BVOCs smell preference, the hawkmoths were reported as the primary pollinators of *D. wrightii* flowers (Riffell et al., 2008). There is evidence that seed dispensers, such as fruit bats (Luft et al., 2003), are able to assess the ripe fruits exclusively by fruit odors, and bats could not only locate fruits by their odor but are also able to discriminate between ripe and unripe fruits of the same species. Pollinator and seed dispenser attraction and plant defense are the most important ecological roles of plant BVOCs, but plant volatiles may have other roles in the plant-environment interaction, such as plant-to-plant signaling to make other plants respond to herbivores and activate defense.

At the population level, plants may eavesdrop on emitted BVOCs from neighboring plants of the same species (intraspecific interaction) (Markovic et al., 2019) or other species at the community level (interspecific interaction) (Frost et al., 2008). In the plant-to-plant communication (Baldwin et al., 2006b; Baldwin and Schultz, 1983; Dicke et al., 2003a; Heil and Karban, 2010; Penuelas et al., 1995; Shulaev et al., 1997), the sensitivity of the receiver plant to specific blends of BVOCs or a single BVOC at different concentrations, coupled with the exposure duration, makes plant responses more complex. The use of BVOC signals as guide cues for predatory insects in tritrophic interactions is sophisticated. Some plants can emit BVOCs as a signal during an attack by specific herbivorous insects that attract predators specialized on that herbivore; thus, these warning signals can induce the expression of defense genes or BVOC emissions in surrounding plants (Arimura et al., 2000; Birkett et al., 2000; Farag et al., 2005;

Kessler and Baldwin, 2001; Ruther and Kleier, 2005) or make these plants ready to respond faster to future herbivory attacks (Engelberth et al., 2004; Frost et al., 2007; Kessler et al., 2006; Rodriguez-Saona et al., 2009). Multiple herbivore species attacking a plant can make this interaction more complex (Gols, 2014; Ponzio et al., 2014).

Plant BVOCs can act as direct herbivore repellents (De Moraes et al., 2001; Holopainen, 2004; Kessler and Baldwin, 2001) or attract natural enemies of herbivores (Heil, 2008; Holopainen, 2004) to defend themselves indirectly. Direct defenses apply negative impacts on herbivores, such as some BVOCs that directly attract or deter herbivores, while indirect defense includes higher trophic levels, such as the attraction of parasitoids or herbivores predators (Arimura et al., 2005; Bowers et al., 1972; Chapman et al., 1981; Dicke et al., 2003b, 2003c; Dicke and Baldwin, 2010; Llusià and Peñuelas, 2001; Matthes et al., 2010; Price et al., 1980). Based on experiments with pure VOCs and transgenic plants engineered to emit modified BVOC mixtures, specific plant terpenes were reported to be involved in attracting herbivore enemies (Degenhardt et al., 2009; Kappers et al., 2005; Kessler and Baldwin, 2001; Schnee et al., 2006; Shiojiri et al., 2006). Several herbivory-induced BVOCs serve as a direct defense strategy against aphids (Dicke and Dijkman, 2001; Hildebrand et al., 1993).

BVOCs can be emitted either constitutively (Holopainen and Gershenzon, 2010) or in response to various stresses, as discussed earlier. These plant BVOCs have low molecular weight and high vapor pressure at ambient temperature. Most BVOCs can be classified into three main chemical groups: terpenoids, green leaf volatiles (GLVs), and aromatic compounds (Holopainen and Blande, 2013). Several small aliphatic BVOCs, such as acetaldehyde, acetone, acetic acid, formic acid, and ethanol, can also be produced in some plants (Rantala et al., 2015). More than 1700 volatile compounds have been identified from the floral headspace of different plant species

(Knudsen et al., 2006), with terpenoids occurring most frequently (Farré-Armengol et al., 2020, 2015; Knudsen et al., 2006). Terpenoids are constructed from five-carbon units from different plant metabolic pathways: the plastidic methylerythritol phosphate (MEP) pathway and the cytosolic mevalonic acid (MVA) pathway (Loreto and Schnitzler, 2010; Maffei, 2010). The simplest form of terpenes is a five-carbon (C5) molecule (isoprene), and the other various multiples of this C5 unit, including two groups that have been found in large amounts in the gas-phase as monoterpenes (C10) and sesquiterpenes (C15). The GLVs, are products of the lipoxygenase (LOX) pathway and are released after mechanical or other destructive damage to cell membranes (Holopainen and Blande, 2013; Maffei, 2010). The last major BVOC group, aromatic compounds, is produced by the shikimate pathway, mainly devoted to aromatic amino acid synthesis (Maffei, 2010; Misztal et al., 2015).

Emission rates of plant BVOCs are primarily controlled by environmental factors such as solar radiation and ambient temperature (Loreto and Schnitzler, 2010). All BVOC emissions from leaves are temperature-dependent, but only some are also light-dependent. BVOCs that are not stored in any specialized structures are both light- and temperature-dependent because their emission rate is a function of biosynthesis rate, which is directly tied to photosynthetic carbon metabolism, so-called "de novo" emissions (Loreto and Schnitzler, 2010). Most broadleaf deciduous trees lack these specialized storage structures. Some plants accumulate volatiles in resin ducts or glandular trichomes (Baldwin, 2010; Duke et al., 2000). This is a common feature of most coniferous plants (Loreto and Schnitzler, 2010). Emission rates of compounds residing in storage structures are exponentially dependent on temperature- and light-independent. Coniferous plants also emit compounds that are not stored, *de novo* emissions, the compounds that are just made, which are light- and temperature-dependent (Loreto and Schnitzler, 2010). Thus, there are both

light-dependent and light-independent fractions of the BVOC emissions from plants that have these storage structures.

In general, plant volatile emissions, BVOCs, can play substantial roles in the ecological processes, providing a common chemical language as a signaling tool from the cellular level to the whole plant, population, and community level.

Evolution and The Adaptive Value of Plant BVOCs

Plants coexist in different communities with unavoidable interactions with neighboring plants and other organisms. BVOCs and their functions can be favored by natural selection on existing heritable variations. The type and intensity of natural selection on these BVOCs may vary by time and location (Allison and Daniel Hare, 2009).

Plants invest a substantial amount of photosynthetic carbon and energy into the BVOC compounds. The plants' benefit from such an investment is still under investigation among plant scientists and ecologists (Dicke and Baldwin, 2010; Hare, 2011; Kessler and Heil, 2011; Vickers et al., 2009a). The carbon investment into BVOC increases under stress, which results in a large amount being released into the atmosphere. The BVOC enhancement happens upon herbivory or pathogen stress (Dicke and Baldwin, 2010) or while coping with abiotic stresses (Loreto and Schnitzler, 2010). Under these stress conditions, carbon is allocated to constitutive and stress-induced BVOCs (Mithöfer and Boland, 2012; Paré and Tumlinson, 1999). The carbon investment can be a substantial carbon loss in stressed leaves and a considerable photochemical energy sink if simultaneous photosynthesis is considered (Sharkey and Yeh, 2001). Plants need to respond to crucial receiving signals to avoid compromising their growth and defense. This makes regulatory mechanisms complex, considering the trade-off between the cost and benefits of carbon investment (Ninkovic et al., 2021). The trade-off between benefits and costs of BVOC emissions as stress

relief compounds is not straightforward and thus difficult to assess. For one of the most abundant BVOC from leaves, isoprene, experiments with transgenic plants showed that the metabolic cost outweighed the benefits (Behnke et al., 2012). Constitutive expression of plant defense may be costly and thus result in seed production reduction (Heidel and Baldwin, 2004; van Hulten et al., 2006); moreover, it may have ecological costs such as interference of BVOCs with pollinator attraction (Dicke and Baldwin, 2010; Kessler and Halitschke, 2009). For example, the floral scents of a plant for pollinator attraction may also attract nectar-robbing bees and folivores, which can negatively impact plant reproduction (Baldwin, 2010). In fact, plants gain a net fitness benefit by investing in the production of floral scent, plant BVOC, as an advertisement of reward (Majetic et al., 2009). Many studies report that pollinators such as bees learn smells faster with higher retention than colors; thus, odors, as BVOCs, can evoke stronger discrimination between plants (Dobson, 1994; Leonard et al., 2011a, 2011b), and this shows an important aspect of the selective environment determining he evolution of plant signals through their impact on plant fitness (Wright and Schiestl, 2009). These studies and examples represent that it is very challenging to clearly understand the trade-off between the costs and benefits of emitting BVOCs, and the way the BVOC emissions would respond to future conditions is still under debate.

The evolutionary perspective can explain inter-and intra-species variability in BVOC emission rates and composition; for instance, it would help to understand why some plants have specific types of BVOCs, such as isoprene or monoterpenes. For example, mosses and ferns, as the early land plants, typically emit constitutive BVOC emissions such as isoprene. The isoprene-emitting plants appeared during the Cretaceous era (a period that lasted from about 145 to 66 million years ago) (Sharkey et al., 2013), and it was suggested that the isoprene emission capacity might have been gained and lost many times during the evolutionary history of plants (Monson et

al., 2013; Sharkey et al., 2008; Welter et al., 2012). The synthase genes of a specific BVOC can frequently arise from mutations of terpene synthase genes. Conifers emit high levels of monoterpenes (Holopainen, 2004), which might indicate that monoterpenes and isoprene emitted by Mediterranean oaks have an isoprene-like protective role against ozone (Loreto et al., 2001, 1996). It has been suggested that the constitutive isoprene emissions make leaf photosynthetic membranes more stable (Velikova et al., 2011). Similar functions have been suggested for constitutive monoterpenes emissions; however, monoterpenes from reservoirs such as resin ducts can also repel herbivores and sterilize wounding locations (Mithöfer and Boland, 2012).

Plant terpenoids may play a role in supporting mutualisms, for example, with pollinators or ants (Farré-Armengol et al., 2013). In plant-insect mutualisms, the plant needs to be easily located and must provide rewards to the mobile partner (the insect), who offers a service but may decide not to visit a particular plant. This plant-pollinator relationship could mean that plants have evolved particular traits contributing to mutualism (Fineschi et al., 2013). Phylogenetic studies also suggest that plant-insect mutualism is not only gained but also lost throughout evolutionary history (Fineschi et al., 2013), whereby losses involve shifts to abiotic alternatives to mutualism such as wind, water, or gravity for pollination and seed dispersal, as well as switches to mutualists other than insects such as birds as pollinators or seed dispersers (Bronstein et al., 2006).

Humans are an important driver of evolution by artificial selection and plant domestication. The intraspecific differences in the BVOC emissions may not have evolutionary significance, but they are associated with productive traits for cultivation. For instance, breeding for productive traits might drive selection for BVOC diversity and, in return, modulate important adaptive mechanisms against stress conditions (Loreto et al., 2009).

Regarding interactions with other organisms, natural selection may have favored BVOC synthesis emitted from plant leaves, just like floral scents and colors were selected to attract pollinators or toxic compounds to repel herbivores and pathogens (Fineschi et al., 2013). It has been suggested that there may be a lot of selective advantages to keeping a large diversity of plant BVOCs in individuals (Gershenzon and Dudareva, 2007); for instance, a more diverse BVOC blend can protect against a broader range of natural enemies. In addition, it may be more effective for a plant to deter herbivores by its BVOCs instead of the sum of its parts (Gershenzon and Dudareva, 2007).

Approaches to Determine BVOCs Adaptive Values

There are several ways to test whether BVOC emissions are adaptive. For instance, the recruitment of natural enemies as an adaptive function of BVOCs can be tested by the ability of an individual plant to attract natural enemies to reduce the damage of herbivores and enhance plant fitness relative to non-emitting genotypes. If BVOCs directly profit plants, then individual plants should emit a high amount of BVOCs to substantially increase fitness even in the absence of natural enemies. This theory can be tested by comparing the fitness of plants that emit different BVOC emissions in the presence and absence of natural enemies. The second approach is the addition of synthetic BVOCs to plants and investigating whether they have a higher fitness or not. Thus, to explain the BVOC-natural enemy signaling function, the evidence of both (a) plant fitness increases due to enemy recruitment and either (b) enemies preferentially learn prey-induced BVOCs, or natural enemies respond innately to prey-host VOCs is required. Plant fitness can be measured in different ways, including growth rates, number of seeds, number of fruits, or probability of survival (Bigio et al., 2017). These two hypotheses, a and b, can be predicted/tested empirically to allow discrimination between enemies' recruitment as a function of or effect of plant

BVOCs (Allison and Daniel Hare, 2009). These suggested methods can be applied for the effect of abiotic stresses on BVOCs or the effect of a combination of biotic and abiotic stresses on plant BVOCs.

Transgenic studies either engineered to emit or knock out specific plant VOC can be applied to address how plant benefits from BVOC emissions. This approach helps to better understand the role of a specific BVOC type, such as isoprene, in tolerating stress and the related mechanism (Niinemets and Monson, 2013; Rosenkranz and Schnitzler, 2013). For instance, to test the hypothesized role of isoprene in the leaf protection against oxidative stress transgenic grey poplar plants with either silenced or upregulated isoprene synthesis gene expression was developed (Behnke et al., 2007). On the other hand, to investigate whether plant fitness would be improved by maintaining isoprene production under drought stress, transgenic *Arabidopsis* plants with isoprene synthesis genes were used, and it was concluded that the presence of this trait did not enhance drought resistance (Sasaki et al., 2007). But in general, many previous works on engineered transgenic isoprene emitters (Sasaki et al., 2007; Velikova et al., 2011; Vickers et al., 2009b) and isoprene silenced (Behnke et al., 2007; Rosenkranz and Schnitzler, 2013) have shown enhanced abiotic stress in isoprene emitting genotypes. Developments in the identification of genes responsible for the synthesis of other BVOCs in addition to isoprene are essential to investigate the potential roles of other BVOCs in plants' stress tolerance mechanism to abiotic, biotic, and combination of both stresses and in survival and fitness. These approaches can help improve BVOC emissions models under various environmental conditions, which would ultimately develop a better understanding of the effects of BVOCs on atmospheric chemistry and climate (Niinemets and Monson, 2013; Vickers et al., 2009a). The complex floral bouquet structure of petunia, which impacted interactions among flowers and their visitors, was investigated with

genetically modified plants (Kessler et al., 2013). Those engineered plants provided a strong tool to test how folivores responded to isogenic plants differing in a single scent expression. This result confirmed that floral bouquets might evolve due to interactions with both mutualists and antagonists, and floral bouquets are not just attractive but also defensive (Kessler et al., 2013). Another study showed that the repellency of a plant BVOC, 2-phenyl ethanol (2PE), was highly sensitive to dosage; for instance, high 2PE emitters in the field repelled both ants (herbivory) and bumblebees (pollinator), while at more moderate emission rates, 2PE increased the amount of nectar left, at no pollination cost. Thus, this dose-dependency on 2PE had an important role in shaping the ecological interactions between plant and its pollinator and/or herbivory (Galen et al., 2011).

For the adaptive evolution of plant BVOCs, its heritability should be estimated (Zu et al., 2016), and it should be evaluated whether the evolutionary change between generations corresponds to a modeling prediction of these parameters (Harder and Johnson, 2009). For adaptive evolution of BVOC emissions to occur, heritable variation among individuals in their BVOC composition is essential, and variation in the BVOC emissions needs to correlate with variation among individuals' fitness. It would need to correlate positively if there is an evolution of greater emissions. This positive correlation between fitness and BVOC emissions can exist if natural enemies respond innately to BVOCs or learn a subset of BVOC emissions. A study estimated the heritability of floral scent and correlated the responses of various plant traits by artificial selection, and fast responses to selection for increased plant VOCs were observed (Zu et al., 2016). The findings by Zu et al. (Zu et al., 2016) provided strong evidence for the conceptual theory of floral scent evolution under natural selection, which could shape the modeling of evolutionary trajectories under different selection scenarios. It is required to combine natural

selection experiments and mathematical modeling to evaluate whether or not the predicted plant BVOC responses to selection from the model would be consistent with observed evolutionary changes.

The herbivory induced BVOC blends are multivariate; thus, the most proper approach for understanding the evolution of BVOC generation is multivariate selection analysis (Hare, 2011), which other studies have proved as a helpful approach for understanding the evolution of the direct mechanism of plant resistance to herbivory stress in natural systems (Mauricio and Rausher, 1997; Shonle and Bergelson, 2000; Simms, 1990; Zangerl et al., 2008). Due to the large number of emitted BVOCs, the actual application of the multivariate selection analysis is complex. Previous studies suggested pre-selecting variables to reduce high dimensionality to solve this issue (Chapurlat et al., 2019; Gfrerer et al., 2021), and selection analyses were performed only on the most abundant compounds or using total BVOCs emission rate (Majetic et al., 2009; Parachnowitsch et al., 2012), or model selection criteria (Ehrlén et al., 2012; Parachnowitsch et al., 2012).

Effect of Biotic and Abiotic Stresses on BVOCs

An external condition that can affect plants' growth, development, or productivity is referred to as stress (Verma et al., 2013). Stresses can cause various types of plant responses, such as altered gene expression, growth rate changes, and cellular metabolism (Gull et al., 2019). In general, some sudden environmental condition changes are usually reflected by plant stresses. Plant stress can be divided into two main groups: abiotic stress and biotic stress. Abiotic stress in plants through the environment may be physical or chemical, imposed on plants by non-living factors, such as drought, flood, extreme temperatures, salinity, sunlight, and mineral toxicity (Gull et al., 2019). On the other hand, biotic stress imposed on plants is caused by living organisms, such

15

as viruses, fungi, pathogens, and insects (Gull et al., 2019). Usually, plants can recover from damage in mild or short-term stresses as the effects are temporary; however, severe stresses can lead to plant death (Verma et al., 2013). Some plants, such as desert plants, can escape the stress altogether (Zhu, 2002).

Abiotic stresses typically make plants more vulnerable to any future or simultaneous stresses (Niinemets, 2010a). Various abiotic factors are known to affect the plant BVOCs. Among the key environmental and stress factors, drought, humidity, ozone, carbon dioxide, light intensity, temperature, and nutrient availability all influence the plant BVOC emissions or the ratios of different compounds in the BVOC blend (Gouinguené and Turlings, 2002; Pinto et al., 2010; Staudt and Lhoutellier, 2011). The growth, development, and quality of seeds and flowers of plants can be negatively impacted by these abiotic stresses, which ultimately can impact the performance of herbivores, predators, and parasitoids. Therefore, the abiotic environment can greatly interfere with multitrophic interactions, specifically those mediated by BVOCs. The effects of increased temperature stress and drought on plant BVOCs have been given much attention because both have been happening alone or in combination in many natural ecosystems (Peñuelas and Llusià, 2003). Previous studies showed that while terpenoid BVOC emission was inhibited by heat stress, the emission of other BVOCs such as GLVs was enhanced (Copolovici et al., 2012; Loreto et al., 2006), and it was observed that these GLV emissions were sustained for the entire heating period and maintained long after the temperature was returned to optimal levels (Niinemets and Monson, 2013). During drought, reducing stomatal conductance and photosynthesis could negatively affect BVOC emissions by reducing carbon supply and increasing the diffusional resistance to emission. The drought effect mainly depends on the level of drought. Mild drought has been shown to neither impact isoprene (Pegoraro et al., 2004; Sharkey and Loreto, 1993) nor monoterpenes emissions

16

(Peñuelas et al., 2009; Staudt et al., 2002). However, prolonged and severe drought suppresses monoterpenes and isoprene (Brilli et al., 2007; Peñuelas et al., 2009; Sharkey and Loreto, 1993; Staudt et al., 2002). Although an increase in drought and temperature individually would normally increase isoprene, it was reported that after drought, the plants in higher temperature experiments had reduced emissions at least for two weeks (Fortunati et al., 2008). Salinity also affects photosynthesis and stomatal conductance, similarly to drought, with strong suppression in BVOCs as salinity increases (Loreto and Delfine, 2000; Teuber et al., 2008). Atmospheric pollutants such as ozone can affect BVOC emission rates positively and negatively or unaffected, depending on temperature, ozone concentrations, species type, BVOC type, and seasons (Blande et al., 2007; Calfapietra et al., 2008; Fares et al., 2007; Heiden et al., 1999; Peñuelas et al., 1999; Rinnan et al., 2005; Ryan et al., 2009; Tiiva et al., 2007; Velikova et al., 2005a, 2005b).

Biotic stresses account for most of the damage caused to trees (Karel and Man, 2017; Michel et al., 2020), and the extent, frequency, and intensity of biotic stresses are predicted to increase in the future (Bale et al., 2002; Cannon, 1998; Harrington et al., 2007; Kurz et al., 2008). The BVOC blend of biotically stressed plants typically includes two major BVOC classes: GLVs, which are emitted immediately after wounding (seconds to minutes), and induced BVOCs that are emitted a few to several hours after attacks (such as monoterpenes and sesquiterpenes, methyl jasmonate, and methyl salicylate) (Šimpraga et al., 2019, 2019). In conifers, a several-fold increase in the BVOC emission rates, such as monoterpenes, was promoted following leaf damage by herbivores (Ghimire et al., 2013; Kivimäenpää et al., 2016; Litvak and Monson, 1998). The effect of herbivory stress on plant BVOC emission rates varies a lot (Yu et al., 2021), depending on many factors such as the type of plants, type and amount of herbivores, and the exposure time. Plant BVOCs at the branch level were increased due to herbivory feeding with increased monoterpene

up to 21-fold, sesquiterpene emissions up to 85-fold, and GLV emissions up to 13-fold compared to control saplings (Blande et al., 2009; Ghimire et al., 2017, 2013; Heijari et al., 2011; Joutsensaari et al., 2015). Scots pine needle BVOC emission rates showed up to 20-fold increases in sesquiterpene emissions due to sawfly feeding effects in a field experiment (Joutsensaari et al., 2015), while laboratory measurements of BVOC emissions of Scots pines and Norway spruce due to bark weevil feeding showed 10-50 fold increases in BVOC emissions due to herbivory stress (Joutsensaari et al., 2015). Kari et al. (2019) observed monoterpene emissions increased on average 90-fold from the baseline emissions and a 180-fold increase from the control in one experiment due to pine weevil feeding (Kari et al., 2019).

Using BVOCs, carnivores can differentiate between plants exposed to different herbivore species. However, most herbivory-induced BVOCs are also constitutively emitted from flowers (Dudareva et al., 2006; Pichersky et al., 2006). Insect herbivory can be classified as external defoliator (leaf and needle chewing), bark borer, and sucking-piercing herbivory (Arneth and Niinemets, 2010; Faiola and Taipale, 2020). Bark borer herbivory studies showed a higher increase in monoterpene emissions than defoliator studies (Faiola and Taipale, 2020). GLVs have been observed notably after defoliator stress (Blande et al., 2010; Brilli et al., 2009; Faiola and Taipale, 2020b; Ghirardo et al., 2012; Maja et al., 2014; Yli-Pirilä et al., 2016), while bark borer stress studies have not reported a significant effect on most GLVs emissions (see Faiola and Taipale, 2020 and references therein). Interestingly, it has been observed that herbivores that are external defoliators induced more total BVOCs and specific classes such as monoterpenes and GLVs than sucking-piercing feeders, and specialist herbivores induced more total BVOCs than generalists (but this was inconsistent across the chemical classes of BVOCs) (Rowen and Kaplan, 2016).

There are other biotic stresses which can induce BVOC emissions as a response to stress. These other biotic stresses include insect oviposition (Hilker and Meiners, 2006; Mumm et al., 2003), gall makers (Borges, 2018; Jiang et al., 2018), and pathogens (Copolovici et al., 2014; Jiang et al., 2016; Toome et al., 2010; Vuorinen et al., 2007), which have been investigated less than herbivory stress. For example, there are very limited studies investigating the pathogenic effects on BVOCs in nature, and most work has been conducted on agricultural crops (Jansen et al., 2011). The composition of emitted BVOCs due to pathogen infection is different from the blend of BVOCs induced by herbivory stress (Copolovici et al., 2017, 2014; Vuorinen et al., 2007). It was observed that the total monoterpenes did not significantly increase due to leaf rust infection (Toome et al., 2010), which was in contrast to what is usually observed from herbivory stressed plants.

Plants are more likely to be simultaneously exposed to multiple stresses in natural conditions, which has great potential to change BVOC emissions (Holopainen and Gershenzon, 2010). There have been some studies performed with plants subjected to two different abiotic stressors simultaneously, for example, see Mittler (2006) and references therein; however, for a better investigation, the stress combinations should be studied in the laboratory or the field by simultaneous exposure of plants to multiple types of stresses. This research is essential since plants' responses to multiple stress combinations cannot always be interpreted from the results of the single stress factor experiments (Mittler, 2006). Simultaneous application of different abiotic and biotic stresses on plants could have additive and opposing effects on BVOC emissions (Gouinguené and Turlings, 2002; Himanen et al., 2009; Pinto et al., 2007; Schmelz et al., 2003; Vuorinen et al., 2004). It was reported that the combination of high temperature and herbivory stress caused greater BVOC emissions in corn plants compared to when either temperature or

herbivory was applied to them (Gouinguené and Turlings, 2002). Another study reported that in maize, the combined and simultaneous exposure to high temperature and herbivory resulted in higher BVOC emissions than when maize was exposed to either of the stresses alone (Gouinguené and Turlings, 2002).

The Effect of BVOCs at the Climate Level

The effect of plant volatile emissions on climate is complex (M. Fiore et al., 2012) due to uncertainties in the magnitude and net climate influence given to developing knowledge of BVOC oxidation chemistry and corresponding oxidant changes such as OH, particularly in pristine regions (Lelieveld et al., 2008; Taraborrelli et al., 2012). For instance, the atmospheric chemical composition and physical properties can be significantly influenced by BVOCs due to their high chemical reactivity and high mass emission rates (Laothawornkitkul et al., 2009). The oxidation of plant BVOCs can remove reactive carbon from the atmosphere and affect the atmosphere's oxidative capacity (Fehsenfeld et al., 1992; Lerdau and Slobodkin, 2002). BVOC can also contribute to the formation of SOA (Carlton et al., 2009a; Ervens et al., 2011) and ozone in the presence of nitrogen oxides (Council, 1992; "Handbook of Weather, Climate, and Water,").

Atmospheric aerosols, including SOA, can influence climate directly and indirectly. Upon release into the atmosphere, plant BVOCs react with atmospheric oxidants (OH radicals, ozone, and nitrate radicals) to form oxidized products with lower vapor pressure (i.e., lower volatility) than the primary BVOCs. The atmospheric SOA can effectively scatter or absorb solar radiation and affect the light transmission through the atmosphere (Ehn et al., 2014; Riccobono et al., 2014). The atmospheric SOA can effectively scatter or absorb solar radiation and affect the light transmission through the atmosphere (Jacobson et al., 2000), and consequently, radiative forcing and visibility would be directly impacted by this effect. SOA can also modify clouds' abundance

and properties and thus indirectly affect local and global climate (Andreae and Rosenfeld, 2008). In general, BVOCs can impact aerosol climate effects by changing particle composition (Faiola et al., 2015; Jimenez et al., 2009; Kiendler-Scharr et al., 2009b), hygroscopicity (Zhao et al., 2017), and optical properties (Lambe et al., 2013; Moise et al., 2015; Zhang et al., 2011).

The BVOC-aerosol-climate interaction is influenced via changes in plant BVOCs that can affect the atmospheric concentration, boundary layer oxidation capacity, and consequently, SOA concentration and size distribution. Increased temperature is predicted to enhance BVOC emission rates leading to SOA formation enhancement (Arneth et al., 2010; Kulmala et al., 2004). Consequently, increased SOA formation can cause two possible effects on plant physiology and BVOC emission rates. First, the aerosol radiative cooling effect resulting from the increased aerosol optical depth and increased number of cloud condensation nuclei (Arneth et al., 2016) would cause BVOC reduction (negative feedback). The reason is that BVOC emission rates are related to temperature exponentially; therefore, the radiative cooling effect would decrease plant emission rates (Guenther et al., 1995). The second impact of SOA on BVOC emission rate is to enhance BVOC emission (positive feedback) through increased plant net primary productivity caused by increased diffuse photosynthetic radiation and vapor pressure deficit suppression (Rap et al., 2018). Considering both positive and negative feedback effects, the Norwegian Earth System Model predicted a net cooling radiative forcing of -0.49 W m^{-2} offsetting warming forcing associated with doubling atmospheric CO_2 (Sporre et al., 2019). Other important factors can change BVOC emissions and thus should be considered in the models for more accurate prediction. For instance, biotic and abiotic stresses can change BVOC composition and emission rates (Arneth and Niinemets, 2010; Holopainen and Gershenzon, 2010; Loreto and Schnitzler, 2010; Niinemets, 2010b, 2010a), and there are range shifts in plant species that can change the plant type distribution

globally (Wieczynski et al., 2019). Changes to the environment driven by human activities, such as global climate change, may perturb the biosphere-atmosphere interactions, leading to adverse and unpredictable consequences for the whole earth system, including BVOC interactions. Applying an Earth system model, NASA GISS ModleE2, the net chemical forcing of global climate due to anthropogenic impacts of BVOC emissions was reported as -0.17 W m^{-2} (cooling effect) that offset the +0.10 W m^{-2} (warming effect) due to anthropogenic VOC emissions (Unger, 2014).

Overall, to investigate the impact of BVOC emissions on climate, one of the crucial tools is a better understanding of the SOA formation potential and SOA properties from BVOCs. SOA laboratory experiments have provided the foundation for SOA model predictions. The SOA formation mechanisms in global climate and air quality models are highly variable, and SOA formation consistently has been under-predicted in current models compared to actual measurements and observations. The uncertainties in the inputs of these models arise from incomplete chemical knowledge of degradation pathways and significant variability in measured SOA yields. Specifically, investigating the SOA formation from real plant mixture upon herbivory stress and studying SOA formation potential and SOA chemical composition of oxygenated monoterpenes would add valuable information to the current body of knowledge about SOA. The increasing prevalence of plant stress conditions, such as the frequency and intensity of herbivorous insect outbreaks, could alter the composition of BVOC emissions, and this impact on SOA formation needs to be investigated as it is unknown. Oxygenated terpenes have been observed in many plant emissions with relatively low contributions to the total plant emission. However, in some plants, such as shrub species in southern California's coastal sage scrub ecosystem, oxygenated terpenes are the dominant contributors to the total plant emission. Regarding SOA

formation, these oxygenated compounds have been studied less than other common terpenes such as α-pinene and isoprene. Thus, the SOA formation and characterization from these compounds would be worth investigating, specifically for a future climate where these drought-tolerant plants will likely experience a large expansion range.

Table 1.1. Ecological functions of plant BVOCs and corresponding examples.

Role/Level	Example
Reproduction: attraction of pollinator and seed dispenser	the attraction of bees, moths, and bats (Chen et al., 2009; Hossaert-McKey et al., 2010; Luft et al., 2003; Shuttleworth and Johnson, 2009)
Defense: defense against herbivory and pathogen (direct/indirect)	repelling of herbivores (De Moraes et al., 2001); the attraction of enemies of herbivores (De Moraes et al., 1998; Rasmann et al., 2005; Turlings et al., 1990); antimicrobial or antifungal effects (De Moraes et al., 2001; Keeling and Bohlmann, 2006; Shiojiri et al., 2006; Shulaev et al., 1997)
Stress tolerance: tolerance against abiotic stress	Dudareva et al., 2006; Holopainen, 2004; Holopainen and Gershenzon, 2010; Peñuelas and Llusià, 2004; Sharkey et al., 2008; Vickers et al., 2009a)
Organism ecology: within-plant signaling	older to younger leaves, damaged to undamaged leaves (Heil and Bueno, 2007; Holopainen and Blande, 2013; Karban et al., 2006)
Population ecology: plant-plant signaling (same species)	activation of defense in a neighbor plant (Arimura et al., 2000; Ton et al., 2007)
Community ecology: plant-plant signaling (different species)	activation of defense in a neighbor plant (Frost et al., 2008; Holopainen and Blande, 2013)

CHAPTER 2

Acyclic terpenes reduce secondary organic aerosol formation from emissions of a riparian shrub

Article

Acyclic Terpenes Reduce Secondary Organic Aerosol Formation from Emissions of a Riparian Shrub

Farzaneh Khalaj, Albert Rivas-Ubach, Christopher R. Anderton, Swarup China, Kailen Mooney, and Celia L. Faiola*

Cite This: ACS Earth Space Chem. 2021, 5, 1242−1253

Read Online

ACCESS | Metrics & More | Article Recommendations | Supporting Information

ABSTRACT: Terrestrial vegetation is a major global source of atmospheric secondary organic aerosol (SOA) through oxidation of biogenic volatile organic compound (BVOC) emissions. Climate change is altering the composition of BVOC emissions by increasing the prevalence of plant stress conditions, such as frequency and intensity of herbivorous insect outbreaks. The impact this will have on SOA formation is unknown. This laboratory study investigated the influence of aphid herbivory (*Uroleucon macolai*) on SOA formation from emissions of a common riparian shrub in California, *Baccharis salicifolia* (Asteraceae). Aphid herbivory increased the relative contribution of β-ocimene and decreased the relative contribution of β-guaiene in the BVOC emission profile. These effects on BVOC emissions did not translate to a significant aphid effect on SOA mass yields. However, for both control and aphid experiments, the fraction of total acyclic monoterpenes in the BVOC emission profile was correlated with reduced SOA mass yield. This is the first study to demonstrate a clear reduction in SOA mass yield as the proportion of acyclic terpenes in a complex BVOC mixture increased. These findings highlight the importance of better understanding acyclic terpene chemistry in the atmosphere to improve predictions of SOA in both current and future climates.

KEYWORDS: *secondary organic aerosol, biogenic volatile organic compounds, plant−atmosphere interactions, atmospheric chemistry, plant stress*
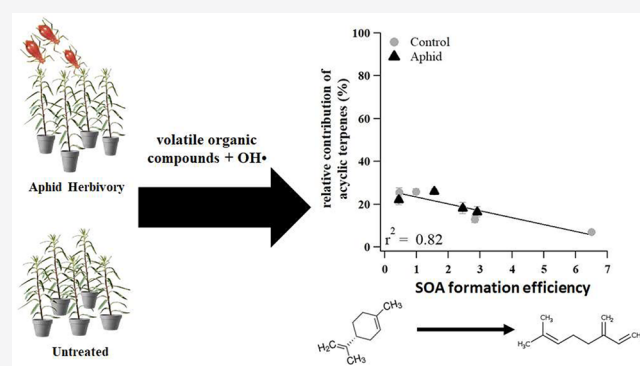
1. INTRODUCTION

Plants produce over one million different chemical metabolites[1] of which at least 1000 are emitted to the atmosphere as biogenic volatile organic compounds (BVOCs).[2,3] These compounds are highly reactive and participate in important atmospheric aerosol processes including particle nucleation[4] and secondary organic aerosol (SOA) formation,[5] whereby they influence aerosol climate effects by altering particle composition,[6−8] hygroscopicity,[9] and optical properties.[10−12] Plant BVOCs, particularly terpenes, are the largest contributor to atmospheric SOA globally.[13,14] The SOA chemistry of a few common terpene compounds (i.e., isoprene, α-pinene, β-pinene, limonene) has been studied extensively in laboratory chamber experiments,[15−18] and this seminal work has provided the foundation for model predictions of SOA production. However, these laboratory experiments represent a small fraction of all BVOCs, which have a diverse range of molecular structures with atmospheric reactivity varying by orders of magnitude even between different types of terpenes.[19,20] The types of BVOCs emitted by plants (or the BVOC emission profile) varies in different environmental contexts[21] and between different plant species,[22] many of which are

undergoing substantial range shifts due to climate change.[23] This presents unique challenges for improving SOA predictions in a rapidly changing world where future spatiotemporal distributions of BVOC profiles could look very different from today. Addressing this challenge necessitates a more complete understanding of the aerosol chemistry associated with these highly complex plant volatile mixtures across a range of environmental conditions.

Each step of the SOA formation process, from BVOC emissions to atmospheric chemistry, is affected by a changing climate, leading to unpredictable BVOC-aerosol-vegetation climate feedbacks. For example, increased temperature and atmospheric carbon dioxide are both predicted to increase BVOC emission rates with subsequent increases in SOA
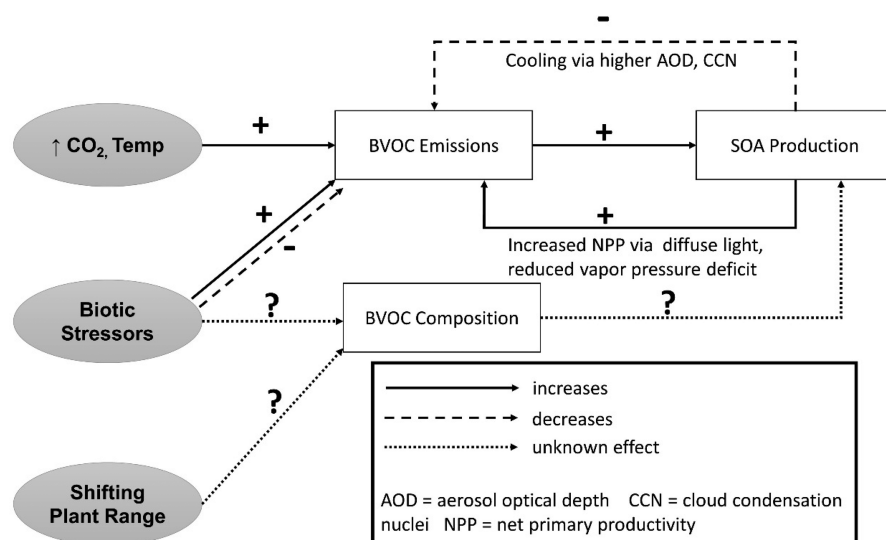
Figure 1. Simplified schematic of the BVOC-aerosol-vegetation feedback associated with changing BVOC emission rates and BVOC composition. We have not included all of the potential sources that could change BVOCs but rather provide a sample to illustrate the process.

production.[24−26] Increased SOA can have two very different effects on plant physiology and BVOC emission rates. The first effect is to reduce BVOC emissions (negative feedback) through aerosol radiative cooling that results from increased aerosol optical depth and increased number of cloud condensation nuclei.[27] This occurs because BVOC emission rates are exponentially related to temperature so any radiative cooling effect will decrease BVOC emission rates.[28] The second effect is to increase BVOC emissions (positive feedback) through increased plant net primary productivity driven by increased diffuse photosynthetic radiation and decreased vapor pressure deficit. The existence of the positive feedback effect has been supported with both modeling[29] and field observations,[30] although there are still questions about the net BVOC-aerosol-vegetation feedback effect due to the inherent complexity of this system.[31] Accounting for both positive and negative feedback effects, the Norwegian Earth System Model estimates a net negative radiative forcing of −0.49 W m^{-2} offsetting 13% of forcing associated with doubling atmospheric CO_2.[32] These results highlight that the BVOC-aerosol-vegetation feedback is worthy of further investigation, including the consideration of important factors other than temperature and CO_2 that could alter BVOC emissions. For example, it could be of equal or greater importance that many abiotic and biotic plant stressors alter both the BVOC emission profile and emission rates,[33−37] and that plant species are currently undergoing drastic range shifts altering the distribution of plant types across Earth's surface.[23] Both of these will change the spatiotemporal distribution of atmospheric BVOC composition. A simplified schematic illustrating this BVOC-aerosol-vegetation feedback is shown in Figure 1. Note that "biotic stressors" can include insect herbivory and pathogens, which could increase BVOC emissions in the short term but could also decrease BVOC emissions in the long term depending on severity and plant mortality. Currently, there are major gaps in our understanding of how BVOC composition could change in the future and how this could influence SOA production.

Changes in BVOC composition from different plant species can alter SOA formation through effects on nucleation rates and condensational growth. Ozonolysis of plant BVOC

emission profiles with a higher contribution of sesquiterpenes (e.g., loblolly pine, *Pinus taeda*) generated much higher particle formation rates than plant systems dominated by monoterpene emissions (e.g., holm oak, *Quercus ilex*).[38] Similarly, new particle formation was enhanced via photooxidation of birch (*Betula pendula*) emissions containing high amounts of oxygenated BVOCs (e.g., 3-hexenol, 3-hexenyl acetate, and methyl salicylate) compared to pine (*Pinus sylvestris*) and spruce (*Picea abies*) emissions.[39] All of these examples demonstrate that variations in the complex mixtures of BVOCs from different plants produce variations in aerosol formation but plant BVOC emission profiles of individuals from the same plant species can also change when a plant experiences stress.

Plant stress can increase SOA production, for example, due to insect herbivory or mechanical wounding.[40−42] Part of the increase in SOA production observed in laboratory chamber experiments is simply due to large increases in BVOC emission rates where increased emissions lead to increased BVOC mixing ratios in the laboratory reaction chamber and higher SOA mass. Of equal interest is the effect of plant stress on SOA yield, which is more nuanced and can vary from plant system to plant system depending on how the BVOC composition is affected by the stress. For example, some plant stressors preferentially increase emissions of monoterpenes over sesquiterpenes, effectively reducing the sesquiterpene-to-monoterpene ratio, leading to decreases in SOA mass yield.[40] Other stressors increase emissions of large cyclic sesquiterpenes or large oxygenated compounds like methyl salicylate, which increase SOA mass yields[43] and decrease hygroscopicity of the resulting particles.[9] None of these plant stress effects on SOA formation are accounted for in global climate models, and their importance for the BVOC-aerosol-vegetation feedback have not been investigated. Currently, there are not enough laboratory SOA studies using real plant emissions to identify the key chemical features in these changing BVOC mixtures that drive SOA formation and climate-relevant properties.

In this study, we investigated the effects of insect herbivory on SOA formation from a common riparian shrub in California, *Baccharis salicifolia*. Plants were exposed to a

specialist sap-feeding aphid herbivore that only feeds on this genus of plant, and emissions from control and aphid-treated plants were used to generate SOA in the laboratory with an oxidation flow reactor. BVOCs were sampled during each SOA experiment to allow us to identify the specific chemical features in the complex mixture that were driving SOA production in the flow reactor. Leaf samples were collected at the completion of the experiment for foliar metabolome analysis to evaluate the effect of aphid herbivory on plant health. To our knowledge, this is the first laboratory study investigating effects of insect herbivory on SOA formation from shrubs, which dominate the vegetation landscape in many regions including the coastal sage scrub and chapparal in California.

2. EXPERIMENTAL METHODS

2.1. Experiment Overview. SOA was generated in the laboratory by oxidizing the emissions of 4−11 plants located inside a Teflon plant enclosure. Multiple plants were required to generate a measurable amount of SOA mass (e.g., condensed phase organic aerosol mass). Each set of plants was used to conduct an SOA "trial", which refers to the generation of an SOA mass yield curve with at least 3−4 SOA yield data points for each curve. The SOA mass yield curves were used to compare SOA formation efficiency between the trials. Experimental replicates were defined as the SOA trial, meaning each SOA mass yield curve constructed from multiple SOA mass loadings is a single replicate (Table 1). Each trial was both time and labor intensive, so replicates were thus restricted to four control trials and four aphid treatment trials. Each aphid trial used 4−5 plants, and each control trial used 8−11 plants. More control plants had to be used to obtain the same SOA mass range because emission rates were likely lower than aphid-exposed plants (as expected). A more detailed description of the methods used for SOA generation is provided in Section 2.3. BVOCs were collected for each condensed mass loading in the SOA trial, but the average BVOC emission profile was used for subsequent volatile analysis and statistics. Leaves were harvested from each plant after the SOA trial was completed to evaluate the effect of the aphid treatment on plant health via its effects on the foliar metabolome. The timing of the treatment and control SOA trials was dependent on plant availability. We note that we were unable to use a randomized block design due to this and consequently all herbivore-treatment SOA trials were performed first followed by all control trials (see dates in Table 1). We acknowledge that there was a time variable separating aphid trials from control trials that we could not necessarily pull out due to the timing of plant availability where all aphid trials were conducted first followed by all control trials. To assess whether the temporal clustering of the trials from the two treatments may have affected our results, we inspected whether variation in the timing of trials within a treatment group differed. This was not the case (see Section 3.1), leading us to conclude that little, if any, of the treatment effects observed were attributable to the sequencing of the trials.

2.2. Plants and Aphid Herbivore Treatment. *Baccharis salicifolia* (Asteraceae) is a woody dioecious shrub native to the southwestern United States and Northern Mexico. Plant cuttings were collected at a field site in the University of California Natural Reserve System San Joaquin Marsh Reserve (33.65°N, 117.85°E; Orange County, CA, U.S.A.). BVOC emission profiles in *Baccharis salicifolia* are independent of plant sex, so cuttings were collected from both plant sexes and

Table 1. Summary of Information for Each SOA Mass Yield Curve Data Point from Each SOA Trial[a]

trial ID	date	point[b]	RH (%)	BVOC$_i$[c]	C$_{OA}$[c]	OH$_{exp}$[d]
aphid 1	03/28/2018	1	58	35	1.4	8.1×10^{11}
		2	55	34	0.8	7.8×10^{11}
		3	50	33	0.4	7.4×10^{11}
aphid 2	04/04/2018	1	70	112	2.5	8.5×10^{11}
		2	68	123	2.7	8.0×10^{11}
		3	60	92	1.8	7.8×10^{11}
		4	55	70	1.1	7.7×10^{11}
aphid 3	05/02/2018	1	80	53	2.1	9.7×10^{11}
		2	80	47	1.4	9.7×10^{11}
		3	75	44	0.9	9.4×10^{11}
		4	70	33	0.5	9.1×10^{11}
aphid 4	05/08/2018	1	75	36	2.7	9.4×10^{11}
		2	80	37	1.9	9.7×10^{11}
		3	85	32	0.9	9.8×10^{11}
control 1	05/16/2018	1	75	15	0.8	9.6×10^{11}
		2	73	16	0.6	9.5×10^{11}
		3	65	14	0.5	8.8×10^{11}
		4	60	15	0.3	8.4×10^{11}
control 2	05/18/2018	1	80	37	2.7	9.8×10^{11}
		2	75	46	1.6	9.3×10^{11}
		3	75	44	1.4	9.4×10^{11}
		4	70	43	0.6	9.0×10^{11}
control 3	05/22/2018	1	60	150	2.7	7.5×10^{11}
		2	55	160	2.6	7.0×10^{11}
		3	50	110	0.9	6.8×10^{11}
		4	45	67	0.5	6.8×10^{11}
control 4	05/24/2018	1	55	190	2.4	6.8×10^{11}
		2	45	147	1.7	6.8×10^{11}
		3	40	66	0.9	6.8×10^{11}
		4	39	76	0.4	6.8×10^{11}

[a]Including date of experiment, relative humidity (RH) in OFR, mass concentration of BVOCs introduced to the OFR (BVOC$_i$), mass concentration of condensed organic aerosol formed in the OFR (C$_{OA}$), and OH exposure (OH$_{exp}$). [b]Points, refers to the point number for the SOA mass yield curve in that SOA trial. [c]Units are μg m^{-3}. [d]Units are molecules cm^3 s^{-1}.

used for the experiment.[44] We imposed an herbivore treatment by an aphid species known to induce changes in *Baccharis salicifolia* volatile emissions.[44] The aphid used in this study, *Uroleucon macolai*,[45] is a dietary specialist herbivore feeding only on two *Baccharis* species, including *Baccharis salicifolia*. Like all aphids, this species is sap-feeding, viviparous, parthenogenetic, and thus has a very short generation time (5−10 days).[46] The aphid laboratory colony, collected in the Marsh reserve, was sourced from a single cluster of aphids and was thus likely to all be of a single genotype.

The *Baccharis salicifolia* stems were cut from mature plants in October 2017. Individual plant stems (from the same plant source cut) were grown in 4 in. pots in a 1:1:1:1 mixture of sand, peat moss, redwood compost, and pumice garden soil in the greenhouse at the University of California, Irvine. In April 2017, plants were randomly selected for aphid colonization and populations were allowed to grow to about 50 individual aphids. To prevent aphid movement to control plants, plants from aphid and control groups were kept in separate greenhouse rooms of an identical size and maintained under consistent environmental conditions. The aphids were introduced to the plants about one month before aphid SOA
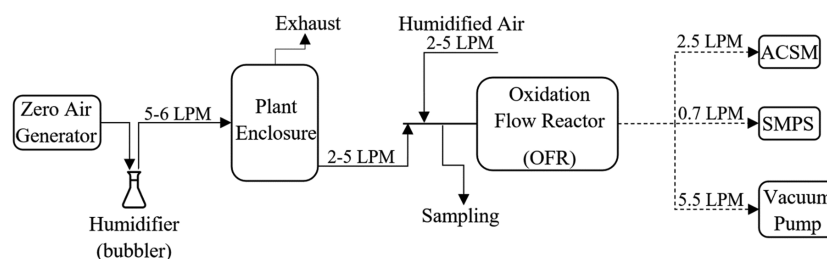
Figure 2. A schematic of the experiment setup. Solid lines refer to PFA tubing and dashed lines refer to copper tubing. LPM refers to liter per min. "Sampling" denotes the location of volatile sampling. ACSM = aerosol chemical speciation monitor and SMPS = scanning mobility particle sizer

experiments were conducted. Before transferring plants to the laboratory to conduct an SOA trial, aphids were removed from plants with a soft brush followed by a gentle water rinse. This was done to eliminate any volatile emissions that might come from the aphids themselves. To account for any effect of the washing treatment, control plants were subjected to the same washing procedure.

2.3. SOA Generation and BVOC Emission Profile Characterization. SOA trials were conducted in a laboratory at University of California, Irvine. Plants were transported from the greenhouse to a custom-built ∼500 L plant enclosure constructed from Teflon sheets and supported by a 1.0 m × 0.7 m × 0.5 m plastic frame. Plants were acclimated to laboratory conditions for a minimum of 24 h to ensure emissions were not elevated due to physical disturbance associated with transportation and the aphid removal processes, which has been shown to be long enough for plant emissions to return to baseline levels.[47] Each trial consisted of generating SOA at a minimum of three different mass loadings to generate an SOA mass yield curve (number of measurement points included in each SOA trial for different replicate sets is shown in Table 1). Aerosol mass loadings <5 $\mu g \ m^{-3}$ were targeted to stay within an atmospherically relevant range in remote areas; the typical range of global ambient biogenic SOA mass loadings vary from 0.1 to 20 $\mu g \ m^{-3}$.[48−50]

SOA was generated via photooxidation of *Baccharis salicifolia* volatile emissions in an oxidation flow reactor (OFR; Aerodyne, Inc.) using the setup shown in Figure 2. Humid clean air was introduced into the plant enclosure continuously with flow rate ranging between 5 to 6 L min^{-1}. Clean air was generated with a zero-air generator (Environics Series 7000) and humidified by passing the air through a bubbler. The plant volatiles were pulled from the plant enclosure headspace into the OFR through 0.25 in PFA tubing at flow rates ranging between 2 to 5 L min^{-1}. This flow rate was controlled by the difference in flow rates between the actively controlled OFR inlet and outlet flows. Humidified air was introduced to the OFR at the inlet and controlled with a mass flow meter between a range of 2.0 to 5.0 L min^{-1}. This range in flows reflect the values required to generate SOA at multiple different mass loadings to generate the SOA mass yield curve. Total flow rate through the OFR was controlled via the outlet flows, which consisted of instrument sampling and an additional vacuum pump flow. Particle size distributions and particle composition were continuously monitored at the outlet with a scanning mobility particle sizer (SMPS; custom-built from TSI, Inc. and Brechtel Inc. components) and time-of-flight aerosol chemical speciation monitor (ToF-ACSM: Aerodyne, Inc.), respectively. The ToF-ACSM sampling line was a 2 m, 3/8″ copper tube that pulled 2.5 L min^{-1} from the same sampling line that served the SMPS. The SMPS pulled

0.7 L min^{-1} with 0.25 in copper tubing. An extra vacuum flow at the outlet was established with a vacuum pump (Thomas, Model 617CA22) and controlled with a needle valve at a flow rate of 5.5 L min^{-1}. Total OFR outlet flow was 8.7 L min^{-1} with a corresponding residence time of 1.49 min. For each SOA mass loading, BVOCs were collected at the OFR inlet on stainless steel adsorbent cartridges containing quartz wool, Tenax TA, and carbograph 5TD (Markes International, Inc.) by pulling 0.42 L min^{-1} through duplicate cartridges in parallel for 4−6 min. Cartridges were capped and stored in a refrigerator until they could be analyzed off-line with a thermo-desorption gas chromatograph mass spectrometer (TD-GC-MS, TD: Markes International Series 2 Unity/ Ultra, GC-MS: Agilent GC 7890B with flame ionization detector (FID), equipped with a 30 m, DB-5 column and a Markes, International mass spectrometer BenchTOF-Select type). Details of the GC operation, volatile quantitation and identification are provided in the BVOC emission profile characterization section of Supporting Information (Section 1).

The Aerodyne OFR has been described in detail elsewhere,[51,52] and we include a brief description of the OFR setup we used here. It is a 13 L (45.7 cm length OD × 19.7 cm ID) aluminum cylinder equipped with two low-pressure mercury 185 and 254 nm lamps (BHK, Inc., model no. 82-904-03) to produce OH radicals through the photolysis of H_2O, O_2, and O_3. In our experiment, the OFR was operated using both 185 and 254 nm lamps (referred to as OFR185 mode) in which OH radicals were produced inside the OFR via reaction of oxygen ($O(^1D)$) radicals with water vapor. The ozone (O_3) was generated within the reactor via UV photolysis of oxygen (O_2) with 185 nm lamps. Then oxygen ($O(^1D)$) radicals were produced by UV photolysis of O_3 with the 254 nm lamps inside the reactor. The OH radicals readily react with BVOCs to generate SOA. Before each SOA trial, the OFR was cleaned by flushing overnight with zero air with OFR lights on, and the SMPS and ToF-ACSM were used to verify the reactor was clean before introducing volatiles to the reactor. The ToF-ACSM operating principles, calibration procedures, and analysis protocols are described in detail elsewhere.[53]

A summary of all SOA trials, including treatment group, date conducted, and other relevant details is given in Table 1. For each SOA trial mass yield point, the OFR relative humidity (RH) and plant volatile concentration at the inlet of the OFR were recorded (Table 1). Each SOA trial used volatiles from the same set of plants in the enclosure and was completed in a single day with each SOA mass loading requiring ∼60−90 min to stabilize the system, collect the volatile cartridge samples, and provide a minimum of 10 min averaging interval from the SMPS and ToF-ACSM before and after cartridge sampling. SOA yield was measured at multiple mass loadings to generate

an SOA mass yield curve. An SOA mass yield curve is a plot of aerosol mass yield versus total condensed organic mass and is a common approach to characterize the SOA formation efficiency of a volatile/oxidant system.[54−59] The SOA mass yield is calculated as the condensed organic aerosol mass generated (ΔC_{OA}) divided by the mass of gas-phase BVOCs that reacted (ΔBVOC). The BVOC concentration at the OFR inlet ranged between 14 to 190 μg m^{-3}. The conditions in the OFR were targeted to be as atmospherically relevant as possible (low BVOC concentrations, high humidity), but the light intensities used were likely high enough to inhibit peroxy radical interactions that normally occur in the ambient environment.[52] Thus, we do not recommend using the SOA yields presented here for direct model integration. Rather, they are used here as a useful metric for comparing SOA formation potential between the different experiments. The integrated OH exposure inside the OFR ranged from 6.8×10^{11} to 9.8×10^{11} molecules cm^{-3} s in all trials. The corresponding equivalent of atmospheric photochemical age of this OH exposure range is 5−8 days assuming an ambient OH concentration of 1.5×10^6 molecules cm^{-3}.[60] In all trials, we assumed ΔBVOC was equal to the inlet concentration (e.g., we assumed all BVOCs reacted) which is a reasonable assumption for the conditions in this study; approximately 530 μg m^{-3} of α-pinene could react (given OH rate constants 5.23×10^{-11} cm^3 molec^{-1} s^{-1})[61] at these OH exposure ranges, which is much higher than the measured BVOC inlet concentrations (14−190 μg m^{-3}). ΔC_{OA} was calculated from SMPS particle size distributions measured at the OFR outlet assuming a background condensed organic aerosol mass of zero (verified before starting each trial) and using a particle density of 1.4 g cm^{-3}, a reasonable value for laboratory biogenic SOA, which has been measured from 1.2 to 1.4 g cm^{-3}.[59,62,63]

2.4. Leaf Sample Collection, Preparation, and Metabolite Extraction. Leaves were harvested from plants at the end of each SOA trial. From each plant in the enclosure, 4−7 "sunlit" leaves (meaning leaves at the top of the plant) from each control and aphid-treated plant were harvested and immediately frozen in liquid N$_2$. Sunlit leaves at the top of the plant were targeted to eliminate known variability between sun and shade leaves, although it should be noted that these plants were small enough that all leaves were exposed to sunlight. The leaves at the top of the plant are the youngest leaves, but all leaves on these *Baccharis Salicifolia* plants were less than 6 months in age because all plants were grown from cuts collected in October of 2017. These samples were lyophilized, ground with a vibration bead mill Qiagen TissueLyzer II (Germantown, MD, U.S.A.) and stored at −80 °C until metabolite extraction. Polar and semipolar compounds were extracted following t'Kind et al. (2008) with minor modifications.[64] Briefly, for each sample, 30 mg of lyophilized powder was introduced into a 2 mL glass vial and 1 mL of methanol/water (80:20) was subsequently added. Samples were shaken for 1 h at 1000 rpm in a Thermoximer at 18 °C, centrifuged for 5 min at 12,000×*g*, and 0.8 mL of supernatants were split and transferred into two different sets of clean 2 mL tubes (0.3 mL for LC-MS and 0.5 mL for GC-MS). LC-MS analysis was performed directly on the methanol/water extracts using a high-resolution LTQ Orbitrap Velos mass spectrometer (HRMS) equipped with a heated electrospray ionization source (HESI) and coupled to a liquid chromatographer Vanquish ultrahigh pressure (UHPLC) (Thermo Fisher Scientific, Waltham, Massachusetts, U.S.A.). Additional details

of chromatography, data filtering, and data analysis methods for GC-MS and LC-MS analysis are provided in Supporting Information (Section 2).

2.5. Statistical Analyses. After data filtering, the metabolomics data set containing both LC-MS and GC-MS foliar metabolome data was composed of one categorical factor with two levels: (control (C1, C2, C3, and C4 trials) and aphid (A1, A2, A3, and A4 trials) treated plants), and 25 001 continuous dependent variables (metabolomic features) where 218 metabolomic features were assigned a metabolite ID (Table S2). The TD-GC-MS data set of the identified plant volatile compounds was composed of a categorial factor with two levels (control (C1, C2, C3, and C4 trials) and aphid (A1, A2, A3, and A4 trials) treated plants) and 13 continuous variables (BVOC compounds). The foliar metabolome and BVOC emission profile of all plants contained in the enclosure for the SOA trial was used for tests of statistical difference between treatment and control.

Variability in the BVOC emission profile and foliar metabolome between control and aphid plants were visualized with a principal component analysis (PCA). PCA of the foliar metabolome was performed using data from individual plants within each trial to visualize intra- and inter-trial variability. PCA of the BVOC emission profiles was performed using the average from the SOA trial because emissions from individual plants were not measured. Differences in the BVOC emission profile and foliar metabolome between control and aphid plants were tested with permutational multivariate analysis of variance (PERMANOVA). Linear regressions were used to fit the SOA yield plots. All statistical analyses were performed using R (version 3.6.1) except for the linear regression, which was performed in Igor Pro software from WaveMetrics Inc. (version 7.0.2.2). The adonis function from the "vegan" package was used for PERMANOVAs.[65] PCAs were plotted using the PCA function from "FactoMineR" package.[66]

3. RESULTS AND DISCUSSION

3.1. Effect of Aphids on the Foliar Metabolome. The foliar metabolome was characterized to assess whether or not aphid herbivory affected the overall plant metabolome. Aphid herbivory altered the overall foliar metabolome (PERMANOVA; $p < 0.05$; Table S5). Principal component (PC)1 and PC2 of the PCA explained 47.9% (PC1 = 32.45% and PC2 = 15.45%) of the total variance and aphid herbivory and control treatments were clustered separately along the PC1 axis (Figure 3). PCA revealed larger metabolome variability between control plants than aphid plants along the PC2. In particular, we found that the total amino acid signal was significantly ($p < 0.01$) increased in aphid-treated plants compared to control groups (Table S7). Individual amino acids that significantly increased in treated plants include proline, histamine, adenine, asparagine, serine, aspartic acid, and tryptophan. Amino acids play important roles in plant stress response including regulating ion transport, modulating stomatal conductance, affecting synthesis and regulation of enzymes, gene expression, and participating in redox-homeostasis.[67] The relative abundance of jasmonic acid (JA), a common stress signaling hormone associated with insect herbivory,[68−71] was increased in aphid plants as well. These results demonstrate that aphid herbivory did affect the plant secondary metabolism and confirm the aphid treatment approach successfully induced an overall plant metabolic response.
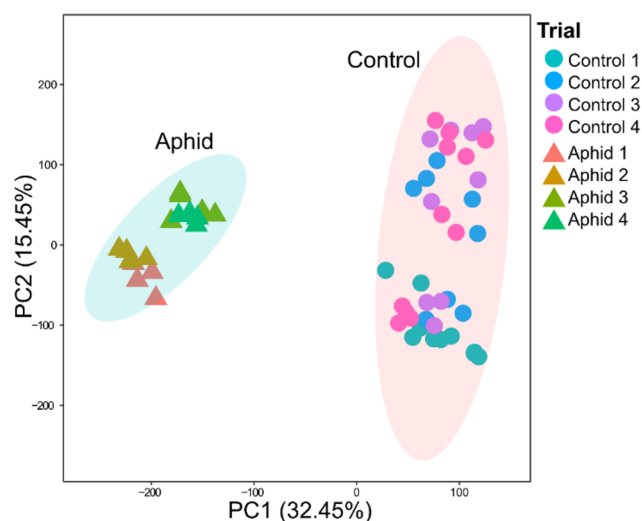
Figure 3. PCA of foliar metabolites from control (circles) and aphid (triangles) plants. Individuals included within each trial are represented in different color. Ellipses represent the distribution at 95% confidence interval for each of the treatments in the plane defined by both PC1 and PC2.

3.2. Effect of Aphids on the Gas-Phase BVOC Emission Profile.

Unlike the foliar metabolome, the BVOC emission profile of control and aphid plants did not exhibit clear clustering based on treatment in a PCA (Figure 4),
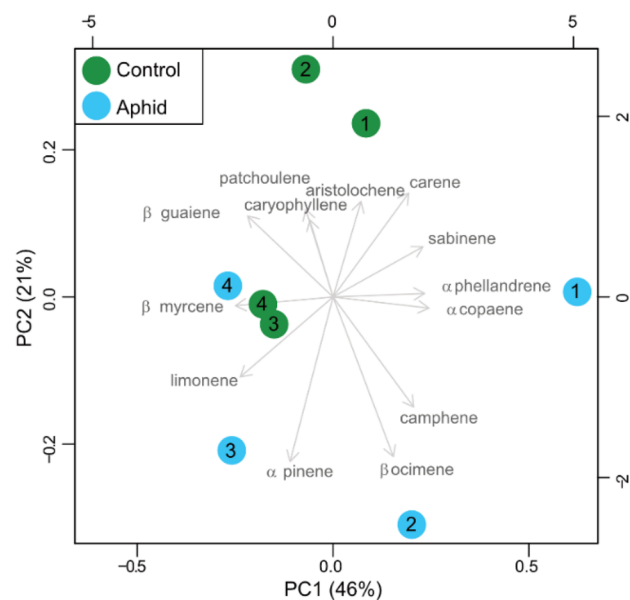
Figure 4. Biplot of the PCA of the gas-phase BVOC profile for control and aphid Baccharis trials. Circles represent the average BVOC profile from SOA trials. Numbers 1−4 indicate the experimental ID number (Table 1).

indicating that aphid herbivory did not have a clear effect on the BVOC emission profile (or the composition of the BVOCs emitted from the plants). PC1 and PC2 of the PCA explained a total variance of 67% (PC1 = 46% and PC2 = 21%). PC1 variability was largely explained by the relative contribution of α-copaene, sabinene, α-phellandrene, camphene, 3-carene, β-ocimene, and by β-guaiene. Variability along PC2 was explained mainly by the relative contribution of 3-carene,

aristolochene, patchoulene, β-guaiene, β-ocimene, α-pinene, and camphene. On the basis of Figure 4, it is clear that there was substantial variation within treatment and control groups. Consistent with the PCA results, there was no significant difference between the BVOC emission profile of control and aphid plants as tested with PERMANOVA analysis (Table S6). This result is in contrast to some other plant-herbivore systems that have been studied previously where significant changes in the BVOC emission profile have been observed after herbivory. For example, gypsy moth herbivory altered the BVOC emission profile of holm oak by increasing β-caryophyllene emissions and inducing new sesquiterpene emissions such as α-humulene and δ-cadinene.[72] Aphid herbivory significantly increased emissions of monoterpenes like linalool and β-ocimene, and sesquiterpenes, such as α-farnesene or β-caryophyllene in European beech and tall fescue grasses.[73,74] On the basis of these previous studies from other plant-herbivore systems, our results were unexpected. We highlight that our results do not suggest the BVOC emission rates were unaffected by aphid herbivory; aphid herbivory has been documented to significantly increase BVOC emission rates from *Baccharis salicifolia*.[44] Indeed, it is likely that BVOC emission rates did increase from the aphid-exposed plants in our study (although this was not directly measured) because we were able to use fewer plants in the enclosure for the aphid SOA trials than the control SOA trials to achieve the same SOA mass loadings. Our measurements were not focused on characterizing BVOC emission rates, but rather the BVOC emission profile and how changes in the composition affect SOA production. Regarding the aphid effect on the BVOC emission profile, the results from this study demonstrated there was just as much variation within treatment groups as between treatment groups (even though all of these plants had been propagated from the same source and were thus genetically identical), and there was no clear impact of the aphid herbivore on the BVOC emission profile. These results highlight the intraspecies variability in BVOC emission profiles, which has been a major challenge in developing predictive models of plant stress emissions following biotic stress.[69,75]

Although the overall BVOC emission profile did not show significant differences between aphid and control plants, there were statistically significant differences in relative emissions of two individual compounds. To illustrate this, the average relative contribution of individual BVOC compounds from aphid and control trials are shown (Figure 5). BVOC emissions of both control and aphid *B. salicifolia* were dominated by limonene. Aphid herbivory significantly increased the relative contribution of β-ocimene and slightly decreased the relative contribution of β-guaiene. The contribution of β-ocimene increased by over 5 times, from 1.72% to 8.72% of the total BVOCs ($p < 0.01$). These results are consistent with a previous study showing *B. salicifolia* emissions are generally dominated by limonene and that aphid herbivory increased β-ocimene emissions.[44] On the other hand, the contribution of β-guaiene was marginally reduced ($p < 0.1$) in aphid plants (5.42%) compared to the control group (9.67%).

3.3. Chemical Controls on SOA Formation.

SOA mass yields were plotted for each SOA trial to compare SOA formation efficiency of the BVOC mixtures from each set of plants (Figure 6). For all trials, the mass yield increased with increased mass loading as expected based on gas-particle partitioning theory.[54,55] Normally, an SOA mass yield curve
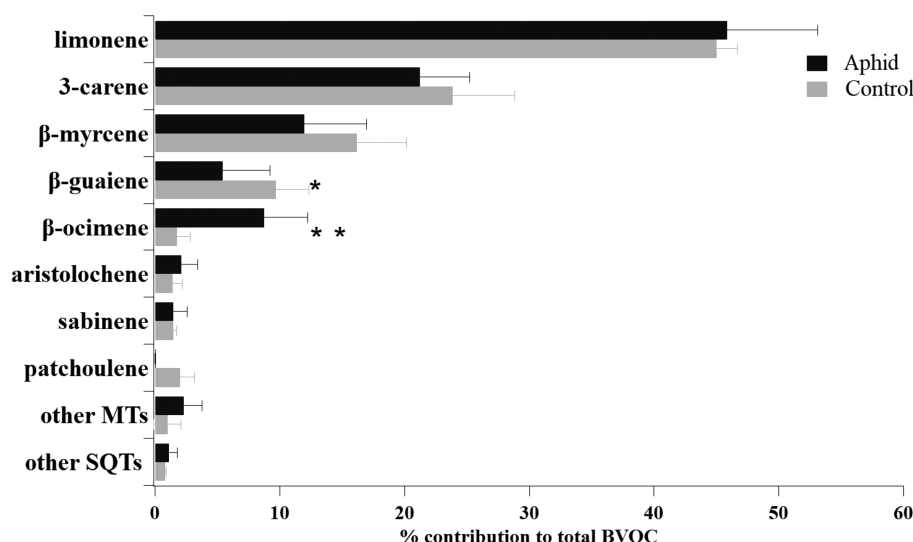
Figure 5. Average percent contribution of individual BVOC compounds during control and aphid Baccharis trials. Asterisk indicates significance level based on t test (*, $p < 0.1$ and **, $p < 0.01$). Other SQTs (sesquiterpenes) included caryophyllene and α-copaene. Other MTs (monoterpenes) included α-pinene, α-phellandrene, and camphene. Error bars denote the standard error of all cartridge samples.
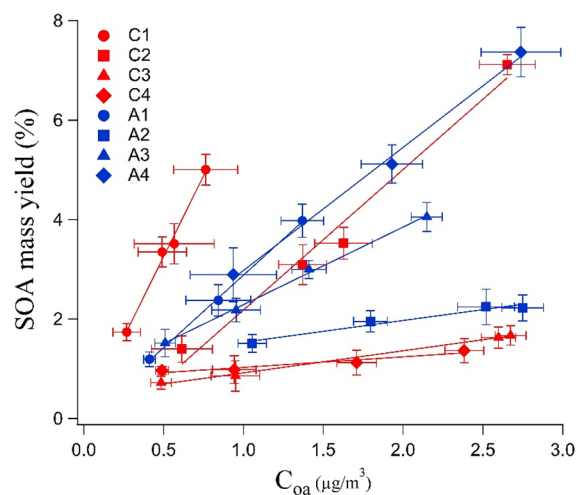
Figure 6. SOA mass yields for aphid and control trials. Lines represent best fits to the data using linear regression. C1–C4 denotes control trials and A1–A4 denotes aphid trials. Error bars denote standard deviation of the measurements.

would not exhibit linearity but would approach a maximum yield at higher condensed organic aerosol (C_{oa}) mass loadings. However, we targeted very low aerosol mass loadings to represent atmospherically relevant conditions in remote areas where BVOCs dominate SOA production, which means we stayed within the linear range of the mass yield curve rather than observing a yield threshold. The SOA yield threshold would typically occur at condensed mass concentrations at least an order of magnitude higher than those used in this study.[56] In both control and aphid trials, the SOA mass yield ranged from 1% to 7% across a condensed organic aerosol mass range of 0.5–3 μg m^{-3} in the OFR. These low-yield values were expected at the low mass loadings targeted in these trials; the estimated SOA mass yields from monoterpene-dominated BVOC mixtures ranged from 3% to 11% at similar organic aerosol mass loadings (0.5–6 μg m^{-3}).[76] Limonene and 3-carene are the dominant terpenes in the BVOC profile for all of the trials, collectively contributing 70–80% of total

BVOCs by mass (Figure 5) and are likely driving a large fraction of the SOA production in the flow reactor. SOA mass yields of laboratory-generated limonene and 3-carene organic aerosols are less than 10% for condensed mass loadings below 10 μg m^{-3},[77,78] and thus these values are comparable with the yield values and corresponding organic aerosol mass values in this study.

SOA formation efficiency was defined as the slope of the line for each SOA mass yield curve; a steeper slope equals higher SOA formation efficiency. The slopes ranged from 0.44 to 2.91 and 0.21 to 6.49 for the aphid and control trials, respectively. This demonstrates there was as much variability in SOA formation efficiency within aphid/control groups as there was between groups. Recall from Section 3.2 that there was quite a bit of variability in the BVOC emission profiles between trials. Detailed BVOC emission profiles for each individual trial are provided in the Supporting Information to help explain some of the variability observed in SOA formation efficiency (Figure S1). The aphid 2 trial had the lowest SOA formation efficiency of all aphid plants and also had the smallest relative contribution from sesquiterpenes in the volatile profile. Aphid 3 and aphid 4 had nearly identical sesquiterpene contributions to the profile, but aphid 3 had a higher contribution from acyclic monoterpenes which can fragment upon oxidation and could explain the reduced SOA formation efficiency.[79] Of particular note, control 1 had the highest SOA formation efficiency with a slope of 6.49. The BVOC profile of the control 1 trial also had the highest cyclic-to-acyclic terpene ratio at 13% compared to the other trials which ranged from 2.7 to 6.5%. However, just qualitatively comparing the BVOC emission profiles of individual trials with the SOA formation efficiency does not indicate which molecular features were driving SOA formation from a more comprehensive perspective.

To systematically investigate relationships between BVOC structural class and SOA formation efficiency for all trials, we calculated the correlation between the slope of the SOA mass yield curve (e.g., the SOA formation efficiency) and the relative contribution of various compound classes and/or structures. This included relative fraction of cyclic terpenes, bicyclic

terpenes, monocyclic terpenes, total monoterpenes, total sesquiterpenes, and all individual compounds. The compounds were grouped as follows: bicyclic terpenes (aristolene, patchoulene, β-guaiene, caryophyllene, sabinene, 3-carene, camphene, α-pinene), acyclic terpenes (β-ocimene, β-myrcene), and monocyclic terpenes (limonene, α-phellandrene). A summary of these results is provided in Table 2. No single

Table 2. Correlation between SOA Formation Efficiency and the Relative Contribution of Different Structural Classes to Total BVOCs

structural class	r^2
cyclic terpenes	0.82
bicyclic terpenes	0.61
monocyclic terpenes	0.08
monoterpenes	0.03
sesquiterpenes	0.03
individual terpenes	0.03–0.50

individual compound was correlated with SOA formation efficiency with correlations ranging from 0.03 to 0.50 (Table S8). Total sesquiterpene contribution was also not correlated with higher SOA formation efficiency. This is in contrast to results presented previously on the effects of bark borer herbivory on SOA mass yield from Scots pines where the sesquiterpene-to-monoterpene ratio was the primary predictor of SOA yield.[59] More recent studies have demonstrated that the large structural diversity in sesquiterpenes can produce different effects on aerosol formation and properties than would be expected if using β-caryophyllene as a model sesquiterpene compound.[80,81] These results further substantiate that sesquiterpene-to-monoterpene ratios cannot be used to estimate SOA mass yield, and that SOA production from a range of sesquiterpene structural classes should be the topic of future studies.

The highest correlation between SOA formation efficiency and BVOC structural class was observed in relation to the relative contribution of cyclic versus acyclic terpenes in the BVOC profile ($r^2 = 0.82$). Acyclic terpenes were negatively correlated with SOA formation efficiency (Figure 7). We note there could be a confounding relationship between SOA mass

yield and OH exposure because we cannot control the OH exposure in the flow reactor with precision. Every effort was made to minimize variations in OH exposure by keeping the light settings the same throughout the experiment. We tested for any confounding relationship with OH exposure by plotting the cyclic-to-acyclic terpene contribution versus the OH exposure and confirmed there was no correlation (Figure S2). Thus, the relationship we observed between the proportion of cyclic terpenes to total BVOCs and SOA formation efficiency cannot be explained by small changes in OH exposure between the SOA trials. From a gas-phase chemistry perspective, a positive correlation between SOA formation efficiency and proportion of cyclic terpenes in the mixture makes sense; breaking endocyclic carbon–carbon double bonds results in ring-opening and retaining the carbon backbone while breaking carbon–carbon double bonds of acyclic compounds results in fragmentation of the molecule. Breaking the carbon–carbon bond at the location of the double bond is common during atmospheric oxidation of terpenes, which is why the dominant oxidation products of α-pinene are pinic acid and pinonic acid, both of which have a single ring while the parent compound, α-pinene, has a bicyclic molecular structure.[82] Fragmentation produces compounds with a smaller carbon backbone, by definition, and thus we would expect fragmentation reaction products from acyclic terpene oxidation to have higher volatility and lower SOA mass yields than ring-opening reaction products from cyclic terpene oxidation. This result is consistent with previous reports. The ozonolysis of Scots pine emissions containing a higher proportion of acyclic sesquiterpenes following aphid herbivory contained more fragmentation reaction products than the ozonolysis of healthy Scots pine emissions.[80] Furthermore, photooxidation of farnesene and bisabolene standards purchased from a chemical supplier have lower SOA mass yields than α-pinene.[81] Farnesene isomers are acyclic sesquiterpenes and bisabolene isomers are sesquiterpenes containing a long, unsaturated acyclic tail. These prior studies provided indirect evidence suggesting that an increased proportion of acyclic terpenes would be expected to decrease SOA mass yields, but this study is the first to more clearly link a reduction in SOA formation efficiency with an increasing proportion of acyclic terpenes in a complex BVOC mixture.

4. CONCLUSION

This study characterized SOA formation potential of a complex mixture of BVOC emissions from a riparian shrub with and without being exposed to aphid herbivory. Foliar metabolome analysis indicated that aphid herbivory had a significant effect on plant metabolism, demonstrating the aphid herbivory treatment did influence plant metabolism and health. In particular, amino acids and jasmonic acid were elevated in aphid-exposed plants, both of which have been implicated in plant stress responses. In contrast, the BVOC emission profile was not significantly different between control and aphid plants. Overall, the BVOC emission profile exhibited a lot of variation between different sets of plants, regardless of aphid herbivory, and this led to measurable differences in the SOA formation potential between different BVOC mixtures. This provided the opportunity to examine the chemical controls on SOA formation related to differences in chemical composition of the BVOC mixture. The single chemical structural characteristic that was most correlated with SOA formation potential was the relative amount of cyclic-to-acyclic terpenes.
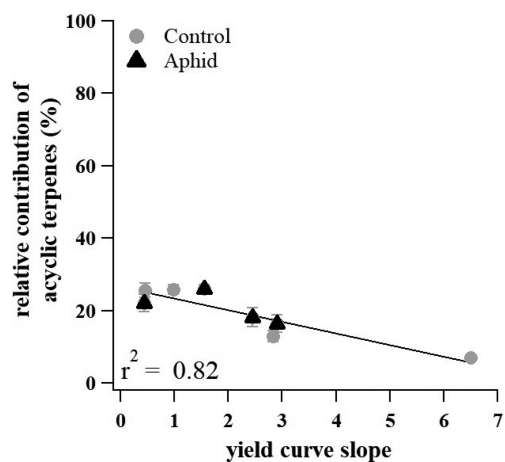

Figure 7. Correlation between the relative contribution of acyclic compounds to total BVOCs and SOA formation efficiency as defined as the SOA mass yield slope. Error bars denote the standard error.

We found a negative correlation between the proportion of acyclic terpenes contributing to the BVOC mixture and the SOA formation efficiency. In this study, the relative contribution of acyclic terpenes to total BVOC emissions was not significantly altered by aphid herbivory. However, other studies have implicated acyclic terpenes as common inducible plant stress BVOCs following herbivory.[33,34,36] Currently, SOA models and chemical transport models do not explicitly account for the atmospheric chemistry of acyclic terpenes. Our results highlight the importance of acyclic terpenes in controlling SOA formation efficiency from a complex mixture, which could become even more prominent in an evolving world with increasing frequency and severity of plant stress conditions. Future studies should target a more comprehensive understanding of the atmospheric chemistry of acyclic terpene compounds including their effect on aerosol chemistry, formation, and climate-relevant properties.

■ ASSOCIATED CONTENT

Ⓢ Supporting Information

The Supporting Information is available free of charge at https://pubs.acs.org/doi/10.1021/acsearthspace-chem.0c00300.

> Details on gas-phase BVOC compound characterization using the TD-GC-ToF-MS, foliar metabolome characterization using GC-MS and LC-MS and related data processing and filtering; brief discussion about statistical analysis results, and plant volatile compounds distribution profile; MZmine parameter details and metabolite assignation information for metabolome (Tables S1 and S2, respectively); metabolite detector parameter details and metabolite assignation information for metabolome (Tables S3 and S4, respectively); summary results of PERMANOVA for metabolome and BVOC (Tables S5 and S6, respectively); student t test summary results for identified metabolites (Table S7); linear trendline r^2 value of yield curve versus relative contribution of individual BVOC to total BVOC (Table S8); plant BVOC distribution profiles of all trials (Figure S1); cyclic-to-acyclic BVOC ratio versus OH exposure curve (Figure S2) (PDF)

■ AUTHOR INFORMATION

Corresponding Author

Celia L. Faiola − *Department of Ecology and Evolutionary Biology and Department of Chemistry, University of California Irvine, Irvine, California 92697, United States;* ⓘ orcid.org/0000-0002-4987-023X; Email: cfaiola@uci.edu

Authors

Farzaneh Khalaj − *Department of Ecology and Evolutionary Biology, University of California Irvine, Irvine, California 92697, United States*

Albert Rivas-Ubach − *Environmental Molecular Science Laboratory, Pacific Northwest National Laboratory, Richland, Washington 99352, United States;* ⓘ orcid.org/0000-0003-1293-7127

Christopher R. Anderton − *Environmental Molecular Science Laboratory, Pacific Northwest National Laboratory, Richland, Washington 99352, United States;* ⓘ orcid.org/0000-0002-6170-1033

Swarup China − *Environmental Molecular Science Laboratory, Pacific Northwest National Laboratory, Richland, Washington 99352, United States;* ⓘ orcid.org/0000-0001-7670-335X

Kailen Mooney − *Department of Ecology and Evolutionary Biology, University of California Irvine, Irvine, California 92697, United States*

Complete contact information is available at:
https://pubs.acs.org/10.1021/acsearthspacechem.0c00300

Notes

The authors declare no competing financial interest.

■ REFERENCES

(1) Afendi, F. M.; Okada, T.; Yamazaki, M.; Hirai-Morita, A.; Nakamura, Y.; Nakamura, K.; Ikeda, S.; Takahashi, H.; Altaf-Ul-Amin, M.; Darusman, L. K.; Saito, K.; Kanaya, S. KNApSAcK Family Databases: Integrated Metabolite-Plant Species Databases for Multifaceted Plant Research. *Plant Cell Physiol.* **2012**, *53* (2), No. e1.

(2) Dudareva, N.; Klempien, A.; Muhlemann, J. K.; Kaplan, I. Biosynthesis, Function and Metabolic Engineering of Plant Volatile Organic Compounds. *New Phytol.* **2013**, *198* (1), 16−32.

(3) Knudsen, J. T.; Eriksson, R.; Gershenzon, J.; Ståhl, B. Diversity and Distribution of Floral Scent. *Bot. Rev.* **2006**, *72* (1), 1.

(4) Riccobono, F.; Schobesberger, S.; Scott, C. E.; Dommen, J.; Ortega, I. K.; Rondo, L.; Almeida, J.; Amorim, A.; Bianchi, F.; Breitenlechner, M.; David, A.; Downard, A.; Dunne, E. M.; Duplissy, J.; Ehrhart, S.; Flagan, R. C.; Franchin, A.; Hansel, A.; Junninen, H.; Kajos, M.; Keskinen, H.; Kupc, A.; Kürten, A.; Kvashin, A. N.; Laaksonen, A.; Lehtipalo, K.; Makhmutov, V.; Mathot, S.; Nieminen, T.; Onnela, A.; Petäjä, T.; Praplan, A. P.; Santos, F. D.; Schallhart, S.; Seinfeld, J. H.; Sipilä, M.; Spracklen, D. V.; Stozhkov, Y.; Stratmann, F.; Tomé, A.; Tsagkogeorgas, G.; Vaattovaara, P.; Viisanen, Y.; Vrtala, A.; Wagner, P. E.; Weingartner, E.; Wex, H.; Wimmer, D.; Carslaw, K. S.; Curtius, J.; Donahue, N. M.; Kirkby, J.; Kulmala, M.; Worsnop, D. R.; Baltensperger, U. Oxidation Products of Biogenic Emissions Contribute to Nucleation of Atmospheric Particles. *Science* **2014**, *344* (6185), 717−721.

(5) Ehn, M.; Thornton, J. A.; Kleist, E.; Sipila, M.; Junninen, H.; Pullinen, I.; Springer, M.; Rubach, F.; Tillmann, R.; Lee, B.; Lopez-Hilfiker, F.; Andres, S.; Acir, I.-H.; Rissanen, M.; Jokinen, T.; Schobesberger, S.; Kangasluoma, J.; Kontkanen, J.; Nieminen, T.; Kurten, T.; Nielsen, L. B.; Jørgensen, S.; Kjaergaard, H. G.; Canagaratna, M.; Maso, M. D.; Berndt, T.; Petaja, T.; Wahner, A.; Kerminen, V.-M.; Kulmala, M.; Worsnop, D. R.; Wildt, J.; Mentel, T. F. A Large Source of Low-Volatility Secondary Organic Aerosol | Nature. *Nature* **2014**, *506*, 476−479.

(6) Kiendler-Scharr, A.; Zhang, Q.; Hohaus, T.; Kleist, E.; Mensah, A.; Mentel, T. F.; Spindler, C.; Uerlings, R.; Tillmann, R.; Wildt, J. Aerosol Mass Spectrometric Features of Biogenic SOA: Observations from a Plant Chamber and in Rural Atmospheric Environments. *Environ. Sci. Technol.* **2009**, *43* (21), 8166−8172.

(7) Faiola, C. L.; Wen, M.; VanReken, T. M. Chemical Characterization of Biogenic Secondary Organic Aerosol Generated from Plant Emissions under Baseline and Stressed Conditions: Inter- and Intra-Species Variability for Six Coniferous Species. *Atmos. Chem. Phys.* **2015**, *15* (7), 3629−3646.

(8) Jimenez, J. L.; Canagaratna, M. R.; Donahue, N. M.; Prevot, A. S. H.; Zhang, Q.; Kroll, J. H.; DeCarlo, P. F.; Allan, J. D.; Coe, H.; Ng, N. L.; Aiken, A. C.; Docherty, K. S.; Ulbrich, I. M.; Grieshop, A. P.; Robinson, A. L.; Duplissy, J.; Smith, J. D.; Wilson, K. R.; Lanz, V. A.; Hueglin, C.; Sun, Y. L.; Tian, J.; Laaksonen, A.; Raatikainen, T.; Rautiainen, J.; Vaattovaara, P.; Ehn, M.; Kulmala, M.; Tomlinson, J. M.; Collins, D. R.; Cubison, M. J.; E Dunlea, J.; Huffman, J. A.; Onasch, T. B.; Alfarra, M. R.; Williams, P. I.; Bower, K.; Kondo, Y.; Schneider, J.; Drewnick, F.; Borrmann, S.; Weimer, S.; Demerjian, K.; Salcedo, D.; Cottrell, L.; Griffin, R.; Takami, A.; Miyoshi, T.; Hatakeyama, S.; Shimono, A.; Sun, J. Y.; Zhang, Y. M.; Dzepina, K.; Kimmel, J. R.; Sueper, D.; Jayne, J. T.; Herndon, S. C.; Trimborn, A. M.; Williams, L. R.; Wood, E. C.; Middlebrook, A. M.; Kolb, C. E.; Baltensperger, U.; Worsnop, D. R. Evolution of Organic Aerosols in the Atmosphere. *Science* **2009**, *326* (5959), 1525−1529.

(9) Zhao, D. F.; Buchholz, A.; Tillmann, R.; Kleist, E.; Wu, C.; Rubach, F.; Kiendler-Scharr, A.; Rudich, Y.; Wildt, J.; Mentel, T. F. Environmental Conditions Regulate the Impact of Plants on Cloud Formation. *Nat. Commun.* **2017**, *8*, 14067.

(10) Lambe, A. T.; Cappa, C. D.; Massoli, P.; Onasch, T. B.; Forestieri, S. D.; Martin, A. T.; Cummings, M. J.; Croasdale, D. R.; Brune, W. H.; Worsnop, D. R.; Davidovits, P. Relationship between Oxidation Level and Optical Properties of Secondary Organic Aerosol. *Environ. Sci. Technol.* **2013**, *47* (12), 6349−6357.

(11) Moise, T.; Flores, J. M.; Rudich, Y. Optical Properties of Secondary Organic Aerosols and Their Changes by Chemical Processes. *Chem. Rev.* **2015**, *115* (10), 4400−4439.

(12) Zhang, X.; Lin, Y.-H.; Surratt, J. D.; Zotter, P.; Prévôt, A. S. H.; Weber, R. J. Light-Absorbing Soluble Organic Aerosol in Los Angeles and Atlanta: A Contrast in Secondary Organic Aerosol. *Geophys. Res. Lett.* **2011**, *38*, L21810 DOI: 10.1029/2011GL049385.

(13) Guenther, A.; Karl, T.; Harley, P.; Wiedinmyer, C.; Palmer, P. I.; Geron, C. Estimates of Global Terrestrial Isoprene Emissions Using MEGAN (Model of Emissions of Gases and Aerosols from Nature). *Atmos. Chem. Phys.* **2006**, *6* (11), 3181−3210.

(14) Hallquist, M.; Wenger, J. C.; Baltensperger, U.; Rudich, Y.; Simpson, D.; Claeys, M.; Dommen, J.; Donahue, N. M.; George, C.; Goldstein, A. H.; Hamilton, J. F.; Herrmann, H.; Hoffmann, T.; Iinuma, Y.; Jang, M.; Jenkin, M. E.; Jimenez, J. L.; Kiendler-Scharr, A.; Maenhaut, W.; McFiggans, G.; Mentel, Th. F.; Monod, A.; Prévôt, A. S. H.; Seinfeld, J. H.; Surratt, J. D.; Szmigielski, R.; Wildt, J. The Formation, Properties and Impact of Secondary Organic Aerosol: Current and Emerging Issues. *Atmos. Chem. Phys.* **2009**, *9* (14), 5155−5236.

(15) Griffin, R. J.; Cocker, D. R.; Flagan, R. C.; Seinfeld, J. H. Organic Aerosol Formation from the Oxidation of Biogenic Hydrocarbons. *J. Geophys. Res. Atmospheres* **1999**, *104* (D3), 3555−3567.

(16) Odum, J. R.; Hoffmann, T.; Bowman, F.; Collins, D.; Flagan, R. C.; Seinfeld, J. H. Gas/Particle Partitioning and Secondary Organic Aerosol Yields. *Environ. Sci. Technol.* **1996**, *30* (8), 2580−2585.

(17) Ng, N. L.; Kroll, J. H.; Keywood, M. D.; Bahreini, R.; Varutbangkul, V.; Flagan, R. C.; Seinfeld, J. H.; Lee, A.; Goldstein, A. H. Contribution of First- versus Second-Generation Products to Secondary Organic Aerosols Formed in the Oxidation of Biogenic Hydrocarbons. *Environ. Sci. Technol.* **2006**, *40* (7), 2283−2297.

(18) Ng, N. L.; Chhabra, P. S.; Chan, A. W. H.; Surratt, J. D.; Kroll, J. H.; Kwan, A. J.; McCabe, D. C.; Wennberg, P. O.; Sorooshian, A.; Murphy, S. M.; Dalleska, N. F.; Flagan, R. C.; Seinfeld, J. H. Effect of NOx Level on Secondary Organic Aerosol (SOA) Formation from the Photooxidation of Terpenes. *Atmos. Chem. Phys.* **2007**, *7* (19), 5159−5174.

(19) Atkinson, R.; Arey, J. Atmospheric Chemistry of Biogenic Organic Compounds. *Acc. Chem. Res.* **1998**, *31* (9), 574−583.

(20) Atkinson, R.; Arey, J. Atmospheric Degradation of Volatile Organic Compounds. *Chem. Rev.* **2003**, *103* (12), 4605−4638.

(21) Loreto, F.; Dicke, M.; Schnitzler, J.-P.; Turlings, T. C. J. Plant Volatiles and the Environment. *Plant, Cell Environ.* **2014**, *37* (8), 1905−1908.

(22) Courtois, E. A.; Paine, C. E. T.; Blandinieres, P.-A.; Stien, D.; Bessiere, J.-M.; Houel, E.; Baraloto, C.; Chave, J. Diversity of the Volatile Organic Compounds Emitted by 55 Species of Tropical Trees: A Survey in French Guiana. *J. Chem. Ecol.* **2009**, *35* (11), 1349.

(23) Wieczynski, D. J.; Boyle, B.; Buzzard, V.; Duran, S. M.; Henderson, A. N.; Hulshof, C. M.; Kerkhoff, A. J.; McCarthy, M. C.; Michaletz, S. T.; Swenson, N. G.; Asner, G. P.; Bentley, L. P.; Enquist, B. J.; Savage, V. M. Climate Shapes and Shifts Functional Biodiversity in Forests Worldwide. *Proc. Natl. Acad. Sci. U. S. A.* **2019**, *116* (2), 587−592.

(24) Kulmala, M.; Suni, T.; Lehtinen, K. E. J.; Dal Maso, M.; Boy, M.; Reissell, A.; Rannik, U.; Aalto, P.; Keronen, P.; Hakola, H.; Back, J.; Hoffmann, T.; Vesala, T.; Hari, P. A New Feedback Mechanism Linking Forests, Aerosols, and Climate. *Atmos. Chem. Phys.* **2004**, *4* (2), 557−562.

(25) Kulmala, M.; Nieminen, T.; Chellapermal, R.; Makkonen, R.; Bäck, J.; Kerminen, V.-M. Climate Feedbacks Linking the Increasing Atmospheric CO2 Concentration, BVOC Emissions, Aerosols and Clouds in Forest Ecosystems. In *Biology, Controls and Models of Tree Volatile Organic Compound Emissions*; Niinemets, Ü., Monson, R. K., Eds.; Tree Physiology; Springer Netherlands: Dordrecht, 2013; pp 489−508.

(26) Arneth, A.; Harrison, S. P.; Zaehle, S.; Tsigaridis, K.; Menon, S.; Bartlein, P. J.; Feichter, J.; Korhola, A.; Kulmala, M.; O'Donnell, D.; Schurgers, G.; Sorvari, S.; Vesala, T. Terrestrial Biogeochemical Feedbacks in the Climate System. *Nat. Geosci.* **2010**, *3* (8), 525−532.

(27) Arneth, A.; Makkonen, R.; Olin, S.; Paasonen, P.; Holst, T.; Kajos, M. K.; Kulmala, M.; Maximov, T.; Miller, P. A.; Schurgers, G. Future Vegetation-Climate Interactions in Eastern Siberia: An Assessment of the Competing Effects of CO_2 and Secondary Organic Aerosols. *Atmos. Chem. Phys.* **2016**, *16* (8), 5243−5262.

(28) Guenther, A.; Hewitt, C. N.; Erickson, D.; Fall, R.; Geron, C.; Graedel, T.; Harley, P.; Klinger, L.; Lerdau, M.; Mckay, W. A.; Pierce, T.; Scholes, B.; Steinbrecher, R.; Tallamraju, R.; Taylor, J.; Zimmerman, P. A Global Model of Natural Volatile Organic Compound Emissions. *J. Geophys. Res.* **1995**, *100* (D5), 8873−8892.

(29) Rap, A.; Scott, C. E.; Reddington, C. L.; Mercado, L.; Ellis, R. J.; Garraway, S.; Evans, M. J.; Beerling, D. J.; MacKenzie, A. R.; Hewitt, C. N.; Spracklen, D. V. Enhanced Global Primary Production by Biogenic Aerosol via Diffuse Radiation Fertilization. *Nat. Geosci.* **2018**, *11* (9), 640.

(30) Wang, X.; Wu, J.; Chen, M.; Xu, X.; Wang, Z.; Wang, B.; Wang, C.; Piao, S.; Lin, W.; Miao, G.; Deng, M.; Qiao, C.; Wang, J.; Xu, S.; Liu, L. Field Evidences for the Positive Effects of Aerosols on Tree Growth. *Glob. Change Biol.* **2018**, *24* (10), 4983−4992.

(31) Wang, B.; Shugart, H. H.; Lerdau, M. T. Complexities between Plants and the Atmosphere. *Nat. Geosci.* **2019**, *12* (9), 693−694.

(32) Sporre, M. K.; Blichner, S. M.; Karset, I. H. H.; Makkonen, R.; Berntsen, T. K. BVOC-Aerosol-Climate Feedbacks Investigated Using NorESM. *Atmos. Chem. Phys.* **2019**, *19* (7), 4763−4782.

(33) Arneth, A.; Niinemets, Ü. Induced BVOCs: How to Bug Our Models? *Trends Plant Sci.* **2010**, *15* (3), 118−125.

(34) Holopainen, J. K.; Gershenzon, J. Multiple Stress Factors and the Emission of Plant VOCs. *Trends Plant Sci.* **2010**, *15* (3), 176−184.

(35) Niinemets, Ü. Mild versus Severe Stress and BVOCs: Thresholds, Priming and Consequences. *Trends Plant Sci.* **2010**, *15* (3), 145−153.

(36) Niinemets, Ü. Responses of Forest Trees to Single and Multiple Environmental Stresses from Seedlings to Mature Plants: Past Stress History, Stress Interactions, Tolerance and Acclimation. *For. Ecol. Manage.* **2010**, *260* (10), 1623−1639.

(37) Loreto, F.; Schnitzler, J.-P. Abiotic Stresses and Induced BVOCs. *Trends Plant Sci.* **2010**, *15* (3), 154−166.

(38) VanReken, T. M.; Greenberg, J. P.; Harley, P. C.; Guenther, A. B.; Smith, J. N. Direct Measurement of Particle Formation and Growth from the Oxidation of Biogenic Emissions. *Atmos. Chem. Phys.* **2006**, *6* (12), 4403−4413.

(39) Mentel, T. F.; Wildt, J.; Kiendler-Scharr, A.; Kleist, E.; Tillmann, R.; Dal Maso, M.; Fisseha, R.; Hohaus, T.; Spahn, H.; Uerlings, R.; Wegener, R.; Griffiths, P. T.; Dinar, E.; Rudich, Y.; Wahner, A. Photochemical Production of Aerosols from Real Plant Emissions. *Atmos. Chem. Phys.* **2009**, *9* (13), 4387−4406.

(40) Faiola, C. L.; Buchholz, A.; Kari, E.; Yli-Pirilä, P.; Holopainen, J. K.; Kivimäenpää, M.; Miettinen, P.; Worsnop, D. R.; Lehtinen, K. E. J.; Guenther, A. B.; Virtanen, A. Terpene Composition Complexity Controls Secondary Organic Aerosol Yields from Scots Pine Volatile Emissions. *Sci. Rep.* **2018**, *8* (1), 3053.

(41) Joutsensaari, J.; Yli-Pirilä, P.; Korhonen, H.; Arola, A.; Blande, J. D.; Heijari, J.; Kivimäenpää, M.; Mikkonen, S.; Hao, L.; Miettinen, P.; Lyytikäinen-Saarenmaa, P.; Faiola, C. L.; Laaksonen, A.; Holopainen, J. K. Biotic Stress Accelerates Formation of Climate-Relevant Aerosols in Boreal Forests. *Atmos. Chem. Phys.* **2015**, *15* (21), 12139−12157.

(42) Yli-Pirilä, P.; Copolovici, L.; Kännaste, A.; Noe, S.; Blande, J. D.; Mikkonen, S.; Klemola, T.; Pulkkinen, J.; Virtanen, A.; Laaksonen, A.; Joutsensaari, J.; Niinemets, Ü.; Holopainen, J. K. Herbivory by an Outbreaking Moth Increases Emissions of Biogenic Volatiles and Leads to Enhanced Secondary Organic Aerosol Formation Capacity. *Environ. Sci. Technol.* **2016**, *50* (21), 11501−11510.

(43) Mentel, Th. F.; Kleist, E.; Andres, S.; Dal Maso, M.; Hohaus, T.; Kiendler-Scharr, A.; Rudich, Y.; Springer, M.; Tillmann, R.; Uerlings, R.; Wahner, A.; Wildt, J. Secondary Aerosol Formation from Stress-Induced Biogenic Emissions and Possible Climate Feedbacks. *Atmos. Chem. Phys.* **2013**, *13* (17), 8755−8770.

(44) Moreira, X.; Nell, C. S.; Katsanis, A.; Rasmann, S.; Mooney, K. A. Herbivore Specificity and the Chemical Basis of Plant-Plant Communication in *Baccharis Salicifolia* (Asteraceae). *New Phytol.* **2018**, *220* (3), 703−713.

(45) Mooney, K. A.; Pratt, R. T.; Singer, M. S. The Tri-Trophic Interactions Hypothesis: Interactive Effects of Host Plant Quality, Diet Breadth and Natural Enemies on Herbivores. *PLoS One* **2012**, *7* (4), e34403.

(46) Dixon, A. F. G. Aphid Ecology: An Optimization Approach, **1998**. London, UK: Chapman & Hall.

(47) Ortega, J.; Helmig, D. Approaches for Quantifying Reactive and Low-Volatility Biogenic Organic Compound Emissions by Vegetation Enclosure Techniques - Part A. *Chemosphere* **2008**, *72* (3), 343−364.

(48) Hallquist, M.; Wenger, J. C.; Baltensperger, U.; Rudich, Y.; Simpson, D.; Claeys, M.; Dommen, J.; Donahue, N. M.; George, C.; Goldstein, A. H.; Hamilton, J. F.; Herrmann, H.; Hoffmann, T.; Iinuma, Y.; Jang, M.; Jenkin, M. E.; Jimenez, J. L.; Kiendler-Scharr, A.; Maenhaut, W.; McFiggans, G.; Mentel, T. F.; Monod, A.; Prévôt, A. S. H.; Seinfeld, J. H.; Surratt, J. D.; Szmigielski, R.; Wildt, J. The Formation, Properties and Impact of Secondary Organic Aerosol: Current and Emerging Issues. *Atmos. Chem. Phys.* **2009**, *9* (14), 5155−5236.

(49) Jimenez, J. L.; Canagaratna, M. R.; Donahue, N. M.; Prevot, A. S. H.; Zhang, Q.; Kroll, J. H.; DeCarlo, P. F.; Allan, J. D.; Coe, H.; Ng, N. L.; Aiken, A. C.; Docherty, K. S.; Ulbrich, I. M.; Grieshop, A. P.; Robinson, A. L.; Duplissy, J.; Smith, J. D.; Wilson, K. R.; Lanz, V. A.; Hueglin, C.; Sun, Y. L.; Tian, J.; Laaksonen, A.; Raatikainen, T.; Rautiainen, J.; Vaattovaara, P.; Ehn, M.; Kulmala, M.; Tomlinson, J. M.; Collins, D. R.; Cubison, M. J.; E Dunlea, J.; Huffman, J. A.; Onasch, T. B.; Alfarra, M. R.; Williams, P. I.; Bower, K.; Kondo, Y.; Schneider, J.; Drewnick, F.; Borrmann, S.; Weimer, S.; Demerjian, K.; Salcedo, D.; Cottrell, L.; Griffin, R.; Takami, A.; Miyoshi, T.; Hatakeyama, S.; Shimono, A.; Sun, J. Y.; Zhang, Y. M.; Dzepina, K.; Kimmel, J. R.; Sueper, D.; Jayne, J. T.; Herndon, S. C.; Trimborn, A. M.; Williams, L. R.; Wood, E. C.; Middlebrook, A. M.; Kolb, C. E.; Baltensperger, U.; Worsnop, D. R. Evolution of Organic Aerosols in the Atmosphere. *Science* **2009**, *326* (5959), 1525−1529.

(50) Zhang, Q.; Jimenez, J. L.; Canagaratna, M. R.; Allan, J. D.; Coe, H.; Ulbrich, I.; Alfarra, M. R.; Takami, A.; Middlebrook, A. M.; Sun, Y. L.; Dzepina, K.; Dunlea, E.; Docherty, K.; DeCarlo, P. F.; Salcedo, D.; Onasch, T.; Jayne, J. T.; Miyoshi, T.; Shimono, A.; Hatakeyama, S.; Takegawa, N.; Kondo, Y.; Schneider, J.; Drewnick, F.; Borrmann, S.; Weimer, S.; Demerjian, K.; Williams, P.; Bower, K.; Bahreini, R.; Cottrell, L.; Griffin, R. J.; Rautiainen, J.; Sun, J. Y.; Zhang, Y. M.; Worsnop, D. R. Ubiquity and Dominance of Oxygenated Species in Organic Aerosols in Anthropogenically-Influenced Northern Hemisphere Midlatitudes. *Geophys. Res. Lett.* **2007**, *34* (13), L13801.

(51) Lambe, A. T.; Ahern, A. T.; Williams, L. R.; Slowik, J. G.; Wong, J. P. S.; Abbatt, J. P. D.; Brune, W. H.; Ng, N. L.; Wright, J. P.; Croasdale, D. R.; Worsnop, D. R.; Davidovits, P.; Onasch, T. B. Characterization of Aerosol Photooxidation Flow Reactors: Heterogeneous Oxidation, Secondary Organic Aerosol Formation and Cloud Condensation Nuclei Activity Measurements. *Atmos. Meas. Tech.* **2011**, *4* (3), 445−461.

(52) Peng, Z.; Jimenez, J. L. Radical Chemistry in Oxidation Flow Reactors for Atmospheric Chemistry Research. *Chem. Soc. Rev.* **2020**, *49* (9), 2570−2616.

(53) Fröhlich, R.; Cubison, M. J.; Slowik, J. G.; Bukowiecki, N.; Prévôt, A. S. H.; Baltensperger, U.; Schneider, J.; Kimmel, J. R.; Gonin, M.; Rohner, U.; Worsnop, D. R.; Jayne, J. T. The ToF-ACSM: A Portable Aerosol Chemical Speciation Monitor with TOFMS Detection. *Atmos. Meas. Tech.* **2013**, *6* (11), 3225−3241.

(54) Odum, J. R.; Hoffmann, T.; Bowman, F.; Collins, D.; Flagan, R. C.; Seinfeld, J. H. Gas/Particle Partitioning and Secondary Organic Aerosol Yields. *Environ. Sci. Technol.* **1996**, *30* (8), 2580−2585.

(55) Pankow, J. F. An Absorption Model of Gas/Particle Partitioning of Organic Compounds in the Atmosphere. *Atmos. Environ.* **1994**, *28* (2), 185−188.

(56) Griffin, R. J.; Cocker, D. R.; Flagan, R. C.; Seinfeld, J. H. Organic Aerosol Formation from the Oxidation of Biogenic Hydrocarbons. *J. Geophys. Res. Atmospheres* **1999**, *104* (D3), 3555−3567.

(57) Ahlberg, E.; Falk, J.; Eriksson, A.; Holst, T.; Brune, W. H.; Kristensson, A.; Roldin, P.; Svenningsson, B. Secondary Organic Aerosol from VOC Mixtures in an Oxidation Flow Reactor. *Atmos. Environ.* **2017**, *161*, 210−220.

(58) Lambe, A. T.; Chhabra, P. S.; Onasch, T. B.; Brune, W. H.; Hunter, J. F.; Kroll, J. H.; Cummings, M. J.; Brogan, J. F.; Parmar, Y.; Worsnop, D. R.; Kolb, C. E.; Davidovits, P. Effect of Oxidant Concentration, Exposure Time, and Seed Particles on Secondary Organic Aerosol Chemical Composition and Yield. *Atmos. Chem. Phys.* **2015**, *15* (6), 3063−3075.

(59) Faiola, C. L.; Buchholz, A.; Kari, E.; Yli-Pirilä, P.; Holopainen, J. K.; Kivimäenpää, M.; Miettinen, P.; Worsnop, D. R.; Lehtinen, K. E. J.; Guenther, A. B.; Virtanen, A. Terpene Composition Complexity Controls Secondary Organic Aerosol Yields from Scots Pine Volatile Emissions. *Sci. Rep.* **2018**, *8*, 3053.

(60) Mao, J.; Ren, X.; Brune, W. H.; Olson, J. R.; Crawford, J. H.; Fried, A.; Huey, L. G.; Cohen, R. C.; Heikes, B.; Singh, H. B.; Blake, D. R.; Sachse, G. W.; Diskin, G. S.; Hall, S. R.; Shetter, R. E. Airborne Measurement of OH Reactivity during INTEX-B. *Atmos. Chem. Phys.* **2009**, *9* (1), 163−173.

(61) Atkinson, R.; Arey, J. Atmospheric Degradation of Volatile Organic Compounds. *Chem. Rev.* **2003**, *103* (12), 4605−4638.

(62) Malloy, Q. G. J.; Nakao, S.; Qi, L.; Austin, R.; Stothers, C.; Hagino, H.; Cocker, D. R. Real-Time Aerosol Density Determination Utilizing a Modified Scanning Mobility Particle Sizer—Aerosol Particle Mass Analyzer System. *Aerosol Sci. Technol.* **2009**, *43* (7), 673−678.

(63) Nakao, S.; Tang, P.; Tang, X.; Clark, C. H.; Qi, L.; Seo, E.; Asa-Awuku, A.; Cocker, D. Density and Elemental Ratios of Secondary Organic Aerosol: Application of a Density Prediction Method. *Atmos. Environ.* **2013**, *68*, 273−277.

(64) t'Kindt, R.; De Veylder, L.; Storme, M.; Deforce, D.; Van Bocxlaer, J. LC-MS Metabolic Profiling of Arabidopsis Thaliana Plant Leaves and Cell Cultures: Optimization of Pre-LC-MS Procedure Parameters. *J. Chromatogr. B: Anal. Technol. Biomed. Life Sci.* **2008**, *871* (1), 37−43.

(65) Oksanen, J.; Blanchet, F. G.; Friendly, M.; Kindt, R.; Legendre, P.; McGlinn, D.; Minchin, P. R.; O'Hara, R. B.; Simpson, G. L.; Solymos, P.; Stevens, M. H. H.; Szoecs, E.; Wagner, H. *Vegan: Community Ecology Package*; **2019**, https://CRAN.R-project.org/package=vegan.

(66) Husson, F.; Josse, J.; Le, S.; Mazet, J. *FactoMineR: Multivariate Exploratory Data Analysis and Data Mining* **2020**, *25* (1), 1−18.

(67) Rai, V. K. Role of Amino Acids in Plant Responses to Stresses. *Biol. Plant.* **2002**, *45* (4), 481−487.

(68) Leitner, M.; Boland, W.; Mithöfer, A. Direct and Indirect Defences Induced by Piercing-Sucking and Chewing Herbivores in Medicago Truncatula. *New Phytol.* **2005**, *167* (2), 597−606.

(69) Faiola, C.; Taipale, D. Impact of Insect Herbivory on Plant Stress Volatile Emissions from Trees: A Synthesis of Quantitative Measurements and Recommendations for Future Research. *Atmospheric Environ. X* **2020**, *5*, 100060.

(70) Wasternack, C. Jasmonates: An Update on Biosynthesis, Signal Transduction and Action in Plant Stress Response, Growth and Development. *Ann. Bot.* **2007**, *100* (4), 681−697.

(71) Staudt, M.; Jackson, B.; El-Aouni, H.; Buatois, B.; Lacroze, J.-P.; Poëssel, J.-L.; Sauge, M.-H.; Niinemets, Ü. Volatile Organic Compound Emissions Induced by the Aphid Myzus Persicae Differ among Resistant and Susceptible Peach Cultivars and a Wild Relative. *Tree Physiol.* **2010**, *30* (10), 1320−1334.

(72) Staudt, M.; Lhoutellier, L. Volatile Organic Compound Emission from Holm Oak Infested by Gypsy Moth Larvae: Evidence for Distinct Responses in Damaged and Undamaged Leaves. *Tree Physiol.* **2007**, *27* (10), 1433−1440.

(73) Joó, É.; Van Langenhove, H.; Šimpraga, M.; Steppe, K.; Amelynck, C.; Schoon, N.; Müller, J.-F.; Dewulf, J. Variation in Biogenic Volatile Organic Compound Emission Pattern of Fagus Sylvatica L. Due to Aphid Infection. *Atmos. Environ.* **2010**, *44* (2), 227−234.

(74) Li, T.; Blande, J. D.; Gundel, P. E.; Helander, M.; Saikkonen, K. Epichloë Endophytes Alter Inducible Indirect Defences in Host Grasses. *PLoS One* **2014**, *9* (6), No. e101331.

(75) Guenther, A. B.; Jiang, X.; Heald, C. L.; Sakulyanontvittaya, T.; Duhl, T.; Emmons, L. K.; Wang, X. The Model of Emissions of Gases and Aerosols from Nature Version 2.1 (MEGAN2.1): An Extended and Updated Framework for Modeling Biogenic Emissions. *Geosci. Model Dev.* **2012**, *5* (6), 1471−1492.

(76) Hao, L. Q.; Romakkaniemi, S.; Yli-Pirilä, P.; Joutsensaari, J.; Kortelainen, A.; Kroll, J. H.; Miettinen, P.; Vaattovaara, P.; Tiitta, P.; Jaatinen, A.; Kajos, M. K.; Holopainen, J. K.; Heijari, J.; Rinne, J.; Kulmala, M.; Worsnop, D. R.; Smith, J. N.; Laaksonen, A. Mass Yields of Secondary Organic Aerosols from the Oxidation of α-Pinene and Real Plant Emissions. *Atmos. Chem. Phys.* **2011**, *11* (4), 1367−1378.

(77) Draper, D. C.; Farmer, D. K.; Desyaterik, Y.; Fry, J. L. A Qualitative Comparison of Secondary Organic Aerosol Yields and Composition from Ozonolysis of Monoterpenes at Varying Concentrations of NO_2. *Atmos. Chem. Phys.* **2015**, *15* (21), 12267−12281.

(78) Friedman, B.; Farmer, D. K. SOA and Gas Phase Organic Acid Yields from the Sequential Photooxidation of Seven Monoterpenes. *Atmos. Environ.* **2018**, *187*, 335−345.

(79) Ziemann, P. J. Effects of Molecular Structure on the Chemistry of Aerosol Formation from the OH-Radical-Initiated Oxidation of Alkanes and Alkenes. *Int. Rev. Phys. Chem.* **2011**, *30* (2), 161−195.

(80) Faiola, C. L.; Pullinen, I.; Buchholz, A.; Khalaj, F.; Ylisirniö, A.; Kari, E.; Miettinen, P.; Holopainen, J. K.; Kivimäenpää, M.; Schobesberger, S.; Yli-Juuti, T.; Virtanen, A. Secondary Organic Aerosol Formation from Healthy and Aphid-Stressed Scots Pine Emissions. *ACS Earth Space Chem.* **2019**, *3* (9), 1756−1772.

(81) Ylisirniö, A.; Buchholz, A.; Mohr, C.; Li, Z.; Barreira, L.; Lambe, A.; Faiola, C.; Kari, E.; Yli-Juuti, T.; Nizkorodov, S. A.; Worsnop, D. R.; Virtanen, A.; Schobesberger, S. Composition and Volatility of Secondary Organic Aerosol (SOA) Formed from Oxidation of Real Tree Emissions Compared to Simplified Volatile Organic Compound (VOC) Systems. *Atmos. Chem. Phys.* **2020**, *20* (9), 5629−5644.

(82) Yu, J.; Griffin, R. J.; Cocker, D. R.; Flagan, R. C.; Seinfeld, J. H.; Blanchard, P. Observation of Gaseous and Particulate Products of Monoterpene Oxidation in Forest Atmospheres. *Geophys. Res. Lett.* **1999**, *26* (8), 1145−1148.

SUPPLEMENTAL INFORMATION

Appendix 2. Supplementary information for chapter 2

Supplementary Information:

Acyclic Terpenes Reduce Secondary Organic Aerosol Formation from Emissions of a Riparian Shrub

Authors: Farzaneh Khalaj[1], Albert Rivas-Ubach[2] , Christopher R. Anderton[2], Swarup China[2], Kailen Mooney[1], and Celia L. Faiola[1,3]

[1]Department of Ecology and Evolutionary Biology, University of California Irvine, Irvine, CA, USA, 92697

[2]Environmental Molecular Science Laboratory, Pacific Northwest National Laboratory, Richland, WA, USA 99352

[3]Department of Chemistry, University of California Irvine, Irvine, CA, USA 92697

*corresponding author: cfaiola@uci.edu

1. Gas-Phase Biogenic Volatile Organic Compound (BVOC) Characterization: TD-GC-ToF-MS Operation and Compound Identification.

Samples were run through a thermo-desorption gas chromatograph mass spectrometer (TD: Markes International Series 2 Unity/Ultra, GC-MS: Agilent GC 7890B with flame ionization detector (FID), equipped with a 30 m, DB-5 column, and mass spectrometers BenchTOF-Select type) using the following method parameters: The Ultra is used to analyze samples which were collected on cartridges. Two internal standards, tetra methylethylene (TME) and cis- and trans- Decahydronaphthalene (DHN), automatically loaded onto the cartridge tubes immediately prior to analysis. The cartridges were heated to release compounds trapped on the absorbents. The sample injection was done with a ratio of 34.4:1 at 350°C, He flow at 15 mL min^{-1}. The oven starting at -30°C; 1 minute hold; then a ramp of 8.0°C min^{-1} up to 194°C (Ramp1), following with a ramp 16°C min^{-1} up to 210°C (Ramp 2), and finally a ramp of 25°C min^{-1} up to 260°C (Ramp3), and a 3 minute hold. Total runtime was 35 min per sample. The integrated FID response for each peak was in the unit of AU-s. Compounds were identified by mass spectrum and the NIST database (version 2.2) with >85% match was used. To quantify the compounds the FID response factor was

used for area peaks in all the runs. The FID response factor was equal to 4.802×10^{-6} in the unit of nanomoles of α-pinene/AU, which was calculated based on the average of the peak areas from the known amount of the introduced α-pinene. To get the compound mass in the unit of µg m^{-3} the calculated mass (µg) of each compound was divided by the volume of sampling, with a flow rate of 0.420 L min^{-1} for 4 to 6 minutes, in the unit of m^3.

2. *Foliar Metabolome Characterization: GC-MS and LC-MS Operation and Data processing.*

2.1. LC-MS

Liquid chromatography was performed at 30°C at a constant flow rate of 0.3 mL/min with a reversed-phase C18 Hypersil Gold column (150 × 2.1 mm, 3 µm particle size; Thermo Scientific, Waltham, Massachusetts, USA). Formic acid in water (A) and acetonitrile/0.1% formic acid in water (90:10) (B) and were used as mobile phases. The chromatographic gradient initiated at 90% A (10% B) and was maintained constant for 5 min before the gradient constantly changed to 10% A (90% B) until minute 20 of the chromatography. Those conditions were maintained for 2 min and the starting conditions (90% A; 10% B) were uniformly recovered over the subsequently 2 min. At the initial conditions, the column was stabilized for 11 minutes before the next sample was injected. All samples randomized and 5 µL of extract of each sample were analyzed in negative and positive ionization modes. The HRMS acquired data in mass range of 50-1000 mass to charge ratio (m/z) at a resolution of 60,000 and FTMS (Fourier Transform Mass Spectrometry) full-scan mode. The HRMS was calibrated to <1ppm error in each ionization mode before starting the sequences. Experimental blanks (methanol: water (80:20)) were analyzed every 8 samples for instrument background filtering purposes.

MZmine v.2.38[1], was used to process the RAW files obtained from the HRMS. Briefly, chromatograms were baseline corrected, MS1 masses were detected and ion chromatograms were generated and deconvoluted to generate individual peaks associated to specific m/z and retention time (RT) values. Chromatographic peaks were aligned and associated to specific compounds according to the exact mass and the RT of our in-home library which includes over 700 common metabolites of plant primary and secondary metabolism. Using m/z and RT for metabolite matching corresponds to a second level of identification.[2] High mass accuracy of Orbitrap technology and high reproducible RT decreases substantially false positive assignations. Peak

areas of all deconvoluted ion chromatograms were thus exported to CSV files. See Tables S1 and S2 for MZmine parameter details and metabolite assignation information, respectively.

2.2. GC-MS

For GC-MS analysis, metabolites were first derivatized to trimethylsilyl esters followed by derivatization of amine, carboxyl and hydroxyl groups. Briefly, extracts were first completely dried in a vacuum evaporator and 20 µL of methoxyamine in pyridine solution (30 mg/mL) was added into each sample followed by 90 min incubation at 37 °C in a Thermomixer (Eppendorf, Hamburg, Germany) operating at 1,200 rpm. After the first incubation period, 80 µL of MSTFA (N-Methyl-N-(trimethylsilyl) trifluoroacetamide) was added to each sample and subsequently incubated for 30 min at 37 °C and 1,200 rpm. After the second incubation, all samples were vortexed for 10 s and centrifuged at 12,000 × g for 1 min. Extracts were transferred into clean HPLC vials with 200 µL glass inserts using Pasteur pipettes. Derivatized extracts were analyzed using an MSD 5975C mass spectrometer coupled to an Agilent 7890C gas chromatographer (Agilent Technologies, Santa Clara, CA) equipped with a HP-5MS column (30 m × 0.25 mm × 0.25 μm; Agilent Technologies). The injector was set at 10 µL and split-less mode, and injection port was maintained at 250 °C. Prior injections, all samples were randomized. Chromatographic gradient started at 60 °C for 1 min constant before temperature raised to 325 °C until minute 26.5 (10 °C/min) and temperature was maintained for 10 min. A combination of fatty acid methyl esters (FAMEs) ranging from chains from 8 to 28 C was analyzed at the beginning of the sequence and were used for retention indices (RIs) calculation of detected peaks. Experimental blanks (derivatized methanol: water (80:20)) were run every 8 samples along the sequence and were used for instrument background filtering purposes. Metabolite Detector 2.5[3] as used to process GC-MS files. First, ".D" files were converted to ".CDF" in Agilent Chemstation that were read and converted to ".bin" files in Metabolite Detector. Metabolite identification in Metabolite Detector was performed using an updated version of FiehnLib[44] containing over 850 metabolites with corroborated spectra and RIs. For that, the calculation of RIs of all detected features was first performed in Metabolite Detector using the FAMEs mixture and chromatograms were then aligned and deconvoluted. All assigned metabolites were manually verified by spectra matching with NIST14 library. See Tables S3 and S4 for Metabolite Detector parameter details and metabolite assignation information, respectively.

2.3. Foliar Metabolomics Dataset Filtering

LC-MS and GC-MS datasets were independently filtered before being merged into a single dataset. For that, five main steps were performed. (1) Number of samples threshold: Variables (metabolomic features) not present in at least 80% of the control or aphid samples were removed from the dataset. (2) Outlier value replacement: Outlier values for specific samples and features represent detected data but its values are far away from the rest of biological replicates of the same group (control or aphid plants). In this study, outlier values for a specific sample and feature were replaced by a random number calculated using the mean and standard deviation of the sample group (control or treated plants). Outlier values were detected as follows:

$$Upper\ outliers \rightarrow value > Q75 + 2 \times IQR$$
$$Lower\ outliers \rightarrow value < Q25 - 2 \times IQR$$

where Q75 and Q25 represent, respectively, the 75th and 25th percentiles, and IQR is the interquartile range (IQR = Q75-Q25). (3) Blank signal threshold: Values of features detected in experimental blanks were kept only if they were present in at least 40% of blanks, otherwise, all values were considered zero for those specific features. (4) Instrument background threshold: Mean values were calculated for each individual feature for the groups of blanks, control and aphid trials. Those features having a ratio Control/Blank and/or Aphid/Blank lower than 25 were removed from the dataset. (5) Zero Filter: When the number of samples with data (value >0) in controls or treated plants was lower than 40% of the biological replicates, all values were converted to zeros. Finally, LC-MS and GC-MS datasets were merged into a single dataset. Identified features with both techniques corresponding to the same metabolite ID were merged into a single variable.

3. Statistical Analysis Results:

The permutational multivariate analysis of variance (PERMANOVA) was used to evaluate the overall metabolome and BVOC differences between control and aphid experimental trials, and Table S5 and Table S6 show the summary results for metabolome and BVOC, respectively. Individual identified metabolites were also submitted to Student t-test to assess for statistical significance between control and aphid trials, and the summary result is presented in the Table S7.

In general, the aphid herbivory changed the overall foliar metabolome ($P < 0.05$; Table S5), and from the 218 identified metabolites, 119 changed significantly between the treatment groups (Table S7). However, there was not a significant difference between the BVOC profile of control and aphid plants ($P>0.05$) (Table S6).

4. *Plant Volatile Compounds Distribution Profile*

Detailed BVOC profile for each individual trial are shown in Figure S1. Overall, the plant BVOC profiles were dominated by limonene. The part b of Figure S1 represents the subset of the plant BVOC profiles to show the sesquiterpene distribution for each trial. The sesquiterpenes profile for each trial was very variable between all the experimental trials. OH exposure can also influence SOA mass yield and is difficult to control in the flow reactor with precision. To test whether or not there was a confounding relationship between the relative proportion of cyclic terpenes and the OH exposure, we plotted the two variables against each other (Figure S2). There was only a very weak correlation between the two, so we do not believe changes in OH exposure could explain the relationship we observed between relative proportion of cyclic vs acyclic terpenes and SOA formation potential.

Table S8 shows correlation between the slope of the SOA mass yield curve and the relative contribution of individual VOCs. The lowest r^2 values were corresponded to the most of the sesquiterpenes, except the aristolochene with r^2 value of 0.26. Among all the monoterpenes, 3-carene had the highest linear r^2 value, which was 0.50.

5. *Tables:*

Table S1. *MZmine parameters applied to LC-MS chromatograms to obtain the datasets of Baccharis plant samples for both positive and negative ionization modes.*

1	**Baseline correction – RollingBall baseline corrector**	
	Chromatogram type	TIC
	Use m/z bins	No
	wm	25
	ws	25
2	**Mass detection** (exact Mass)	
	Noise level	1×10^3
3	FTMS shoulder peak filter	
	Mass resolution	60,000
	Peak model function	Lorentzian
4	**Chromatogram builder**	
	Minimum time span	0.04
	Min highest intensity	1×10^3
	m/z tolerance	0.0005 Da or 7ppm
5	**Smoothing**	
	Filter width	5
6	**Chromatogram deconvolution (local minimum search)**	
	Chromatographic threshold	40%
	Search minimum in RT range (min)	0.3
	Minimum relative height	30%
	Minimum absolute height	1×10^3
	Minimum ratio of peak top/edge	2
	Peak duration range	0-0.5 min
7	**Retention Time Normalizer**	
	m/z tolerance	0.0005 Da or 7ppm
	RT tolerance	0.25
	Min Standard intensity	1×10^5
8	**Chromatogram alignment (join alignment)**	
	m/z tolerance	0.0005 Da or 7ppm
	Weight for m/z	65
	RT tolerance	0.3
	Weight for RT	35
9	**Gap filling (Peak Finder)**	
	Intensity tolerance	50%
	m/z tolerance	0.0005 Da or 6ppm
	Retention time tolerance	0.25
	RT correction	Yes
10	**Filtering (Duplicate Peak Filter)**	
	Filter mode	New Average
	m/z Tolerance	0.0005 m/z or 6ppm
	RT Tolerance	0.4 min
11	**Metabolite Assignation**	
	m/z tolerance	0.001 Da or 15ppm*
	RT tolerance	0.5*

* Metabolite IDs posteriorly filtered (see table S2).

Table S2. Retention time (RT) and mass to charge ratio (m/z) of the deconvoluted ion chromatograms analyzed in both positive and negative ionization modes assigned to metabolites with the LC-MS data. RT and m/z of the standards are shown in the table. RT and m/z matching error of assigned features are shown. Due deconvolution algorithms, several ion chromatograms may have been deconvoluted into two or more independent peaks slightly different retention times which may result in separate peaks with the same identity. This table shows all peaks assigned to a molecular compound based on the exact mass of their precursor ion (in negative and positive mode) and retention time. Therefore, some independent peaks may have the same identity. For statistical purposes and as explained in the main manuscript, all identified metabolic features assigned to a same metabolite were combined into a single variable. Only "good matches" were considered as reliable metabolite identifications and "non-good-matches" were kept as unassigned features. The diverse criteria for determining whether a match was good enough as to keep the putative identification are described at the bottom of the table.

NEGATIVE IONIZATION MODE								
		Standard parent ion		Measured in samples (calibrated)		m/z Error After Calibration		RT Error After Calibration
	KEGG ID	m/z	RT	m/z	RT	Dalton	PPM	min	Good Match?
(S)-dihydroorotate	C00337	157.0255	1.57	157.0274	1.34	0.001945	12.38	-0.23	NO
1- kestose	G00339	503.1617	1.29	503.1575	1.29	-0.0042	-8.34	0.00	NO
1-aminocyclopropane-1-carboxylate	C01234	100.0404	1.29	100.0406	1.71	0.000173	1.73	0.42	NO
1-methyladenine	C02216	148.0628	1.3	148.0615	1.31	-0.00134	-9.05	0.01	NO
2,3-dihydroxybenzoate	C00196	153.0193	7.49	153.0194	7.55	3.36E-05	0.22	0.06	YES
2,4-dihydroxypyrimidine-5-carboxylic acid	C03030	155.0098	1.38	155.0116	1.36	0.001788	11.53	-0.02	NO
2,5-dihydroxybenzoate	C00628	153.0193	5.4	153.0193	5.58	-1.3E-05	-0.08	0.18	YES
2,6-dihydroxypyridine	C03056	110.0247	1.41	110.0251	1.70	0.000321	2.92	0.29	NO
2-deoxy-d ribose	C01801	133.0506	1.4	133.0507	1.58	6.86E-05	0.52	0.18	YES
2-deoxy-d-glucose	C00586	163.0612	1.35	163.0612	1.38	9.95E-06	0.06	0.03	YES
2-hydroxyphenylacetic acid	C05852	151.0401	8.82	151.0399	8.99	-0.00015	-1.00	0.17	YES
2-oxoadipate	C00322	159.0299	1.88	159.0299	1.51	4.16E-05	0.26	-0.37	NO
2-oxovaleric acid	C06255	115.04	3.47	115.0402	3.71	0.000185	1.61	0.24	YES
3-(2-hydroxyphenyl)propanoate	C01198	165.0557	10.74	165.0553	10.48	-0.00038	-2.32	-0.26	YES
3,4-Dihydroxybenzoic acid	C00230	153.0193	3.01	153.0194	2.93	0.000128	0.84	-0.08	YES
3,4-dihydroxy-l-phenylalanine	C00355	196.0615	1.36	196.0575	1.22	-0.00407	-20.76	-0.14	NO
3,4-dihydroxyphenyl glycol	C05576	169.0506	1.45	169.0508	1.78	0.000195	1.16	0.33	NO
3-dehydroshikimate	C02637	171.0299	1.45	171.0299	1.36	2.64E-06	0.02	-0.09	YES
3-hydroxy-3-methylglutarate	C03761	161.0456	1.85	161.0456	1.70	8.14E-05	0.51	-0.15	YES
3-hydroxybenzoate	C00587	137.0244	7.45	137.0245	7.55	3.91E-05	0.29	0.10	YES
3-Hydroxycinnamic acid		163.04	9.39	163.0399	9.36	-0.00015	-0.90	-0.03	YES
3-hydroxyphenylacetate	C05593	151.0401	7.74	151.0401	7.55	-1.4E-05	-0.09	-0.19	YES
3-methoxy-4-hydroxymandelate	C05584	197.0456	2.3	197.0489	2.45	0.003352	17.01	0.15	NO
4-acetamidobutanoate	C02946	144.0666	1.38	144.0668	1.74	0.000215	1.49	0.36	NO
4-aminobutanoate	C00334	102.0561	1.25	102.0562	1.33	0.000129	1.26	0.08	YES
4-hydroxy-2-quinolinecarboxylic acid	C01717	188.0353	4.49	188.0352	4.23	-7.2E-05	-0.38	-0.26	YES
4-hydroxybenzoate	C00156	137.0244	5.21	137.0244	5.58	2.1E-05	0.15	0.37	NO
4-Hydroxybenzoic acid	C00156	137.0244	5	137.0244	4.72	1.95E-05	0.14	-0.28	YES
5,6-dihydrouracil	C00429	113.0357	1.36	113.0357	1.31	7.23E-05	0.64	-0.05	YES
5-aminolevulinic acid	C00430	130.051	1.26	130.0512	1.63	0.000231	1.77	0.37	NO
5-hydroxy-l-tryptophan	C01017	219.0775	1.4	219.0776	1.84	0.000113	0.52	0.44	NO
5-oxo-l-proline	C01879	128.0353	1.37	128.0355	1.45	0.000178	1.39	0.08	YES
Abscisic acid	C06082	263.1289	12.66	263.1282	12.25	-0.00072	-2.75	-0.41	YES
Abscisic acid	C06082	263.1289	12.66	263.1283	12.93	-0.00067	-2.54	0.27	YES
Acacetin	C01470	283.0612	15.62	283.0605	15.62	-0.00074	-2.61	0.00	YES
Adenine	C00147	134.0472	1.35	134.0473	1.34	3.25E-05	0.24	-0.01	YES
Adipic acid	C06104	145.0506	3.26	145.0508	3.61	0.00014	0.96	0.35	NO
Allantoin	C01551	157.0367	1.36	157.0366	1.36	-6.3E-05	-0.40	0.00	YES
Alpha-d-glucose 1-phosphate	C00103	259.0224	1.54	259.022	1.36	-0.00041	-1.57	-0.18	YES
Alpha-hydroxybutyric acid	C01188	103.0401	1.95	103.0402	1.64	0.000166	1.61	-0.31	NO
Alpha-ketoglutaric acid	C00026	145.0143	1.79	145.0143	1.46	6.76E-05	0.47	-0.33	NO
Ascorbate	C00072	175.0248	1.36	175.0248	1.38	-5.3E-05	-0.30	0.02	YES
Aspartate	C00049	132.0302	1.41	132.0304	1.32	0.000155	1.17	-0.09	YES
Astilbin	C17449	449.1089	10.3	449.1071	9.92	-0.00181	-4.02	-0.38	NO
Azelaic acid	C08261	187.0976	11.3	187.0973	11.20	-0.0003	-1.62	-0.10	YES

Beta-alanine	C00099	88.0404	1.28	88.04056	1.32	0.000157	1.78	0.04	**YES**
Betaine	C00719	116.0717	1.34	116.0718	1.40	6.96E-05	0.60	0.06	**YES**
Biliverdin	C00500	581.2406	14.84	581.2385	14.96	-0.00203	-3.50	0.12	**YES**
Catechin	C06562	289.0717	1.49	289.0688	1.35	-0.0029	-10.03	-0.14	**NO**
Catechol	C00090	109.0295	3.08	109.0297	2.93	0.000214	1.96	-0.15	**YES**
Chlorogenic acid	C00852	353.0878	5.94	353.087	5.57	-0.00085	-2.39	-0.37	**NO**
Chlorogenic acid	C00852	353.0878	5.94	353.0877	6.11	-7.7E-05	-0.22	0.17	**YES**
Chlorogenic acid	C00852	353.0878	5	353.0868	4.82	-0.00098	-2.78	-0.18	**YES**
Chrysin	C10028	253.0506	15.56	253.0505	15.62	-0.00018	-0.70	0.06	**YES**
Cinnamaldehyde	C00903	131.0502	13.43	131.0502	13.58	2.3E-05	0.18	0.15	**YES**
Citrate	C00158	191.0197	1.48	191.0198	1.67	0.000103	0.54	0.19	**YES**
Cytidine	C00475	242.0783	1.29	242.0785	1.52	0.000276	1.14	0.23	**YES**
Dehydroascorbate	C05422	173.0092	1.51	173.0093	1.57	9.23E-05	0.53	0.06	**YES**
Deoxyuridine	C00526	227.0673	1.37	227.0655	1.30	-0.00187	-8.24	-0.07	**NO**
D-gulonic acid gama-lactone	C01040	177.0405	1.36	177.0404	1.42	-2.6E-05	-0.14	0.06	**YES**
Dihydroxymandelic acid	C05580	183.0299	1.45	183.0276	1.79	-0.00232	-12.65	0.34	**NO**
D-ornithine	C00515	131.0826	1.24	131.0825	1.28	-6.9E-05	-0.52	0.04	**YES**
D-pinitol	C03844	193.0717	1.31	193.0714	1.38	-0.00029	-1.49	0.07	**YES**
D-ribose 5-phosphate	C00117	229.0119	1.48	229.0115	1.34	-0.00042	-1.84	-0.14	**YES**
D-saccharic acid	C00818	209.0303	1.51	209.0301	1.35	-0.00022	-1.04	-0.16	**YES**
D-sorbitol	C00749	181.0717	1.31	181.0716	1.31	-7.4E-05	-0.41	0.00	**YES**
D-xylose	C01394	149.0456	1.32	149.0456	1.39	8.48E-05	0.57	0.07	**YES**
Emodin	C10343	269.0455	17.41	269.045	17.58	-0.00053	-1.98	0.17	**YES**
Emodin	C10343	269.0455	18.36	269.0449	18.65	-0.00062	-2.29	0.29	**YES**
Epigallocatechin	C12136	305.0667	1.46	305.0638	1.33	-0.00295	-9.66	-0.13	**NO**
Ethylmalonic acid	CA1366	131.035	3.08	131.0352	2.72	0.000239	1.83	-0.36	**NO**
Fumaric acid	C00122	115.0037	1.79	115.0039	1.42	0.000183	1.59	-0.37	**NO**
Galacturonic acid	C00333	193.0354	1.34	193.0351	1.35	-0.00031	-1.62	0.01	**YES**
Galangin	C10044	269.0455	15.88	269.0448	15.93	-0.00076	-2.81	0.05	**YES**
Galangin	C10044	269.0455	15.88	269.0404	15.61	-0.00509	-18.93	-0.27	**NO**
Gluconic acid	C00257	195.051	1.52	195.0507	1.34	-0.00028	-1.41	-0.18	**YES**
Glucosaminate	C03752	194.067	1.32	194.0632	1.35	-0.0038	-19.61	0.03	**NO**
Glutamic acid	C00025	146.0459	1.29	146.046	1.32	5.78E-05	0.40	0.03	**YES**
Glutarate	C00489	131.035	1.78	131.0352	1.48	0.000182	1.39	-0.30	**NO**
Glutarate	C00489	131.035	1.78	131.0353	2.15	0.000293	2.24	0.37	**NO**
Gluthathione reduced	C00051	306.0765	1.35	306.0761	1.56	-0.00039	-1.28	0.21	**YES**
Glyceraldehyde	C02154	89.02442	1.39	89.02464	1.41	0.000218	2.45	0.02	**YES**
Glycerate	C00258	105.0193	1.58	105.0195	1.38	0.00016	1.53	-0.20	**YES**
Glycine	C00037	74.02475	1.31	74.02491	1.30	0.000158	2.14	-0.01	**YES**
Glycolate	C00160	75.00877	1.75	75.009	1.41	0.000231	3.08	-0.34	**NO**
Glyoxilic acid	C00048	72.99312	1.45	72.99332	1.39	0.000202	2.77	-0.06	**YES**
Guanine	C00242	150.0421	1.33	150.0422	1.36	6.1E-05	0.41	0.03	**YES**
Guanosine 5'-monophosphate	C00144	362.0507	1.53	362.0517	1.36	0.000994	2.75	-0.17	**YES**
Hesperetin	C01709	301.0717	13.51	301.0709	13.08	-0.00082	-2.73	-0.43	**YES**
Hesperetin	C01709	301.0717	13.51	301.0708	13.61	-0.00089	-2.96	0.10	**YES**
Hippurate	C01586	178.051	6	178.0509	5.54	-8.4E-05	-0.47	-0.46	**NO**
Homogentisate	C00544	167.035	2.51	167.0353	2.11	0.000312	1.87	-0.40	**NO**
Homogentisate	C00544	167.035	2.51	167.0351	2.80	0.000157	0.94	0.29	**YES**
Hydroxypyruvate	C00168	103.0037	1.58	103.0039	1.50	0.000208	2.02	-0.08	**YES**
Hypoxanthine	C00262	135.0312	1.4	135.0299	1.36	-0.0013	-9.63	-0.04	**NO**
Inosine	C00294	267.0735	1.41	267.0716	1.34	-0.0019	-7.12	-0.07	**NO**
Isorhamnetin	C10084	315.051	13.65	315.0501	13.60	-0.00094	-2.97	-0.05	**YES**
Jasmonic acid	C08491	209.1183	13.47	209.1181	13.48	-0.00026	-1.25	0.01	**YES**
Kaempferol	C05903	285.0404	13.49	285.0396	13.49	-0.0008	-2.80	0.00	**YES**
Kaempferol	C05903	285.0404	13.49	285.0361	13.48	-0.00428	-15.00	-0.01	**NO**
L-arginine	C00062	173.1044	1.25	173.1042	1.27	-0.00016	-0.94	0.02	**YES**
L-asparagine	C00152	131.0462	1.31	131.0464	1.31	0.000154	1.17	0.00	**YES**
Leucine	C16439	130.0874	1.37	130.0876	1.67	0.000203	1.56	0.30	**NO**
L-glutamine	C00064	145.0619	1.32	145.0619	1.31	6.06E-05	0.42	-0.01	**YES**
L-histidine	C00135	154.0622	1.26	154.0622	1.28	-3E-05	-0.20	0.02	**YES**
Ll-2,6-diaminoheptanedioate	C00666	189.0881	1.31	189.0879	1.33	-0.0018	-0.96	0.02	**YES**
L-phenylalanine	C00079	164.0717	1.36	164.0717	1.33	-1.3E-05	-0.08	-0.03	**YES**
L-phenylalanine	C00079	164.0717	2.19	164.0719	2.26	0.000244	1.49	0.07	**YES**
L-pipecolic acid	C00408	128.0717	1.35	128.0718	1.40	0.000116	0.90	0.05	**YES**
L-proline	C00148	114.0561	1.35	114.0561	1.41	7.05E-05	0.62	0.06	**YES**
L-serine	C00065	104.0353	1.29	104.0354	1.30	0.000128	1.23	0.01	**YES**
L-sorbose	C01452	179.0561	1.29	179.0562	1.37	4.4E-05	0.25	0.08	**YES**
L-threonine	C00188	118.051	1.31	118.0511	1.31	0.000104	0.88	0.00	**YES**
L-tyrosine	C00082	180.0666	1.37	180.0667	1.72	0.000112	0.62	0.35	**NO**
Lumazine	C03212	163.0257	1.36	163.0249	1.40	-0.00085	-5.21	0.04	**YES**
Malic acid	C00149	133.0143	1.41	133.0144	1.40	0.000172	1.29	-0.01	**YES**
Mandelic acid	C01984	151.0401	5.35	151.0401	5.56	-1E-05	-0.07	0.21	**YES**
Mangiferin	C10077	421.0776	1.37	421.0717	1.35	-0.00589	-14.00	-0.02	**NO**
Mangiferin	C10077	421.0776	1.37	421.0775	1.35	-0.00015	-0.36	-0.02	**YES**
Melibiose	C05402	341.1089	1.24	341.1079	1.41	-0.00106	-3.10	0.17	**YES**

	KEGG ID	m/z	RT	m/z	RT	Dalton	PPM	min	Good Match?
Methyleugenol	C10454	177.0921	16.1	177.0922	16.20	4.78E-05	0.27	0.10	YES
N-acetyl-d-glucosamine	C00140	220.0827	1.35	220.0822	1.37	-0.00042	-1.90	0.02	YES
N-acetyl-dl-glutamic acid	C00624	188.0564	1.39	188.0565	1.41	0.000103	0.55	0.02	YES
N-acetyl-d-tryptophan	C03137	245.0932	10.29	245.0922	10.32	-0.00095	-3.88	0.03	YES
N-acetylglycine	CA1212	116.0353	1.55	116.0354	1.39	0.000125	1.08	-0.16	YES
N-acetyl-l-aspartic acid	C01042	174.0408	1.57	174.0408	1.39	-7.7E-07	0.00	-0.18	YES
N-acetyl-l-leucine	C02710	172.0979	9.01	172.0977	9.04	-0.00024	-1.42	0.03	YES
N-acetyl-l-phenylalanine	C03519	206.0823	9.98	206.0818	9.54	-0.00048	-2.35	-0.44	NO
N-acetylneuraminate	C00270	308.0987	1.53	308.0971	1.27	-0.00155	-5.04	-0.26	NO
N-alpha-acetyl-l-asparagine	CA1214	173.0568	1.54	173.0567	1.43	-0.00012	-0.68	-0.11	YES
N-amidino-l-aspartate	C03139	174.052	1.34	174.0488	1.40	-0.00318	-18.29	0.06	NO
Naringenin	C00509	271.0612	13.31	271.0606	13.59	-0.0006	-2.22	0.28	YES
N-formylglycine	CA1268	102.0197	1.41	102.0198	1.43	0.000115	1.13	0.02	YES
Nicotinate	C00253	122.0248	1.55	122.0249	1.36	0.000122	1.00	-0.19	YES
N-methyl-l-glutamate	C01046	160.0615	1.34	160.0616	1.52	2.27E-05	0.14	0.18	YES
Omega-hydroxydodecanoic acid	C08317	215.1653	14.78	215.165	14.84	-0.00026	-1.20	0.06	YES
Ophthalmic acid	C21016	288.1201	1.38	288.1203	1.38	0.000228	0.79	0.00	YES
O-succinyl-l-homoserine	C01118	218.067	1.36	218.0667	1.39	-0.00033	-1.51	0.03	YES
Oxalic acid	C00209	88.98803	1.36	88.98821	1.24	0.000185	2.08	-0.12	YES
Oxalic acid	C00209	88.98803	1.36	88.98835	1.70	0.000317	3.56	0.34	NO
Oxaloacetic acid	C00036	130.9986	1.43	130.9989	1.41	0.000256	1.96	-0.02	YES
Phenylpyruvic acid	C00166	163.0401	13.36	163.0398	13.10	-0.00024	-1.49	-0.26	YES
Pterin	CA1303	162.0421	1.4	162.0407	1.40	-0.00141	-8.69	0.00	NO
Purine	C00465	119.0363	1.38	119.0351	1.34	-0.00123	-10.37	-0.04	NO
Pyruvic acid	C00022	87.00877	1.51	87.00901	1.49	0.000238	2.73	-0.02	YES
Pyruvic aldehyde	C00546	71.01385	1.38	71.01408	1.40	0.000229	3.22	0.02	YES
Quercitin	C00389	301.0354	12.41	301.0345	12.36	-0.00089	-2.97	-0.05	YES
Quercitin	C00389	301.0354	12.41	301.0309	12.76	-0.00453	-15.04	0.35	NO
Quinate	C00296	191.0561	1.57	191.056	1.38	-0.00014	-0.76	-0.19	YES
Resorcinol monoacetate	C12064	151.0401	10.87	151.0398	10.59	-0.00024	-1.61	-0.28	YES
Resorcinol monoacetate	C12064	151.0401	10.87	151.0399	11.27	-0.00014	-0.95	0.40	YES
Rhamnetin	C10176	315.051	14.66	315.0496	14.73	-0.00138	-4.38	0.07	YES
Rhapontin	C10288	419.1347	10.64	419.1335	10.78	-0.00125	-2.97	0.14	YES
Rhein	C10401	283.0248	15.44	283.025	15.19	0.000133	0.47	-0.25	YES
Ribitol	C00474	151.0612	1.31	151.0612	1.36	3.58E-05	0.24	0.05	YES
Riboflavin	C00255	375.131	8.29	375.1299	8.03	-0.00106	-2.84	-0.26	YES
Rs-mevalonic acid lithium salt	C00418	147.0663	1.78	147.0664	1.76	6.97E-05	0.47	-0.02	YES
S-(5'-adenosyl)-l-homocysteine	C00021	383.1143	1.34	383.1172	1.36	0.002878	7.51	0.02	NO
S-(5'-adenosyl)-l-homocysteine	C00021	383.1143	1.34	383.1204	1.36	0.006088	15.89	0.02	NO
Salicylate	C00805	137.0244	11.39	137.0243	11.16	-0.00015	-1.10	-0.23	YES
Salicylate	C00805	137.0244	11.39	137.0243	11.61	-0.00012	-0.88	0.22	YES
Secologanin	C01852	387.1296	9.36	387.1285	9.36	-0.00109	-2.82	0.00	YES
Shikimic acid	C00493	173.0456	1.38	173.0456	1.39	2.86E-05	0.17	0.01	YES
Sinapic acid	C00482	223.0612	10	223.0638	9.73	0.00257	11.52	-0.27	NO
Sn-glycerol 3-phosphate	C00093	171.0064	1.55	171.0063	1.33	-8.2E-05	-0.48	-0.22	YES
Sorbate	CA1411	111.0452	11.02	111.045	10.90	-0.00011	-0.96	-0.12	YES
Suberic acid	C08278	173.0819	9.84	173.0816	9.75	-0.00033	-1.92	-0.09	YES
Succinate semialdehyde	C00232	101.0244	1.79	101.0246	1.38	0.00015	1.49	-0.41	NO
Succinate	C00042	117.0193	1.41	117.0195	1.77	0.000204	1.74	0.36	NO
Syringaldehyde		181.0507	9.42	181.0535	9.82	0.002737	15.12	0.40	NO
Taxifolin	C01617	303.051	10.13	303.0499	10.45	-0.00116	-3.84	0.32	YES
Tryptophan	C00078	203.0826	3.5	203.0826	3.65	-1.3E-05	-0.06	0.15	YES
Uracil	C00106	111.02	1.37	111.0201	1.35	0.000126	1.14	-0.02	YES
Urate	C00366	167.0211	1.39	167.0227	1.33	0.00159	9.52	-0.06	NO
Uridine 5'-diphosphoglucose	C00029	565.0478	1.68	565.0424	1.41	-0.00531	-9.40	-0.27	NO
Uridine 5'-diphosphoglucose	C00029	565.0478	1.68	565.051	1.46	0.003252	5.76	-0.22	YES
Uridine	C00299	243.0623	1.37	243.0621	1.65	-0.00015	-0.61	0.28	NO
Urocanate	C00785	137.0357	1.33	137.0342	1.35	-0.00144	-10.48	0.02	NO
Urocanate	C00785	137.0357	1.33	137.0352	1.34	-0.00047	-3.46	0.01	YES
Vitexin	C01460	431.0983	9.85	431.0967	9.83	-0.0016	-3.72	-0.02	YES
Xanthine	C00385	151.0262	1.36	151.0261	1.71	-6.9E-05	-0.46	0.35	NO
Xanthosine 5'-monophosphate	C00655	363.0347	1.72	363.0304	1.41	-0.00435	-11.99	-0.31	NO
Xanthosine 5'-monophosphate	C00655	363.0347	1.72	363.0352	1.40	0.000474	1.31	-0.32	NO
Zeatin	C00371	218.1047	2.06	218.1035	2.28	-0.00118	-5.40	0.22	YES

POSITIVE IONIZATION MODE

		Standard parent ion		Measured in samples (calibrated)		m/z Error After Calibration		RT Error After Calibration	
	KEGG ID	m/z	RT	m/z	RT	Dalton	PPM	min	Good Match?
(S)-dihydroorotate	C00337	159.04	1.57	159.0434	1.19	0.003331	20.95	-0.26	NO
1-aminocyclopropane-1-carboxylate	C01234	102.055	1.29	102.0549	1.28	-8E-05	-0.79	0.09	YES
1-methyladenine	C02216	150.0774	1.3	150.0773	1.39	-0.00012	-0.77	0.20	YES
1-methyladenosine	C02494	282.1197	1.37	282.1207	1.62	0.001033	3.66	0.36	NO
2,1-hydroxypregnenolone	C05485	333.2424	15.63	333.2431	15.83	0.000708	2.13	0.25	YES

9

2-aminophenol	C01987	110.06	1.39	110.06	1.32	-2.4E-05	-0.22	0.04	**YES**
2-deoxy-d-glucose	C00586	165.0758	1.35	165.0773	1.19	0.001502	9.10	-0.05	**NO**
2-hydroxyphenylacetic acid	C05852	153.0546	8.82	153.0545	8.89	-7.9E-05	-0.52	0.15	**YES**
2-hydroxyphenylacetic acid	C05852	153.0546	8.82	153.0546	8.31	-4.9E-05	-0.32	-0.43	**NO**
2-methylmaleate	C02226	131.0339	2.06	131.034	1.62	6.12E-05	0.47	-0.33	**NO**
3-(2-hydroxyphenyl)propanoate	C01198	167.0703	10.74	167.0701	10.73	-0.00018	-1.08	0.06	**YES**
3,4-Dihydroxybenzoic acid	C00230	155.0339	3.01	155.0339	3.22	2.98E-05	0.19	0.31	**NO**
3-amino-4-hydroxybenzoic acid	C12115	154.0499	1.39	154.0499	1.65	-1.7E-05	-0.11	0.37	**NO**
3-Hydroxycinnamic acid		165.0546	9.39	165.0545	9.44	-6.7E-05	-0.41	0.13	**YES**
3-methoxytyramine	C05587	168.1019	1.78	168.1019	1.73	1.41E-05	0.08	0.06	**YES**
3-methyl-2-oxindole	CA1325	148.0757	11.21	148.0756	10.89	-8.6E-05	-0.58	-0.25	**YES**
4-acetamidobutanoate	C02946	146.0812	1.38	146.0811	1.54	-4.9E-05	-0.33	0.27	**NO**
4-aminobutanoate	C00334	104.0706	1.25	104.0705	1.25	-7.2E-05	-0.69	0.10	**YES**
4-guanidinobutanoate	C01035	146.0924	1.32	146.0922	1.28	-0.00022	-1.49	0.07	**YES**
4-hydroxy-2-quinolinecarboxylic acid	C01717	190.0499	4.49	190.0499	4.20	7.42E-05	0.39	-0.19	**YES**
4'-hydroxyacetophenone	C10700	137.0597	8.94	137.0596	9.13	-5.9E-05	-0.43	0.26	**YES**
4-hydroxy-l-phenylglycine	CA1445	168.0655	1.35	168.0654	1.37	-0.0001	-0.62	0.13	**YES**
4-hydroxy-l-proline	C01157	132.0655	1.33	132.0656	1.63	5.56E-05	0.42	0.41	**NO**
4-imidazoleacetic acid	C02835	127.0502	1.32	127.0499	1.22	-0.00028	-2.18	0.01	**YES**
4-imidazoleacetic acid	C02835	127.0502	1.32	127.0502	1.63	-2.2E-05	-0.17	0.42	**NO**
5,6-dihydrouracil	C00429	115.0502	1.36	115.0503	1.50	0.000103	0.89	0.24	**YES**
5-aminopentanoate	C00431	118.0863	1.28	118.0862	1.21	-9E-05	-0.77	0.04	**YES**
5-hydroxy-l-tryptophan	C01017	221.0921	1.4	221.0923	1.70	0.00019	0.86	0.40	**NO**
5-hydroxy-l-tryptophan	C01017	221.0921	1.4	221.0921	1.29	2.22E-05	0.10	0.00	**YES**
5-methylcytosine hydrocloride	C02376	126.0662	1.28	126.0659	1.23	-0.00025	-1.98	0.06	**YES**
5'-methylthioadenosine	C00170	298.0968	2.86	298.0972	2.77	0.000371	1.24	0.01	**YES**
6-benzylaminopurine	C11263	226.1087	8.92	226.1075	8.75	-0.00118	-5.23	-0.10	**YES**
6-Phosphogluconic acid	C00345	277.0319	1.55	277.0328	1.27	0.000919	3.32	-0.17	**YES**
6-Phosphogluconic acid	C00345	277.0319	1.55	277.0303	1.26	-0.0016	-5.77	-0.18	**YES**
Abscisic acid	C06082	265.1435	12.66	265.1436	12.96	7.35E-05	0.28	0.36	**YES**
Acacetin	C01470	285.0758	15.62	285.0758	15.64	4.83E-05	0.17	0.07	**YES**
Acetoacetate	C00164	103.039	1.82	103.0389	1.62	-5.7E-05	-0.56	-0.09	**YES**
Adenine	C00147	136.0618	1.35	136.0617	1.34	-0.00011	-0.81	0.10	**YES**
Adenosine	C00212	268.104	1.38	268.1045	1.61	0.000493	1.84	0.34	**NO**
Adenosine	C00212	268.104	1.38	268.1023	1.25	-0.00171	-6.36	-0.02	**NO**
Agmatine sulfate	C00179	131.1291	1.22	131.1293	1.17	0.00021	1.60	0.06	**YES**
Alpha-aminoadipate	C00956	162.0761	1.34	162.0761	1.57	-2.5E-06	-0.02	0.34	**NO**
Alpha-d-glucose 1-phosphate	C00103	261.037	1.54	261.0379	1.26	0.000935	3.58	-0.17	**YES**
Anethole	C10428	149.0961	17.85	149.0961	17.76	4.38E-05	0.29	-0.05	**YES**
Aniline	C00292	94.06512	1.93	94.06499	1.59	-0.00013	-1.33	-0.23	**YES**
Ascorbate	C00072	177.0394	1.36	177.0391	1.18	-0.00025	-1.43	-0.07	**YES**
Ascorbate	C00072	177.0394	1.36	177.038	1.15	-0.0014	-7.89	-0.10	**NO**
Aspartate	C00049	134.0448	1.41	134.0447	1.26	-0.00011	-0.83	-0.04	**YES**
Benzaldehyde	C00261	107.0492	10.58	107.049	10.94	-0.00012	-1.11	0.43	**YES**
Benzaldehyde	C00261	107.0492	10.58	107.049	10.18	-0.00011	-1.03	-0.33	**YES**
Beta-alanine	C00099	90.05496	1.28	90.05477	1.22	-0.00019	-2.06	0.05	**YES**
Carvone	C11383	151.1118	16.1	151.1118	15.85	3.92E-06	0.03	-0.20	**YES**
Carvone	C11383	151.1118	16.1	151.1118	16.40	2.78E-05	0.18	0.35	**YES**
Caryophyllene	C09629	205.1951	20.2	205.195	20.60	-6.7E-05	-0.32	0.43	**YES**
Caryophyllene	C09629	205.1951	20.2	205.195	20.11	-0.00013	-0.62	-0.06	**YES**
Catechin	C06562	291.0863	1.47	291.0851	1.26	-0.00121	-4.16	-0.10	**YES**
Chlorogenic acid	C00852	355.1024	1.41	355.1014	1.37	-0.00093	-2.63	0.07	**YES**
Chlorogenic acid	C00852	355.1024	5	355.1028	4.79	0.000422	1.19	-0.12	**YES**
Chrysin	C10028	255.0652	15.56	255.0654	15.64	0.000189	0.74	0.13	**YES**
Corticosterone	C02140	347.2217	13.82	347.2218	13.39	0.000107	0.31	-0.37	**YES**
Creatine phosphate	C02305	212.0431	1.51	212.0442	1.23	0.001087	5.13	-0.17	**YES**
Cytidine	C00475	244.0928	1.29	244.0932	1.24	0.00043	1.76	0.06	**YES**
Cytosine	C00380	112.0505	1.26	112.0506	1.31	1.07E-05	0.10	0.16	**YES**
Cytosine	C00380	112.0505	1.26	112.0523	1.19	0.001725	15.39	0.04	**NO**
Dehydroascorbate	C05422	175.0237	1.39	175.0238	1.61	5.77E-05	0.33	0.33	**NO**
Deoxycarnitine	C05543	146.1176	1.29	146.1174	1.37	-0.00015	-1.02	0.18	**YES**
Emodin	C10343	271.0601	17.41	271.0606	17.60	0.000485	1.79	0.23	**YES**
Emodin	C10343	271.0601	18.36	271.0606	18.30	0.00054	1.99	-0.02	**YES**
Epigallocatechin	C12136	307.0813	1.44	307.0843	1.61	0.002971	9.67	0.27	**NO**
Epigallocatechin	C12136	307.0813	1.44	307.0802	1.25	-0.00109	-3.54	-0.08	**YES**
Epigallocatechin	C12136	307.0813	4.27	307.0821	3.98	0.000776	2.53	-0.19	**YES**
Eriodictyol	C05631	289.0707	12.26	289.0707	12.31	-1.3E-05	-0.04	0.11	**YES**
Ferulate	C01494	195.0652	10.14	195.0651	9.95	-4.9E-05	-0.25	-0.12	**YES**
Fisetin	C10041	287.055	10.13	287.055	10.27	-1.3E-05	-0.05	0.21	**YES**
Galangin	C10044	271.0601	15.88	271.0601	15.93	5.49E-05	0.20	0.10	**YES**
Gallic acid	CA1424	171.0288	1.67	171.0288	1.67	3.82E-05	0.22	0.11	**YES**
Gamma-linolenic acid	C06426	279.2319	18.1	279.232	18.05	0.00015	0.54	-0.01	**YES**
Gamma-linolenic acid	C06426	279.2319	19.34	279.232	19.39	0.00014	0.50	0.08	**YES**
Gibberellin A3	C01699	347.1489	9.86	347.1493	9.93	0.000462	1.33	0.15	**YES**
Glutamic acid	C00025	148.0605	1.29	148.0604	1.24	-8.3E-05	-0.56	0.06	**YES**

Gluthathione reduced	C00051	308.0911	1.35	308.0921	1.48	0.001013	3.29	0.24	**YES**
Guanine	C00242	152.0567	1.33	152.0567	1.46	-2.6E-05	-0.17	0.24	**YES**
Guanosine	C00387	284.099	1.36	284.1001	1.62	0.001166	4.10	0.37	**NO**
Hesperetin	C01709	303.0863	13.51	303.0864	13.07	7.75E-05	0.26	-0.38	**YES**
Hesperetin	C01709	303.0863	13.51	303.0862	13.86	-3.6E-05	-0.12	0.41	**YES**
Histamine	C00388	112.0869	1.3	112.0869	1.15	-4.9E-05	-0.43	-0.04	**YES**
Homogentisate	C00544	169.0495	2.51	169.0495	2.11	-6.9E-05	-0.41	-0.30	**YES**
Homogentisate	C00544	169.0495	2.51	169.0495	2.66	-5.9E-05	-0.35	0.26	**YES**
Hypoxanthine	C00262	137.0458	1.4	137.0457	1.58	-9.1E-05	-0.67	0.29	**NO**
Indole-3-ethanol	C00955	162.0913	11.34	162.0914	11.45	8.26E-05	0.51	0.18	**YES**
Isocitric acid	C00311	193.0343	1.58	193.0344	1.61	0.000129	0.67	0.14	**YES**
Isorhamnetin	C10084	317.0656	13.65	317.0657	13.59	0.000152	0.48	0.00	**YES**
Jasmonic acid	C08491	211.1329	13.47	211.133	13.68	0.000157	0.74	0.27	**YES**
Kaempferol	C05903	287.055	13.49	287.0551	13.47	0.000123	0.43	0.04	**YES**
L-arginine	C00062	175.119	1.25	175.119	1.16	6.88E-05	0.39	0.02	**YES**
L-asparagine	C00152	133.0608	1.31	133.0605	1.25	-0.0003	-2.27	0.05	**YES**
L-carnitine	C00318	162.1125	1.27	162.1123	1.51	-0.00016	-1.02	0.35	**NO**
L-cystine	C01420	241.0311	1.28	241.0297	1.26	-0.00141	-5.87	0.09	**YES**
Leucine	C16439	132.1019	1.37	132.1019	1.58	-5.2E-05	-0.39	0.32	**NO**
L-glutamine	C00064	147.0764	1.32	147.0763	1.24	-8.4E-05	-0.57	0.03	**YES**
L-histidine	C00135	156.0768	1.26	156.0767	1.18	-4.4E-05	-0.28	0.03	**YES**
Ll-2,6-diaminoheptanedioate	C00666	191.1026	1.31	191.1027	1.30	5.19E-05	0.27	0.10	**YES**
L-lysine	C16440	147.1128	1.23	147.1129	1.13	0.000119	0.81	0.01	**YES**
L-methionine	C01733	150.0583	1.37	150.0582	1.62	-9.5E-05	-0.63	0.36	**NO**
L-phenylalanine	C00079	166.0863	2.15	166.0862	2.13	-9.8E-05	-0.59	0.08	**YES**
L-pipecolic acid	C00408	130.0863	1.35	130.0861	1.27	-0.00014	-1.06	0.03	**YES**
L-proline	C00148	116.0706	1.35	116.0708	1.23	0.000141	1.22	-0.01	**YES**
L-serine	C00065	106.0499	1.29	106.0498	1.25	-8.4E-05	-0.79	0.07	**YES**
L-threonine	C00188	120.0655	1.31	120.0652	1.25	-0.00033	-2.73	0.04	**YES**
L-tyrosine	C00082	182.0812	1.37	182.0812	1.59	1.36E-05	0.07	0.33	**NO**
Maleamate	C01596	116.0342	1.44	116.0344	1.26	0.000226	1.95	-0.08	**YES**
Methyl jasmonate	C11512	225.1485	16.43	225.149	16.29	0.00045	2.00	-0.09	**YES**
Methyleugenol	C10454	179.1067	16.1	179.1067	16.26	-5.2E-07	0.00	0.21	**YES**
Methylmalonate	C02170	119.0339	1.99	119.034	2.08	0.000102	0.85	0.20	**YES**
Myristicin	C10480	193.0859	18.17	193.086	17.77	0.000103	0.53	-0.36	**YES**
Myristicin	C10480	193.0859	18.17	193.086	18.32	0.000144	0.75	0.19	**YES**
N-acetyl-dl-glutamic acid	C00624	190.071	1.77	190.0711	1.76	0.000106	0.56	0.10	**YES**
N-acetyl-d-tryptophan	C03137	247.1077	10.29	247.1077	10.44	-2.1E-05	-0.09	0.22	**YES**
N-acetyl-l-aspartic acid	C01042	176.0554	1.57	176.0554	1.62	7.28E-06	0.04	0.16	**YES**
N-acetyl-l-leucine	C02710	174.1125	9.01	174.1125	8.97	-1.3E-06	-0.01	0.04	**YES**
Nalpha-acetyl-l-lysine	C12989	189.1234	1.28	189.1235	1.56	9.05E-05	0.48	0.39	**NO**
Naringenin	C00509	273.0758	13.31	273.0759	13.58	0.000122	0.45	0.33	**YES**
Naringin	C09789	581.1865	10.7	581.1885	10.69	0.002058	3.54	0.06	**YES**
Nepsilon,nepsilon,nepsilon-trimethyllysine	C03793	189.1598	1.3	189.1601	1.16	0.000362	1.91	-0.03	**YES**
Nicotinamide	C00153	123.0553	1.36	123.0552	1.54	-0.0001	-0.85	0.29	**NO**
Ophthalmic acid	C21016	290.1347	1.38	290.1357	1.57	0.001061	3.66	0.30	**NO**
P-Anisaldehyde	C10761	137.0597	12.72	137.0596	12.36	-3.7E-05	-0.27	-0.30	**YES**
P-Anisaldehyde	C10761	137.0597	12.72	137.0597	12.91	-1.3E-05	-0.10	0.25	**YES**
Picolinic acid	C10164	124.0393	1.35	124.0392	1.62	-7.9E-05	-0.64	0.38	**NO**
Picolinic acid	C10164	124.0393	1.35	124.0411	1.06	0.001768	14.25	-0.18	**NO**
Quercitin	C00389	303.05	12.41	303.05	12.35	6.32E-05	0.21	0.01	**YES**
Quinate	C00296	193.0707	1.57	193.0706	1.29	-2.4E-05	-0.12	-0.17	**YES**
Rac-glycerol 1-myristate	CA1370	303.253	21.31	303.2538	21.33	0.000836	2.76	0.05	**YES**
Resorcinol monoacetate	C12064	153.0546	10.87	153.0545	10.65	-9.6E-05	-0.63	-0.15	**YES**
Rhamnetin	C10176	317.0656	14.66	317.0662	14.79	0.000613	1.93	0.18	**YES**
Rhapontin	C10288	421.1493	10.64	421.1474	10.77	-0.00186	-4.41	0.20	**YES**
Ribitol	C00474	153.0758	1.31	153.0754	1.29	-0.00034	-2.23	0.09	**YES**
Riboflavin	C00255	377.1456	8.29	377.1471	8.00	0.001544	4.09	-0.20	**YES**
S-carboxymethyl-l-cysteine	C03727	180.0325	1.5	180.0339	1.51	0.001387	7.70	0.12	**NO**
Serotonin	C00780	177.1022	1.86	177.1023	1.82	2.02E-05	0.11	0.07	**YES**
Sphinganine	C00836	302.3054	17.66	302.3057	17.31	0.000361	1.19	-0.31	**YES**
Succinate	C00042	119.0339	1.41	119.0349	1.53	0.001043	8.76	0.23	**NO**
Syringaldehyde		183.0653	9.42	183.0651	9.39	-0.00016	-0.87	0.05	**YES**
Taxifolin	C01617	305.0656	10.13	305.0658	10.13	0.000211	0.69	0.08	**YES**
Theobromine	C07480	181.072	2.23	181.0733	1.84	0.001326	7.33	-0.28	**NO**
Trigonelline	C01004	138.055	1.36	138.0549	1.22	-8E-05	-0.58	-0.03	**YES**
Trimethylamine	C00565	60.08078	1.28	60.08054	1.19	-0.00024	-3.96	0.02	**YES**
Tryptophan	C00078	205.0972	3.5	205.0972	3.62	8.59E-05	0.42	0.22	**YES**
Uracil	C00106	113.0346	1.37	113.0346	1.60	7.7E-06	0.07	0.34	**NO**
Urate	C00366	169.0356	1.39	169.0343	1.29	-0.00128	-7.57	0.01	**NO**
Uridine	C00299	245.0768	1.37	245.0774	1.62	0.000601	2.45	0.36	**NO**
Uridine-5-monophosphate	C00105	325.0432	1.68	325.0409	1.18	-0.00225	-6.92	-0.39	**NO**
Vitexin	C01460	433.1129	9.85	433.1139	9.79	0.000972	2.24	0.01	**YES**
Xanthine	C00385	153.0407	1.36	153.0407	1.62	-2.4E-05	-0.16	0.37	**NO**
Zeatin	C00371	220.1193	2.08	220.1181	2.18	-0.00121	-5.48	0.20	**YES**

Metabolite assignations were kept as valid when met the following criteria:
· If m/z error (PPM) < 6.
· If RT error between min 1-2 < 0.25 min.
· If RT error > 0.3 min for features with RT > 10 min only if m/z error (PPM) < 4.
· If RT error between min 2-10 < 0.3min.

Table S3. *Parameters applied to GC-MS chromatograms in Metabolite Detector 2.5 to obtain the GC-MS metabolomics dataset for Baccharis plants.*

Tool settings		
Centroid	Threshold begins	10
	Peak threshold end	-5
	Maximal baseline	30
	FWHM	0.1
Deconvolution	Peak threshold	10
	Minimum peak height	10
	Deconvolution width (scans)	8
Identification	Max RI difference	20
	Cutoff score	0.6
	Pure/Impure	0.6
	Scaled lib	Yes
	Combined score	Yes
Quantification	Minimal distance	0.5
	Minimal required quality index	1
	Exclude	72.5 to 73.5 146.5 to 147.5
Batch quantification Settings		
Compound matching	ARI	20
	Pure/Impure	0.6
	Req. Score	0.6
	RI+Spec	OK
Identification	ARI	20
	Pure/Impure	0.6
	RI+Spec	OK
Other settings	Compound reproducibility	0
	Max. Peak drisc. index	100
	S/N	15
	Number of ions	4
	Extended SIC Scan	Yes

Table S4. *Matching score, retention time of standard (RT), measured RT (Average in min) and signal to noise ratio (S/N) for the assigned metabolites in GC-MS chromatograms. Decision on whether a metabolite match was considered for the study as a good identification (YES) or kept as unknown (NO) is indicated. Decision on whether the metabolite match was considered as reliable identification was made on whether the metabolite mass fragmentation pattern could be verified using NIST GC-MS library.*

	Matching Score	RT (Standard)	Measured Avg. RT (Min)	Avg. S/N	Considered as good match
glyceric.acid	0.99	10.74	10.75	177.1	YES
L.serine.2	0.99	11.23	11.15	294.7	YES
D.arabinose	0.97	15.2	15.24	193.8	YES
D.mannose.1	0.97	17.67	17.7	583.8	YES
L.threonine.2.	0.97	11.6	11.52	144.6	YES
D.malic.acid	0.96	12.79	12.83	350.8	YES
D.mannose.2	0.95	17.83	17.89	288.2	YES
porphine.1	0.95	10.77	10.79	21.5	YES
quinic.acid	0.95	17.34	17.29	404.9	YES
chlorogenic.acid	0.93	27.38	27.52	196.4	YES
citric.acid	0.93	16.84	16.75	334.3	YES
pyrrole.2.carboxylic.acid	0.93	10.97	11.05	9.4	NO
shikimic.acid	0.93	16.43	16.58	210.5	YES
fructose.2	0.92	17.29	17.43	539	YES
kaempferol.1	0.92	26.86	26.99	175.6	YES
L.glutamic.acid.2	0.92	14.4	14.41	253.9	YES
norvaline.2	0.92	9.47	9.13	138	YES
scyllo.inositol	0.92	19.1	18.99	525.3	YES
Sucrose	0.92	24.41	24.35	88.1	YES
myo.inositol	0.91	19.71	19.59	581.7	YES
D.gluconic.acid.3	0.9	18.8	18.9	27.6	YES
ferulic.acid	0.9	19.31	19.35	50.6	YES
L.aspartic.acid.2	0.9	13.03	13.23	317.7	YES
lactose.1	0.9	24.92	25.11	98.7	NO
talose.2	0.9	17.58	17.62	60.4	YES
4.guanidinobutyric.acid.2	0.9	13.35	13.31	33.9	NO
citramalic.acid	0.89	12.75	12.65	72.6	YES
salicylic.acid	0.89	13.08	13.1	37.9	NO
xylitol	0.89	15.7	15.81	29.5	NO
arabitol	0.88	15.6	15.47	143.1	YES
isomaltose.1	0.88	25.63	25.64	94.7	YES
L.glutamic.acid.1	0.88	13.34	13.29	104.5	YES
L.ornithine.2	0.88	16.63	16.68	18.4	YES
D.lyxose.1	0.87	15.01	14.99	77.4	YES
D.lyxose.2	0.87	15.11	15.07	51.1	YES
glycerol.3.phosphate	0.87	16.06	16.14	55.4	YES
linoleic.acid	0.87	20.4	20.36	68.5	YES
palatinitol.1	0.87	25.92	25.97	48.6	YES
arachidic.acid	0.85	22.37	22.29	66.8	YES
D.allose.2	0.85	17.52	17.59	18.1	NO
kaempferol.2	0.85	26.93	27.11	194.9	YES
D.melezitose	0.83	29.95	29.92	78.7	YES
D.lyxosylamine.2	0.83	14.86	14.91	44	YES
D.threitol	0.83	13.13	13.14	32.1	YES
DL.isoleucine.1	0.83	8.58	8.27	14	YES
urea	0.83	9.6	9.46	8.2	NO
chrysin	0.82	24.71	24.82	48.8	NO
methyl.caffeate	0.82	18.62	18.58	29.8	NO
fumaric.acid	0.81	10.94	10.88	161.4	YES
L.proline.2	0.81	10.32	10.27	128.2	YES
D.mannitol	0.8	18.13	18.15	13.8	NO
4.hydroxy.3.methoxybenzoic.acid	0.8	15.99	16.04	3.2	NO
6.deoxy.D.glucose.2	0.8	15.75	15.81	31	YES
D.glucose.2	0.79	17.99	18.06	283.9	NO
L.asparagine.2	0.79	14.98	15.13	85.9	YES
D.galactaric.acid	0.78	19.23	19.18	118.5	NO

maleic.acid	0.78	10.32	10.34	23.3	NO
phytol.2	0.78	20.03	20.05	427.9	YES
turanose.1	0.78	24.81	24.71	177	YES
acetol.2	0.77	15.29	15.3	73.1	NO
beta.cyano.L.alanine	0.77	11.29	11.3	38.8	NO
lactose.2	0.77	25	25.18	91.4	YES
maltose.1	0.77	25.22	25.22	19	NO
melibiose.2	0.77	26.36	26.61	38.8	NO
palatinitol.2	0.77	26.01	26.08	62.9	NO
lactulose.1	0.76	23.87	23.97	117.9	YES
tagatose.2	0.76	17.21	17.53	418.7	YES
tartaric.acid	0.76	14.59	14.31	92.2	YES
isomaltose.2	0.75	25.86	25.94	29.6	YES
L.asparagine.1	0.74	14.5	14.35	9.8	NO
liquiritigenin.1	0.74	24.71	24.6	137.2	NO
maltose.2	0.74	25.4	25.33	183.5	NO
melibiose.1	0.74	26.11	26.38	46.4	NO
1.hexadecanol	0.74	18.05	17.98	84.8	YES
D.maltitol	0.73	25.97	26.21	73.4	NO
L.leucine.2	0.73	9.95	9.91	60	NO
valproic.acid.glucuronide	0.73	21.97	22.06	154.6	NO
D.glucose.6.phosphate.1	0.72	21.84	21.89	5.8	NO
L.alanine.1	0.71	7.54	7.51	101.8	YES
lactobionic.acid.1	0.71	24.58	24.63	32.2	NO
raffinose	0.71	29.94	30.29	44.9	NO
resorcinol	0.71	11.53	11.41	31.6	NO
ribitol	0.71	15.66	15.55	34	NO
4.nitroquinoline	0.71	13.64	13.38	112.7	NO
galacturonic.acid.2	0.7	18.11	18.1	15.2	NO
D.gluconic.acid.2	0.69	18.32	18.53	78.2	NO
gluconolactone.1	0.69	17.56	17.49	197.9	NO
fructose.1	0.68	17.18	17.14	51.7	NO
L.tyrosine.2	0.68	17.86	17.93	32.9	NO
melezitose	0.68	29.88	29.99	93.8	NO
phenylethylamine	0.68	13.77	13.98	120.4	NO
alpha.tocophereol	0.67	27.38	27.47	31.3	NO
D.galactose.2	0.67	18	18.1	5.8	NO
L.sorbose.1	0.67	17.19	17.01	16.7	NO
maltotriose.1	0.67	29.27	29.21	59.1	NO
N.formylglycine.2	0.67	11.53	11.34	87	NO
alizarin	0.66	23.46	23.62	305.9	NO
D.fructose.6.phosphate.2	0.66	21.71	21.62	24.3	NO
erythritol	0.66	13.18	13.43	70.5	NO
gentisic.acid	0.66	16.12	16.25	62.3	NO
lactulose.3	0.65	24.43	24.56	28.5	NO
trans.trans.farnesol	0.65	16.43	16.46	127.1	NO
lactobionic.acid.3	0.64	25.41	25.43	37.8	NO
sialic.acid	0.64	22.25	22.51	3.7	NO
3.aminopropionitrile.2	0.64	9.93	9.83	178.4	NO
ethyl.glucuronide	0.63	18.62	18.45	130.5	NO
iminodiacetic.acid.1	0.62	12.49	12.36	21.5	NO
oleic.acid	0.62	20.5	20.43	90.4	NO
6.deoxy.D.glucose.1	0.62	15.6	15.71	204.9	NO
guanidinosuccinic.acid.2	0.61	18.62	18.4	75	NO
maltotriitol	0.61	31.8	31.8	14.1	NO
p.toluenesulfonic.acid	0.61	14.27	14.62	16.8	NO
3.indolelactic.acid.1	0.61	19.81	19.72	71.2	NO
acetol.3	0.6	15.38	15.39	61.6	NO
naringin	0.6	29.08	29.12	513	NO

Score: Score value obtained for each metabolite matching with the library.

T (Standard): Retention Time from the specific standard

Avg. RT (min): Average Retention Time (minutes)

Avg. S/N: Average Signal to Noise

Hits: number of samples where the metabolite was detected

Table S5. *The result of PERMANOVA analysis on plant foliar metabolome*

	Degrees of freedom	Sums of squares	Mean square	Pseudo-F	R^2	*P* value
Aphid Treatment	1	1.89×10^{19}	1.89×10^{19}	17.3	0.203	< 0.0001
Residuals	68	7.44×10^{19}	1.09×10^{18}		0.78	
Total	69	9.33×10^{19}			1	

Table S6. *The result of PERMANOVA analysis on plant volatile compounds*

	Degrees of freedom	Sums of squares	Mean square	Pseudo-F	R^2	*P* value
Aphid Treatment	1	162.89	162.89	0.65	0.1	0.5969
Residuals	6	1509.49	251.58		0.9	
Total	7	1672.38			1	

Table S7. *The individual t-test for all identified metabolite and total amino acids*

Metabolite	Control_Mean	Control_SE	Aphid_Mean	Aphid_SE	T	P_value
1.hexadecanol	1.77E+06	1.66E+05	6.43E+05	6.67E+04	6.30E+00	6.27E-08
1-methyladenine	1.03E+04	8.80E+02	7.49E+04	1.11E+04	-5.78E+00	1.12E-05
1-hydroxypregnenolone	4.61E+04	3.20E+03	1.23E+04	1.55E+03	9.50E+00	2.77E-13
3-dihydroxybenzoate	1.00E+04	7.38E+02	2.50E+04	2.53E+03	-5.68E+00	8.10E-06
5-dihydroxybenzoate	5.20E+04	1.95E+03	9.85E+03	9.49E+02	1.94E+01	1.29E-26
6-diaminoheptanedioate	1.32E+03	4.62E+02	2.19E+04	8.37E+03	-2.46E+00	2.31E-02
2-deoxy-d ribose	1.58E+05	1.10E+04	4.84E+04	6.14E+03	8.67E+00	4.19E-12
2-hydroxyphenylacetic acid	2.94E+04	7.54E+02	2.18E+04	1.28E+03	5.12E+00	1.16E-05
2-oxovaleric acid	4.27E+03	3.49E+02	7.41E+03	5.84E+02	-4.61E+00	5.25E-05
4-dihydroxybenzoic acid	5.31E+04	1.62E+03	2.88E+04	2.86E+03	7.38E+00	1.69E-08
3.aminopropionitrile.2	3.68E+06	1.32E+05	4.35E+06	3.35E+05	-1.84E+00	7.66E-02
3.indolelactic.acid.1	1.00E+06	3.70E+04	4.64E+05	4.67E+04	9.08E+00	1.09E-11
3-dehydroshikimate	3.25E+04	1.35E+03	9.34E+03	1.75E+03	1.05E+01	1.76E-13
3-hydroxy-3-methylglutarate	7.29E+05	3.86E+04	5.39E+05	7.59E+04	2.23E+00	3.34E-02
3-hydroxybenzoate	5.63E+04	3.44E+03	1.38E+05	1.11E+04	-7.06E+00	2.73E-07
3-hydroxycinnamic acid	4.83E+04	3.40E+03	5.88E+04	7.60E+03	-1.26E+00	2.17E-01
3-hydroxyphenylacetate	8.94E+03	6.92E+02	1.85E+04	1.64E+03	-5.41E+00	9.81E-06
3-methyl-2-oxindole	4.11E+04	2.92E+03	2.32E+04	2.03E+03	5.02E+00	4.86E-06
4.guanidinobutyric.acid.2	1.41E+06	9.34E+04	3.37E+06	1.19E+06	-1.65E+00	1.15E-01
4.hydroxy.3.methoxybenzoic.acid	3.26E+06	2.90E+05	2.76E+06	3.06E+05	1.19E+00	2.40E-01
4.nitroquinoline	1.58E+06	1.17E+05	3.28E+06	4.90E+05	-3.37E+00	2.74E-03
4-aminobutanoate	2.64E+05	1.27E+04	3.26E+05	2.05E+04	-2.56E+00	1.48E-02
4-guanidinobutanoate	1.11E+04	1.16E+03	7.93E+04	1.03E+04	-6.57E+00	1.86E-06
4-hydroxy-2-quinolinecarboxylic acid	1.41E+06	7.12E+04	2.46E+06	1.07E+05	-8.18E+00	6.44E-10
4-hydroxybenzoic acid	7.18E+05	1.76E+04	2.21E+06	2.62E+05	-5.66E+00	1.48E-05
4-imidazoleacetic acid	7.03E+04	5.83E+03	3.50E+04	4.74E+03	4.71E+00	1.54E-05
6-dihydrouracil	6.04E+04	7.29E+03	7.34E+05	1.66E+05	-4.04E+00	6.35E-04
5-aminopentanoate	7.73E+08	1.78E+07	9.64E+08	2.27E+07	-6.60E+00	4.36E-08

5-methylcytosine hydrocloride	1.15E+04	1.24E+03	2.00E+04	2.04E+03	-3.55E+00	1.12E-03
5'-methylthioadenosine	2.21E+05	2.07E+04	2.40E+05	3.67E+04	-4.47E-01	6.58E-01
5-oxo-l-proline	1.80E+05	1.37E+04	2.05E+05	3.00E+04	-7.39E-01	4.66E-01
6-deoxy.d.glucose	6.02E+06	2.99E+05	4.55E+06	3.68E+05	3.10E+00	3.34E-03
6-phosphogluconic acid	1.75E+06	1.15E+05	4.53E+05	7.06E+04	9.67E+00	7.10E-14
abscisic acid	5.49E+07	3.90E+06	3.17E+07	5.80E+06	3.33E+00	1.94E-03
acacetin	2.67E+08	9.12E+06	2.65E+08	1.34E+07	1.51E-01	8.81E-01
acetol	2.52E+06	8.43E+04	1.49E+06	1.09E+05	7.43E+00	2.94E-09
adenine	7.83E+06	7.28E+05	4.92E+06	9.17E+05	2.48E+00	1.69E-02
alanine	4.41E+06	1.95E+05	4.03E+06	5.41E+05	6.61E-01	5.15E-01
alizarin	1.13E+07	7.04E+05	8.16E+06	3.79E+05	3.92E+00	2.32E-04
allose.2	1.78E+05	1.27E+04	2.34E+05	1.60E+04	-2.69E+00	9.91E-03
alpha.tocopherol	2.26E+05	3.14E+04	2.46E+05	4.13E+04	-3.96E-01	6.94E-01
alpha-d-glucose 1-phosphate	3.27E+05	1.71E+04	3.17E+05	3.48E+04	2.68E-01	7.90E-01
anethole	4.83E+05	1.40E+04	2.23E+05	2.15E+04	1.01E+01	2.81E-12
arabinose	4.12E+06	2.63E+05	3.40E+06	2.28E+05	2.07E+00	4.32E-02
arabitol	2.47E+06	8.75E+04	2.57E+06	1.41E+05	-6.29E-01	5.33E-01
arachidic.acid	6.33E+05	4.24E+04	1.19E+06	8.32E+04	-5.97E+00	1.39E-06
arginine	2.79E+05	3.95E+04	9.13E+06	3.02E+06	-2.93E+00	8.32E-03
ascorbate	1.07E+05	3.47E+03	1.13E+05	1.12E+04	-4.57E-01	6.52E-01
asparagine	4.30E+06	5.01E+05	6.68E+07	1.54E+07	-4.06E+00	6.14E-04
aspartic acid	1.23E+07	6.57E+05	1.42E+07	1.79E+06	-9.76E-01	3.38E-01
azelaic acid	2.46E+04	9.58E+02	1.35E+05	4.60E+04	-2.40E+00	2.63E-02
beta.cyano.alanine	4.22E+06	1.73E+05	4.28E+06	3.67E+05	-1.63E-01	8.72E-01
betaine	5.24E+03	6.38E+02	1.74E+04	4.84E+03	-2.49E+00	2.11E-02
biliverdin	8.12E+04	1.44E+04	4.24E+04	6.86E+03	2.43E+00	1.84E-02
caryophyllene	1.96E+08	6.75E+06	9.33E+07	6.64E+06	1.08E+01	3.45E-15
catechol	5.91E+04	1.70E+03	2.70E+04	2.68E+03	1.01E+01	4.40E-12
chlorogenic acid	3.72E+08	1.10E+07	1.71E+08	1.54E+07	1.06E+01	3.23E-13
chrysin	5.24E+08	1.25E+07	4.30E+08	1.23E+07	5.32E+00	2.00E-06
cinnamaldehyde	1.84E+03	1.99E+02	1.08E+03	2.17E+02	2.57E+00	1.32E-02
citramalic.acid	9.20E+05	4.46E+04	9.09E+05	1.42E+05	7.99E-02	9.37E-01
citrate	2.00E+07	1.23E+06	6.39E+06	7.76E+05	9.36E+00	2.26E-13
cytidine	1.92E+04	2.78E+03	2.43E+04	6.13E+03	-7.50E-01	4.60E-01
cytosine	1.27E+05	1.89E+04	4.81E+04	1.53E+04	3.23E+00	2.01E-03
dehydroascorbate	4.22E+05	4.60E+04	2.66E+05	3.68E+04	2.65E+00	1.03E-02
disoleucine	2.14E+05	1.73E+04	5.17E+05	1.25E+05	-2.40E+00	2.60E-02
emodin	3.04E+05	1.29E+04	2.62E+05	1.52E+04	2.10E+00	4.12E-02
epigallocatechin	3.40E+05	3.54E+04	2.35E+05	2.60E+04	2.39E+00	1.98E-02
eriodictyol	3.58E+05	2.45E+04	3.44E+05	3.28E+04	3.43E-01	7.33E-01
erythritol	8.67E+05	3.18E+04	8.63E+05	6.82E+04	4.62E-02	9.63E-01
ethyglucuronide	2.61E+06	1.26E+05	1.38E+06	1.24E+05	6.97E+00	4.51E-09
ferulic.acid	5.55E+05	1.69E+04	3.82E+05	2.73E+04	5.39E+00	4.62E-06

fisetin	2.25E+06	7.67E+04	1.99E+06	2.30E+05	1.08E+00	2.91E-01
fructose.6.phosphate	2.66E+05	9.96E+03	1.58E+05	1.66E+04	5.58E+00	2.84E-06
fructose	2.95E+07	1.52E+06	3.61E+07	3.16E+06	-1.87E+00	7.12E-02
fumaric.acid	2.53E+06	1.97E+05	4.33E+06	5.48E+05	-3.09E+00	4.81E-03
galactaric.acid	2.17E+06	7.30E+04	2.04E+06	1.27E+05	8.67E-01	3.92E-01
galactose	2.93E+05	2.13E+04	4.19E+05	3.33E+04	-3.18E+00	2.99E-03
galacturonic acid	5.71E+05	6.16E+04	6.37E+05	5.26E+04	-8.22E-01	4.14E-01
galangin	8.23E+08	2.83E+07	6.83E+08	2.30E+07	3.83E+00	3.12E-04
gallic acid	5.81E+04	3.58E+03	9.76E+04	1.68E+04	-2.30E+00	3.15E-02
gamma-linolenic acid	3.82E+05	1.77E+04	6.69E+05	1.35E+05	-2.10E+00	4.80E-02
gentisic.acid	8.85E+05	3.22E+04	3.68E+05	2.92E+04	1.19E+01	3.94E-17
gibberellin a3	2.33E+05	1.32E+04	3.44E+04	3.83E+03	1.44E+01	5.14E-19
gluconic acid	4.59E+06	1.14E+05	5.60E+06	7.74E+05	-1.30E+00	2.09E-01
gluconolactone.1	5.31E+06	2.03E+05	4.15E+06	5.02E+05	2.14E+00	4.13E-02
glucose.6.phosphate	2.86E+05	2.70E+04	5.43E+05	7.57E+04	-3.20E+00	3.72E-03
glucose	9.53E+06	3.22E+05	5.62E+06	4.74E+05	6.83E+00	3.86E-08
glutamic acid	2.06E+07	8.85E+05	1.79E+07	1.64E+06	1.44E+00	1.60E-01
glutamine	7.80E+05	8.96E+04	5.75E+06	1.55E+06	-3.19E+00	4.52E-03
gluthathione reduced	3.59E+04	1.49E+04	2.95E+05	9.62E+04	-2.66E+00	1.45E-02
glyceraldehyde	5.62E+05	1.41E+04	3.11E+05	2.28E+04	9.33E+00	4.04E-11
glycerate	3.65E+06	1.14E+05	2.66E+06	1.20E+05	5.99E+00	2.07E-07
glycero.3.phosphate	5.76E+05	2.43E+04	8.10E+05	8.04E+04	-2.79E+00	1.03E-02
glycine	4.37E+03	3.17E+02	8.42E+03	9.79E+02	-3.93E+00	6.14E-04
glyoxilic acid	4.08E+04	1.96E+03	1.70E+04	1.32E+03	1.01E+01	1.30E-14
guanidinosuccinic.acid	5.68E+05	2.26E+04	4.61E+05	2.95E+04	2.89E+00	6.00E-03
guanine	8.18E+05	1.25E+05	9.19E+04	1.40E+04	5.78E+00	8.14E-07
gulonic acid gama-lactone	3.38E+04	1.59E+03	3.21E+04	3.01E+03	5.14E-01	6.11E-01
hesperetin	2.47E+07	8.70E+05	2.33E+07	1.42E+06	8.13E-01	4.22E-01
histamine	2.35E+04	1.14E+03	1.45E+05	2.43E+04	-4.99E+00	6.92E-05
histidine	3.59E+05	4.82E+04	4.88E+06	1.23E+06	-3.67E+00	1.50E-03
homogentisate	1.90E+04	3.94E+02	1.25E+04	9.05E+02	6.63E+00	3.57E-07
hydroxypyruvate	8.19E+05	5.82E+04	4.79E+05	1.06E+05	2.81E+00	8.41E-03
iminodiacetic.acid	3.82E+05	3.43E+04	2.51E+05	2.82E+04	2.94E+00	4.61E-03
indole-3-ethanol	1.05E+03	3.02E+01	1.94E+04	1.07E+04	-1.72E+00	1.00E-01
isocitric acid	4.06E+04	2.32E+03	7.87E+03	1.55E+03	1.17E+01	3.04E-17
isomaltose	3.70E+06	1.61E+05	5.24E+06	3.12E+05	-4.38E+00	1.25E-04
isorhamnetin	1.73E+08	8.73E+06	1.63E+08	1.22E+07	6.14E-01	5.43E-01
jasmonic acid	9.59E+01	3.14E+01	4.73E+03	9.03E+02	-5.12E+00	5.13E-05
kaempferol	2.85E+08	1.36E+07	2.29E+08	9.24E+06	3.36E+00	1.33E-03
lactobionic.acid	4.12E+06	1.07E+05	5.81E+06	3.35E+05	-4.79E+00	6.98E-05
lactose	7.25E+06	2.95E+05	4.85E+06	4.08E+05	4.76E+00	2.42E-05
lactulose	2.44E+06	2.98E+05	2.95E+06	2.25E+05	-1.38E+00	1.72E-01
leucine	5.57E+05	6.97E+04	5.24E+05	1.30E+05	2.20E-01	8.27E-01

linoleic.acid	1.25E+06	5.34E+04	1.20E+06	1.04E+05	3.77E-01	7.09E-01
liquiritigenin	3.16E+06	2.54E+05	3.31E+06	2.55E+05	-4.07E-01	6.86E-01
lumazine	1.73E+05	1.33E+04	5.88E+04	1.40E+04	5.90E+00	2.82E-07
lysine	9.63E+04	1.04E+04	1.73E+05	4.20E+04	-1.78E+00	8.87E-02
lyxose	2.22E+06	9.13E+04	1.88E+06	2.31E+05	1.40E+00	1.74E-01
lyxosylamine	4.36E+05	2.27E+04	7.81E+05	1.42E+05	-2.40E+00	2.56E-02
maleamate	1.23E+05	1.31E+04	5.07E+05	1.25E+05	-3.05E+00	6.18E-03
maleic.acid	3.63E+05	5.60E+04	2.12E+05	3.72E+04	2.24E+00	2.88E-02
malic acid	3.22E+07	1.96E+06	1.25E+07	1.31E+06	8.35E+00	1.10E-11
maltitol	2.60E+06	1.00E+05	4.50E+06	3.12E+05	-5.80E+00	5.45E-06
maltose	1.24E+07	4.83E+05	5.72E+06	4.91E+05	9.75E+00	1.92E-13
maltotriitol	6.57E+05	7.03E+04	0.00E+00	0.00E+00	9.35E+00	1.02E-11
maltotriose	3.41E+06	2.55E+05	1.96E+06	2.40E+05	4.13E+00	1.23E-04
mandelic acid	5.32E+04	1.47E+03	8.63E+03	9.46E+02	2.56E+01	3.39E-34
mangiferin	4.23E+04	4.26E+03	1.48E+03	1.83E+02	9.56E+00	5.28E-12
mannitol	2.98E+05	1.80E+04	3.02E+05	1.58E+04	-1.66E-01	8.69E-01
mannose	4.07E+07	2.34E+06	4.04E+07	2.93E+06	7.27E-02	9.42E-01
melezitose	5.70E+06	3.67E+05	7.57E+06	7.60E+05	-2.22E+00	3.45E-02
melibiose	1.35E+06	9.53E+04	1.62E+06	3.31E+05	-7.84E-01	4.41E-01
melibiose	2.55E+06	1.25E+05	1.65E+06	8.64E+04	5.94E+00	1.49E-07
methycaffeate	3.36E+05	2.51E+04	2.02E+05	2.87E+04	3.53E+00	9.30E-04
methylmalonate	2.13E+04	1.46E+03	4.93E+04	5.95E+03	-4.57E+00	1.42E-04
myo.inositol	3.69E+07	1.16E+06	2.20E+07	8.24E+05	1.04E+01	3.29E-15
n.formylglycine	1.25E+06	3.55E+04	7.00E+05	5.23E+04	8.71E+00	1.20E-10
n-acetyl-d-glucosamine	8.27E+03	6.70E+02	2.38E+04	3.00E+03	-5.04E+00	4.74E-05
n-acetyl-dl-glutamic acid	5.24E+04	2.19E+03	8.01E+04	7.88E+03	-3.39E+00	2.51E-03
n-acetyl-d-tryptophan	1.67E+04	1.02E+03	4.92E+05	2.03E+05	-2.34E+00	2.97E-02
n-acetyl-l-aspartic acid	9.60E+03	5.17E+02	2.98E+04	3.06E+03	-6.51E+00	1.82E-06
n-acetyl-l-leucine	5.21E+03	9.36E+02	2.23E+03	4.54E+02	2.86E+00	5.86E-03
n-alpha-acetyl-l-asparagine	1.07E+02	3.05E+01	4.57E+03	1.72E+03	-2.59E+00	1.74E-02
naringenin	1.46E+08	6.75E+06	1.21E+08	6.51E+06	2.70E+00	9.12E-03
naringin	5.42E+07	2.66E+06	4.64E+07	2.44E+06	2.15E+00	3.60E-02
nepsilon	3.93E+04	2.31E+03	2.82E+05	5.44E+04	-4.46E+00	2.39E-04
n-methyl-l-glutamate	3.30E+04	1.80E+03	5.74E+04	5.78E+03	-4.02E+00	4.96E-04
norvaline	1.27E+06	1.00E+05	3.99E+06	8.88E+05	-3.04E+00	6.39E-03
oleic.acid	1.43E+06	8.11E+04	1.36E+06	1.34E+05	4.59E-01	6.49E-01
omega-hydroxydodecanoic acid	5.44E+02	4.57E+01	5.86E+02	6.65E+01	-5.12E-01	6.11E-01
ophthalmic acid	0.00E+00	0.00E+00	2.40E+03	9.83E+02	-2.44E+00	2.41E-02
ornitine	2.92E+03	5.23E+02	1.01E+06	3.18E+05	-3.18E+00	4.71E-03
o-succinyl-l-homoserine	6.91E+03	3.90E+02	8.21E+03	9.68E+02	-1.24E+00	2.24E-01
oxaloacetic acid	1.11E+04	9.93E+02	2.05E+03	5.75E+02	7.92E+00	7.20E-11
p.toluenesulfonic.acid	0.00E+00	0.00E+00	9.33E+05	2.34E+05	-3.99E+00	7.28E-04
palatinitol	3.45E+06	1.74E+05	6.83E+06	4.96E+05	-6.44E+00	9.50E-07

phenylalanine	1.51E+07	1.14E+06	2.16E+07	5.43E+06	-1.18E+00	2.53E-01
phenylethylamine	1.25E+06	1.11E+05	3.33E+06	5.42E+05	-3.76E+00	1.10E-03
phenylpyruvic acid	1.99E+04	1.33E+03	1.70E+04	2.74E+03	9.46E-01	3.52E-01
pinitol	3.91E+05	1.19E+04	2.71E+05	2.70E+04	4.08E+00	3.39E-04
pipecolic acid	1.12E+07	1.10E+06	5.75E+06	6.76E+05	4.21E+00	8.51E-05
porphine	5.86E+04	5.26E+03	7.44E+04	6.80E+03	-1.85E+00	7.18E-02
proline	3.13E+06	1.12E+05	6.77E+07	1.56E+07	-4.14E+00	5.02E-04
pyrrole.2.carboxylic.acid	1.07E+05	6.07E+03	2.06E+05	2.71E+04	-3.55E+00	1.78E-03
pyruvic acid	3.26E+05	3.18E+04	2.21E+05	1.97E+04	2.82E+00	6.49E-03
pyruvic aldehyde	2.05E+05	7.76E+03	1.14E+05	6.30E+03	9.12E+00	6.60E-13
quercitin	3.83E+07	2.05E+06	4.49E+07	4.20E+06	-1.42E+00	1.67E-01
quinic acid	8.18E+07	4.05E+06	1.39E+07	1.89E+06	1.52E+01	1.96E-21
rac-glycerol 1-myristate	3.84E+02	7.13E+01	1.41E+04	2.36E+03	-5.80E+00	1.12E-05
raffinose	8.20E+05	7.16E+04	8.74E+05	1.03E+05	-4.33E-01	6.68E-01
resorcinol monoacetate	3.12E+04	2.09E+03	5.48E+05	6.74E+04	-7.66E+00	2.25E-07
resorcinol	2.32E+05	9.34E+03	1.69E+05	9.05E+03	4.84E+00	1.10E-05
rhamnetin	3.05E+05	1.70E+04	3.64E+05	3.19E+04	-1.64E+00	1.11E-01
rhapontin	1.34E+06	5.96E+04	1.18E+06	8.28E+04	1.56E+00	1.26E-01
rhein	5.56E+03	5.70E+02	3.21E+03	4.96E+02	3.10E+00	2.96E-03
riboflavin	1.05E+05	7.67E+03	1.95E+05	1.66E+04	-4.91E+00	3.30E-05
ribose 5-phosphate	5.41E+03	4.05E+02	3.78E+03	6.29E+02	2.18E+00	3.55E-02
rs-mevalonic acid lithium salt	2.95E+04	4.29E+03	8.57E+03	7.67E+02	4.81E+00	1.84E-05
saccharic acid	2.05E+04	1.34E+03	1.46E+04	1.05E+03	3.50E+00	8.75E-04
salicylate	6.21E+05	1.74E+04	2.44E+06	3.36E+05	-5.39E+00	2.76E-05
scyllo.inositol	2.71E+07	8.39E+05	2.08E+07	1.40E+06	3.86E+00	4.73E-04
secologanin	7.33E+04	5.52E+03	1.51E+05	1.74E+04	-4.25E+00	2.77E-04
serine	4.52E+06	4.48E+05	1.65E+07	1.93E+06	-6.05E+00	4.17E-06
serotonin	1.27E+04	1.07E+03	5.96E+03	1.11E+03	4.35E+00	6.35E-05
shikimic acid	8.58E+06	2.99E+05	1.94E+06	1.52E+05	1.98E+01	3.08E-27
sialic.acid	0.00E+00	0.00E+00	2.83E+05	8.77E+04	-3.23E+00	4.24E-03
sn-glycerol 3-phosphate	3.20E+04	4.44E+03	2.21E+04	4.79E+03	1.50E+00	1.39E-01
sorbate	5.00E+04	2.33E+03	2.24E+04	2.07E+03	8.87E+00	2.36E-12
sorbose	3.32E+05	1.25E+04	2.90E+05	1.78E+04	1.92E+00	6.25E-02
suberic acid	5.84E+03	2.91E+02	1.02E+04	6.06E+02	-6.42E+00	4.60E-07
sucrose	1.47E+06	4.12E+04	1.81E+06	5.65E+04	-4.73E+00	2.67E-05
sugar-alcohol-hexoses	1.25E+04	5.97E+02	3.23E+04	4.33E+03	-4.54E+00	1.82E-04
sugars-alcohol-pentoses	5.11E+05	2.00E+04	3.44E+05	3.59E+04	4.07E+00	2.78E-04
sugars-deoxy-hexoses	4.60E+04	1.48E+03	3.65E+04	4.69E+03	1.93E+00	6.54E-02
sugars-monosaccharides-hexoses	1.58E+06	3.55E+04	1.26E+06	8.43E+04	3.50E+00	1.64E-03
sugars-monosaccharides-pentoses	1.89E+06	6.28E+04	1.70E+06	1.14E+05	1.50E+00	1.43E-01
tagatose	2.38E+07	1.46E+06	2.63E+07	2.69E+06	-8.08E-01	4.25E-01
talose	1.82E+06	1.28E+05	1.11E+06	5.96E+04	5.02E+00	5.60E-06
tartaric.acid	1.74E+06	1.15E+05	3.80E+05	3.24E+04	1.14E+01	4.01E-15

taxifolin	5.39E+04	6.21E+03	4.33E+04	3.01E+03	1.53E+00	1.32E-01
threitol	1.97E+05	8.48E+03	2.97E+05	1.25E+04	-6.61E+00	7.65E-08
threonine	2.00E+06	1.12E+05	3.72E+06	4.79E+05	-3.50E+00	1.99E-03
trans.trans.farnesol	4.50E+06	2.97E+05	7.65E+05	7.01E+04	1.22E+01	5.77E-16
trigonelline	3.97E+06	4.55E+05	7.40E+06	4.93E+05	-5.10E+00	5.08E-06
trimethylamine	3.67E+04	1.81E+03	2.05E+04	1.74E+03	6.45E+00	2.98E-08
tryptophan	1.19E+07	6.61E+05	5.82E+07	7.38E+06	-6.26E+00	3.84E-06
turanose	4.86E+06	2.02E+05	4.18E+06	2.36E+05	2.20E+00	3.30E-02
tyrosine	3.65E+05	1.52E+04	1.07E+05	1.61E+04	1.17E+01	4.33E-16
uracil	3.53E+03	4.94E+02	1.08E+04	2.53E+03	-2.81E+00	1.02E-02
urea	0.00E+00	0.00E+00	5.34E+05	1.35E+05	-3.95E+00	7.95E-04
uridine 5'-diphosphoglucose	6.90E+03	5.98E+02	4.05E+03	4.56E+02	3.79E+00	3.47E-04
urocanate	7.24E+03	5.54E+02	4.10E+03	5.95E+02	3.87E+00	3.08E-04
valproic.acid.glucuronide	5.39E+06	3.38E+05	2.05E+06	1.61E+05	8.92E+00	2.54E-12
vitexin	8.24E+05	4.35E+04	3.86E+05	3.84E+04	7.55E+00	3.60E-10
xylitol	1.03E+06	4.35E+04	1.41E+06	8.61E+04	-4.02E+00	3.51E-04
zeatin	1.08E+05	1.08E+05	3.80E+06	4.11E+05	4.21E-01	6.78E-01
Total amino acids	7.87E+09	1.10E+10	4.99E+09	7.23E+08	-4.37E+00	2.36E-03

Table S8: Linear trendline r^2 value of yield curve slopes vs. relative contribution of individual compounds to total VOCs for all trials.

Compound	r^2 of linear trendline
α-pinene	0.42
camphene	0.10
α-phellandrene	0.02
β-myrcene	0.21
3-carene	0.50
limonene	0.07
β-ocimene	0.19
sabinene	0.12
α-copaene	0.03
caryophyllene	0.03
β-guaiene	0.03
patchoulene	0.03
aristolochene	0.26

6. Figures:
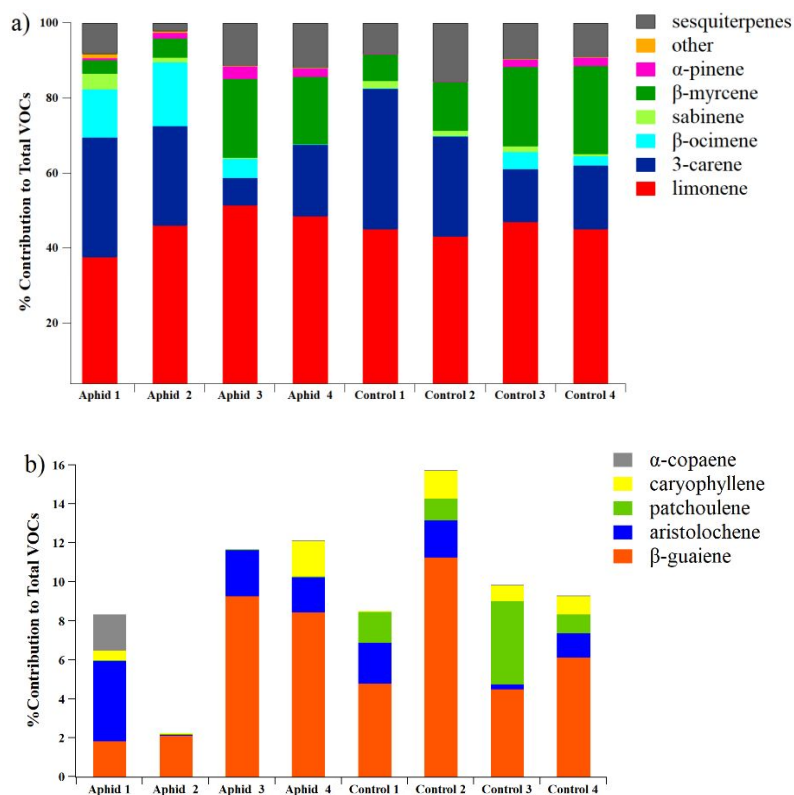
Figure S1: a) Average relative contribution of mono- & sesqui-terpene distribution for each control and aphid trials, other refers to α-phellandrene and camphene, b) sesquiterpenes average relative contribution to total BVOCs for each control and aphid trials. Aphid and Control refer to treated and control Baccharis trials, respectively. The error bars were removed to be able to see the detailed profiles.
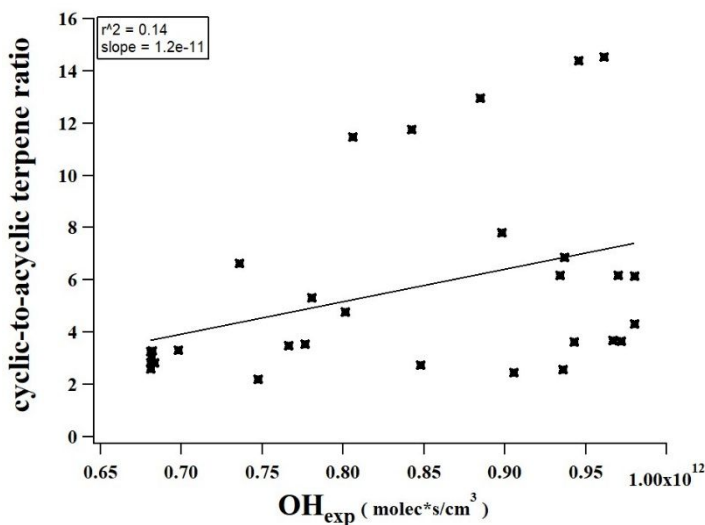
Figure S2: cyclic-to-acyclic terpene ratio versus OH exposure.

References:

(1)   Pluskal, T.; Castillo, S.; Villar-Briones, A.; Orešič, M. MZmine 2: Modular Framework for Processing, Visualizing, and Analyzing Mass Spectrometry-Based Molecular Profile Data. *BMC Bioinformatics* **2010**, *11* (1), 395. https://doi.org/10.1186/1471-2105-11-395.

(2)   Sumner, L. W.; Amberg, A.; Barrett, D.; Beale, M. H.; Beger, R.; Daykin, C. A.; Fan, T. W.-M.; Fiehn, O.; Goodacre, R.; Griffin, J. L.; Hankemeier, T.; Hardy, N.; Harnly, J.; Higashi, R.; Kopka, J.; Lane, A. N.; Lindon, J. C.; Marriott, P.; Nicholls, A. W.; Reily, M. D.; Thaden, J. J.; Viant, M. R. Proposed Minimum Reporting Standards for Chemical Analysis Chemical Analysis Working Group (CAWG) Metabolomics Standards Initiative (MSI). *Metabolomics Off. J. Metabolomic Soc.* **2007**, *3* (3), 211–221. https://doi.org/10.1007/s11306-007-0082-2.

(3)   Hiller, K.; Hangebrauk, J.; Jäger, C.; Spura, J.; Schreiber, K.; Schomburg, D. MetaboliteDetector: Comprehensive Analysis Tool for Targeted and Nontargeted GC/MS Based Metabolome Analysis. *Anal. Chem.* **2009**, *81* (9), 3429–3439. https://doi.org/10.1021/ac802689c.

CHAPTER 3

Secondary organic aerosol from the photooxidation of oxygenated biogenic volatile organic

compounds

INTRODUCTION

Biogenic volatile organic compounds (BVOCs) released primarily from terrestrial

vegetation are estimated to contribute up to 90% of total atmospheric VOCs (Carlton et al., 2009b;

Claeys et al., 2004; Guenther et al., 1995). These volatile compounds are highly reactive and can

contribute to the formation of secondary organic aerosol (SOA) (Ehn et al., 2014). Atmospheric

aerosols, including SOA, impact atmospheric chemistry (D. Abbatt et al., 2012; Pöschl and

Shiraiwa, 2015; Shiraiwa et al., 2011), and contribute to air pollution (Huang et al., 2014;

Volkamer et al., 2006), and affect human health negatively (Baltensperger et al., 2008; Lelieveld

et al., 2015; Nault et al., 2021; Nel, 2005; Shiraiwa et al., 2017b). They also can impact climate

directly by scattering and absorbing solar radiation and indirectly by affecting cloud properties and

formation when acting as cloud condensation nuclei (CCN). The type of plant VOCs varies

between plant species (Courtois et al., 2009) and environmental regions (Loreto et al., 2014).

Various types of plant species are undergoing significant range shifts due to climate change

(Wieczynski et al., 2019), and it is expected that there will be range expansion of plants that can

better tolerate drought and high temperatures (Bradley et al., 2012; Seager and Vecchi, 2010). This

complexity (Guenther, 2013) means that it is required to investigate SOA formation from different

VOCs with different chemical structures and chemical functional groups for regions with different

BVOC compositions. SOA chemistry of a couple of plant emissions has been studied well in

laboratory experiments (Griffin et al., 1999a; Ng et al., 2006; Odum et al., 1996). These studies

have provided the foundation for SOA model predictions. The SOA formation mechanisms in

global climate and air quality models are highly variable (Kanakidou et al., 2005; Lee et al., 2016), and SOA formation consistently has been under-predicted in current models compared to actual measurements and observations (Hodzic et al., 2010, 2009; Yang et al., 2018). The uncertainties in the inputs of these models arise from incomplete chemical knowledge of degradation pathways and significant variability in measured SOA yields (Fry et al., 2014; Marais et al., 2017; M. Donahue et al., 2005). For instance, oxygenated terpenes, one type of plant VOCs, dominate emissions from drought-tolerant shrubs in southern California's coastal sage scrub ecosystem (Mehra et al., 2020), but very few studies have investigated SOA generated from the oxidation of these types of plant VOCs.

Isoprene and α-pinene, as the most abundant BVOCs from plants, have been the subject of many SOA studies (Carlton et al., 2009b; Després et al., 2012; Guenther et al., 2012; Kroll et al., 2006; Zhang et al., 2015), while other types of BVOCs have gotten less attention as oxygenated terpenes. Oxygenated terpenes can play important roles in ecosystems (Hallquist et al., 2009; Hamilton et al., 2009), and it has been suggested that oxygenated terpenes are the possible cause of the discrepancies between single component and actual plant emissions experiments (Mentel et al., 2009). The oxygenated monoterpene emissions and their ambient mixing ratios, dominated by linalool and perillene, were higher than anthropogenic and monoterpene emissions, with approximately four times higher average diurnal mixing ratios, in some agricultural regions in California (Gentner et al., 2014), which suggests that this type of BOVCs may be more significant for SOA production than other types in this area. Another study reported that BVOC profiles of coastal sage scrub shrubs consisted of more than 80% oxygenated monoterpenes such as camphor and 1,8-cineol (Mehra et al., 2020). These oxygenated terpenes can react with the OH radical (rate constants with OH are provided in Table 1) and form SOA. These types of shrubs are widely spread

across the U.S. and Canada (USDA Plants Database), and SOA mass is extremely underestimated across the western U.S., with a broad distribution of this plant type (Carlton et al., 2018).

Among oxygenated terpenes, camphor and 1,8-cineole have received more attention because of their contributions from essential oils, candles, and cleaning products to the indoor environment. For instance, the indoor total VOC mixing ratio, including 1,8-cineole as one of the major contributors, significantly increased upon evaporating essential oils (Su et al., 2007), potentially contributing to indoor secondary pollutants such as SOA in the presence of ozone. However, the impact of the oxygenated terpenes on atmospheric chemistry has not been studied well. Another less-studied oxygenated terpene is bornyl acetate which was reported as the major terpene of Siberian fir needle oil emission, with approximately 32% contribution to the total plant BVOCs (Hatfield and Huff Hartz, 2011). Bornyl acetate was the most frequently associated with insect infestation, increasing during the defoliation of the Calabrian pine needle tree (Foti et al., 2020). Borneol emissions could be increased due to biotic or abiotic stresses; for instance, increased temperature impacted the BVOC emission profiles of pine seedlings, which included a significant increase in the proportions of linalool and borneol (Kivimäenpää et al., 2016). Despite all of these potential significant impacts of oxygenated terpenes on atmospheric SOA chemistry, they have not been represented in detail in the literature.

This study investigated SOA formation and composition from the photooxidation of four oxygenated terpenes and α-pinene, as a reference compound, in an oxidation flow reactor (OFR) (Table 3.1). The investigation of these types of SOA produced important new knowledge on oxidation products, SOA yields, and SOA condensed phase composition from these important SOA precursors.

MATERIALS AND METHODS

SOA generation and collection. All the experiments were conducted in a laboratory at the University of California, Irvine. SOAs were generated in an oxidation flow reactor (OFR; Aerodyne, Inc.) with photooxidation of α-pinene (Acros Organics Inc., 98%) as a model compound, and four oxygenated terpenes, including camphor (Alfa Aesar Inc., 98%), 1,8-cineol (Sigma Aldrich Inc., 99%), borneol (Acros Organics Inc., 97%), and bornyl acetate (Sigma Aldrich Inc., 95%) using the set-up shown in Figure 3.1, and a summary of experimental conditions is provided in Table 3.2. Clean air was generated with a zero-air generator (Environics® Series 7000) and humidified by passing the clean air through a bubbler to produce and hold relative humidity (RH) in the OFR. Humid clean air was introduced into the glass sealed jar continuously as the VOC source with a flow rate of 10 L min^{-1}. The VOC from the VOC source and the humidified air was introduced to the inlet OFR. At the OFR outlet, there was a vacuum line with a vacuum pump (Thomas, Model 617CA22) and controlled with a needle valve at a flow rate of 6.8 L min^{-1}, which was applied for SOA mass yield curve and SOA mass yield versus OH exposure experiments. This vacuum flow was used for SOA collection for aerosol chemical composition analysis through a filter holder. Particle size distributions were continuously monitored at the OFR outlet with a scanning mobility particle sizer (SMPS; custom-built from TSI, Inc. and Brechtel Inc. components) with a pulling flow of 0.35 L min^{-1}. An ozone monitor (2B Technologies Inc., Model 106-M) was used to monitor the ozone level during experiments with a pulling flow of 1 L min^{-1}. The total outlet flow of the OFR was 8.15 L min^{-1} with a corresponding residence time of 1.59 min. For each point of each experiment, VOCs were collected at the OFR inlet and outlet on stainless steel vapor adsorbtion cartridges containing quartz wool, Tenax TA, and carbograph 5TD (Markes International, Inc.) by pulling 0.42 L min^{-1} through duplicate cartridges in a row for 4 to

5 min. Cartridges were capped and stored in a refrigerator until they were analyzed off-line with a thermos-desorption gas chromatograph-mass spectrometer (TD-GC-MS, Markes International TD-100xr autosampler, Agilent GC 7890B, equipped with a 30 m, DB-5 column, and Agilent 5975 MS). For each SOA sample type, two Teflon filters were collected in two separate experiments with exactly the same experimental design. Details of the GC operation and VOC quantification are provided in Appendix 3.

Detailed information about this Aerodyne OFR has been provided elsewhere (Lambe et al., 2015, 2011a, 2011b; Peng et al., 2019; Peng and Jimenez, 2020), and we explain briefly the OFR setting we used in this study here. The OFR in this study is a 13 L (45.7 cm length OD × 19.7 cm ID) aluminum cylinder equipped with two low-pressure mercury 185 and 254 nm lamps (BHK, Inc., model no. 82-904-03) to generate hydroxyl radicals (OH) through the photolysis of H_2O, O_2, and O_3. The OFR was operated in 185 mode; both 185 nm and 254 nm lamps were used in all experiments. This OFR 185 mode can reproduce conditions that better represent more realistic atmospheric conditions that drive aerosol chemistry (such as the ratio of RO_2/HO_x radicals) (Peng and Jimenez, 2020). These more realistic conditions were met by keeping RH more than 50% and keeping VOC mixing ratios relatively low (between 20 to 90 ppb). In this OFR mode, OH radicals were produced inside the OFR with the reaction of oxygen $O(^1D)$ radicals with water vapor, where $O(^1D)$ was produced via UV photolysis of ozone with 254 nm lamps inside the reactor. The ozone (O_3) was generated within the OFR with UV photolysis of oxygen with 185 nm lamps. The OH radicals then reacted with introduced VOCs to form SOA. For OFR calibration, the OH concentrations were varied by changing the UV light intensity by stepping the lamps' settings, and toluene (Alfa Aesar Inc., ≥ 99.5%) was introduced to the OFR as an OH tracer. Detailed information about the OFR calibration is provided in Appendix 3.

To generate SOA mass yield vs. OH exposure curves, the oxidant concentration, OH concentration, was adjusted by increasing and decreasing UV light intensity. The SOA mass yields were calculated for the OH exposure range of 4.2×10^{11} to 3.6×10^{12} molec s cm^{-3} with the corresponding equivalent of atmospheric photochemical ages of 3.2 to 27.8 days, respectively. The equivalent of the atmospheric photochemical ages was calculated assuming an ambient OH concentration of 1.5×10^{6} molec cm^{-3} (Mao et al., 2009).

The SOA mass yield was calculated as formed condensed organic aerosol mass (C_{OA}) divided by the mass of gas-phase VOCs that reacted (ΔVOC) inside the OFR. C_{OA} was calculated from SMPS particle size distributions measured at the OFR outlet by assuming a particle density of 1.4 g cm^{-3}, which is a reasonable value for these types of SOA (Faiola et al., 2018; Malloy et al., 2009; Nakao et al., 2013). SOA mass yield curve is a plot of aerosol mass yield versus total condensed organic mass, which has been applied as a common approach to characterize the SOA formation efficiency of VOCs (Ahlberg et al., 2017; Faiola et al., 2018; Griffin et al., 1999a; Odum et al., 1996; Pankow, 1994). For generating the SOA mass yield curves for each sample, the SOA mass yield was measured at multiple mass loadings. SOA mass yield curves for each chemical system were fit via two methods:

The first method is the two-product model developed by Odum et al. (1996) with the following equation:

$$Y = M_0 \left[\frac{\alpha_1 \, K_{OM1}}{1 + K_{OM1} \, M_0} + \frac{\alpha_2 \, K_{OM2}}{1 + K_{OM2} \, M_0} \right]$$

where Y is mass yield; M_0 is the organic particle mass ($\mu g/m^3$); K_{OMi} is the partitioning coefficient of product i, and α_i is the mass-based stoichiometric yield of product i.

The second method is the volatility-basis set (VBS) model proposed by Donahue et al. (Donahue et al., 2006) with the following equation:

$$Y = \sum \alpha_i \left(\frac{1}{1 + \frac{c_i^*}{C_{OA}}}\right)$$

where Y is mass yield; α_i is the mass-based stoichiometric yield for product i, and c_i^* is the effective saturation concentration in µg/m³ of i. For fitting a curve to the data point in the SOA mass yield plots, a four-product basin set was used with $\alpha_1, \alpha_2, \alpha_3,$ and α_4, where $c^* = \{1, 10, 100, 1000\}$ µg/m³. The c_i^* values were fixed while the α_i values were the free parameters in the basis set.

High-resolution mass spectrometry sample run and data analysis. For each sample type, generated SOA particles were collected at the outlet of OFR on Teflon filters (MilliporeSigma, Sigma Aldrich Inc., 0.2 µm PTFE membrane) for high-resolution Orbitrap mass spectrometry. The composition of each SOA type was determined from duplicate samples. Immediately after collection, the filter samples were kept in a -80°C freezer until the analysis time. For chemical composition analysis, each filter was thawed and extracted into 4 mL of a mixture of 1:1 acetonitrile (ACN) (Honeywell Inc., Burdick & Jackson®, ≥ 99.93%) and water (18.2 MW cm; Thermo Scientific, Barnstead; model 7146). The SOA extracts were then analyzed using an ultra-performance liquid chromatography-mass spectrometer (UPLC-MS) equipped with a Vanquish Horizon UPLC system (including a binary liquid chromatography pump, an autosampler, a column manager, and a diode array detector) coupled to a high-resolution Q Exactive Plus Orbitrap mass spectrometer. A Luna Omega 1.6 µm particle size Polar C18 150 × 2.1 mm (Phenomenex) column fitted with a SecurityGuard ULTRA cartridge (porous polar C18, 2.1 mm; Phenomenex) maintained at 30°C was used for the compound separation. The mobile phase combination was

(A) 0.1% formic acid (Fisher Chemical) in HPLC grade water (Fisher Chemical) and (B) 0.1 %

formic acid in HPLC grade acetonitrile (Fisher Chemical). The eluent gradient was as follows: 0-

3 min hold at 5% B, 3-14 min linear gradient to 95% B, 14-16 min hold at 95% B, 16-22 min linear

gradient back to 5% B with a flow rate of 300 μL min^{-1}. Analysis was carried out using the heated

electrospray source (HESI), and the source conditions were as follows: capillary voltage, 2.50 kV

(negative mode) and 3.50 kV (positive mode); capillary temperature 320 °C (negative mode) and

325°C (positive mode); sheath gas flow rate, 50; auxiliary gas flow rate, 10; sweep gas flow rate,

1; S-lens RF level 50; auxiliary gas heater temp, 300C. The analysis for each sample (injection

volume = 10 mL) was performed in both positive (ESI (+)) and negative (ESI (-)) ion modes using

a full scan data-dependent MS/MS (FS-ddMS^2) approach. In this approach, full MS scans were

recorded over the *m/z* 50-750 mass range with a resolution of 140,000 and an AGC target of 10^6

(max. IT = 100 ms), while MS/MS scans were recorded for the top 3 most abundant ions from the

adjacent full MS scan (res. 17,500; AGC target 5 × 10^4; max. IT 50 ms) using normalized collision

energies (NCE) of 10, 30 and 50. The data were acquired using Xcalibur 4.2 software (Thermo

Scientific) and then processed using FreeStyle^{TM} version 1.6.75.20 (from Thermo Scientific Inc.).

Almost no peaks were observed in the ESI (+) modes; thus, only the ESI (-) mode results are

presented in the result and discussion section. In addition to SOA extracts, two types of blank

samples were run with SOA samples so that the background spectra could be subtracted from the

sample spectra. The first blank sample was just the solvent (water and ACN) and the second blank

sample type was an extract of a Teflon filter from the collection at the OFR outlet when only clean

humid air was through the OFR without any introduced VOCs at the OFR inlet.

The analysis of the high-resolution mass spectrometry (HR-MS) and assignment of the

molecular formulas was performed following similar previous works (Fleming et al., 2018;

Nizkorodov et al., 2011; Romonosky et al., 2015). Briefly, peaks and their intensities were determined using the Decon2LS software (https://omics.pnl. gov/software/decontools-decon2ls). ^{13}C isotopes and obvious impurities (if they existed) with anomalous mass defects were removed from peaks. All peaks were assigned to the formulas $C_XH_YO_Z$ with an accuracy of ±0.001 m/z units, while elemental ratios for assigning were constrained to 0.30 < H/C < 2.25 and 0 < O/C < 2.30 (Smith et al., 2021), where O/C is the oxygen to carbon ratio and H/C is the hydron to carbon ratio. The high-resolution mass spectra results presented in this paper were reported as formulas of neutral SOA compounds.

To get further insight into the SOA chemical composition of samples, based on chemical composition analysis, each organic compound identified in the SOA samples was plotted in two-dimensional space, including the oxidation state of carbon (OS_C) and carbon number, which has been referred to as a "Kroll diagram" (Kroll et al., 2011). OS_C for each compound was calculated as $OS_C=2×O/C-H/C$ based on methods presented by Kroll et al. (Kroll et al., 2011), where O/C is the oxygen to carbon ratio and H/C is the hydron to carbon ratio.

SOA formation mechanism. SOA formation was investigated using the Generator for Explicit Chemistry and Kinetics of Organics in the Atmosphere (GECKO-A). The description of the GECKO-A is provided in detail by Aumont et al. (Aumont et al., 2005), and updates have been provided (Aumont et al., 2013; La et al., 2016; McVay et al., 2016; Valorso et al., 2011). This model is a tool to generate nearly explicit gas-phase oxidation mechanisms for organic compounds, as well as the properties, to show the gas-particle partitioning of organic compounds in the mechanism.

Volatility and viscosity predictions. The volatility of oxidation products in each SOA sample was determined via assigned molecular formulas from the high-resolution MS data, and it was

estimated based on the number of carbon and oxygen atoms in each molecule based on the parameterizations of pure compound saturation mass concentration (C_0) reported in Li et al. (Li et al., 2016) for CHO compounds using the following equation:

$$log_{10} C_0 = (n_C^0 - n_C)b_C - n_O b_O - 2\frac{n_C n_O}{n_C + n_O}b_{CO}$$

where n_C^0 is the reference carbon number, and n_C and n_O are the number of carbon and oxygen atoms, respectively. The values for n_C^0, b_C, b_O, and b_{CO} were 22.6, 0.448, 1.656, and -0.779, respectively, for reference CHO compounds recommended by (Li et al., 2016).

The viscosity of each SOA sample was estimated using the method presented by DeRieux et al. (DeRieux et al., 2018a). The glass transition temperature ($T_{g,i}$), at which between amorphous solid and semi-solidstatates a phase transition happens (Koop et al., 2011), was predicted as a function of molecular composition for each SOA compound in each SOA sample as following equation (DeRieux et al., 2018a):

$$T_{g,i} = (n_C^0 + \ln(n_C))b_C + \ln(n_H)\,b_H + \ln(n_C)\ln(n_H)\,b_{CH} + \ln(n_O)\,b_O + \ln(n_C)\ln(n_O)b_{CO}$$

where n_C, n_H, and n_O are the numbers of carbon, hydrogen, and oxygen atoms, respectively. For CHO compounds, the coefficients n_C^0, b_C, b_H, b_{CH}, b_O, and b_{CO} were 12.13, 10.95, -41.82, 21.61, 118.96, and -24.38, respectively (DeRieux et al., 2018b). The glass transition temperature of the SOA under dry conditions ($T_{g,org}$) was calculated based on the Gordon-Taylor equation, assuming the Gordon-Taylor constant (κ_{GT}) as 1 for each organic compound (Dette et al., 2014):

$$T_{g,org} = \sum \omega_i T_{g,i}$$

where ω_i is the mass fraction of an organic compound i from mass spectra. The water content in SOA was calculated using the effective hygroscopicity parameter (κ) (Petters and Kreidenweis, 2007). The value of κ was from cloud condensation nuclei measurements of 0.15 by Zhao et al.

(Zhao et al., 2017). T_g for organic-water mixtures ($T_{g,mix}$) was calculated by Gordon-Taylor equationwith constant of $k_{GT}= 2.5$ (Koop et al., 2011; Zobrist et al., 2008) as following:

$$T_{g,mix} = \frac{(1 - w_{org})T_{g,H_2O} + \frac{1}{k_{GT}}w_{org}T_{g,ORG}}{(1 - w_{org}) + \frac{1}{k_{GT}}w_{org}}$$

where T_{g,H_2O} and $T_{g,org}$ are the glass transition temperatures of water and SOA organics and w_{org} is the mass fraction of the organic compounds. The mass of water (m_{H_2O}) and SOA (m_{SOA}) were used to calculate w_{org} as $w_{org} = \frac{m_{SOA}}{(m_{SOA}+m_{H_2O})}$, and can be estimated by the effective hygroscopicity factor (κ) (Petters and Kreidenweis, 2007) as following:

$$m_{H_2O} = \frac{\kappa\rho_w m_{SOA}}{\rho_{SOA}(\frac{1}{a_w} - 1)}$$

The density of water (ρ_w) is 1 g cm⁻³, and the density of SOA (ρ_{SOA}) is assumed to be as 1.4 g cm⁻³ (Faiola et al., 2018; Malloy et al., 2009; Nakao et al., 2013), and a_w is the water activity is RH/100 (Kuwata and Martin, 2012).

The Vogel-Tammann-Fulcher (VTF) equation was used to calculate the temperature-dependence of viscosity using $T_{g,mix}$:

$$\log(\eta) = -5 + 0.434\frac{T_0 D_f}{T - T_0}$$

where T_0 is the Vogel temperature as : $T_0 = \frac{39.17 T_g}{D_f + 39.17}$ with assumed viscosity of 10^{12} Pa s at the glass transition temperature (Angell, 2002), and T is the temperature at which measurements were done, which was 291 K. The fragility parameter (D_f) was assumed to be 10 (DeRieux et al., 2018a). This parameter characterizes temperature dependence of viscosity deviation from the Arrhenius behavior (Angell, 1991; DeRieux et al., 2018a).

Aerosol Mass Spectrometer Measurements of SOA from Real Plants. We included SOA results from previous work (Mehra et al., 2020) to compare SOA formed from real plant emissions as a complex system and SOA formed from single pure VOCs. The plants used for SOA generation are among common plant species in southern California's coastal sage ecosystem (www.calflora.org), with BVOC emission profiles dominated by oxygenated terpenes. Details of how this study was conducted are provided in Mehra et al., 2020. Briefly, SOA was formed inside an OFR from the photooxidation of black sage (*Salvia mellifera*; Sage) and California sagebrush (*Artemisia californica*; Artemisia) and pure standards, including oxygenated terpenes (Mehra et al., 2020). The Sage BVOC emission profile was dominated by camphor with 57% contribution to the total and 13% contribution of 1,8-cineole. The Artemisia plant BVOC emission profile included 25% contribution of 1,8-cineole and 5% contribution of camphor.SOA composition was continuously measured at the OFR outlet with a high-resolution long-time-of-flight aerosol mass spectrometer (HR-LToF-AMS; Aerodyne Research, Inc.), described in detail elsewhere (DeCarlo et al., 2006). The AMS data was analyzed using the Squirrel (v1.60P) and Pika (v1.20P) ToF-AMS toolkits in Igor Pro (v6.37; WaveMetrics, Inc.).

Statistical Analysis. The hierarchical clustering analyses on the chemical composition of SOA samples were performed using R (version1.2.5001). Heatmap was plotted using the function heatmap.2 from the "gplots" package (Warnes et al., 2022).

RESULTS and Discussion

SOA Mass Yield versus Oxidant Exposure

The OH concentration influenced the mass yields of each SOA type generated in the OFR, as expected (Lambe et al., 2015; Li et al., 2019; Palm et al., 2018, 2017, 2016; Zhao et al., 2021),

and this effect was shown for each chemical system included in this study (Figure 3.2). Between all chemical systems, maximum SOA mass yield values are 0.47±0.04, 0.35±0.06, 0.33±0.06, 0.31±0.04, and 0.21±0.04 for camphor, 1,8-cineole, borneol, α-pinene, and bornyl acetate, respectively (± represent standard deviation). These maximum SOA yield values occurred at corresponding OH exposures as 5.02×10^{11}, 5.08×10^{11}, 5.14×10^{11}, 5.14×10^{11}, and 5.13×10^{11} molec s cm^{-3} for camphor, 1,8-cineole, borneol, α-pinene, and bornyl acetate, respectively. The OH exposures ranged from 4.2×10^{11} to 3.7×10^{12} molec s cm $^{-3}$, corresponding to equivalent atmospheric photochemical ages of ~3-28 days, respectively, assuming the ambient OH concentration of 1.5×10^{6} molec s cm^{-3} (Mao et al., 2009). Overall oxidation of bornyl acetate formed SOA (BAC) had low yields, while α-pinene formed SOA (API) with moderate yields as expected based on a previous study on α-pinene (Eddingsaas et al., 2012; Lambe et al., 2015). Camphor SOA (CAM) had the highest yields compared to the other compounds. The OH exposure inflection points, where SOA yields shift from increasing with increasing OH exposure to decreasing with increasing OH exposure, were similar across all the chemical systems in this study, occurring at OH$_{exp}$~ 5.1×10^{11} molec s cm $^{-3}$. This suggests that the chemistry of all the systems moved from being dominated by functionalization to fragmentation reactions at approximately the same level of OH exposure (equivalent to 4 atmospheric photochemical age) regardless of their different chemical structures and reactivities (Table 3.1). At low OH exposures (less than 5.1×10^{11} molec s cm $^{-3}$) with increasing the OH exposure, the photooxidation of precursors generated more condensation products with lower volatility compared to the region with high OH levels (greater than 5.1×10^{11} molec s cm $^{-3}$), and these condensation products increased the SOA yields. While at high OH levels, fragmentation reaction became a significant mechanism with increasing OH exposure. Previous studies reported that the SOA mass yields for α-pinene reached a maximum

yield of 0.39 (Zhao et al., 2021) and 0.35 (Lambe et al., 2015) at approximately 6×10^{11} molec s cm^{-3} within an OFR. These results are comparable to the maximum α-pinene yield measured in this study of 0.31 (Figure 3.2). Comparing the α-pinene plot to the previous study, the yield of α-pinene dropped more rapidly at the lower OH exposure values (left side of the inflection point), which may be due to the losses of low-volatility compounds inside the OFR in this study. Borneol yields did not decrease as rapidly as 1,8-cineole, α-pinene, and bornyl acetate by increasing OH exposure, which could possibly mean that borneol is more resistant to fragmentation, causing higher yields.

SOA Mass Yield Curves

SOA mass yields were calculated as a function of total condensed organic mass loading for each SOA precursor to compare the SOA formation efficiency of the four oxygenated terpenes with α-pinene as a reference compound (Figure 3.3). The experimental conditions used for these experiments correspond to the OH exposure that led to the highest SOA yields in Figure 3.2. SOA mass yield curves for each chemical system were fit via two methods. The estimated coefficients are summarized in Table 3.3 for these two models. Overall, the range of SOA mass yield was from 3% to 56% across a condensed organic aerosol (C_{OA}) mass range of 3-176 μg/m^3 in the OFR. Bornyl acetate (BAC) had the lowest SOA mass yields and was the only oxygenated terpene with a lower yield than α-pinene (API). Borneol (BOR) and 1,8-cineole (CIN) had very similar SOA mass yields slightly higher than α-pinene. Camphor (CAM) had the highest SOA mass yield among these oxygenated terpenes and α-pinene. At mass loading C_{OA}=40 μg/m^3 the corresponding yields were 11%, 20%, 24%, 25%, and 33% for bornyl acetate, α-pinene, 1,8-cineole, borneol, and camphor, respectively.

These results for SOA from oxygenated terpenes were compared to SOA generated from blends of BVOC emissions of Salvia mellifera (Sage) and Artemisia californica (Artemisia) in an OFR via OH oxidation obtained in a previous study (Mehra et al., 2020). The plant emissions in this study were dominated by oxygenated monoterpenes such as camphor and 1,8-cineol. The SOA mass yields for Sage and Artemisia were reported as 9%±4% and 6%±1% at mass loadings of 11.4±6.3 μg/m^3 and 11.2±2.7 μg/m^3, respectively, which are comparable with SOA mass yields of 15% and 13% for camphor and 1,8-cineole with mass loadings of 8 μg/m^3 and 11 μg/m^3, respectively. These low yields for SOA from real plant emissions could be due to the VOC mixture effects. Sage plant BVOC emissions were dominated by camphor with 57% contribution and with 13% contribution of 1,8-cineole. Artemisia emissions included 25% of 1,8-cineole and 5% of camphor. It should be considered that the BVOC profiles of these plant emissions include other BVOCs, which might differ in SOA mass yield. Deviations from expected yields for complex systems such as VOC mixtures were reported previously; for instance, a higher than expected yield was reported in mixtures containing myrcene which was attributed to producing a significantly higher number of nucleation particles compared to the other precursors in the mixture (Ahlberg et al., 2017). Thus, SOA from complex VOC systems, such as plant emissions, can impact oxidant reactivity and subsequent generated products compared to single VOC systems (McFiggans et al., 2019); thus, this causes deviation from expectation from SOA mass yields of single VOC systems. This highlights the importance of investigating the SOA formed from mixed plant volatiles instead of SOA from a single precursor.

SOA Chemical Composition

High-resolution Mass Spectra. The high-resolution mass spectra of CAM, BOR, CIN, and BAC in ESI (-) modes, compared to API, are shown in Figure 3.4. The five most abundant peaks of each

SOA type, with assigned formula, are presented. The relative contributions of these five dominant peaks to the total detected peaks were 28%, 27%, 24%, 22%, and 13% for BOR, CIN, CAM, API, and BAC, respectively. Most of the abundant peaks detected in API were consistent with previous studies, including $C_8H_{12}O_4$, $C_8H_{12}O_5$, $C_{10}H_{16}O_5$, $C_{10}H_{14}O_6$, and $C_{10}H_{16}O_6$ (Jia and Xu, 2020; Kourtchev et al., 2015; Kristensen et al., 2014; Romonosky et al., 2017; Winterhalter et al., 2003; Wong et al., 2021; Zhang et al., 2015). Some of the abundantly detected peaks in the API sample were also observed among the most abundant compounds in other SOA types, such as $C_8H_{12}O_4$, $C_{10}H_{16}O_5$, $C_{10}H_{14}O_6$, $C_9H_{14}O_4$, $C_{10}H_{16}O_6$, and further investigation about the peaks with the same assigned formulas is provided in the results from GECKO-A model further in this section. In BOR and CAM sample, $C_9H_{14}O_3$ was among top-5 detected peaks, and this chemical formula was assigned to pinalic acid in the α-pinene oxidation experiment (Jia and Xu, 2020; Wong et al., 2021). The monomer-to-dimer transition point on each mass spectra is mentioned in the caption of Figure 3.4. The shift of the mass spectrum toward the molecules with higher mass was expected for BAC as a C_{12}-compound, retaining its backbone, compared to the other SOAs, which are C_{10}-compounds. There were large contributions of C_8, C_9, and C_{10} compounds for all SOA types and a large C_{10} and C_{12} contribution for BAC.

The general carbon contributions (Figure 3.5) were comparable with a previous study for SOA from monoterpenes (Dam et al., 2022), and it demonstrates that the mass spectrum of CAM had the largest contribution of dimeric compounds (17%) than those of API (15.5%), CIN (14.5%), BOR (14%), and BAC (10%), and the order of distribution of monomeric compounds was exactly in contract with dimeric compounds as BAC (90%), BOR (86%), CIN (85.5%), API (84.5%), and CAM (83%). Thus, the order of dimer to monomer ratio from the highest to the lowest was as follows, CAM with the highest and BAC with the lowest dimer to monomer ratio, CAM (0.21),

76

API (0.18), CIN (0.17), BOR (0.16), and BAC (0.11). This order of dimer to monomeric ratio agrees with the order of mass yield curves from the highest to the lowest in Figure 3.3, in which camphor had the highest and bornyl acetate showed the lowest SOA mass yields. The carbon distribution in dimeric and monomeric regions was as expected. For instance, there were more C_8, C_9, and C_{10} for API, CAM, BOR, CIN (as C_{10}-compounds), and more C_{11}-C_{14} for BAC (as a C_{12}-compound), in the monomeric region. There was a large contribution of C_{18} compounds in the dimeric region of API and BAC, while BOR, CAM, and CIN had the highest contribution of C_{12}-C_{14} in this region, which is in agreement with the orders of SOA mass yields (Figure 3.3), as these dimeric compounds can contribute effectively to SOA formation. The oxygen distributions for monomeric and dimeric regions are also provided in the summary table to get further insight into oxidation. BAC had distributions of oxygen evenly in both dimeric and monomeric regions; however, API, CAM, and BOR showed the highest contributions of O_4 and O_5 in the monomeric region and O_9 in the dimeric region.

The reaction pathways of OH oxidation of camphor, 1,8-cineole, and bornyl acetate are shown in Figure S3.1. I modeled these three compounds with GECKO-A, as borneol had a very similar chemical SOA composition (Figures 3.4), and α-pinene has been modeled previously (Afreh et al., 2021). A couple of reaction products had the matched chemical formulas with the peaks detected by HR-MS data analysis. These matched compounds with matched formulas are shown in Figure S3.1. To compare the result with oxidation products for α-pinene, the potential structures associated with the masses/formulas from HR-MS data analysis, we used a previous work that analyzed SOA from the photooxidation of α-pinene with HR-MS equipped with orbitrap in ESI (-) mode (Jia and Xu, 2020). The summary of these aligned peaks between HR-MS data analysis and GECKO-A mechanisms with potential structures associated with formulas is shown

in Table S3.3. Some of these matched masses also corresponded to exact masses with the same predicted chemical formulas that were expected for α-pinene oxidation. For instance, comparing the chemical formulas between HR-MS and GECKO-A model results, $C_7H_{10}O_4$, $C_9H_{14}O_4$, $C_{10}H_{16}O_4$, and $C_{10}H_{16}O_5$ were observed in both API and CAM. $C_9H_{14}O_5$ was present in BAC, API, CAM, and $C_9H_{16}O_6$ was observed in both API and CIN. $C_9H_{16}O_5$ was seen in all samples, including BAC, CIN, CAM, and API. Comparing the proposed structures associated with these chemical formulas (Table S3.3), they were actually different compounds with different chemical structures but the same chemical formulas/masses. However, $C_7H_{10}O_5$ observed in CAM and API had the same proposed chemical structure. Those different compounds with the same chemical formulas highlight that just looking at the HR-MS data from ambient SOA samples and assigning chemical structures might be misleading and need further investigation. Based on the GECKO model outputs, BAC and CAM had more matches between the model predicted compound and HR-MS data analysis than CIN.

Figure 3.6 shows that highly oxidized organic compounds in aerosols have $OS_C \geq +1$, while the reduced compounds have $OS_C \leq 0$ (Kroll et al., 2011). Figure 3.6 shows that consistent with previous studies, the majority of compounds in each SOA had OS_C between -1 and +1 with carbon numbers up to 30 (Benoit et al., 2021; Chhabra et al., 2015; Kourtchev et al., 2015; Kroll et al., 2015, 2011; Zhang et al., 2015). It has been suggested that multi-step oxidation reactions generate semivolatile and low volatility oxidized organic aerosols with OS_C between -1 and +1 carbon number ≤ 1 (Kroll et al., 2011). It should be considered that the large clusters of molecules with carbon numbers ≥ 15 are likely related to dimers and trimers of the oxidation products. The clusters with more compounds at higher carbon numbers (between 25 to 30) at $OS_C < -1$ in BAC, BOR, and API samples can indicate oligomerization (Kroll et al., 2011). The relative intensities of

these highly reduced large molecules are very small. In general, contributions of higher-order oligomers tend to have lower OS_c than monomers and dimers, which can favor lower O:C ratios in larger particles (Tu and Johnston, 2017). Overall, the average O:C ratios calculated from the high-resolution mass spectrometry data were 0.66±0.25 for CIN, 0.60±0.22 for CAM, 0.60±0.25 for BOR, 0.60±0.24 for API, and 0.59±0.24 for BAC. These average O:C ratios (average ± standard deviation) are within a very similar range, meaning that the SOA compounds were approximately oxidized at the same level inside the OFR.

Estimated SOA Properties. To investigate the chemical characteristics of these oxygenated terpenes SOAs further, the glass transition temperatures (T_g) of SOA were plotted as a function of saturation mass concentration of individual compounds (defined as C_0) (Figure 3.7). Four regions representing extremely low volatility organic compounds (ELVOC, $C_0 < 3\times10^{-4}$ μg/m^3), low-volatility organic compounds (LVOC, $3\times10^{-4} < C_0 < 0.3$ μg/m^3), semi-volatile organic compounds (SVOC, $0.3 < C_0 < 300$ μg/m^3), and intermediate volatility organic compounds (IVOC, $300 < C_0 < 3\times10^6$ μg/m^3) (Li et al., 2020) are shown. Because CAM and BOR had very similar $T_{g,org}$ plots, which agree with Figure 3.4 and Figure 3.5, only CAM is shown in Figure 3.7.

For all SOA experiments, $T_{g,org}$ decreases with increasing C_0, and this is because smaller compounds tend to be more volatile (Shiraiwa et al., 2014) and less viscous (Rothfuss and Petters, 2017; Thomas et al., 1979). There are more individual compounds with large abundance across the SVOC region in BAC than API, CAM, and CIN. The larger abundance of lower volatility compounds in BAC with larger $T_{g,org}$ could cause SOA with higher viscosity. CAM and API showed individual compounds with larger abundance within the IVOC region. CIN also has more individual compounds with a larger abundance within the IVOC region; however, the most abundant compounds were in the threshold of the SVOC region.

The SOA viscosity is affected by molecular weight, the degree of chemical constituent oxidation, temperature, and RH (Dette et al., 2014; Koop et al., 2011; Saukko et al., 2012; Shiraiwa et al., 2017a). A parameterization method has been developed and applied for predicting the viscosity of several types of SOA (DeRieux et al., 2018a; Li et al., 2016; Shiraiwa et al., 2017a). Based on this method, estimated viscosity values were 2700 Pa s, 1800 Pa s, 1600 Pa s, 1300 Pa s, and 780 Pa s for SOA generated from bornyl acetate, α-pinene, camphor, borneol, and 1,8-cineole, respectively. This parameterization has been used to estimate the viscosity of SOA from α-pinene in previous studies (DeRieux et al., 2018a; Renbaum-Wolff et al., 2013; Smith et al., 2021), and at RH around 50%, the predicted viscosity was between 103 to 104 Pa s. Bornyl acetate with the lowest SOA mass yields had the highest estimated viscosity. Overall, there were small differences in predicted viscosity values of these different SOA types, which seem internally consistent in this study. However, the overall variation observed between these systems is very small. These systems all have quite similar viscosity relative to ambient aerosol ranges.

SOA Composition Comparison. Figure 3.8 shows the hierarchical clustering analysis result, heatmap, for HR-ToF-AMS and HR-MS equipped with Orbitrap data. These heatmaps can help compare/contrast and link SOA composition from single precursors with SOA from a complex system, such as real plant emissions. Interestingly, hierarchical clustering of the HR-ToF-AMS data (Figure 3.8a) showed that the real plant SOA were most similar to each other and were equally dissimilar to SOA formed from 1,8-cineole. Based on the analysis on SOA chemical composition from HR-MS data (Figure 3.8b), the composition of borneol and camphor SOA were most similar to one another, while 1,8-cineole SOA had the largest differences in composition compared to all other samples (Figure 3.7b). This result is consistent with Figure 3.4, in which camphor and borneol had similar MS plots, while 1,8-cineole and bornyl acetate had the most different mass

spectra plots compared to all samples. Mehra et al. (2020) reported that sage. These results suggest that SOA formed from simple standards does not accurately represent the complexity of real plant emissions.

CONCLUSION

Our study suggests that among oxygenated monoterpenes that we study, camphor had the highest SOA formation potential, and bornyl acetate had the lowest SOA formation potential in the following order from the highest to the lowest: camphor, borneol, 1,8-cineol, α-pinene, and bornyl acetate. Based on the GECKO-A oxidation schemes for camphor, 1,8-cineole, and borneol, there were a couple of matched products with the same chemical formulas from the HR-MS data. However, it was observed that the proposed chemical structures of these matched compounds were different from the chemical structures of the compounds with the same mass/formulas for α-pinene SOA. This result highlights that by looking at the HR-MS data, this would be misleading to assign chemical structures to ambient SOA samples using the common previously reported structures based on the exact mass or chemical formulas. Based on the GECKO model outputs, BAC and CAM had more matches between the model predicted compound and HR-MS data analysis than CIN Hierarchical clustering analysis of HR-MS data showed that the composition of borneol and camphor SOA were most similar to each other. 1,8-cineole SOA had the largest differences in composition compared to the other SOA types. The hierarchical clustering analysis of HR-ToF-AMS data showed that the SOA formed from real plants emissions, dominated by oxygenated monoterpenes, was most similar to each other and were equally dissimilar to SOA formed from oxygenated monoterpenes, such as camphor. In agreement with the other hierarchical clustering analysis on SOA from oxygenated monoterpenes, 1,8-cineole SOA was the most different in this

analysis. This suggests that SOA formed from single VOC systems is not accurately representing

the real plant emissions complexity.
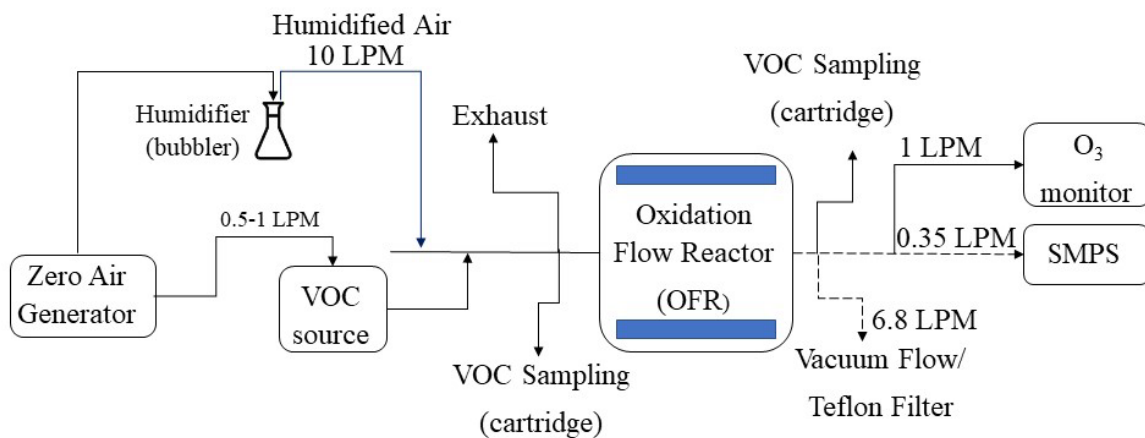
Figure 3.1. Experimental design. A schematic of the experimental setup. Solid lines represent PFA tubing, and dashed lines refer to copper tubing. LPM indicates liter per minute. Sampling refers to VOC and SOA sampling locations on cartridges and Teflon filters, respectively. SMPS refers to a scanning mobility particle sizer.
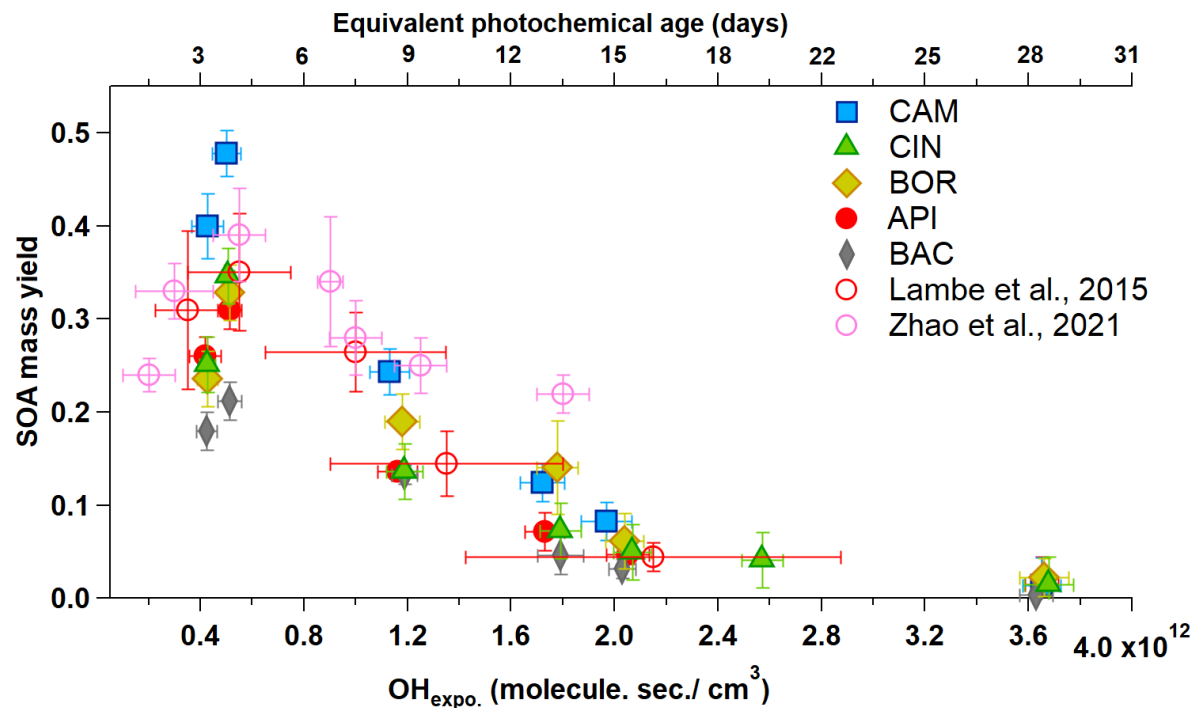
Figure 3.2. SOA mass yield versus oxidant exposure. SOA yields from photooxidation in an OFR/PAM as a function of OH exposure. The error bars indicate standard deviations of OH exposures and SOA mass yield over x- and y-axis from duplicate points, respectively. Red un-filled circles indicate data from Lambe et al. (2015), and un-filled pink circles indicate data from Zhao et al. (2021).
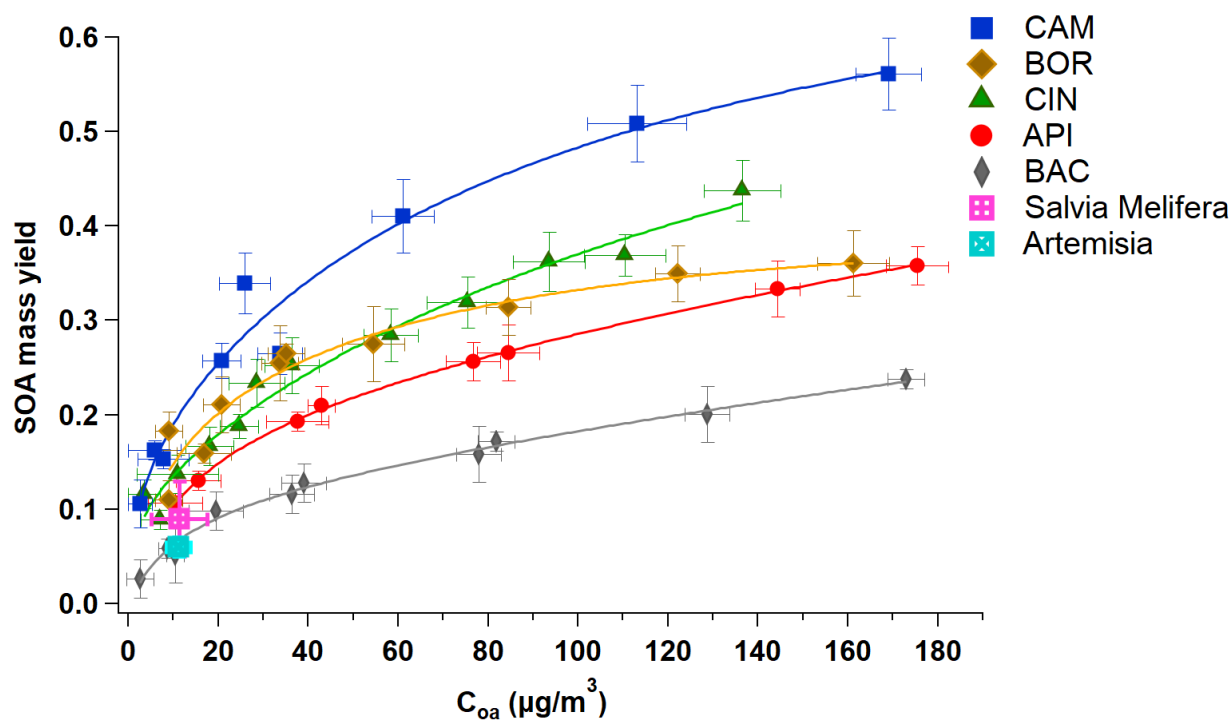
Figure 3.3. SOA mass yield curves. SOA mass yield curves for camphor (CAM), borneol (BOR), 1,8-cineole (CIN), α-pinene (API), and bornyl acetate (BAC), and SOA mass yields from real plant emissions of Salvia *mellifera* and Artemisia *californica* (from a previous work of Mehra et al. (2020)). Error bars denote standard deviations of measurements.
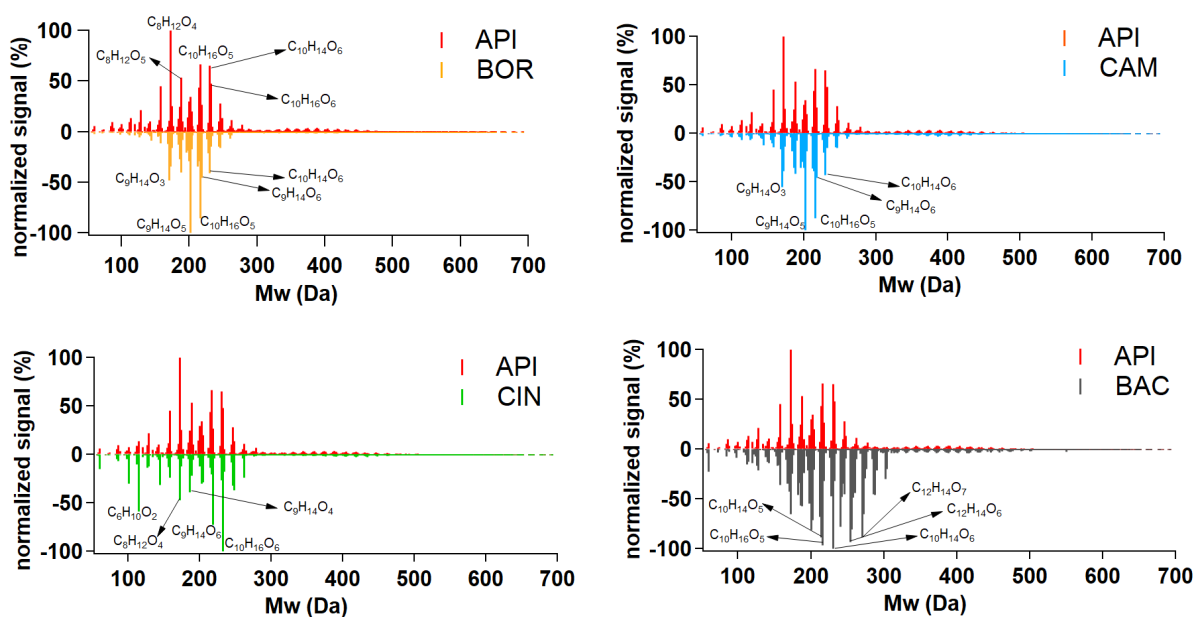
Figure 3.4. SOA mass spectra. High-resolution mass spectra in ESI (-) modes (normalized intensities) of α-pinene SOA (API), borneol SOA (BOR), camphor SOA (CAM), 1,8-cineol SOA (CIN), and bornyl acetate SOA (BAC). The monomeric and dimeric are as follows: the monomeric region for α-pinene is $Mw < 300$ Da, and the dimeric region is 300 Da $<Mw < 500$ Da; the monomeric region for borneol and camphor is $Mw < 260$ Da, and the dimeric region is 260 Da $<Mw < 500$ Da; the monomeric region for 1,8-cineole is $Mw < 250$ Da, and the dimeric region is 250 Da $<Mw < 500$ Da; the monomeric region for bornyl acetate is $Mw < 320$ Da, and the dimeric region is 320 Da $<Mw < 600$ Da.

		API	CAM	BOR	CIN	BAC
	monomer	84.5%	83%	86%	85.5%	90%
	dimer	15.5%	17%	14%	14.5%	10%
monomer carbon	< C6	5%	2%	1%	7%	2%
	C6	5%	3%	1%	13%	2%
	C7	13%	8%	8%	11%	6%
	C8	20%	17%	16%	15%	11%
	C9	18%	34%	37%	23%	18%
	C10	38%	36%	36%	30%	27%
	C11-14	0%	0%	0%	0%	33%
dimer carbon	C12-14	13%	19%	25%	20%	0%
	C15	10%	9%	9%	10%	11%
	C16	15%	11%	11%	13%	13%
	C17	16%	16%	15%	16%	15%
	C18	18%	19%	21%	17%	20%
	C19	12%	15%	12%	16%	14%
	C20	10%	8%	6%	6%	13%
	C21-28	6%	2%	2%	2%	14%
$C_{7-12}O_X$	< O3	4%	4%	3%	4%	4%
	O3	3%	11%	9%	1%	6%
	O4	23%	21%	17%	18%	16%
	O5	29%	37%	39%	19%	25%
	O6	23%	19%	21%	34%	22%
	O7	12%	6%	8%	17%	15%
	O8	5%	2%	2%	5%	8%
	O9-13	2%	0%	0%	1%	4%
$C_{14-21}O_X$	< O7	3%	6%	7%	2%	7%
	O7	9%	11%	11%	6%	9%
	O8	16%	17%	14%	11%	12%
	O9	23%	19%	19%	17%	18%
	O10	19%	17%	19%	20%	19%
	O11	13%	14%	12%	19%	13%
	O12-15	17%	16%	17%	24%	22%

Relative to total	0%	15%	50%	80%	100%

Figure 3.5. Carbon and oxygen distributions. Ratios of oxidized products separated into categories for α-pinene SOA (API), borneol SOA (BOR), camphor SOA (CAM), 1,8-cineol SOA (CIN), and bornyl acetate SOA (BAC) from HR-MS results in ESI (-) mode; the color axis indicates the relative contribution to the total. In each section of the table in Figure 3.5, including monomer and dimer, monomer carbon, dimer carbon, $C_{7-12}O_X$, and $C_{14-21}OX$, the sum of the distributions for each sample in each column adds up to 100. The color of each cell is based on the relative abundance of signal intensity of the corresponding detected peak/s to the total.
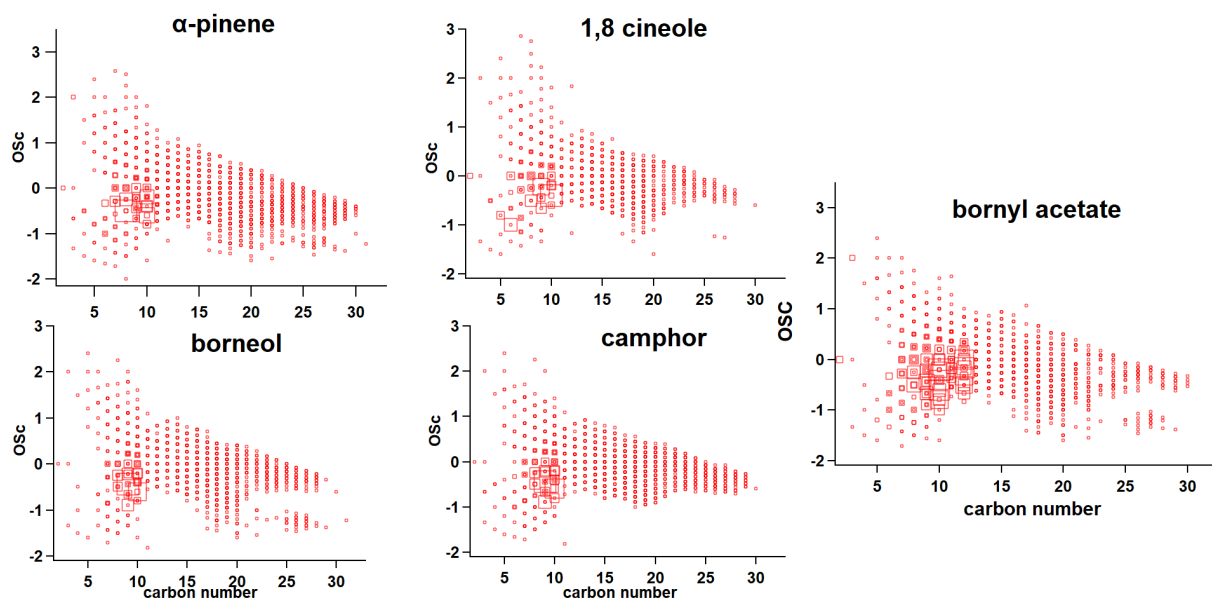
Figure 3.6. Kroll diagrams. Carbon oxidation state (OS$_C$) versus the number of carbon atoms for assigned compounds from HR-MS results in ESI (-) mode for α-pinene SOA (API), borneol SOA (BOR), camphor SOA (CAM), 1,8-cineol SOA (CIN), and bornyl acetate SOA (BAC). Each marker denotes a detected peak, and the size of the marker indicates the relative abundance of the intensity.
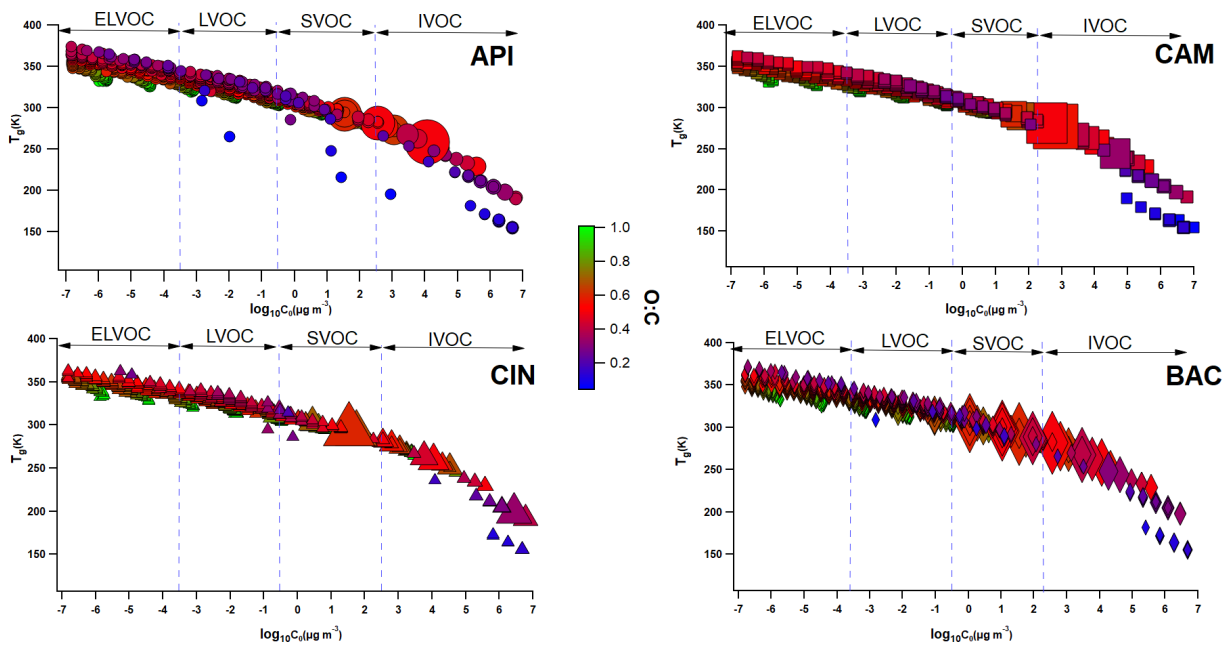
Figure 3.7. Glass transition temperature. Glass transition temperature (T_g) of α-pinene SOA (API), camphor SOA (CAM), 1,8-cineol SOA (CIN), and bornyl acetate SOA (BAC) as a function of saturation mass concentration of individual compounds (C_0). The warmer the color, the higher the O/C ratio. The size of the marker indicates the relative abundance (normalized to the maximum signal intensity) of the species based on the HR-MS results in ESI (-) mode.
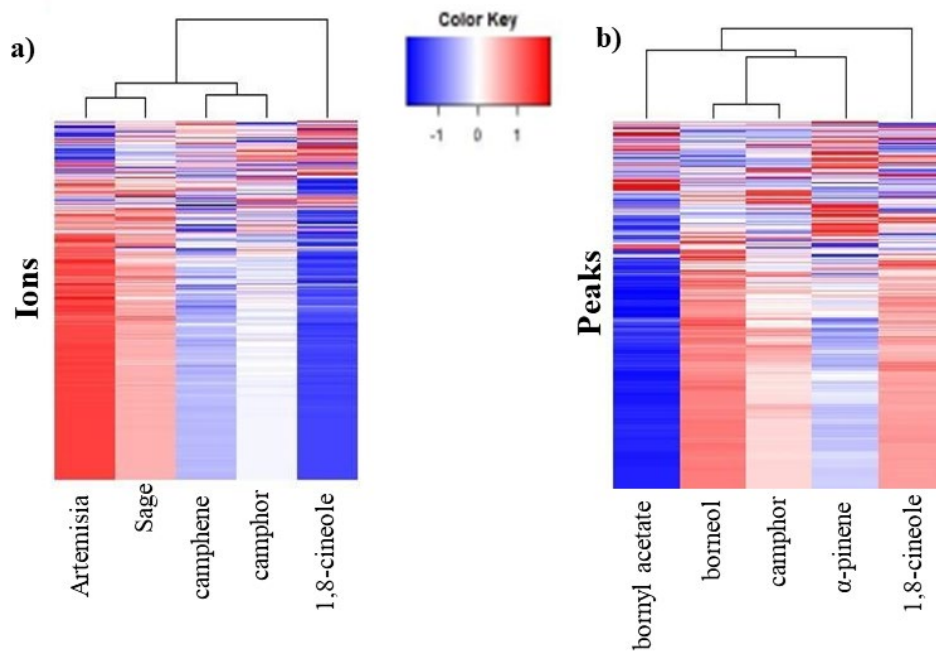
Figure 3.8. Heatmaps of SOA composition. Heatmap of a) SOA from sages and camphor, camphene, and 1,8-cineole form HR-ToF-AMS data, b) CAM, BOR, API, BAC, and CIN from SOA chemical composition analysis of HR-MS data in ESI (-) mode. The values are based on mean values over two replicates for each SOA type.

Table 3.1. SOA precursors that are investigated in this study:
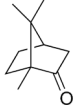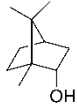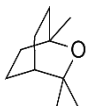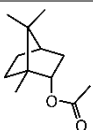
SOA Precursor	Formula	Structure	K_{OH} (cm^3 molec $^{-1}$ s^{-1})
α-pinene	$C_{10}H_{16}$		5.23×10^{-11} (Atkinson and Arey, 2003)
camphor	$C_{10}H_{16}O$		3.8×10^{-12} (Ceacero-Vega et al., 2012)
borneol	$C_{10}H_{18}O$		1.24×10^{-11} (Jenkin et al., 2018)
1,8-cineol	$C_{10}H_{18}O$		1.11×10^{-11} (Corchnoy and Atkinson, 1990)
bornyl acetate	$C_{12}H_{20}O_2$		1.25×10^{-11} (Jenkin et al., 2018)

Table 3.2. Summary of experimental conditions:

Experiment	Precursor	ID	Introduced VOC (ppb)	RH (%)	O$_3$ (ppm)
SOA mass yield versus OH exposure	α-pinene	API	81± 5	59±3	1.8 - 25
	camphor	CAM	56±8	60±3	2 - 26
	borneol	BOR	72±2	57±4	1.6 - 27
	1,8-cineole	CIN	78±6	59±4	2.5 - 26
	bornyl acetate	BAC	58±5	58±4	1.8 - 27
SOA mass yield curve	α-pinene	API	19 - 88	62±3	4.0±0.2
	camphor	CAM	6 - 51	60±2	4.1±0.3
	borneol	BOR	8 - 70	60±1	4.0±0.1
	1,8-cineole	CIN	5 - 51	61±2	4.2±0.1
	bornyl acetate	BAC	12 - 92	61±2	4.1±0.2

Table 3.3. SOA parameterization. The coefficients form a two-product model and volatility-basis set (VBS) model with 4 bins for fitting lines to SOA mass yield curves. (values ± standard deviations)

	two-product model				volatility-basis set model			
	α_1	α_2	K_{OM1}	K_{OM2}	α_1 ($C^*_1 = 1$ µg/m^3)	α_2 ($C^*_2 = 10$ µg/m^3)	α_3 ($C^*_3 = 10^2$ µg/m^3)	α_4 ($C^*_4 = 10^3$ µg/m^3)
α-pinene	0.94	0.20	0.001	0.08	0.01	0.15	0.12	0.84
camphor	0.63	0.16	0.01	0.46	0.07	0.17	0.31	0.95
borneol	0.41	0.31	0.001	0.08	0.03	0.22	0.10	0.50
1,8-cineole	0.98	0.15	0.003	0.31	0.09	0.02	0.37	0.81
bornyl acetate	2.27	0.13	0.0003	0.07	0.01	0.08	0.09	0.62

SUPPLEMENTAL MATERIALS

Appendix 3: Supplementary information

Gas-Phase Characterization: TD-GC-ToF-MS Operation and Compound Identification.

Cartridge samples were run through a thermo-desorption gas chromatograph-mass spectrometer (TD-GC-MS, Markes International TD-100xr autosampler, Agilent GC 7890B, equipped with a 30 m, DB-5 column, and Agilent 5975 MS) using the following method parameters: Samples were desorbed and injected through TD100-xr automated thermal desorber (Markes International Inc.). The cartridges were heated to release compounds trapped in the absorbents. The sample injection was done at 350°C, He flow at 15 mL min^{-1}. The oven starts at -30°C; 1-minute hold; then a ramp of 8.0°C min^{-1} up to 194°C (Ramp1), followed by a ramp 16°C min^{-1} up to 210°C (Ramp 2), and finally a ramp of 25°C min^{-1} up to 260°C (Ramp3), and a 3-minute hold. The total runtime was 35 min per sample. Compounds were identified by mass spectrum, and the NIST database (version 2.2) with >85% match was used. The calibration factor was used to quantify the compounds for area peaks in all the runs. The calibration factor for each sample was calculated based on the average of the peak areas from the known amount of the introduced standard (Table S3.1). To get the compound mass in the unit of µg m^{-3}, the calculated mass in the unit of µg of each compound was divided by the sampling volume, with a flow rate of 0.420 L min^{-1} for 4 to 5 minutes, in the unit of m^3.

Oxidation Flow Reactor Calibration

For OFR calibration, OH concentrations were varied by changing the UV light intensity with changing the lamp's settings. Toluene was introduced at the OFR inlet by passing clean air through a glass jar (Figure 3.1). Calibration was conducted at the same relative humidity used in the SOA experiments. The OFR setting and toluene mixing ratios at the OFR inlet (initial VOC, VOC$_i$) and the OFR outlet (final VOC, VOC$_f$) are presented in Table S3.2. At each lamp setting, OH exposures were calculated using the following equation and applying the known OH rate constant with toluene ($k_{OH,toluene}$= 5.63e-12 cm^3 molec^{-1} s^{-1}) (Atkinson and Arey, 2003):

$$\text{OH exposure} = \frac{-1}{k_{OH,toluene}} \times \ln\left(\frac{[VOC_f]}{[VOC_i]}\right)$$

GECKO-A Model Predictions:

     SOA formation from OH oxidation of three precursors (camphor, 1,8-cineole, and bornyl acetate) was modeled using GECKO-A. The oxidation scheme of each precursor is shown in Figure S3.1. Compounds that had matched chemical formulas with the HR-MS data analysis are indicated with red circles along with their corresponding formulas. To compare results from the model and the HR-MS data analysis, the peaks aligned between both methods are summarized in Table S3.3 The suggested corresponding chemical structure for a couple of major components of SOA formed from α-pinene based on previous studies are also provided in the table.

a)
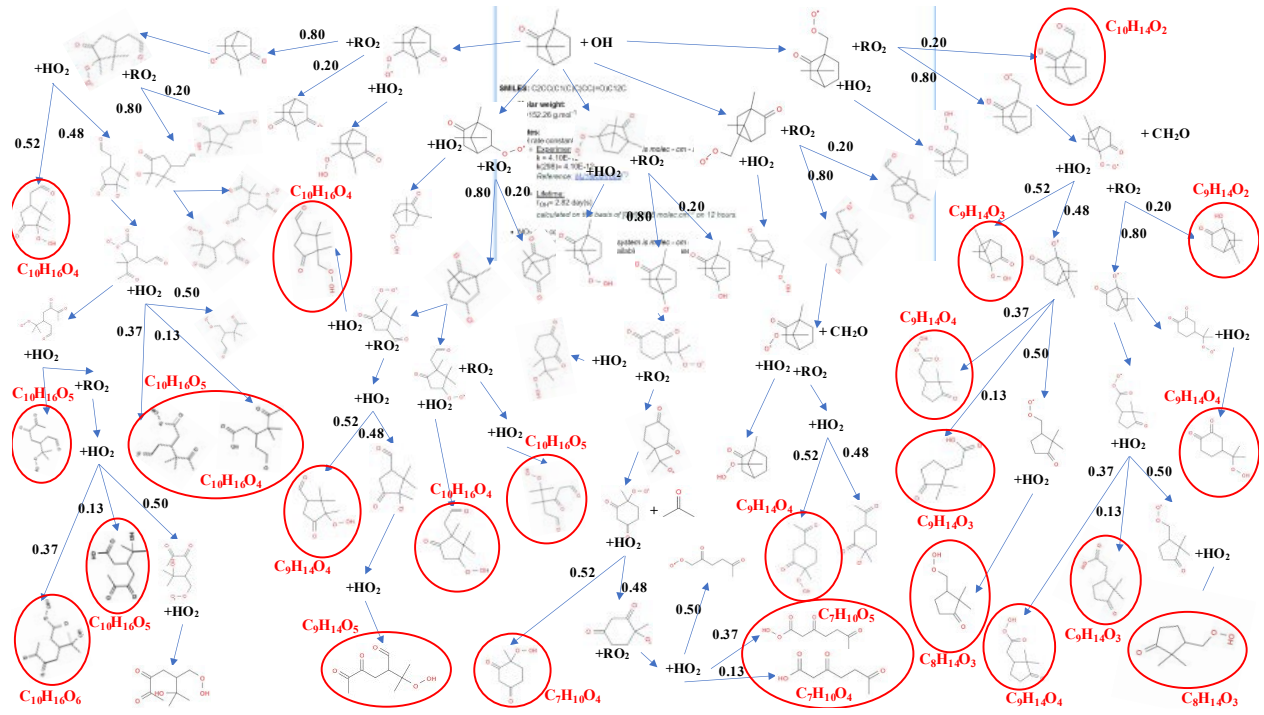
b)
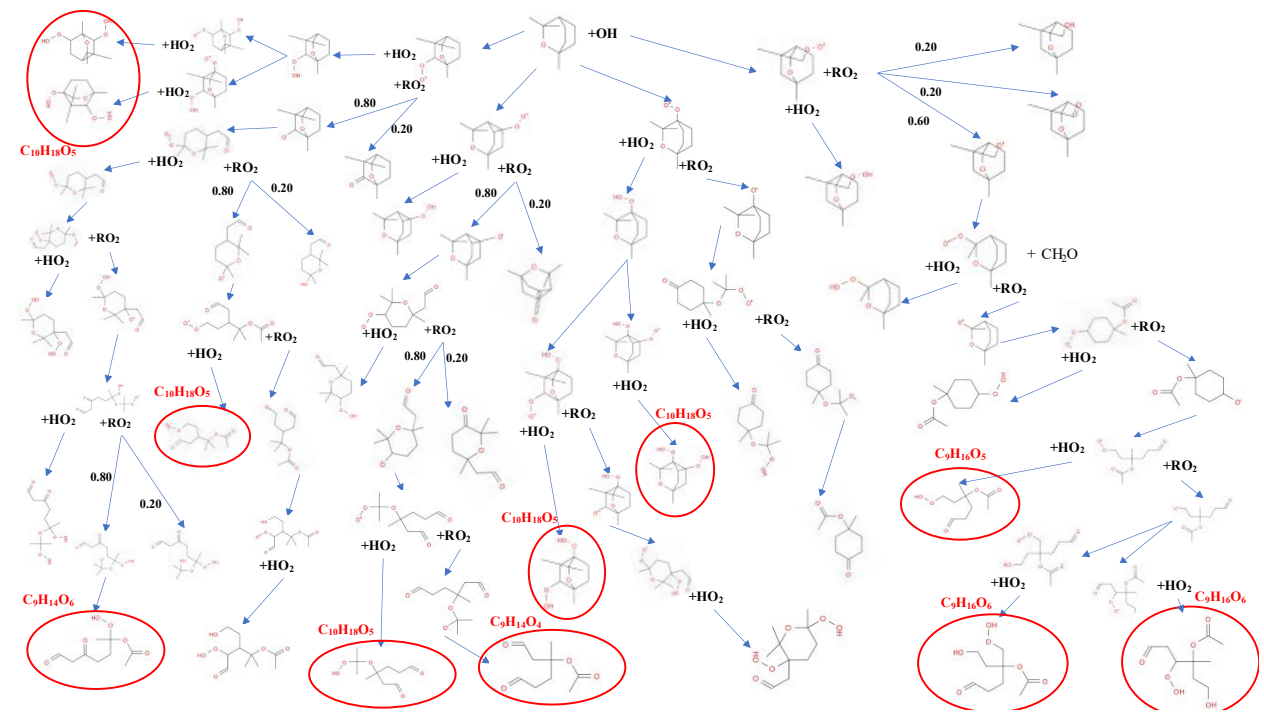
c)
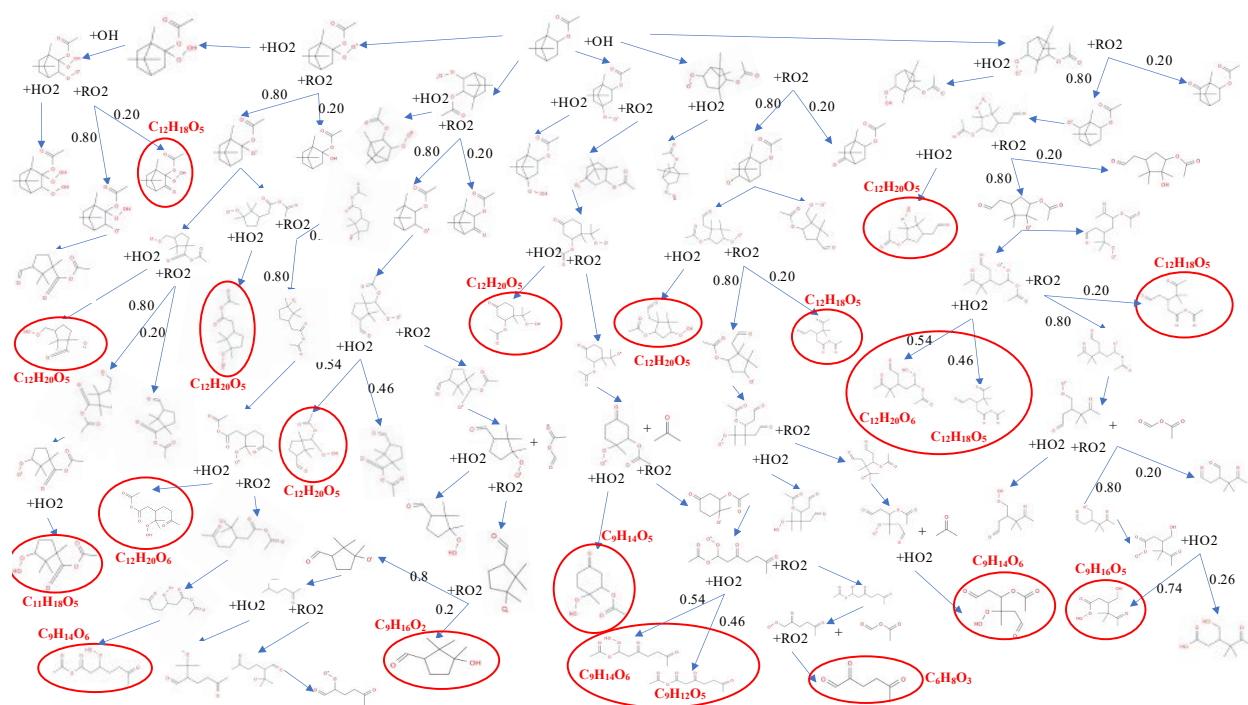
Figure S3.1 Oxidation schemes from GECKO-A. GECKO-A reaction pathways of OH-oxidation of a) camphor, b) 1,8-cineole, and c) bornyl acetate. The matched products with detected peaks via HR-MS data are shown with chemical formulas and red circles. HO₂ and RO₂ refer to hydroxyalkyl radicals and peroxy radicals, respectively.

Table S3.1. The calibration factors for quantification of peaks from GC-MS results
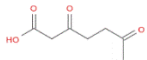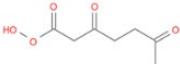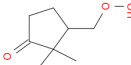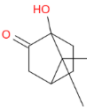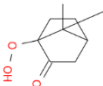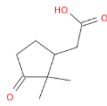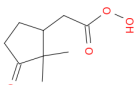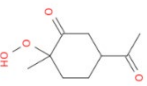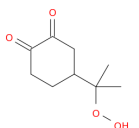
Compound	Calibration factor (mass (ng)/area)
α-pinene	2.37e-6
camphor	2.08e-6
1,8-cineole	2.29e-6
borneol	2.59e-6
bornyl acetate	4.01e-6
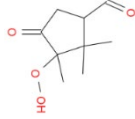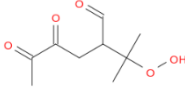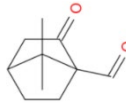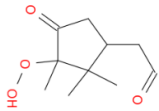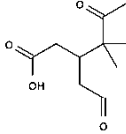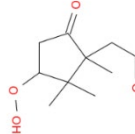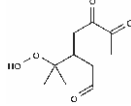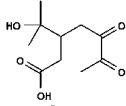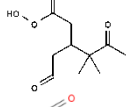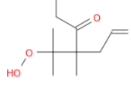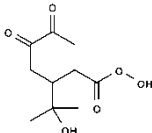
Table S3.2. OFR calibration setting using toluene to determine the impact of UV photon flux changes on OH exposure at a constant RH with three lamp settings.
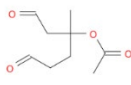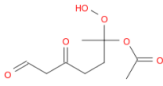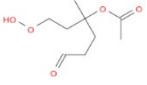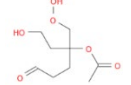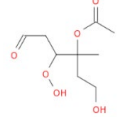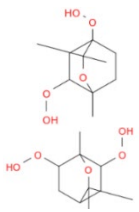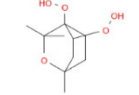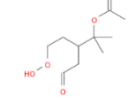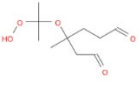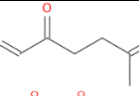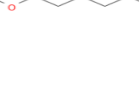
Irradiance ($\mu W/cm^2$)	**RH (%)**	Initial VOC (ppb)	Final VOC (ppb)	OH_{exp} (molec s cm^{-3})
1.48		641	73	3.87e+11
12.15	60	655	22	5.99e+11
51.17		782	10	1.01e+12
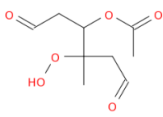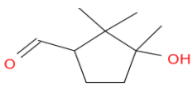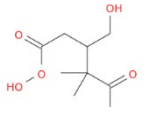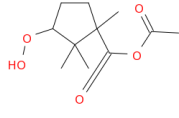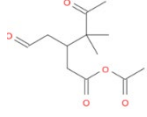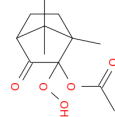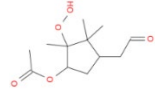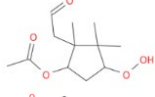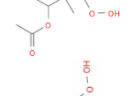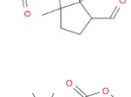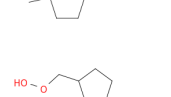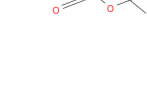
Table S3.3. The matched oxidation products detected by negative HR-MS, ESI (-) mode, and the corresponding chemical structure from GECKO-A for SOA formed from camphor, 1,8-cineole, and bornyl acetate.
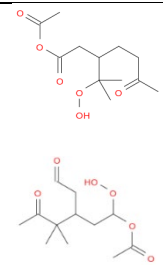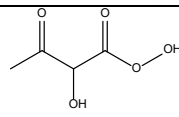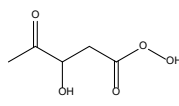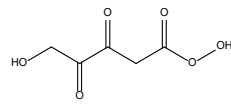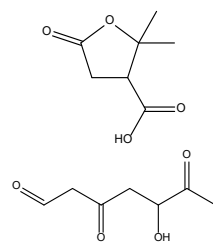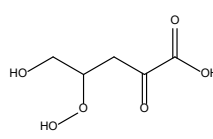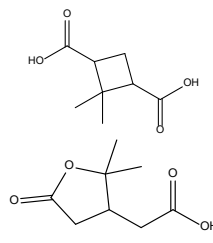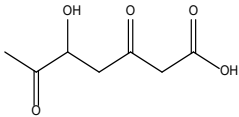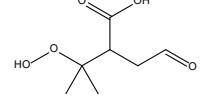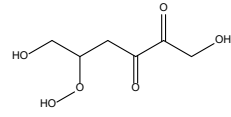
*The predicted/suggested chemical structures for observed oxidation products from previous studies (cited in the main text of the chapter) for α-pinene SOA (Jia and Xu, 2020) are also provided.
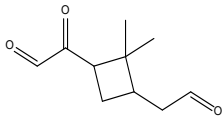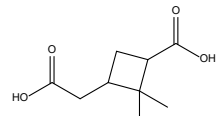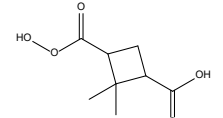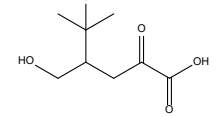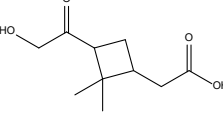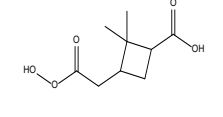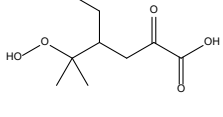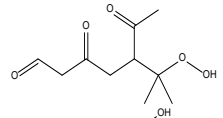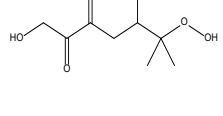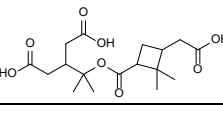
Sample	MW (Da)	Formula	Molecular structure from GECKO-A
Camphor	158.05	$C_7H_{10}O_4$	
	174.05	$C_7H_{10}O_5$	
	158.09	$C_8H_{14}O_3$	
	154.09	$C_9H_{14}O_2$	
	170.08	$C_9H_{14}O_3$	
	186.08	$C_9H_{14}O_4$	

	202.08	$C_9H_{14}O_5$	
	166.09	$C_{10}H_{14}O_2$	
	200.09	$C_{10}H_{16}O_4$	
	216.09	$C_{10}H_{16}O_5$	
	232.08	$C_{10}H_{16}O_6$	

1,8-cineole	186.08	$C_9H_{14}O_4$	
	218.07	$C_9H_{14}O_6$	
	204.09	$C_9H_{16}O_5$	
	220.07	$C_9H_{16}O_6$	
	218.11	$C_{10}H_{18}O_5$	
bornyl acetate	128.04	$C_6H_8O_3$	
	200.06	$C_9H_{12}O_5$	
	202.07	$C_9H_{14}O_5$	
	218.07	$C_9H_{14}O_6$	

	156.11	$C_9H_{16}O_2$	
	204.09	$C_9H_{16}O_5$	
	230.11	$C_{11}H_{18}O_5$	
	242.11	$C_{12}H_{18}O_5$	
	244.12	$C_{12}H_{20}O_5$	

	260.12	C$_{12}$H$_{20}$O$_6$	
α-pinene*	134.04	C$_4$H$_6$O$_5$	
	148.03	C$_5$H$_8$O$_5$	
	162.01	C$_5$H$_6$O$_6$	
	158.05	C$_7$H$_{10}$O$_4$	
	164.02	C$_5$H$_8$O$_6$	
	172.07	C$_8$H$_{12}$O$_4$	
	174.05	C$_7$H$_{10}$O$_5$	
	176.06	C$_7$H$_{12}$O$_5$	
	178.04	C$_6$H$_{10}$O$_6$	

	182.09	$C_{10}H_{14}O_3$	
	186.08	$C_9H_{14}O_4$	
	188.06	$C_8H_{12}O_5$	
	190.08	$C_8H_{14}O_5$	
	200.09	$C_{10}H_{16}O_4$	
	202.08	$C_9H_{14}O_5$	
	206.07	$C_8H_{14}O_6$	
	216.09	$C_{10}H_{16}O_5$	
	220.08	$C_9H_{16}O_6$	
	358.16	$C_{17}H_{26}O_8$	

REFERENCES

Afreh, I.K., Aumont, B., Camredon, M., Barsanti, K.C., 2021. Using GECKO-A to derive mechanistic understanding of secondary organic aerosol formation from the ubiquitous but understudied camphene. Atmospheric Chemistry and Physics 21, 11467–11487. https://doi.org/10.5194/acp-21-11467-2021

Ahlberg, E., Falk, J., Eriksson, A., Holst, T., Brune, W.H., Kristensson, A., Roldin, P., Svenningsson, B., 2017. Secondary organic aerosol from VOC mixtures in an oxidation flow reactor. Atmospheric Environment 161, 210–220. https://doi.org/10.1016/j.atmosenv.2017.05.005

Allison, J.D., Daniel Hare, J., 2009. Learned and naïve natural enemy responses and the interpretation of volatile organic compounds as cues or signals. New Phytologist 184, 768–782. https://doi.org/10.1111/j.1469-8137.2009.03046.x

Andreae, M.O., Rosenfeld, D., 2008. Aerosol–cloud–precipitation interactions. Part 1. The nature and sources of cloud-active aerosols. Earth-Science Reviews 89, 13–41. https://doi.org/10.1016/j.earscirev.2008.03.001

Angell, C.A., 2002. Liquid Fragility and the Glass Transition in Water and Aqueous Solutions. Chem. Rev. 102, 2627–2650. https://doi.org/10.1021/cr000689q

Angell, C.A., 1991. Relaxation in liquids, polymers and plastic crystals — strong/fragile patterns and problems. Journal of Non-Crystalline Solids, Proceedings of the International Discussion Meeting on Relaxations in Complex Systems 131–133, 13–31. https://doi.org/10.1016/0022-3093(91)90266-9

Arimura, G., Kost, C., Boland, W., 2005. Herbivore-induced, indirect plant defences. Biochimica et Biophysica Acta (BBA) - Molecular and Cell Biology of Lipids 1734, 91–111. https://doi.org/10.1016/j.bbalip.2005.03.001

Arimura, G., Matsui, K., Takabayashi, J., 2009. Chemical and Molecular Ecology of Herbivore-Induced Plant Volatiles: Proximate Factors and Their Ultimate Functions. Plant and Cell Physiology 50, 911–923. https://doi.org/10.1093/pcp/pcp030

Arimura, G., Ozawa, R., Shimoda, T., Nishioka, T., Boland, W., Takabayashi, J., 2000. Herbivory-induced volatiles elicit defence genes in lima bean leaves. Nature 406, 512–515. https://doi.org/10.1038/35020072

Arneth, A., Harrison, S.P., Zaehle, S., Tsigaridis, K., Menon, S., Bartlein, P.J., Feichter, J., Korhola, A., Kulmala, M., O'Donnell, D., Schurgers, G., Sorvari, S., Vesala, T., 2010. Terrestrial biogeochemical feedbacks in the climate system. Nature Geosci 3, 525–532. https://doi.org/10.1038/ngeo905

Arneth, A., Makkonen, R., Olin, S., Paasonen, P., Holst, T., Kajos, M.K., Kulmala, M., Maximov, T., Miller, P.A., Schurgers, G., 2016. Future vegetation–climate interactions in Eastern Siberia: an assessment of the competing effects of CO_2 and secondary organic aerosols. Atmospheric Chemistry and Physics 16, 5243–5262. https://doi.org/10.5194/acp-16-5243-2016

Arneth, A., Niinemets, Ü., 2010. Induced BVOCs: how to bug our models? Trends in Plant Science, Special Issue: Induced biogenic volatile organic compounds from plants 15, 118–125. https://doi.org/10.1016/j.tplants.2009.12.004

Atkinson, R., Arey, J., 2003. Atmospheric Degradation of Volatile Organic Compounds. Chem. Rev. 103, 4605–4638. https://doi.org/10.1021/cr0206420

Aumont, B., Camredon, M., Mouchel-Vallon, C., La, S., Ouzebidour, F., Valorso, R., Lee-Taylor, J., Madronich, S., 2013. Modeling the influence of alkane molecular structure on secondary organic aerosol formation. Faraday Discuss. 165, 105–122. https://doi.org/10.1039/C3FD00029J

Aumont, B., Szopa, S., Madronich, S., 2005. Modelling the evolution of organic carbon during its gas-phase tropospheric oxidation: development of an explicit model based on a self generating approach. Atmospheric Chemistry and Physics 5, 2497–2517. https://doi.org/10.5194/acp-5-2497-2005

Baldwin, I.T., 2010. Plant volatiles. Current Biology 20, R392–R397. https://doi.org/10.1016/j.cub.2010.02.052

Baldwin, I.T., Halitschke, R., Paschold, A., von Dahl, C.C., Preston, C.A., 2006a. Volatile Signaling in Plant-Plant Interactions: "Talking Trees" in the Genomics Era. Science 311, 812–815. https://doi.org/10.1126/science.1118446

Baldwin, I.T., Halitschke, R., Paschold, A., von Dahl, C.C., Preston, C.A., 2006b. Volatile Signaling in Plant-Plant Interactions: "Talking Trees" in the Genomics Era. Science 311, 812–815. https://doi.org/10.1126/science.1118446

Baldwin, I.T., Schultz, J.C., 1983. Rapid Changes in Tree Leaf Chemistry Induced by Damage: Evidence for Communication Between Plants. Science 221, 277–279. https://doi.org/10.1126/science.221.4607.277

Bale, J.S., Masters, G.J., Hodkinson, I.D., Awmack, C., Bezemer, T.M., Brown, V.K., Butterfield, J., Buse, A., Coulson, J.C., Farrar, J., Good, J.E.G., Harrington, R., Hartley, S., Jones, T.H., Lindroth, R.L., Press, M.C., Symrnioudis, I., Watt, A.D., Whittaker, J.B., 2002. Herbivory in global climate change research: direct effects of rising temperature on insect herbivores. Global Change Biology 8, 1–16. https://doi.org/10.1046/j.1365-2486.2002.00451.x

Baltensperger, U., Dommen, J., Alfarra, M.R., Duplissy, J., Gaeggeler, K., Metzger, A., Facchini, M.C., Decesari, S., Finessi, E., Reinnig, C., Schott, M., Warnke, J., Hoffmann, T., Klatzer, B., Puxbaum, H., Geiser, M., Savi, M., Lang, D., Kalberer, M., Geiser, T., 2008. Combined determination of the chemical composition and of health effects of secondary organic aerosols: the POLYSOA project. J Aerosol Med Pulm Drug Deliv 21, 145–154. https://doi.org/10.1089/jamp.2007.0655

Behnke, K., Ehlting, B., Teuber, M., Bauerfeind, M., Louis, S., Hänsch, R., Polle, A., Bohlmann, J., Schnitzler, J.-P., 2007. Transgenic, non-isoprene emitting poplars don't like it hot. The Plant Journal 51, 485–499. https://doi.org/10.1111/j.1365-313X.2007.03157.x

Behnke, K., Grote, R., Brüggemann, N., Zimmer, I., Zhou, G., Elobeid, M., Janz, D., Polle, A., Schnitzler, J.-P., 2012. Isoprene emission-free poplars – a chance to reduce the impact from poplar plantations on the atmosphere. New Phytologist 194, 70–82. https://doi.org/10.1111/j.1469-8137.2011.03979.x

Benoit, R., Belhadj, N., Lailliau, M., Dagaut, P., 2021. Autoxidation of terpenes, a common pathway in tropospheric and low temperature combustion conditions: the case of limonene and α-pinene. Atmospheric Chemistry and Physics Discussions 1–21. https://doi.org/10.5194/acp-2021-964

Bigio, L., Lebel, M., Sapir, Y., 2017. Do different measures of maternal fitness affect estimation of natural selection on floral traits? A lesson from Linum pubescens (Linaceae). Journal of Plant Ecology 10, 406–413. https://doi.org/10.1093/jpe/rtw035

Birkett, M.A., Campbell, C.A.M., Chamberlain, K., Guerrieri, E., Hick, A.J., Martin, J.L., Matthes, M., Napier, J.A., Pettersson, J., Pickett, J.A., Poppy, G.M., Pow, E.M., Pye, B.J., Smart, L.E., Wadhams, G.H., Wadhams, L.J., Woodcock, C.M., 2000. New roles for cis-jasmone as an insect semiochemical and in plant defense. PNAS 97, 9329–9334. https://doi.org/10.1073/pnas.160241697

Blande, J.D., 2017. Chapter Eleven - Plant Communication With Herbivores, in: Becard, G. (Ed.), Advances in Botanical Research, How Plants Communicate with Their Biotic Environment. Academic Press, pp. 281–304. https://doi.org/10.1016/bs.abr.2016.09.004

Blande, J.D., Korjus, M., Holopainen, J.K., 2010. Foliar methyl salicylate emissions indicate prolonged aphid infestation on silver birch and black alder. Tree Physiology 30, 404–416. https://doi.org/10.1093/treephys/tpp124

Blande, J.D., Tiiva, P., Oksanen, E., Holopainen, J.K., 2007. Emission of herbivore-induced volatile terpenoids from two hybrid aspen (Populus tremula×tremuloides) clones under ambient and elevated ozone concentrations in the field. Global Change Biology 13, 2538–2550. https://doi.org/10.1111/j.1365-2486.2007.01453.x

Blande, J.D., Turunen, K., Holopainen, J.K., 2009. Pine weevil feeding on Norway spruce bark has a stronger impact on needle VOC emissions than enhanced ultraviolet-B radiation. Environmental Pollution 157, 174–180. https://doi.org/10.1016/j.envpol.2008.07.007

Borges, R.M., 2018. The Galling Truth: Limited Knowledge of Gall-Associated Volatiles in Multitrophic Interactions. Frontiers in Plant Science 9.

Bowers, W.S., Nault, L.R., Webb, R.E., Dutky, S.R., 1972. Aphid alarm pheromone: isolation, identification, synthesis. Science 177, 1121–1122. https://doi.org/10.1126/science.177.4054.1121

Bradley, B.A., Blumenthal, D.M., Early, R., Grosholz, E.D., Lawler, J.J., Miller, L.P., Sorte, C.J., D'Antonio, C.M., Diez, J.M., Dukes, J.S., Ibanez, I., Olden, J.D., 2012. Global change, global trade, and the next wave of plant invasions. Frontiers in Ecology and the Environment 10, 20–28. https://doi.org/10.1890/110145

Brilli, F., Barta, C., Fortunati, A., Lerdau, M., Loreto, F., Centritto, M., 2007. Response of isoprene emission and carbon metabolism to drought in white poplar (Populus alba) saplings. New Phytol 175, 244–254. https://doi.org/10.1111/j.1469-8137.2007.02094.x

Brilli, F., Ciccioli, P., Frattoni, M., Prestininzi, M., Spanedda, A.F., Loreto, F., 2009. Constitutive and herbivore-induced monoterpenes emitted by Populus × euroamericana leaves are key volatiles that orient Chrysomela populi beetles. Plant, Cell & Environment 32, 542–552. https://doi.org/10.1111/j.1365-3040.2009.01948.x

Bronstein, J.L., Alarcón, R., Geber, M., 2006. The evolution of plant-insect mutualisms. New Phytol 172, 412–428. https://doi.org/10.1111/j.1469-8137.2006.01864.x

Calfapietra, C., Scarascia Mugnozza, G., Karnosky, D.F., Loreto, F., Sharkey, T.D., 2008. Isoprene emission rates under elevated CO2 and O3 in two field-grown aspen clones differing in their sensitivity to O3. New Phytologist 179, 55–61. https://doi.org/10.1111/j.1469-8137.2008.02493.x

Cannon, R.J.C., 1998. The implications of predicted climate change for insect pests in the UK, with emphasis on non-indigenous species. Global Change Biology 4, 785–796. https://doi.org/10.1046/j.1365-2486.1998.00190.x

Carlton, A.G., Pye, H.O.T., Baker, K.R., Hennigan, C.J., 2018. Additional Benefits of Federal Air-Quality Rules: Model Estimates of Controllable Biogenic Secondary Organic Aerosol. Environ. Sci. Technol. 52, 9254–9265. https://doi.org/10.1021/acs.est.8b01869

Carlton, A.G., Wiedinmyer, C., Kroll, J.H., 2009a. A review of Secondary Organic Aerosol (SOA) formation from isoprene. Atmospheric Chemistry and Physics 9, 4987–5005. https://doi.org/10.5194/acp-9-4987-2009

Carlton, A.G., Wiedinmyer, C., Kroll, J.H., 2009b. A review of Secondary Organic Aerosol (SOA) formation from isoprene. Atmospheric Chemistry and Physics 9, 4987–5005. https://doi.org/10.5194/acp-9-4987-2009

Ceacero-Vega, A.A., Ballesteros, B., Bejan, I., Barnes, I., Jiménez, E., Albaladejo, J., 2012. Kinetics and Mechanisms of the Tropospheric Reactions of Menthol, Borneol, Fenchol, Camphor, and Fenchone with Hydroxyl Radicals (OH) and Chlorine Atoms (Cl). J. Phys. Chem. A 116, 4097–4107. https://doi.org/10.1021/jp212076g

Chapman, R.F., Bernays, E.A., Simpson, S.J., 1981. Attraction and repulsion of the aphid,Cavariella aegopodii, by Plant Odors. J Chem Ecol 7, 881–888. https://doi.org/10.1007/BF00992385

Chapurlat, E., Ågren, J., Anderson, J., Friberg, M., Sletvold, N., 2019. Conflicting selection on floral scent emission in the orchid Gymnadenia conopsea. New Phytologist 222, 2009–2022. https://doi.org/10.1111/nph.15747

Chen, C., Song, Q., Proffit, M., Bessière, J.-M., Li, Z., Hossaert-McKey, M., 2009. Private channel: a single unusual compound assures specific pollinator attraction in Ficus semicordata. Functional Ecology 23, 941–950. https://doi.org/10.1111/j.1365-2435.2009.01622.x

Chhabra, P.S., Lambe, A.T., Canagaratna, M.R., Stark, H., Jayne, J.T., Onasch, T.B., Davidovits, P., Kimmel, J.R., Worsnop, D.R., 2015. Application of high-resolution time-of-flight chemical ionization mass spectrometry measurements to estimate volatility distributions of α-pinene and

naphthalene oxidation products. Atmospheric Measurement Techniques 8, 1–18. https://doi.org/10.5194/amt-8-1-2015

Claeys, M., Wang, W., Ion, A.C., Kourtchev, I., Gelencsér, A., Maenhaut, W., 2004. Formation of secondary organic aerosols from isoprene and its gas-phase oxidation products through reaction with hydrogen peroxide. Atmospheric Environment 38, 4093–4098. https://doi.org/10.1016/j.atmosenv.2004.06.001

Copolovici, L., Kännaste, A., Pazouki, L., Niinemets, U., 2012. Emissions of green leaf volatiles and terpenoids from Solanum lycopersicum are quantitatively related to the severity of cold and heat shock treatments. J Plant Physiol 169, 664–672. https://doi.org/10.1016/j.jplph.2011.12.019

Copolovici, L., Kännaste, A., Remmel, T., Niinemets, Ü., 2014. Volatile organic compound emissions from Alnus glutinosa under interacting drought and herbivory stresses. Environmental and Experimental Botany 100, 55–63. https://doi.org/10.1016/j.envexpbot.2013.12.011

Copolovici, L., Pag, A., Kännaste, A., Bodescu, A., Tomescu, D., Copolovici, D., Soran, M.-L., Niinemets, Ü., 2017. Disproportionate photosynthetic decline and inverse relationship between constitutive and induced volatile emissions upon feeding of Quercus robur leaves by large larvae of gypsy moth (Lymantria dispar). Environmental and Experimental Botany 138, 184–192. https://doi.org/10.1016/j.envexpbot.2017.03.014

Copolovici, L.O., Filella, I., Llusià, J., Niinemets, Ü., Peñuelas, J., 2005. The Capacity for Thermal Protection of Photosynthetic Electron Transport Varies for Different Monoterpenes in Quercus ilex. Plant Physiology 139, 485–496. https://doi.org/10.1104/pp.105.065995

Corchnoy, S.B., Atkinson, R., 1990. Kinetics of the gas-phase reactions of hydroxyl and nitrogen oxide (NO3) radicals with 2-carene, 1,8-cineole, p-cymene, and terpinolene. https://doi.org/10.1021/ES00080A007

Council, N.R., 1992. Rethinking the Ozone Problem in Urban and Regional Air Pollution. https://doi.org/10.17226/1889

Courtois, E.A., Paine, C.E.T., Blandinieres, P.-A., Stien, D., Bessiere, J.-M., Houel, E., Baraloto, C., Chave, J., 2009. Diversity of the Volatile Organic Compounds Emitted by 55 Species of Tropical Trees: a Survey in French Guiana. J Chem Ecol 35, 1349. https://doi.org/10.1007/s10886-009-9718-1

D. Abbatt, J.P., Y. Lee, A.K., A. Thornton, J., 2012. Quantifying trace gas uptake to tropospheric aerosol: recent advances and remaining challenges. Chemical Society Reviews 41, 6555–6581. https://doi.org/10.1039/C2CS35052A

Dam, M., Draper, D.C., Marsavin, A., Fry, J.L., Smith, J.N., 2022. Observations of gas-phase products from the nitrate radical-initiated oxidation of four monoterpenes. Atmospheric Chemistry and Physics Discussions 1–22. https://doi.org/10.5194/acp-2021-1020

De Moraes, C.M., Mescher, M.C., Tumlinson, J.H., 2001. Caterpillar-induced nocturnal plant volatiles repel conspecific females. Nature 410, 577–580. https://doi.org/10.1038/35069058

DeCarlo, P.F., Kimmel, J.R., Trimborn, A., Northway, M.J., Jayne, J.T., Aiken, A.C., Gonin, M., Fuhrer, K., Horvath, T., Docherty, K.S., Worsnop, D.R., Jimenez, J.L., 2006. Field-Deployable, High-Resolution, Time-of-Flight Aerosol Mass Spectrometer. Anal. Chem. 78, 8281–8289. https://doi.org/10.1021/ac061249n

Degenhardt, J., Hiltpold, I., Köllner, T.G., Frey, M., Gierl, A., Gershenzon, J., Hibbard, B.E., Ellersieck, M.R., Turlings, T.C.J., 2009. Restoring a maize root signal that attracts insect-killing nematodes to control a major pest. Proceedings of the National Academy of Sciences 106, 13213–13218. https://doi.org/10.1073/pnas.0906365106

Delfine, S., Csiky, O., Seufert, G., Loreto, F., 2000. Fumigation with exogenous monoterpenes of a non-isoprenoid-emitting oak (Quercus suber): monoterpene acquisition, translocation, and effect on the photosynthetic properties at high temperatures. The New Phytologist 146, 27–36. https://doi.org/10.1046/j.1469-8137.2000.00612.x

DeRieux, W.-S.W., Li, Y., Lin, P., Laskin, J., Laskin, A., Bertram, A.K., Nizkorodov, S.A., Shiraiwa, M., 2018a. Predicting the glass transition temperature and viscosity of secondary organic material

using molecular composition. Atmospheric Chemistry and Physics 18, 6331–6351. https://doi.org/10.5194/acp-18-6331-2018

DeRieux, W.-S.W., Li, Y., Lin, P., Laskin, J., Laskin, A., Bertram, A.K., Nizkorodov, S.A., Shiraiwa, M., 2018b. Predicting the glass transition temperature and viscosity of secondary organic material using molecular composition. Atmospheric Chemistry and Physics 18, 6331–6351. https://doi.org/10.5194/acp-18-6331-2018

Després, VivianeR., Huffman, J.A., Burrows, S.M., Hoose, C., Safatov, AleksandrS., Buryak, G., Fröhlich-Nowoisky, J., Elbert, W., Andreae, MeinratO., Pöschl, U., Jaenicke, R., 2012. Primary biological aerosol particles in the atmosphere: a review. Tellus B: Chemical and Physical Meteorology 64, 15598. https://doi.org/10.3402/tellusb.v64i0.15598

Dette, H.P., Qi, M., Schröder, D.C., Godt, A., Koop, T., 2014. Glass-Forming Properties of 3-Methylbutane-1,2,3-tricarboxylic Acid and Its Mixtures with Water and Pinonic Acid. J. Phys. Chem. A 118, 7024–7033. https://doi.org/10.1021/jp505910w

Dicke, M., 2004. Tritrophic Interactions. Encyclopedia of Entomology.

Dicke, M., Agrawal, A.A., Bruin, J., 2003a. Plants talk, but are they deaf? Trends in Plant Science 8, 403–405. https://doi.org/10.1016/S1360-1385(03)00183-3

Dicke, M., Baldwin, I.T., 2010. The evolutionary context for herbivore-induced plant volatiles: beyond the 'cry for help.' Trends in Plant Science, Special Issue: Induced biogenic volatile organic compounds from plants 15, 167–175. https://doi.org/10.1016/j.tplants.2009.12.002

Dicke, M., De Boer, J.G., Höfte, M., Rocha-Granados, M.C., 2003b. Mixed blends of herbivore-induced plant volatiles and foraging success of carnivorous arthropods. Oikos 101, 38–48. https://doi.org/10.1034/j.1600-0706.2003.12571.x

Dicke, M., Dijkman, H., 2001. Within-plant circulation of systemic elicitor of induced defence and release from roots of elicitor that affects neighbouring plants. Biochemical Systematics and Ecology, Chemical information transfer between wounded and unwounded plants 29, 1075–1087. https://doi.org/10.1016/S0305-1978(01)00051-5

Dicke, M., van Poecke, R.M.P., de Boer, J.G., 2003c. Inducible indirect defence of plants: from mechanisms to ecological functions. Basic and Applied Ecology 4, 27–42. https://doi.org/10.1078/1439-1791-00131

Dobson, H.E.M., 1994. Floral Volatiles in Insect Biology, in: Insect-Plant Interactions. CRC Press.

Donahue, N.M., Robinson, A.L., Stanier, C.O., Pandis, S.N., 2006. Coupled Partitioning, Dilution, and Chemical Aging of Semivolatile Organics. Environ. Sci. Technol. 40, 2635–2643. https://doi.org/10.1021/es052297c

Dudareva, N., Klempien, A., Muhlemann, J.K., Kaplan, I., 2013. Biosynthesis, function and metabolic engineering of plant volatile organic compounds. New Phytologist 198, 16–32. https://doi.org/10.1111/nph.12145

Dudareva, N., Negre, F., Nagegowda, D.A., Orlova, I., 2006. Plant Volatiles: Recent Advances and Future Perspectives. Critical Reviews in Plant Sciences 25, 417–440. https://doi.org/10.1080/07352680600899973

Duke, S.O., Canel, C., Rimando, A.M., Telle, M.R., Duke, M.V., Paul, R.N., 2000. Current and potential exploitation of plant glandular trichome productivity, in: Advances in Botanical Research. Academic Press, pp. 121–151. https://doi.org/10.1016/S0065-2296(00)31008-4

Eddingsaas, N.C., Loza, C.L., Yee, L.D., Chan, M., Schilling, K.A., Chhabra, P.S., Seinfeld, J.H., Wennberg, P.O., 2012. α-pinene photooxidation under controlled chemical conditions – Part 2: SOA yield and composition in low- and high-NO$_x$ environments. Atmospheric Chemistry and Physics 12, 7413–7427. https://doi.org/10.5194/acp-12-7413-2012

Ehn, M., Thornton, J.A., Kleist, E., Sipilä, M., Junninen, H., Pullinen, I., Springer, M., Rubach, F., Tillmann, R., Lee, B., Lopez-Hilfiker, F., Andres, S., Acir, I.-H., Rissanen, M., Jokinen, T., Schobesberger, S., Kangasluoma, J., Kontkanen, J., Nieminen, T., Kurtén, T., Nielsen, L.B., Jørgensen, S., Kjaergaard, H.G., Canagaratna, M., Maso, M.D., Berndt, T., Petäjä, T., Wahner, A., Kerminen, V.-M., Kulmala, M., Worsnop, D.R., Wildt, J., Mentel, T.F., 2014. A large source

of low-volatility secondary organic aerosol. Nature 506, 476–479. https://doi.org/10.1038/nature13032

Ehrlén, J., Borg-Karlson, A.-K., Kolb, A., 2012. Selection on plant optical traits and floral scent: Effects via seed development and antagonistic interactions. Basic and Applied Ecology 13, 509–515. https://doi.org/10.1016/j.baae.2012.08.001

Engelberth, J., Alborn, H.T., Schmelz, E.A., Tumlinson, J.H., 2004. Airborne signals prime plants against insect herbivore attack. PNAS 101, 1781–1785. https://doi.org/10.1073/pnas.0308037100

Ervens, B., Turpin, B.J., Weber, R.J., 2011. Secondary organic aerosol formation in cloud droplets and aqueous particles (aqSOA): a review of laboratory, field and model studies. Atmospheric Chemistry and Physics 11, 11069–11102. https://doi.org/10.5194/acp-11-11069-2011

Faiola, C., Taipale, D., 2020. Impact of insect herbivory on plant stress volatile emissions from trees: A synthesis of quantitative measurements and recommendations for future research. Atmospheric Environment: X 5, 100060. https://doi.org/10.1016/j.aeaoa.2019.100060

Faiola, C.L., Buchholz, A., Kari, E., Yli-Pirilä, P., Holopainen, J.K., Kivimäenpää, M., Miettinen, P., Worsnop, D.R., Lehtinen, K.E.J., Guenther, A.B., Virtanen, A., 2018. Terpene Composition Complexity Controls Secondary Organic Aerosol Yields from Scots Pine Volatile Emissions. Sci Rep 8, 3053. https://doi.org/10.1038/s41598-018-21045-1

Faiola, C.L., Pullinen, I., Buchholz, A., Khalaj, F., Ylisirniö, A., Kari, E., Miettinen, P., Holopainen, J.K., Kivimäenpää, M., Schobesberger, S., Yli-Juuti, T., Virtanen, A., 2019. Secondary Organic Aerosol Formation from Healthy and Aphid-Stressed Scots Pine Emissions. ACS Earth Space Chem. 3, 1756–1772. https://doi.org/10.1021/acsearthspacechem.9b00118

Faiola, C.L., VanderSchelden, G.S., Wen, M., Elloy, F.C., Cobos, D.R., Watts, R.J., Jobson, B.T., VanReken, T.M., 2014. SOA Formation Potential of Emissions from Soil and Leaf Litter. Environ. Sci. Technol. 48, 938–946. https://doi.org/10.1021/es4040045

Faiola, C.L., Wen, M., VanReken, T.M., 2015. Chemical characterization of biogenic secondary organic aerosol generated from plant emissions under baseline and stressed conditions: inter- and intra-species variability for six coniferous species. Atmospheric Chemistry and Physics 15, 3629–3646. https://doi.org/10.5194/acp-15-3629-2015

Farag, M.A., Fokar, M., Abd, H., Zhang, H., Allen, R.D., Paré, P.W., 2005. (Z)-3-Hexenol induces defense genes and downstream metabolites in maize. Planta 220, 900–909. https://doi.org/10.1007/s00425-004-1404-5

Fares, S., Loreto, F., Kleist, E., Wildt, J., 2007. Stomatal Uptake and Stomatal Deposition of Ozone in Isoprene and Monoterpene Emitting Plants. Plant Biol (Stuttg) 9, e69–e78. https://doi.org/10.1055/s-2007-965257

Farré-Armengol, G., Fernández-Martínez, M., Filella, I., Junker, R.R., Peñuelas, J., 2020. Deciphering the Biotic and Climatic Factors That Influence Floral Scents: A Systematic Review of Floral Volatile Emissions. Frontiers in Plant Science 11.

Farré-Armengol, G., Filella, I., Llusià, J., Peñuelas, J., 2015. Pollination mode determines floral scent. Biochemical Systematics and Ecology 61, 44–53. https://doi.org/10.1016/j.bse.2015.05.007

Farré-Armengol, G., Filella, I., Llusia, J., Peñuelas, J., 2013. Floral volatile organic compounds: Between attraction and deterrence of visitors under global change. Perspectives in Plant Ecology, Evolution and Systematics 15, 56–67. https://doi.org/10.1016/j.ppees.2012.12.002

Fehsenfeld, F., Calvert, J., Fall, R., Goldan, P., Guenther, A.B., Hewitt, C.N., Lamb, B., Liu, S., Trainer, M., Westberg, H., Zimmerman, P., 1992. Emissions of volatile organic compounds from vegetation and the implications for atmospheric chemistry. Global Biogeochemical Cycles 6, 389–430. https://doi.org/10.1029/92GB02125

Fineschi, S., Loreto, F., Staudt, M., Peñuelas, J., 2013. Diversification of Volatile Isoprenoid Emissions from Trees: Evolutionary and Ecological Perspectives, in: Niinemets, Ü., Monson, R.K. (Eds.), Biology, Controls and Models of Tree Volatile Organic Compound Emissions, Tree Physiology. Springer Netherlands, Dordrecht, pp. 1–20. https://doi.org/10.1007/978-94-007-6606-8_1

Fleming, L.T., Lin, P., Laskin, A., Laskin, J., Weltman, R., Edwards, R.D., Arora, N.K., Yadav, A., Meinardi, S., Blake, D.R., Pillarisetti, A., Smith, K.R., Nizkorodov, S.A., 2018. Molecular composition of particulate matter emissions from dung and brushwood burning household cookstoves in Haryana, India. Atmospheric Chemistry and Physics 18, 2461–2480. https://doi.org/10.5194/acp-18-2461-2018

Fortunati, A., Barta, C., Brilli, F., Centritto, M., Zimmer, I., Schnitzler, J.-P., Loreto, F., 2008. Isoprene emission is not temperature-dependent during and after severe drought-stress: a physiological and biochemical analysis. Plant J 55, 687–697. https://doi.org/10.1111/j.1365-313X.2008.03538.x

Foti, V., Araniti, F., Manti, F., Alicandri, E., Giuffrè, A.M., Bonsignore, C.P., Castiglione, E., Sorgonà, A., Covino, S., Paolacci, A.R., Ciaffi, M., Badiani, M., 2020. Profiling Volatile Terpenoids from Calabrian Pine Stands Infested by the Pine Processionary Moth. Plants 9, 1362. https://doi.org/10.3390/plants9101362

Frost, C.J., Appel, H.M., Carlson, J.E., De Moraes, C.M., Mescher, M.C., Schultz, J.C., 2007. Within-plant signalling via volatiles overcomes vascular constraints on systemic signalling and primes responses against herbivores. Ecology Letters 10, 490–498. https://doi.org/10.1111/j.1461-0248.2007.01043.x

Frost, C.J., Mescher, M.C., Dervinis, C., Davis, J.M., Carlson, J.E., De Moraes, C.M., 2008. Priming defense genes and metabolites in hybrid poplar by the green leaf volatile cis-3-hexenyl acetate. New Phytologist 180, 722–734. https://doi.org/10.1111/j.1469-8137.2008.02599.x

Fry, J.L., Draper, D.C., Barsanti, K.C., Smith, J.N., Ortega, J., Winkler, P.M., Lawler, M.J., Brown, S.S., Edwards, P.M., Cohen, R.C., Lee, L., 2014. Secondary Organic Aerosol Formation and Organic Nitrate Yield from NO3 Oxidation of Biogenic Hydrocarbons. Environ. Sci. Technol. 48, 11944–11953. https://doi.org/10.1021/es502204x

Galen, C., Kaczorowski, R., Todd, S.L., Geib, J., Raguso, R.A., 2011. Dosage-Dependent Impacts of a Floral Volatile Compound on Pollinators, Larcenists, and the Potential for Floral Evolution in the Alpine Skypilot Polemonium viscosum. The American Naturalist 177, 258–272. https://doi.org/10.1086/657993

Gentner, D.R., Ormeño, E., Fares, S., Ford, T.B., Weber, R., Park, J.-H., Brioude, J., Angevine, W.M., Karlik, J.F., Goldstein, A.H., 2014. Emissions of terpenoids, benzenoids, and other biogenic gas-phase organic compounds from agricultural crops and their potential implications for air quality. Atmospheric Chemistry and Physics 14, 5393–5413. https://doi.org/10.5194/acp-14-5393-2014

Gershenzon, J., Dudareva, N., 2007. The function of terpene natural products in the natural world. Nat Chem Biol 3, 408–414. https://doi.org/10.1038/nchembio.2007.5

Gervasi, D.D.L., Schiestl, F.P., 2017. Real-time divergent evolution in plants driven by pollinators. Nat Commun 8, 14691. https://doi.org/10.1038/ncomms14691

Gfrerer, E., Laina, D., Gibernau, M., Fuchs, R., Happ, M., Tolasch, T., Trutschnig, W., Hörger, A.C., Comes, H.P., Dötterl, S., 2021. Floral Scents of a Deceptive Plant Are Hyperdiverse and Under Population-Specific Phenotypic Selection. Frontiers in Plant Science 12.

Ghimire, R.P., Kivimäenpää, M., Kasurinen, A., Häikiö, E., Holopainen, T., Holopainen, J.K., 2017. Herbivore-induced BVOC emissions of Scots pine under warming, elevated ozone and increased nitrogen availability in an open-field exposure. Agricultural and Forest Meteorology 242, 21–32. https://doi.org/10.1016/j.agrformet.2017.04.008

Ghimire, R.P., Markkanen, J.M., Kivimäenpää, M., Lyytikäinen-Saarenmaa, P., Holopainen, J.K., 2013. Needle Removal by Pine Sawfly Larvae Increases Branch-Level VOC Emissions and Reduces Below-Ground Emissions of Scots Pine. Environ. Sci. Technol. 47, 4325–4332. https://doi.org/10.1021/es4006064

Ghirardo, A., Heller, W., Fladung, M., Schnitzler, J.-P., Schroeder, H., 2012. Function of defensive volatiles in pedunculate oak (Quercus robur) is tricked by the moth Tortrix viridana. Plant, Cell & Environment 35, 2192–2207. https://doi.org/10.1111/j.1365-3040.2012.02545.x

Gols, R., 2014. Direct and indirect chemical defences against insects in a multitrophic framework. Plant, Cell & Environment 37, 1741–1752. https://doi.org/10.1111/pce.12318

Gouinguené, S.P., Turlings, T.C.J., 2002. The effects of abiotic factors on induced volatile emissions in corn plants. Plant Physiol 129, 1296–1307. https://doi.org/10.1104/pp.001941

Griffin, R.J., Cocker, D.R., Flagan, R.C., Seinfeld, J.H., 1999a. Organic aerosol formation from the oxidation of biogenic hydrocarbons. Journal of Geophysical Research D 104, 3555–3567.

Griffin, R.J., Cocker III, D.R., Flagan, R.C., Seinfeld, J.H., 1999b. Organic aerosol formation from the oxidation of biogenic hydrocarbons. Journal of Geophysical Research: Atmospheres 104, 3555–3567. https://doi.org/10.1029/1998JD100049

Gross, K., Sun, M., Schiestl, F.P., 2016. Why Do Floral Perfumes Become Different? Region-Specific Selection on Floral Scent in a Terrestrial Orchid. PLOS ONE 11, e0147975. https://doi.org/10.1371/journal.pone.0147975

Guenther, A., 2013. Biological and Chemical Diversity of Biogenic Volatile Organic Emissions into the Atmosphere. ISRN Atmospheric Sciences 2013, e786290. https://doi.org/10.1155/2013/786290

Guenther, A., Hewitt, C.N., Erickson, D., Fall, R., Geron, C., Graedel, T., Harley, P., Klinger, L., Lerdau, M., Mckay, W.A., Pierce, T., Scholes, B., Steinbrecher, R., Tallamraju, R., Taylor, J., Zimmerman, P., 1995. A global model of natural volatile organic compound emissions. Journal of Geophysical Research: Atmospheres 100, 8873–8892. https://doi.org/10.1029/94JD02950

Guenther, A.B., Jiang, X., Heald, C.L., Sakulyanontvittaya, T., Duhl, T., Emmons, L.K., Wang, X., 2012. The Model of Emissions of Gases and Aerosols from Nature version 2.1 (MEGAN2.1): an extended and updated framework for modeling biogenic emissions. Geoscientific Model Development 5, 1471–1492. https://doi.org/10.5194/gmd-5-1471-2012

Gull, A., Lone, A.A., Wani, N.U.I., 2019. Biotic and Abiotic Stresses in Plants, Abiotic and Biotic Stress in Plants. IntechOpen. https://doi.org/10.5772/intechopen.85832

Hallquist, M., Wenger, J.C., Baltensperger, U., Rudich, Y., Simpson, D., Claeys, M., Dommen, J., Donahue, N.M., George, C., Goldstein, A.H., Hamilton, J.F., Herrmann, H., Hoffmann, T., Iinuma, Y., Jang, M., Jenkin, M.E., Jimenez, J.L., Kiendler-Scharr, A., Maenhaut, W., McFiggans, G., Mentel, T.F., Monod, A., Prévôt, A.S.H., Seinfeld, J.H., Surratt, J.D., Szmigielski, R., Wildt, J., 2009. The formation, properties and impact of secondary organic aerosol: current and emerging issues. Atmospheric Chemistry and Physics 9, 5155–5236. https://doi.org/10.5194/acp-9-5155-2009

Hamilton, J.F., Lewis, A.C., Carey, T.J., Wenger, J.C., Borrás i Garcia, E., Muñoz, A., 2009. Reactive oxidation products promote secondary organic aerosol formation from green leaf volatiles. Atmospheric Chemistry and Physics 9, 3815–3823. https://doi.org/10.5194/acp-9-3815-2009

Handbook of Weather, Climate, and Water: Dynamics, Climate, Physical Meteorology, Weather Systems, and Measurements | Wiley [WWW Document], n.d. . Wiley.com. URL https://www.wiley.com/en-us/Handbook+of+Weather%2C+Climate%2C+and+Water%3A+Dynamics%2C+Climate%2C+Physical+Meteorology%2C+Weather+Systems%2C+and+Measurements+-p-9780471214908 (accessed 5.14.22).

Hao, L.Q., Romakkaniemi, S., Yli-Pirilä, P., Joutsensaari, J., Kortelainen, A., Kroll, J.H., Miettinen, P., Vaattovaara, P., Tiitta, P., Jaatinen, A., Kajos, M.K., Holopainen, J.K., Heijari, J., Rinne, J., Kulmala, M., Worsnop, D.R., Smith, J.N., Laaksonen, A., 2011. Mass yields of secondary organic aerosols from the oxidation of α-pinene and real plant emissions. Atmospheric Chemistry and Physics 11, 1367–1378. https://doi.org/10.5194/acp-11-1367-2011

Harder, L.D., Johnson, S.D., 2009. Darwin's beautiful contrivances: evolutionary and functional evidence for floral adaptation. New Phytologist 183, 530–545. https://doi.org/10.1111/j.1469-8137.2009.02914.x

Hare, J.D., 2011. Ecological role of volatiles produced by plants in response to damage by herbivorous insects. Annu Rev Entomol 56, 161–180. https://doi.org/10.1146/annurev-ento-120709-144753

Harrington, R., Clark, S.J., Welham, S.J., Verrier, P.J., Denholm, C.H., Hullé, M., Maurice, D., Rounsevell, M.D., Cocu, N., Consortium, E.U.E., 2007. Environmental change and the phenology

of European aphids. Global Change Biology 13, 1550–1564. https://doi.org/10.1111/j.1365-2486.2007.01394.x

Hatfield, M.L., Huff Hartz, K.E., 2011. Secondary organic aerosol from biogenic volatile organic compound mixtures. Atmospheric Environment 45, 2211–2219. https://doi.org/10.1016/j.atmosenv.2011.01.065

Heidel, A.J., Baldwin, I.T., 2004. Microarray analysis of salicylic acid- and jasmonic acid-signalling in responses of Nicotiana attenuata to attack by insects from multiple feeding guilds. Plant, Cell & Environment 27, 1362–1373. https://doi.org/10.1111/j.1365-3040.2004.01228.x

Heiden, A.C., Hoffmann, T., Kahl, J., Kley, D., Klockow, D., Langebartels, C., Mehlhorn, H., Sandermann Jr., H., Schraudner, M., Schuh, G., Wildt, J., 1999. Emission of Volatile Organic Compounds from Ozone-Exposed Plants. Ecological Applications 9, 1160–1167. https://doi.org/10.1890/1051-0761(1999)009[1160:EOVOCF]2.0.CO;2

Heijari, J., Blande, J.D., Holopainen, J.K., 2011. Feeding of large pine weevil on Scots pine stem triggers localised bark and systemic shoot emission of volatile organic compounds. Environmental and Experimental Botany 71, 390–398. https://doi.org/10.1016/j.envexpbot.2011.02.008

Heil, M., 2008. Indirect defence via tritrophic interactions. New Phytologist 178, 41–61. https://doi.org/10.1111/j.1469-8137.2007.02330.x

Heil, M., Bueno, J.C.S., 2007. Within-plant signaling by volatiles leads to induction and priming of an indirect plant defense in nature. PNAS 104, 5467–5472. https://doi.org/10.1073/pnas.0610266104

Heil, M., Karban, R., 2010. Explaining evolution of plant communication by airborne signals. Trends in Ecology & Evolution 25, 137–144. https://doi.org/10.1016/j.tree.2009.09.010

Hildebrand, D.F., Brown, G.C., Jackson, D.M., Hamilton-Kemp, T.R., 1993. Effects of some leaf-emitted volatile compounds on aphid population increase. J Chem Ecol 19, 1875–1887. https://doi.org/10.1007/BF00983793

Hilker, M., Meiners, T., 2006. Early Herbivore Alert: Insect Eggs Induce Plant Defense. J Chem Ecol 32, 1379–1397. https://doi.org/10.1007/s10886-006-9057-4

Himanen, S.J., Nerg, A.-M., Nissinen, A., Pinto, D.M., Stewart Jr, C.N., Poppy, G.M., Holopainen, J.K., 2009. Effects of elevated carbon dioxide and ozone on volatile terpenoid emissions and multitrophic communication of transgenic insecticidal oilseed rape (Brassica napus). New Phytologist 181, 174–186. https://doi.org/10.1111/j.1469-8137.2008.02646.x

Hodzic, A., Jimenez, J.L., Madronich, S., Aiken, A.C., Bessagnet, B., Curci, G., Fast, J., Lamarque, J.-F., Onasch, T.B., Roux, G., Schauer, J.J., Stone, E.A., Ulbrich, I.M., 2009. Modeling organic aerosols during MILAGRO: importance of biogenic secondary organic aerosols. Atmospheric Chemistry and Physics 9, 6949–6981. https://doi.org/10.5194/acp-9-6949-2009

Hodzic, A., Jimenez, J.L., Madronich, S., Canagaratna, M.R., DeCarlo, P.F., Kleinman, L., Fast, J., 2010. Modeling organic aerosols in a megacity: potential contribution of semi-volatile and intermediate volatility primary organic compounds to secondary organic aerosol formation. Atmospheric Chemistry and Physics 10, 5491–5514. https://doi.org/10.5194/acp-10-5491-2010

Holopainen, J., Blande, J., 2013. Where do herbivore-induced plant volatiles go? Frontiers in Plant Science 4, 185. https://doi.org/10.3389/fpls.2013.00185

Holopainen, J.K., 2004. Multiple functions of inducible plant volatiles. Trends in Plant Science 9, 529–533. https://doi.org/10.1016/j.tplants.2004.09.006

Holopainen, J.K., Gershenzon, J., 2010. Multiple stress factors and the emission of plant VOCs. Trends in Plant Science, Special Issue: Induced biogenic volatile organic compounds from plants 15, 176–184. https://doi.org/10.1016/j.tplants.2010.01.006

Holopainen, J.K., Virjamo, V., Ghimire, R.P., Blande, J.D., Julkunen-Tiitto, R., Kivimäenpää, M., 2018. Climate Change Effects on Secondary Compounds of Forest Trees in the Northern Hemisphere. Frontiers in Plant Science 9, 1445. https://doi.org/10.3389/fpls.2018.01445

Hossaert-McKey, M., Soler, C., Schatz, B., Proffit, M., 2010. Floral scents: their roles in nursery pollination mutualisms. Chemoecology 20, 75–88. https://doi.org/10.1007/s00049-010-0043-5

Jacobson, M.C., Hansson, H.-C., Noone, K.J., Charlson, R.J., 2000. Organic atmospheric aerosols: Review and state of the science. Reviews of Geophysics 38, 267–294. https://doi.org/10.1029/1998RG000045

Jansen, R.M.C., Wildt, J., Kappers, I.F., Bouwmeester, H.J., Hofstee, J.W., van Henten, E.J., 2011. Detection of Diseased Plants by Analysis of Volatile Organic Compound Emission. Annual Review of Phytopathology 49, 157–174. https://doi.org/10.1146/annurev-phyto-072910-095227

Jenkin, M.E., Valorso, R., Aumont, B., Rickard, A.R., Wallington, T.J., 2018. Estimation of rate coefficients and branching ratios for gas-phase reactions of OH with aliphatic organic compounds for use in automated mechanism construction. Atmospheric Chemistry and Physics 18, 9297–9328. https://doi.org/10.5194/acp-18-9297-2018

Jia, L., Xu, Y., 2020. The role of functional groups in the understanding of secondary organic aerosol formation mechanism from α-pinene. Science of The Total Environment 738, 139831. https://doi.org/10.1016/j.scitotenv.2020.139831

Jiang, Y., Veromann-Jürgenson, L.-L., Ye, J., Niinemets, Ü., 2018. Oak gall wasp infections of Quercus robur leaves lead to profound modifications in foliage photosynthetic and volatile emission characteristics. Plant, Cell & Environment 41, 160–175. https://doi.org/10.1111/pce.13050

Jiang, Y., Ye, J., Veromann, L.-L., Niinemets, Ü., 2016. Scaling of photosynthesis and constitutive and induced volatile emissions with severity of leaf infection by rust fungus (Melampsora larici-populina) in Populus balsamifera var. suaveolens. Tree Physiology 36, 856–872. https://doi.org/10.1093/treephys/tpw035

Jimenez, J.L., Canagaratna, M.R., Donahue, N.M., Prevot, A.S.H., Zhang, Q., Kroll, J.H., DeCarlo, P.F., Allan, J.D., Coe, H., Ng, N.L., Aiken, A.C., Docherty, K.S., Ulbrich, I.M., Grieshop, A.P., Robinson, A.L., Duplissy, J., Smith, J.D., Wilson, K.R., Lanz, V.A., Hueglin, C., Sun, Y.L., Tian, J., Laaksonen, A., Raatikainen, T., Rautiainen, J., Vaattovaara, P., Ehn, M., Kulmala, M., Tomlinson, J.M., Collins, D.R., Cubison, M.J., E., Dunlea, J., Huffman, J.A., Onasch, T.B., Alfarra, M.R., Williams, P.I., Bower, K., Kondo, Y., Schneider, J., Drewnick, F., Borrmann, S., Weimer, S., Demerjian, K., Salcedo, D., Cottrell, L., Griffin, R., Takami, A., Miyoshi, T., Hatakeyama, S., Shimono, A., Sun, J.Y., Zhang, Y.M., Dzepina, K., Kimmel, J.R., Sueper, D., Jayne, J.T., Herndon, S.C., Trimborn, A.M., Williams, L.R., Wood, E.C., Middlebrook, A.M., Kolb, C.E., Baltensperger, U., Worsnop, D.R., 2009. Evolution of Organic Aerosols in the Atmosphere. Science 326, 1525–1529. https://doi.org/10.1126/science.1180353

Joutsensaari, J., Loivamäki, M., Vuorinen, T., Miettinen, P., Nerg, A.-M., Holopainen, J.K., Laaksonen, A., 2005. Nanoparticle formation by ozonolysis of inducible plant volatiles. Atmospheric Chemistry and Physics 5, 1489–1495. https://doi.org/10.5194/acp-5-1489-2005

Joutsensaari, J., Yli-Pirilä, P., Korhonen, H., Arola, A., Blande, J.D., Heijari, J., Kivimäenpää, M., Mikkonen, S., Hao, L., Miettinen, P., Lyytikäinen-Saarenmaa, P., Faiola, C.L., Laaksonen, A., Holopainen, J.K., 2015. Biotic stress accelerates formation of climate-relevant aerosols in boreal forests. Atmospheric Chemistry and Physics 15, 12139–12157. https://doi.org/10.5194/acp-15-12139-2015

Kanakidou, M., Seinfeld, J.H., Pandis, S.N., Barnes, I., Dentener, F.J., Facchini, M.C., Van Dingenen, R., Ervens, B., Nenes, A., Nielsen, C.J., Swietlicki, E., Putaud, J.P., Balkanski, Y., Fuzzi, S., Horth, J., Moortgat, G.K., Winterhalter, R., Myhre, C.E.L., Tsigaridis, K., Vignati, E., Stephanou, E.G., Wilson, J., 2005. Organic aerosol and global climate modelling: a review. Atmospheric Chemistry and Physics 5, 1053–1123. https://doi.org/10.5194/acp-5-1053-2005

Kantsa, A., Raguso, R.A., Lekkas, T., Kalantzi, O.-I., Petanidou, T., 2019. Floral volatiles and visitors: A meta-network of associations in a natural community. Journal of Ecology 107, 2574–2586. https://doi.org/10.1111/1365-2745.13197

Kappers, I.F., Aharoni, A., van Herpen, T.W.J.M., Luckerhoff, L.L.P., Dicke, M., Bouwmeester, H.J., 2005. Genetic Engineering of Terpenoid Metabolism Attracts Bodyguards to Arabidopsis. Science 309, 2070–2072. https://doi.org/10.1126/science.1116232

Karban, R., Shiojiri, K., Huntzinger, M., McCall, A.C., 2006. Damage-induced resistance in sagebrush: volatiles are key to intra- and interplant communication. Ecology 87, 922–930. https://doi.org/10.1890/0012-9658(2006)87[922:drisva]2.0.co;2

Karel, T.H., Man, G., 2017. Major forest insect and disease conditions in the United States: 2015. Major forest insect and disease conditions in the United States: 2015.

Kari, E., Faiola, C., Isokääntä, S., Miettinen, P., Yli-Pirilä, P., Buchholz, A., Kivimäenpää, M., Mikkonen, S., Holopainen, J., Virtanen, A., 2019. Time-resolved characterization of biotic stress emissions from Scots pines being fed upon by pine weevil by means of PTR-ToF-MS. Boreal Environment Research 24, 25–49.

Kessler, A., Baldwin, I.T., 2001. Defensive Function of Herbivore-Induced Plant Volatile Emissions in Nature. Science 291, 2141–2144. https://doi.org/10.1126/science.291.5511.2141

Kessler, A., Halitschke, R., 2009. Testing the Potential for Conflicting Selection on Floral Chemical Traits by Pollinators and Herbivores: Predictions and Case Study. Functional Ecology 23, 901–912.

Kessler, A., Halitschke, R., Diezel, C., Baldwin, I.T., 2006. Priming of plant defense responses in nature by airborne signaling between Artemisia tridentata and Nicotiana attenuata. Oecologia 148, 280–292. https://doi.org/10.1007/s00442-006-0365-8

Kessler, A., Heil, M., 2011. The multiple faces of indirect defences and their agents of natural selection. Functional Ecology 25, 348–357. https://doi.org/10.1111/j.1365-2435.2010.01818.x

Kessler, D., Diezel, C., Clark, D.G., Colquhoun, T.A., Baldwin, I.T., 2013. Petunia flowers solve the defence/apparency dilemma of pollinator attraction by deploying complex floral blends. Ecology Letters 16, 299–306. https://doi.org/10.1111/ele.12038

Khalaj, F., Rivas-Ubach, A., Anderton, C.R., China, S., Mooney, K., Faiola, C.L., 2021. Acyclic Terpenes Reduce Secondary Organic Aerosol Formation from Emissions of a Riparian Shrub. ACS Earth Space Chem. 5, 1242–1253. https://doi.org/10.1021/acsearthspacechem.0c00300

Kiendler-Scharr, A., Andres, S., Bachner, M., Behnke, K., Broch, S., Hofzumahaus, A., Holland, F., Kleist, E., Mentel, T.F., Rubach, F., Springer, M., Steitz, B., Tillmann, R., Wahner, A., Schnitzler, J.-P., Wildt, J., 2012. Isoprene in poplar emissions: effects on new particle formation and OH concentrations. Atmospheric Chemistry and Physics 12, 1021–1030. https://doi.org/10.5194/acp-12-1021-2012

Kiendler-Scharr, A., Wildt, J., Maso, M.D., Hohaus, T., Kleist, E., Mentel, T.F., Tillmann, R., Uerlings, R., Schurr, U., Wahner, A., 2009a. New particle formation in forests inhibited by isoprene emissions. Nature 461, 381–384. https://doi.org/10.1038/nature08292

Kiendler-Scharr, A., Zhang, Q., Hohaus, T., Kleist, E., Mensah, A., Mentel, T.F., Spindler, C., Uerlings, R., Tillmann, R., Wildt, J., 2009b. Aerosol Mass Spectrometric Features of Biogenic SOA: Observations from a Plant Chamber and in Rural Atmospheric Environments. Environ. Sci. Technol. 43, 8166–8172. https://doi.org/10.1021/es901420b

Kivimäenpää, M., Ghimire, R.P., Sutinen, S., Häikiö, E., Kasurinen, A., Holopainen, T., Holopainen, J.K., 2016. Increases in volatile organic compound emissions of Scots pine in response to elevated ozone and warming are modified by herbivory and soil nitrogen availability. Eur J Forest Res 135, 343–360. https://doi.org/10.1007/s10342-016-0939-x

Knudsen, J.T., Eriksson, R., Gershenzon, J., Ståhl, B., 2006. Diversity and distribution of floral scent. Bot. Rev 72, 1. https://doi.org/10.1663/0006-8101(2006)72[1:DADOFS]2.0.CO;2

Koop, T., Bookhold, J., Shiraiwa, M., Pöschl, U., 2011. Glass transition and phase state of organic compounds: dependency on molecular properties and implications for secondary organic aerosols in the atmosphere. Physical Chemistry Chemical Physics 13, 19238–19255. https://doi.org/10.1039/C1CP22617G

Kourtchev, I., Doussin, J.-F., Giorio, C., Mahon, B., Wilson, E.M., Maurin, N., Pangui, E., Venables, D.S., Wenger, J.C., Kalberer, M., 2015. Molecular composition of fresh and aged secondary organic aerosol from a mixture of biogenic volatile compounds: a high-resolution mass

spectrometry study. Atmospheric Chemistry and Physics 15, 5683–5695. https://doi.org/10.5194/acp-15-5683-2015

Kristensen, K., Cui, T., Zhang, H., Gold, A., Glasius, M., Surratt, J.D., 2014. Dimers in α-pinene secondary organic aerosol: effect of hydroxyl radical, ozone, relative humidity and aerosol acidity. Atmospheric Chemistry and Physics 14, 4201–4218. https://doi.org/10.5194/acp-14-4201-2014

Kroll, J.H., Donahue, N.M., Jimenez, J.L., Kessler, S.H., Canagaratna, M.R., Wilson, K.R., Altieri, K.E., Mazzoleni, L.R., Wozniak, A.S., Bluhm, H., Mysak, E.R., Smith, J.D., Kolb, C.E., Worsnop, D.R., 2011. Carbon oxidation state as a metric for describing the chemistry of atmospheric organic aerosol. Nature Chem 3, 133–139. https://doi.org/10.1038/nchem.948

Kroll, J.H., Lim, C.Y., Kessler, S.H., Wilson, K.R., 2015. Heterogeneous Oxidation of Atmospheric Organic Aerosol: Kinetics of Changes to the Amount and Oxidation State of Particle-Phase Organic Carbon. J. Phys. Chem. A 119, 10767–10783. https://doi.org/10.1021/acs.jpca.5b06946

Kroll, J.H., Ng, N.L., Murphy, S.M., Flagan, R.C., Seinfeld, J.H., 2006. Secondary Organic Aerosol Formation from Isoprene Photooxidation. Environ. Sci. Technol. 40, 1869–1877. https://doi.org/10.1021/es0524301

Kulmala, M., Suni, T., Lehtinen, K.E.J., Dal Maso, M., Boy, M., Reissell, A., Rannik, Ü., Aalto, P., Keronen, P., Hakola, H., Bäck, J., Hoffmann, T., Vesala, T., Hari, P., 2004. A new feedback mechanism linking forests, aerosols, and climate. Atmospheric Chemistry and Physics 4, 557–562. https://doi.org/10.5194/acp-4-557-2004

Kurz, W.A., Dymond, C.C., Stinson, G., Rampley, G.J., Neilson, E.T., Carroll, A.L., Ebata, T., Safranyik, L., 2008. Mountain pine beetle and forest carbon feedback to climate change. Nature 452, 987–990. https://doi.org/10.1038/nature06777

Kuwata, M., Martin, S.T., 2012. Phase of atmospheric secondary organic material affects its reactivity. Proceedings of the National Academy of Sciences 109, 17354–17359. https://doi.org/10.1073/pnas.1209071109

La, Y.S., Camredon, M., Ziemann, P.J., Valorso, R., Matsunaga, A., Lannuque, V., Lee-Taylor, J., Hodzic, A., Madronich, S., Aumont, B., 2016. Impact of chamber wall loss of gaseous organic compounds on secondary organic aerosol formation: explicit modeling of SOA formation from alkane and alkene oxidation. Atmospheric Chemistry and Physics 16, 1417–1431. https://doi.org/10.5194/acp-16-1417-2016

Lambe, A.T., Ahern, A.T., Williams, L.R., Slowik, J.G., Wong, J.P.S., Abbatt, J.P.D., Brune, W.H., Ng, N.L., Wright, J.P., Croasdale, D.R., Worsnop, D.R., Davidovits, P., Onasch, T.B., 2011a. Characterization of aerosol photooxidation flow reactors: heterogeneous oxidation, secondary organic aerosol formation and cloud condensation nuclei activity measurements. Atmospheric Measurement Techniques 4, 445–461. https://doi.org/10.5194/amt-4-445-2011

Lambe, A.T., Cappa, C.D., Massoli, P., Onasch, T.B., Forestieri, S.D., Martin, A.T., Cummings, M.J., Croasdale, D.R., Brune, W.H., Worsnop, D.R., Davidovits, P., 2013. Relationship between Oxidation Level and Optical Properties of Secondary Organic Aerosol. Environ. Sci. Technol. 47, 6349–6357. https://doi.org/10.1021/es401043j

Lambe, A.T., Chhabra, P.S., Onasch, T.B., Brune, W.H., Hunter, J.F., Kroll, J.H., Cummings, M.J., Brogan, J.F., Parmar, Y., Worsnop, D.R., Kolb, C.E., Davidovits, P., 2015. Effect of oxidant concentration, exposure time, and seed particles on secondary organic aerosol chemical composition and yield. Atmospheric Chemistry and Physics 15, 3063–3075. https://doi.org/10.5194/acp-15-3063-2015

Lambe, A.T., Onasch, T.B., Massoli, P., Croasdale, D.R., Wright, J.P., Ahern, A.T., Williams, L.R., Worsnop, D.R., Brune, W.H., Davidovits, P., 2011b. Laboratory studies of the chemical composition and cloud condensation nuclei (CCN) activity of secondary organic aerosol (SOA) and oxidized primary organic aerosol (OPOA). Atmospheric Chemistry and Physics 11, 8913–8928. https://doi.org/10.5194/acp-11-8913-2011

Laothawornkitkul, J., Taylor, J.E., Paul, N.D., Hewitt, C.N., 2009. Biogenic volatile organic compounds in the Earth system. New Phytologist 183, 27–51. https://doi.org/10.1111/j.1469-8137.2009.02859.x

Lee, L.A., Reddington, C.L., Carslaw, K.S., 2016. On the relationship between aerosol model uncertainty and radiative forcing uncertainty. PNAS 113, 5820–5827. https://doi.org/10.1073/pnas.1507050113

Lelieveld, J., Butler, T.M., Crowley, J.N., Dillon, T.J., Fischer, H., Ganzeveld, L., Harder, H., Lawrence, M.G., Martinez, M., Taraborrelli, D., Williams, J., 2008. Atmospheric oxidation capacity sustained by a tropical forest. Nature 452, 737–740. https://doi.org/10.1038/nature06870

Lelieveld, J., Evans, J.S., Fnais, M., Giannadaki, D., Pozzer, A., 2015. The contribution of outdoor air pollution sources to premature mortality on a global scale. Nature 525, 367–371. https://doi.org/10.1038/nature15371

Leonard, A.S., Dornhaus, A., Papaj, D.R., 2011a. Forget-me-not: Complex floral displays, inter-signal interactions, and pollinator cognition. Current Zoology 57, 215–224. https://doi.org/10.1093/czoolo/57.2.215

Leonard, A.S., Dornhaus, A., Papaj, D.R., 2011b. Flowers help bees cope with uncertainty: signal detection and the function of floral complexity. Journal of Experimental Biology 214, 113–121. https://doi.org/10.1242/jeb.047407

Lerdau, M., Slobodkin, L., 2002. Trace gas emissions and species-dependent ecosystem services. Trends in Ecology & Evolution 17, 309–312. https://doi.org/10.1016/S0169-5347(02)02535-1

Li, K., Liggio, J., Lee, P., Han, C., Liu, Q., Li, S.-M., 2019. Secondary organic aerosol formation from α-pinene, alkanes, and oil-sands-related precursors in a new oxidation flow reactor. Atmospheric Chemistry and Physics 19, 9715–9731. https://doi.org/10.5194/acp-19-9715-2019

Li, Y., Day, D.A., Stark, H., Jimenez, J.L., Shiraiwa, M., 2020. Predictions of the glass transition temperature and viscosity of organic aerosols from volatility distributions. Atmospheric Chemistry and Physics 20, 8103–8122. https://doi.org/10.5194/acp-20-8103-2020

Li, Y., Pöschl, U., Shiraiwa, M., 2016. Molecular corridors and parameterizations of volatility in the chemical evolution of organic aerosols. Atmospheric Chemistry and Physics 16, 3327–3344. https://doi.org/10.5194/acp-16-3327-2016

Litvak, M.E., Monson, R.K., 1998. Patterns of induced and constitutive monoterpene production in conifer needles in relation to insect herbivory. Oecologia 114, 531–540. https://doi.org/10.1007/s004420050477

Llusià, J., Peñuelas, J., 2001. Emission of volatile organic compounds by apple trees under spider mite attack and attraction of predatory mites. Exp Appl Acarol 25, 65–77. https://doi.org/10.1023/A:1010659826193

Loreto, F., Bagnoli, F., Fineschi, S., 2009. One species, many terpenes: matching chemical and biological diversity. Trends in Plant Science 14, 416–420. https://doi.org/10.1016/j.tplants.2009.06.003

Loreto, F., Barta, C., Brilli, F., Nogues, I., 2006. On the induction of volatile organic compound emissions by plants as consequence of wounding or fluctuations of light and temperature. Plant Cell Environ 29, 1820–1828. https://doi.org/10.1111/j.1365-3040.2006.01561.x

Loreto, F., Ciccioli, P., Cecinato, A., Brancaleoni, E., Frattoni, M., Tricoli, D., 1996. Influence of Environmental Factors and Air Composition on the Emission of [alpha]-Pinene from Quercus ilex Leaves. Plant Physiology 110, 267–275. https://doi.org/10.1104/pp.110.1.267

Loreto, F., Delfine, S., 2000. Emission of Isoprene from Salt-Stressed Eucalyptus globulus Leaves1. Plant Physiology 123, 1605–1610. https://doi.org/10.1104/pp.123.4.1605

Loreto, F., Dicke, M., Schnitzler, J.-P., Turlings, T.C.J., 2014. Plant volatiles and the environment. Plant, Cell & Environment 37, 1905–1908. https://doi.org/10.1111/pce.12369

Loreto, F., Mannozzi, M., Maris, C., Nascetti, P., Ferranti, F., Pasqualini, S., 2001. Ozone Quenching Properties of Isoprene and Its Antioxidant Role in Leaves. Plant Physiology 126, 993–1000. https://doi.org/10.1104/pp.126.3.993

Loreto, F., Schnitzler, J.-P., 2010. Abiotic stresses and induced BVOCs. Trends in Plant Science, Special Issue: Induced biogenic volatile organic compounds from plants 15, 154–166. https://doi.org/10.1016/j.tplants.2009.12.006

Luft, S., Curio, E., Tacud, B., 2003. The use of olfaction in the foraging behaviour of the golden-mantled flying fox, Pteropus pumilus, and the greater musky fruit bat, Ptenochirus jagori (Megachiroptera: Pteropodidae). Naturwissenschaften 90, 84–87. https://doi.org/10.1007/s00114-002-0393-0

Maffei, M.E., 2010. Sites of synthesis, biochemistry and functional role of plant volatiles. South African Journal of Botany, Chemical diversity and biological functions of plant volatiles 76, 612–631. https://doi.org/10.1016/j.sajb.2010.03.003

Maja, M.M., Kasurinen, A., Yli-Pirilä, P., Joutsensaari, J., Klemola, T., Holopainen, T., Holopainen, J.K., 2014. Contrasting responses of silver birch VOC emissions to short- and long-term herbivory. Tree Physiology 34, 241–252. https://doi.org/10.1093/treephys/tpt127

Majetic, C.J., Raguso, R.A., Ashman, T.-L., 2009. The sweet smell of success: floral scent affects pollinator attraction and seed fitness in Hesperis matronalis. Functional Ecology 23, 480–487. https://doi.org/10.1111/j.1365-2435.2008.01517.x

Malloy, Q.G.J., Nakao, S., Qi, L., Austin, R., Stothers, C., Hagino, H., Cocker, D.R., 2009. Real-Time Aerosol Density Determination Utilizing a Modified Scanning Mobility Particle Sizer—Aerosol Particle Mass Analyzer System. Aerosol Science and Technology 43, 673–678. https://doi.org/10.1080/02786820902832960

Mao, J., Ren, X., Brune, W.H., Olson, J.R., Crawford, J.H., Fried, A., Huey, L.G., Cohen, R.C., Heikes, B., Singh, H.B., Blake, D.R., Sachse, G.W., Diskin, G.S., Hall, S.R., Shetter, R.E., 2009. Airborne measurement of OH reactivity during INTEX-B. Atmospheric Chemistry and Physics 9, 163–173. https://doi.org/10.5194/acp-9-163-2009

Marais, E.A., Jacob, D.J., Turner, J.R., Mickley, L.J., 2017. Evidence of 1991–2013 decrease of biogenic secondary organic aerosol in response to SO 2 emission controls. Environ. Res. Lett. 12, 054018. https://doi.org/10.1088/1748-9326/aa69c8

Markovic, D., Colzi, I., Taiti, C., Ray, S., Scalone, R., Gregory Ali, J., Mancuso, S., Ninkovic, V., 2019. Airborne signals synchronize the defenses of neighboring plants in response to touch. Journal of Experimental Botany 70, 691–700. https://doi.org/10.1093/jxb/ery375

Matthes, M.C., Bruce, T.J.A., Ton, J., Verrier, P.J., Pickett, J.A., Napier, J.A., 2010. The transcriptome of cis-jasmone-induced resistance in Arabidopsis thaliana and its role in indirect defence. Planta 232, 1163–1180. https://doi.org/10.1007/s00425-010-1244-4

Mauricio, R., Rausher, M.D., 1997. Experimental Manipulation of Putative Selective Agents Provides Evidence for the Role of Natural Enemies in the Evolution of Plant Defense. Evolution 51, 1435–1444. https://doi.org/10.1111/j.1558-5646.1997.tb01467.x

McFiggans, G., Mentel, T.F., Wildt, J., Pullinen, I., Kang, S., Kleist, E., Schmitt, S., Springer, M., Tillmann, R., Wu, C., Zhao, D., Hallquist, M., Faxon, C., Le Breton, M., Hallquist, Å.M., Simpson, D., Bergström, R., Jenkin, M.E., Ehn, M., Thornton, J.A., Alfarra, M.R., Bannan, T.J., Percival, C.J., Priestley, M., Topping, D., Kiendler-Scharr, A., 2019. Secondary organic aerosol reduced by mixture of atmospheric vapours. Nature 565, 587–593. https://doi.org/10.1038/s41586-018-0871-y

McVay, R.C., Zhang, X., Aumont, B., Valorso, R., Camredon, M., La, Y.S., Wennberg, P.O., Seinfeld, J.H., 2016. SOA formation from the photooxidation of α-pinene: systematic exploration of the simulation of chamber data. Atmospheric Chemistry and Physics 16, 2785–2802. https://doi.org/10.5194/acp-16-2785-2016

M. Donahue, N., Hartz, K.E.H., Chuong, B., A. Presto, A., O. Stanier, C., Rosenhørn, T., L. Robinson, A., N. Pandis, S., 2005. Critical factors determining the variation in SOA yields from terpene ozonolysis: A combined experimental and computational study. Faraday Discussions 130, 295–309. https://doi.org/10.1039/B417369D

Mehra, A., Krechmer, J.E., Lambe, A., Sarkar, C., Williams, L., Khalaj, F., Guenther, A., Jayne, J., Coe, H., Worsnop, D., Faiola, C., Canagaratna, M., 2020. Oligomer and highly oxygenated organic

molecule formation from oxidation of oxygenated monoterpenes emitted by California sage plants. Atmospheric Chemistry and Physics 20, 10953–10965. https://doi.org/10.5194/acp-20-10953-2020

Mentel, T.F., Wildt, J., Kiendler-Scharr, A., Kleist, E., Tillmann, R., Dal Maso, M., Fisseha, R., Hohaus, T., Spahn, H., Uerlings, R., Wegener, R., Griffiths, P.T., Dinar, E., Rudich, Y., Wahner, A., 2009. Photochemical production of aerosols from real plant emissions. Atmospheric Chemistry and Physics 9, 4387–4406. https://doi.org/10.5194/acp-9-4387-2009

M. Fiore, A., Naik, V., V. Spracklen, D., Steiner, A., Unger, N., Prather, M., Bergmann, D., J. Cameron-Smith, P., Cionni, I., J. Collins, W., Dalsøren, S., Eyring, V., A. Folberth, G., Ginoux, P., W. Horowitz, L., Josse, B., Lamarque, J.-F., A. MacKenzie, I., Nagashima, T., M. O'Connor, F., Righi, M., T. Rumbold, S., T. Shindell, D., B. Skeie, R., Sudo, K., Szopa, S., Takemura, T., Zeng, G., 2012. Global air quality and climate. Chemical Society Reviews 41, 6663–6683. https://doi.org/10.1039/C2CS35095E

Michel, A., Prescher, A.-K., Schwärzel, K., 2020. Forest Condition in Europe: 2019 Technical Report of ICP Forests. Report under the UNECE Convention on Long-Range Transboundary Air Pollution (Air Convention).

Misztal, P.K., Hewitt, C.N., Wildt, J., Blande, J.D., Eller, A.S.D., Fares, S., Gentner, D.R., Gilman, J.B., Graus, M., Greenberg, J., Guenther, A.B., Hansel, A., Harley, P., Huang, M., Jardine, K., Karl, T., Kaser, L., Keutsch, F.N., Kiendler-Scharr, A., Kleist, E., Lerner, B.M., Li, T., Mak, J., Nölscher, A.C., Schnitzhofer, R., Sinha, V., Thornton, B., Warneke, C., Wegener, F., Werner, C., Williams, J., Worton, D.R., Yassaa, N., Goldstein, A.H., 2015. Atmospheric benzenoid emissions from plants rival those from fossil fuels. Sci Rep 5, 12064. https://doi.org/10.1038/srep12064

Mithöfer, A., Boland, W., 2012. Plant Defense Against Herbivores: Chemical Aspects. Annual Review of Plant Biology 63, 431–450. https://doi.org/10.1146/annurev-arplant-042110-103854

Mittler, R., 2006. Abiotic stress, the field environment and stress combination. Trends in Plant Science 11, 15–19. https://doi.org/10.1016/j.tplants.2005.11.002

Moise, T., Flores, J.M., Rudich, Y., 2015. Optical Properties of Secondary Organic Aerosols and Their Changes by Chemical Processes. Chem. Rev. 115, 4400–4439. https://doi.org/10.1021/cr5005259

Monson, R.K., Jones, R.T., Rosenstiel, T.N., Schnitzler, J.-P., 2013. Why only some plants emit isoprene. Plant, Cell & Environment 36, 503–516. https://doi.org/10.1111/pce.12015

Moreira, X., Nell, C.S., Katsanis, A., Rasmann, S., Mooney, K.A., 2018a. Herbivore specificity and the chemical basis of plant–plant communication in Baccharis salicifolia (Asteraceae). New Phytologist 220, 703–713. https://doi.org/10.1111/nph.14164

Moreira, X., Nell, C.S., Meza-Lopez, M.M., Rasmann, S., Mooney, K.A., 2018b. Specificity of plant–plant communication for Baccharis salicifolia sexes but not genotypes. Ecology 99, 2731–2739. https://doi.org/10.1002/ecy.2534

Mumm, R., Schrank, K., Wegener, R., Schulz, S., Hilker, M., 2003. Chemical Analysis of Volatiles Emitted by Pinus sylvestris After Induction by Insect Oviposition. J Chem Ecol 29, 1235–1252. https://doi.org/10.1023/A:1023841909199

Nakao, S., Tang, P., Tang, X., Clark, C.H., Qi, L., Seo, E., Asa-Awuku, A., Cocker, D., 2013. Density and elemental ratios of secondary organic aerosol: Application of a density prediction method. Atmospheric Environment 68, 273–277. https://doi.org/10.1016/j.atmosenv.2012.11.006

Nault, B.A., Jo, D.S., McDonald, B.C., Campuzano-Jost, P., Day, D.A., Hu, W., Schroder, J.C., Allan, J., Blake, D.R., Canagaratna, M.R., Coe, H., Coggon, M.M., DeCarlo, P.F., Diskin, G.S., Dunmore, R., Flocke, F., Fried, A., Gilman, J.B., Gkatzelis, G., Hamilton, J.F., Hanisco, T.F., Hayes, P.L., Henze, D.K., Hodzic, A., Hopkins, J., Hu, M., Huey, L.G., Jobson, B.T., Kuster, W.C., Lewis, A., Li, M., Liao, J., Nawaz, M.O., Pollack, I.B., Peischl, J., Rappenglück, B., Reeves, C.E., Richter, D., Roberts, J.M., Ryerson, T.B., Shao, M., Sommers, J.M., Walega, J., Warneke, C., Weibring, P., Wolfe, G.M., Young, D.E., Yuan, B., Zhang, Q., de Gouw, J.A., Jimenez, J.L., 2021. Secondary organic aerosols from anthropogenic volatile organic compounds contribute

substantially to air pollution mortality. Atmospheric Chemistry and Physics 21, 11201–11224. https://doi.org/10.5194/acp-21-11201-2021

Nel, A., 2005. Atmosphere. Air pollution-related illness: effects of particles. Science 308, 804–806. https://doi.org/10.1126/science.1108752

Ng, N.L., Chhabra, P.S., Chan, A.W.H., Surratt, J.D., Kroll, J.H., Kwan, A.J., McCabe, D.C., Wennberg, P.O., Sorooshian, A., Murphy, S.M., Dalleska, N.F., Flagan, R.C., Seinfeld, J.H., 2007. Effect of NOx level on secondary organic aerosol (SOA) formation from the photooxidation of terpenes. Atmospheric Chemistry and Physics 7, 5159–5174.

Ng, N.L., Kroll, J.H., Keywood, M.D., Bahreini, R., Varutbangkul, V., Flagan, R.C., Seinfeld, J.H., Lee, A., Goldstein, A.H., 2006. Contribution of first- versus second-generation products to secondary organic aerosols formed in the oxidation of biogenic hydrocarbons. Environ Sci Technol 40, 2283–2297. https://doi.org/10.1021/es052269u

Niinemets, Ü., 2010a. Responses of forest trees to single and multiple environmental stresses from seedlings to mature plants: Past stress history, stress interactions, tolerance and acclimation. Forest Ecology and Management 260, 1623–1639. https://doi.org/10.1016/j.foreco.2010.07.054

Niinemets, Ü., 2010b. Mild versus severe stress and BVOCs: thresholds, priming and consequences. Trends in Plant Science, Special Issue: Induced biogenic volatile organic compounds from plants 15, 145–153. https://doi.org/10.1016/j.tplants.2009.11.008

Niinemets, Ü., Kännaste, A., Copolovici, L., 2013. Quantitative patterns between plant volatile emissions induced by biotic stresses and the degree of damage. Frontiers in Plant Science 4, 262. https://doi.org/10.3389/fpls.2013.00262

Niinemets, Ü., Monson, R.K. (Eds.), 2013. Biology, Controls and Models of Tree Volatile Organic Compound Emissions, Tree Physiology. Springer Netherlands, Dordrecht. https://doi.org/10.1007/978-94-007-6606-8

Ninkovic, V., Markovic, D., Rensing, M., 2021. Plant volatiles as cues and signals in plant communication. Plant, Cell & Environment 44, 1030–1043. https://doi.org/10.1111/pce.13910

Nizkorodov, S.A., Laskin, J., Laskin, A., 2011. Molecular chemistry of organic aerosols through the application of high resolution mass spectrometry. Phys. Chem. Chem. Phys. 13, 3612–3629. https://doi.org/10.1039/C0CP02032J

Nozière, B., Kalberer, M., Claeys, M., Allan, J., D'Anna, B., Decesari, S., Finessi, E., Glasius, M., Grgić, I., Hamilton, J.F., Hoffmann, T., Iinuma, Y., Jaoui, M., Kahnt, A., Kampf, C.J., Kourtchev, I., Maenhaut, W., Marsden, N., Saarikoski, S., Schnelle-Kreis, J., Surratt, J.D., Szidat, S., Szmigielski, R., Wisthaler, A., 2015. The Molecular Identification of Organic Compounds in the Atmosphere: State of the Art and Challenges. Chem. Rev. 115, 3919–3983. https://doi.org/10.1021/cr5003485

Odum, J.R., Hoffmann, T., Bowman, F., Collins, D., Flagan, R.C., Seinfeld, J.H., 1996. Gas/Particle Partitioning and Secondary Organic Aerosol Yields. Environ. Sci. Technol. 30, 2580–2585. https://doi.org/10.1021/es950943+

Palm, B.B., Campuzano-Jost, P., Day, D.A., Ortega, A.M., Fry, J.L., Brown, S.S., Zarzana, K.J., Dube, W., Wagner, N.L., Draper, D.C., Kaser, L., Jud, W., Karl, T., Hansel, A., Gutiérrez-Montes, C., Jimenez, J.L., 2017. Secondary organic aerosol formation from in situ OH, O_3, and NO_3 oxidation of ambient forest air in an oxidation flow reactor. Atmospheric Chemistry and Physics 17, 5331–5354. https://doi.org/10.5194/acp-17-5331-2017

Palm, B.B., Campuzano-Jost, P., Ortega, A.M., Day, D.A., Kaser, L., Jud, W., Karl, T., Hansel, A., Hunter, J.F., Cross, E.S., Kroll, J.H., Peng, Z., Brune, W.H., Jimenez, J.L., 2016. In situ secondary organic aerosol formation from ambient pine forest air using an oxidation flow reactor. Atmospheric Chemistry and Physics 16, 2943–2970. https://doi.org/10.5194/acp-16-2943-2016

Palm, B.B., de Sá, S.S., Day, D.A., Campuzano-Jost, P., Hu, W., Seco, R., Sjostedt, S.J., Park, J.-H., Guenther, A.B., Kim, S., Brito, J., Wurm, F., Artaxo, P., Thalman, R., Wang, J., Yee, L.D., Wernis, R., Isaacman-VanWertz, G., Goldstein, A.H., Liu, Y., Springston, S.R., Souza, R., Newburn, M.K., Alexander, M.L., Martin, S.T., Jimenez, J.L., 2018. Secondary organic aerosol

formation from ambient air in an oxidation flow reactor in central Amazonia. Atmospheric Chemistry and Physics 18, 467–493. https://doi.org/10.5194/acp-18-467-2018

Pankow, J.F., 1994. An absorption model of gas/particle partitioning of organic compounds in the atmosphere. Atmospheric Environment 28, 185–188. https://doi.org/10.1016/1352-2310(94)90093-0

Parachnowitsch, A.L., Raguso, R.A., Kessler, A., 2012. Phenotypic selection to increase floral scent emission, but not flower size or colour in bee-pollinated Penstemon digitalis. New Phytologist 195, 667–675. https://doi.org/10.1111/j.1469-8137.2012.04188.x

Paré, P.W., Tumlinson, J.H., 1999. Plant Volatiles as a Defense against Insect Herbivores. Plant Physiology 121, 325–332. https://doi.org/10.1104/pp.121.2.325

Pegoraro, E., Rey, A., Greenberg, J., Harley, P., Grace, J., Malhi, Y., Guenther, A., 2004. Effect of drought on isoprene emission rates from leaves of Quercus virginiana Mill. Atmospheric Environment 38, 6149–6156. https://doi.org/10.1016/j.atmosenv.2004.07.028

Peng, Z., Jimenez, J.L., 2020. Radical chemistry in oxidation flow reactors for atmospheric chemistry research. Chem. Soc. Rev. 49, 2570–2616. https://doi.org/10.1039/C9CS00766K

Peng, Z., Lee-Taylor, J., Orlando, J.J., Tyndall, G.S., Jimenez, J.L., 2019. Organic peroxy radical chemistry in oxidation flow reactors and environmental chambers and their atmospheric relevance. Atmospheric Chemistry and Physics 19, 813–834. https://doi.org/10.5194/acp-19-813-2019

Peñuelas, J., Filella, I., Seco, R., Llusià, J., 2009. Increase in isoprene and monoterpene emissions after re-watering of droughted Quercus ilex seedlings. Biol Plant 53, 351–354. https://doi.org/10.1007/s10535-009-0065-4

Peñuelas, J., Llusià, J., 2004. Plant VOC emissions: making use of the unavoidable. Trends in Ecology & Evolution 19, 402–404. https://doi.org/10.1016/j.tree.2004.06.002

Peñuelas, J., Llusià, J., 2003. BVOCs: plant defense against climate warming? Trends Plant Sci 8, 105–109. https://doi.org/10.1016/S1360-1385(03)00008-6

Penuelas, J., Llusia, J., Estiarte, M., 1995. Terpenoids: a plant language. Trends Ecol Evol 10, 289. https://doi.org/10.1016/0169-5347(95)90025-x

Peñuelas, J., Llusià, J., Gimeno, B.S., 1999. Effects of ozone concentrations on biogenic volatile organic compounds emission in the Mediterranean region. Environmental Pollution 105, 17–23. https://doi.org/10.1016/S0269-7491(98)00214-0

Petters, M.D., Kreidenweis, S.M., 2007. A single parameter representation of hygroscopic growth and cloud condensation nucleus activity. Atmospheric Chemistry and Physics 7, 1961–1971. https://doi.org/10.5194/acp-7-1961-2007

Pichersky, E., Gang, D.R., 2000. Genetics and biochemistry of secondary metabolites in plants: an evolutionary perspective. Trends in Plant Science 5, 439–445. https://doi.org/10.1016/S1360-1385(00)01741-6

Pichersky, E., Lewinsohn, E., 2011. Convergent Evolution in Plant Specialized Metabolism. Annual Review of Plant Biology 62, 549–566. https://doi.org/10.1146/annurev-arplant-042110-103814

Pichersky, E., Noel, J.P., Dudareva, N., 2006. Biosynthesis of Plant Volatiles: Nature's Diversity and Ingenuity. Science 311, 808–811. https://doi.org/10.1126/science.1118510

Pinto, D.M., Blande, J.D., Nykänen, R., Dong, W.-X., Nerg, A.-M., Holopainen, J.K., 2007. Ozone Degrades Common Herbivore-Induced Plant Volatiles: Does This Affect Herbivore Prey Location by Predators and Parasitoids? J Chem Ecol 33, 683–694. https://doi.org/10.1007/s10886-007-9255-8

Pinto, D.M., Blande, J.D., Souza, S.R., Nerg, A.-M., Holopainen, J.K., 2010. Plant volatile organic compounds (VOCs) in ozone (O3) polluted atmospheres: the ecological effects. J Chem Ecol 36, 22–34. https://doi.org/10.1007/s10886-009-9732-3

Ponzio, C., Gols, R., Weldegergis, B.T., Dicke, M., 2014. Caterpillar-induced plant volatiles remain a reliable signal for foraging wasps during dual attack with a plant pathogen or non-host insect herbivore. Plant, Cell & Environment 37, 1924–1935. https://doi.org/10.1111/pce.12301

Pöschl, U., Shiraiwa, M., 2015. Multiphase Chemistry at the Atmosphere–Biosphere Interface Influencing Climate and Public Health in the Anthropocene. Chem. Rev. 115, 4440–4475. https://doi.org/10.1021/cr500487s

Price, P.W., Bouton, C.E., Gross, P., McPheron, B.A., Thompson, J.N., Weis, A.E., 1980. Interactions Among Three Trophic Levels: Influence of Plants on Interactions Between Insect Herbivores and Natural Enemies. Annual Review of Ecology and Systematics 11, 41–65. https://doi.org/10.1146/annurev.es.11.110180.000353

Raguso, R.A., 2006. Behavioral responses to floral scent: Experimental manipulations and the interplay of sensory modalities, in: Biology of Floral Scent. pp. 297–318.

Rantala, P., Aalto, J., Taipale, R., Ruuskanen, T.M., Rinne, J., 2015. Annual cycle of volatile organic compound exchange between a boreal pine forest and the atmosphere. Biogeosciences 12, 5753–5770. https://doi.org/10.5194/bg-12-5753-2015

Rap, A., Scott, C.E., Reddington, C.L., Mercado, L., Ellis, R.J., Garraway, S., Evans, M.J., Beerling, D.J., MacKenzie, A.R., Hewitt, C.N., Spracklen, D.V., 2018. Enhanced global primary production by biogenic aerosol via diffuse radiation fertilization. Nature Geosci 11, 640–644. https://doi.org/10.1038/s41561-018-0208-3

Renbaum-Wolff, L., Grayson, J.W., Bateman, A.P., Kuwata, M., Sellier, M., Murray, B.J., Shilling, J.E., Martin, S.T., Bertram, A.K., 2013. Viscosity of α-pinene secondary organic material and implications for particle growth and reactivity. Proceedings of the National Academy of Sciences 110, 8014–8019. https://doi.org/10.1073/pnas.1219548110

Riccobono, F., Schobesberger, S., Scott, C.E., Dommen, J., Ortega, I.K., Rondo, L., Almeida, J., Amorim, A., Bianchi, F., Breitenlechner, M., David, A., Downard, A., Dunne, E.M., Duplissy, J., Ehrhart, S., Flagan, R.C., Franchin, A., Hansel, A., Junninen, H., Kajos, M., Keskinen, H., Kupc, A., Kürten, A., Kvashin, A.N., Laaksonen, A., Lehtipalo, K., Makhmutov, V., Mathot, S., Nieminen, T., Onnela, A., Petäjä, T., Praplan, A.P., Santos, F.D., Schallhart, S., Seinfeld, J.H., Sipilä, M., Spracklen, D.V., Stozhkov, Y., Stratmann, F., Tomé, A., Tsagkogeorgas, G., Vaattovaara, P., Viisanen, Y., Vrtala, A., Wagner, P.E., Weingartner, E., Wex, H., Wimmer, D., Carslaw, K.S., Curtius, J., Donahue, N.M., Kirkby, J., Kulmala, M., Worsnop, D.R., Baltensperger, U., 2014. Oxidation Products of Biogenic Emissions Contribute to Nucleation of Atmospheric Particles. Science 344, 717–721. https://doi.org/10.1126/science.1243527

Riffell, J.A., Alarcón, R., Abrell, L., Davidowitz, G., Bronstein, J.L., Hildebrand, J.G., 2008. Behavioral consequences of innate preferences and olfactory learning in hawkmoth–flower interactions. Proceedings of the National Academy of Sciences 105, 3404–3409. https://doi.org/10.1073/pnas.0709811105

Rinnan, R., Rinnan, Å., Holopainen, T., Holopainen, J.K., Pasanen, P., 2005. Emission of non-methane volatile organic compounds (VOCs) from boreal peatland microcosms—effects of ozone exposure. Atmospheric Environment 39, 921–930. https://doi.org/10.1016/j.atmosenv.2004.09.076

Rodriguez-Saona, C.R., Rodriguez-Saona, L.E., Frost, C.J., 2009. Herbivore-Induced Volatiles in the Perennial Shrub, Vaccinium corymbosum, and Their Role in Inter-branch Signaling. J Chem Ecol 35, 163–175. https://doi.org/10.1007/s10886-008-9579-z

Romonosky, D.E., Laskin, A., Laskin, J., Nizkorodov, S.A., 2015. High-Resolution Mass Spectrometry and Molecular Characterization of Aqueous Photochemistry Products of Common Types of Secondary Organic Aerosols. J. Phys. Chem. A 119, 2594–2606. https://doi.org/10.1021/jp509476r

Romonosky, D.E., Li, Y., Shiraiwa, M., Laskin, A., Laskin, J., Nizkorodov, S.A., 2017. Aqueous Photochemistry of Secondary Organic Aerosol of α-Pinene and α-Humulene Oxidized with Ozone, Hydroxyl Radical, and Nitrate Radical. J. Phys. Chem. A 121, 1298–1309. https://doi.org/10.1021/acs.jpca.6b10900

Rosenkranz, M., Schnitzler, J.-P., 2013. Genetic Engineering of BVOC Emissions from Trees, in: Niinemets, Ü., Monson, R.K. (Eds.), Biology, Controls and Models of Tree Volatile Organic

Compound Emissions, Tree Physiology. Springer Netherlands, Dordrecht, pp. 95–118. https://doi.org/10.1007/978-94-007-6606-8_4

Rothfuss, N.E., Petters, M.D., 2017. Influence of Functional Groups on the Viscosity of Organic Aerosol. Environ. Sci. Technol. 51, 271–279. https://doi.org/10.1021/acs.est.6b04478

Rowen, E., Kaplan, I., 2016. Eco-evolutionary factors drive induced plant volatiles: a meta-analysis. New Phytologist 210, 284–294. https://doi.org/10.1111/nph.13804

Ruther, J., Kleier, S., 2005. Plant–Plant Signaling: Ethylene Synergizes Volatile Emission In Zea mays Induced by Exposure to (Z)-3-Hexen-1-ol. J Chem Ecol 31, 2217–2222. https://doi.org/10.1007/s10886-005-6413-8

Ryan, A., Cojocariu, C., Possell, M., Davies, W.J., Hewitt, C.N., 2009. Defining hybrid poplar (Populus deltoides × Populus trichocarpa) tolerance to ozone: identifying key parameters. Plant, Cell & Environment 32, 31–45. https://doi.org/10.1111/j.1365-3040.2008.01897.x

Sasaki, K., Saito, T., Lämsä, M., Oksman-Caldentey, K.-M., Suzuki, M., Ohyama, K., Muranaka, T., Ohara, K., Yazaki, K., 2007. Plants Utilize Isoprene Emission as a Thermotolerance Mechanism. Plant and Cell Physiology 48, 1254–1262. https://doi.org/10.1093/pcp/pcm104

Saukko, E., Lambe, A.T., Massoli, P., Koop, T., Wright, J.P., Croasdale, D.R., Pedernera, D.A., Onasch, T.B., Laaksonen, A., Davidovits, P., Worsnop, D.R., Virtanen, A., 2012. Humidity-dependent phase state of SOA particles from biogenic and anthropogenic precursors. Atmospheric Chemistry and Physics 12, 7517–7529. https://doi.org/10.5194/acp-12-7517-2012

Schiestl, F.P., Johnson, S.D., 2013. Pollinator-mediated evolution of floral signals. Trends in Ecology & Evolution 28, 307–315. https://doi.org/10.1016/j.tree.2013.01.019

Schmelz, E.A., Alborn, H.T., Engelberth, J., Tumlinson, J.H., 2003. Nitrogen Deficiency Increases Volicitin-Induced Volatile Emission, Jasmonic Acid Accumulation, and Ethylene Sensitivity in Maize. Plant Physiology 133, 295–306. https://doi.org/10.1104/pp.103.024174

Schnee, C., Köllner, T.G., Held, M., Turlings, T.C.J., Gershenzon, J., Degenhardt, J., 2006. The products of a single maize sesquiterpene synthase form a volatile defense signal that attracts natural enemies of maize herbivores. Proceedings of the National Academy of Sciences 103, 1129–1134. https://doi.org/10.1073/pnas.0508027103

Seager, R., Vecchi, G.A., 2010. Greenhouse warming and the 21st century hydroclimate of southwestern North America. Proceedings of the National Academy of Sciences 107, 21277–21282. https://doi.org/10.1073/pnas.0910856107

Sharkey, T.D., Gray, D.W., Pell, H.K., Breneman, S.R., Topper, L., 2013. Isoprene Synthase Genes Form a Monophyletic Clade of Acyclic Terpene Synthases in the Tps-B Terpene Synthase Family. Evolution 67, 1026–1040. https://doi.org/10.1111/evo.12013

Sharkey, T.D., Loreto, F., 1993. Water stress, temperature, and light effects on the capacity for isoprene emission and photosynthesis of kudzu leaves. Oecologia 95, 328–333. https://doi.org/10.1007/BF00320984

Sharkey, T.D., Singsaas, E.L., 1995. Why plants emit isoprene. Nature 374, 769–769. https://doi.org/10.1038/374769a0

Sharkey, T.D., Wiberley, A.E., Donohue, A.R., 2008. Isoprene Emission from Plants: Why and How. Annals of Botany 101, 5–18. https://doi.org/10.1093/aob/mcm240

Sharkey, T.D., Yeh, S., 2001. Isoprene Emission from Plants. Annual Review of Plant Physiology and Plant Molecular Biology 52, 407–436. https://doi.org/10.1146/annurev.arplant.52.1.407

Shiojiri, K., Kishimoto, K., Ozawa, R., Kugimiya, S., Urashimo, S., Arimura, G., Horiuchi, J., Nishioka, T., Matsui, K., Takabayashi, J., 2006. Changing green leaf volatile biosynthesis in plants: An approach for improving plant resistance against both herbivores and pathogens. Proceedings of the National Academy of Sciences 103, 16672–16676. https://doi.org/10.1073/pnas.0607780103

Shiraiwa, M., Ammann, M., Koop, T., Pöschl, U., 2011. Gas uptake and chemical aging of semisolid organic aerosol particles. Proceedings of the National Academy of Sciences 108, 11003–11008. https://doi.org/10.1073/pnas.1103045108

Shiraiwa, M., Berkemeier, T., Schilling-Fahnestock, K.A., Seinfeld, J.H., Pöschl, U., 2014. Molecular corridors and kinetic regimes in the multiphase chemical evolution of secondary organic aerosol. Atmospheric Chemistry and Physics 14, 8323–8341. https://doi.org/10.5194/acp-14-8323-2014

Shiraiwa, M., Li, Y., Tsimpidi, A.P., Karydis, V.A., Berkemeier, T., Pandis, S.N., Lelieveld, J., Koop, T., Pöschl, U., 2017a. Global distribution of particle phase state in atmospheric secondary organic aerosols. Nat Commun 8, 15002. https://doi.org/10.1038/ncomms15002

Shiraiwa, M., Ueda, K., Pozzer, A., Lammel, G., Kampf, C.J., Fushimi, A., Enami, S., Arangio, A.M., Fröhlich-Nowoisky, J., Fujitani, Y., Furuyama, A., Lakey, P.S.J., Lelieveld, J., Lucas, K., Morino, Y., Pöschl, U., Takahama, S., Takami, A., Tong, H., Weber, B., Yoshino, A., Sato, K., 2017b. Aerosol Health Effects from Molecular to Global Scales. Environ. Sci. Technol. 51, 13545–13567. https://doi.org/10.1021/acs.est.7b04417

Shonle, I., Bergelson, J., 2000. Evolutionary Ecology of the Tropane Alkaloids of Datura Stramonium L. (solanaceae). Evolution 54, 778–788. https://doi.org/10.1111/j.0014-3820.2000.tb00079.x

Shrivastava, M., Easter, R.C., Liu, X., Zelenyuk, A., Singh, B., Zhang, K., Ma, P.-L., Chand, D., Ghan, S., Jimenez, J.L., Zhang, Q., Fast, J., Rasch, P.J., Tiitta, P., 2015. Global transformation and fate of SOA: Implications of low-volatility SOA and gas-phase fragmentation reactions. Journal of Geophysical Research: Atmospheres 120, 4169–4195. https://doi.org/10.1002/2014JD022563

Shulaev, V., Silverman, P., Raskin, I., 1997. Airborne signalling by methyl salicylate in plant pathogen resistance. Nature 385, 718–721. https://doi.org/10.1038/385718a0

Shuttleworth, A., Johnson, S.D., 2009. A key role for floral scent in a wasp-pollination system in Eucomis (Hyacinthaceae). Annals of Botany 103, 715–725. https://doi.org/10.1093/aob/mcn261

Simms, E.L., 1990. Examining Selection on the Multivariate Phenotype: Plant Resistance to Herbivores. Evolution 44, 1177–1188. https://doi.org/10.1111/j.1558-5646.1990.tb05224.x

Šimpraga, M., Ghimire, R.P., Van Der Straeten, D., Blande, J.D., Kasurinen, A., Sorvari, J., Holopainen, T., Adriaenssens, S., Holopainen, J.K., Kivimäenpää, M., 2019. Unravelling the functions of biogenic volatiles in boreal and temperate forest ecosystems. Eur J Forest Res 138, 763–787. https://doi.org/10.1007/s10342-019-01213-2

Smith, N.R., Crescenzo, G.V., Huang, Y., Hettiyadura, A.P.S., Siemens, K., Li, Y., Faiola, C.L., Laskin, A., Shiraiwa, M., Bertram, A.K., Nizkorodov, S.A., 2021. Viscosity and liquid–liquid phase separation in healthy and stressed plant SOA. Environ. Sci.: Atmos. 1, 140–153. https://doi.org/10.1039/D0EA00020E

Sporre, M.K., Blichner, S.M., Karset, I.H.H., Makkonen, R., Berntsen, T.K., 2019. BVOC–aerosol–climate feedbacks investigated using NorESM. Atmospheric Chemistry and Physics 19, 4763–4782. https://doi.org/10.5194/acp-19-4763-2019

Staudt, M., Lhoutellier, L., 2011. Monoterpene and sesquiterpene emissions from *Quercus coccifera* exhibit interacting responses to light and temperature. Biogeosciences 8, 2757–2771. https://doi.org/10.5194/bg-8-2757-2011

Staudt, M., Rambal, S., Joffre, R., Kesselmeier, J., 2002. Impact of drought on seasonal monoterpene emissions from Quercus ilex in southern France. Journal of Geophysical Research: Atmospheres 107, ACH 15-1-ACH 15-9. https://doi.org/10.1029/2001JD002043

Su, H.-J., Chao, C.-J., Chang, H.-Y., Wu, P.-C., 2007. The effects of evaporating essential oils on indoor air quality. Atmospheric Environment 41, 1230–1236. https://doi.org/10.1016/j.atmosenv.2006.09.044

Taraborrelli, D., Lawrence, M.G., Crowley, J.N., Dillon, T.J., Gromov, S., Groß, C.B.M., Vereecken, L., Lelieveld, J., 2012. Hydroxyl radical buffered by isoprene oxidation over tropical forests. Nature Geosci 5, 190–193. https://doi.org/10.1038/ngeo1405

Teuber, M., Zimmer, I., Kreuzwieser, J., Ache, P., Polle, A., Rennenberg, H., Schnitzler, J.-P., 2008. VOC emissions of Grey poplar leaves as affected by salt stress and different N sources. Plant Biol (Stuttg) 10, 86–96. https://doi.org/10.1111/j.1438-8677.2007.00015.x

Thomas, L.H., Meatyard, R., Smith, H., Davies, G.H., 1979. Viscosity behavior of associated liquids at lower temperatures and vapor pressures. J. Chem. Eng. Data 24, 161–164. https://doi.org/10.1021/je60082a011

Tiiva, P., Rinnan, R., Holopainen, T., Mörsky, S.K., Holopainen, J.K., 2007. Isoprene emissions from boreal peatland microcosms; effects of elevated ozone concentration in an open field experiment. Atmospheric Environment 41, 3819–3828. https://doi.org/10.1016/j.atmosenv.2007.01.005

Toome, M., Randjärv, P., Copolovici, L., Niinemets, Ü., Heinsoo, K., Luik, A., Noe, S.M., 2010. Leaf rust induced volatile organic compounds signalling in willow during the infection. Planta 232, 235–243. https://doi.org/10.1007/s00425-010-1169-y

Tu, P., Johnston, M.V., 2017. Particle size dependence of biogenic secondary organic aerosol molecular composition. Atmospheric Chemistry and Physics 17, 7593–7603. https://doi.org/10.5194/acp-17-7593-2017

Unger, N., 2014. On the role of plant volatiles in anthropogenic global climate change. Geophysical Research Letters 41, 8563–8569. https://doi.org/10.1002/2014GL061616

Valorso, R., Aumont, B., Camredon, M., Raventos-Duran, T., Mouchel-Vallon, C., Ng, N.L., Seinfeld, J.H., Lee-Taylor, J., Madronich, S., 2011. Explicit modelling of SOA formation from α-pinene photooxidation: sensitivity to vapour pressure estimation. Atmospheric Chemistry and Physics 11, 6895–6910. https://doi.org/10.5194/acp-11-6895-2011

van Hulten, M., Pelser, M., van Loon, L.C., Pieterse, C.M.J., Ton, J., 2006. Costs and benefits of priming for defense in Arabidopsis. Proceedings of the National Academy of Sciences 103, 5602–5607. https://doi.org/10.1073/pnas.0510213103

VanReken, T.M., Greenberg, J.P., Harley, P.C., Guenther, A.B., Smith, J.N., 2006. Direct measurement of particle formation and growth from the oxidation of biogenic emissions. Atmospheric Chemistry and Physics 6, 4403–4413. https://doi.org/10.5194/acp-6-4403-2006

Velikova, V., Pinelli, P., Pasqualini, S., Reale, L., Ferranti, F., Loreto, F., 2005a. Isoprene decreases the concentration of nitric oxide in leaves exposed to elevated ozone. New Phytologist 166, 419–426. https://doi.org/10.1111/j.1469-8137.2005.01409.x

Velikova, V., Tsonev, T., Pinelli, P., Alessio, G.A., Loreto, F., 2005b. Localized ozone fumigation system for studying ozone effects on photosynthesis, respiration, electron transport rate and isoprene emission in field-grown Mediterranean oak species. Tree Physiology 25, 1523–1532. https://doi.org/10.1093/treephys/25.12.1523

Velikova, V., Várkonyi, Z., Szabó, M., Maslenkova, L., Nogues, I., Kovács, L., Peeva, V., Busheva, M., Garab, G., Sharkey, T.D., Loreto, F., 2011. Increased Thermostability of Thylakoid Membranes in Isoprene-Emitting Leaves Probed with Three Biophysical Techniques. Plant Physiology 157, 905–916. https://doi.org/10.1104/pp.111.182519

Verma, S., Nizam, S., Verma, P.K., 2013. Biotic and Abiotic Stress Signaling in Plants, in: Sarwat, M., Ahmad, A., Abdin, M. (Eds.), Stress Signaling in Plants: Genomics and Proteomics Perspective, Volume 1. Springer, New York, NY, pp. 25–49. https://doi.org/10.1007/978-1-4614-6372-6_2

Vickers, C.E., Gershenzon, J., Lerdau, M.T., Loreto, F., 2009a. A unified mechanism of action for volatile isoprenoids in plant abiotic stress. Nat Chem Biol 5, 283–291. https://doi.org/10.1038/nchembio.158

Vickers, C.E., Possell, M., Cojocariu, C.I., Velikova, V.B., Laothawornkitkul, J., Ryan, A., Mullineaux, P.M., Nicholas Hewitt, C., 2009b. Isoprene synthesis protects transgenic tobacco plants from oxidative stress. Plant, Cell & Environment 32, 520–531. https://doi.org/10.1111/j.1365-3040.2009.01946.x

Vuorinen, T., Nerg, A.-M., Syrjälä, L., Peltonen, P., Holopainen, J.K., 2007. Epirrita autumnata induced VOC emission of silver birch differ from emission induced by leaf fungal pathogen. Arthropod-Plant Interactions 1, 159. https://doi.org/10.1007/s11829-007-9013-4

Vuorinen, T., Reddy, G.V.P., Nerg, A.-M., Holopainen, J.K., 2004. Monoterpene and herbivore-induced emissions from cabbage plants grown at elevated atmospheric CO2 concentration. Atmospheric Environment 38, 675–682. https://doi.org/10.1016/j.atmosenv.2003.10.029

Warnes, G.R., Bolker, B., Bonebakker, L., Gentleman, R., Huber, W., Liaw, A., Lumley, T., Maechler, M., Magnusson, A., Moeller, S., Schwartz, M., Venables, B., Galili, T., 2022. gplots: Various R Programming Tools for Plotting Data.

Welter, S., Bracho-Nuñez, A., Mir, C., Zimmer, I., Kesselmeier, J., Lumaret, R., Schnitzler, J.-P., Staudt, M., 2012. The diversification of terpene emissions in Mediterranean oaks: lessons from a study of Quercus suber, Quercus canariensis and its hybrid Quercus afares. Tree Physiol 32, 1082–1091. https://doi.org/10.1093/treephys/tps069

Wieczynski, D.J., Boyle, B., Buzzard, V., Duran, S.M., Henderson, A.N., Hulshof, C.M., Kerkhoff, A.J., McCarthy, M.C., Michaletz, S.T., Swenson, N.G., Asner, G.P., Bentley, L.P., Enquist, B.J., Savage, V.M., 2019. Climate shapes and shifts functional biodiversity in forests worldwide. Proc Natl Acad Sci U S A 116, 587–592. https://doi.org/10.1073/pnas.1813723116

Wink, M., 2003. Evolution of secondary metabolites from an ecological and molecular phylogenetic perspective. Phytochemistry 64, 3–19. https://doi.org/10.1016/S0031-9422(03)00300-5

Winterhalter, R., Van Dingenen, R., Larsen, B.R., Jensen, N.R., Hjorth, J., 2003. LC-MS analysis of aerosol particles from the oxidation of α-pinene by ozone and OH-radicals. Atmospheric Chemistry and Physics Discussions 3, 1–39. https://doi.org/10.5194/acpd-3-1-2003

Wong, C., Vite, D., Nizkorodov, S.A., 2021. Stability of α-Pinene and d-Limonene Ozonolysis Secondary Organic Aerosol Compounds Toward Hydrolysis and Hydration. ACS Earth Space Chem. 5, 2555–2564. https://doi.org/10.1021/acsearthspacechem.1c00171

Wright, G.A., Schiestl, F.P., 2009. The evolution of floral scent: the influence of olfactory learning by insect pollinators on the honest signalling of floral rewards. Functional Ecology 23, 841–851. https://doi.org/10.1111/j.1365-2435.2009.01627.x

Yang, W., Li, J., Wang, M., Sun, Y., Wang, Z., 2018. A Case Study of Investigating Secondary Organic Aerosol Formation Pathways in Beijing using an Observation-based SOA Box Model. Aerosol Air Qual. Res. 18, 1606–1616. https://doi.org/10.4209/aaqr.2017.10.0415

Yli-Pirilä, P., Copolovici, L., Kännaste, A., Noe, S., Blande, J.D., Mikkonen, S., Klemola, T., Pulkkinen, J., Virtanen, A., Laaksonen, A., Joutsensaari, J., Niinemets, Ü., Holopainen, J.K., 2016. Herbivory by an Outbreaking Moth Increases Emissions of Biogenic Volatiles and Leads to Enhanced Secondary Organic Aerosol Formation Capacity. Environ. Sci. Technol. 50, 11501–11510. https://doi.org/10.1021/acs.est.6b02800

Ylisirniö, A., Buchholz, A., Mohr, C., Li, Z., Barreira, L., Lambe, A., Faiola, C., Kari, E., Yli-Juuti, T., Nizkorodov, S.A., Worsnop, D.R., Virtanen, A., Schobesberger, S., 2020. Composition and volatility of secondary organic aerosol (SOA) formed from oxidation of real tree emissions compared to simplified volatile organic compound (VOC) systems. Atmospheric Chemistry and Physics 20, 5629–5644. https://doi.org/10.5194/acp-20-5629-2020

Yu, H., Holopainen, J.K., Kivimäenpää, M., Virtanen, A., Blande, J.D., 2021. Potential of Climate Change and Herbivory to Affect the Release and Atmospheric Reactions of BVOCs from Boreal and Subarctic Forests. Molecules 26, 2283. https://doi.org/10.3390/molecules26082283

Yuan, J.S., Himanen, S.J., Holopainen, J.K., Chen, F., Stewart, C.N., 2009. Smelling global climate change: mitigation of function for plant volatile organic compounds. Trends in Ecology & Evolution 24, 323–331. https://doi.org/10.1016/j.tree.2009.01.012

Zangerl, A.R., Stanley, M.C., Berenbaum, M.R., 2008. Selection for chemical trait remixing in an invasive weed after reassociation with a coevolved specialist. PNAS 105, 4547–4552. https://doi.org/10.1073/pnas.0710280105

Zhang, X., Lin, Y.-H., Surratt, J.D., Zotter, P., Prévôt, A.S.H., Weber, R.J., 2011. Light-absorbing soluble organic aerosol in Los Angeles and Atlanta: A contrast in secondary organic aerosol. Geophysical Research Letters 38. https://doi.org/10.1029/2011GL049385

Zhang, X., McVay, R.C., Huang, D.D., Dalleska, N.F., Aumont, B., Flagan, R.C., Seinfeld, J.H., 2015. Formation and evolution of molecular products in α-pinene secondary organic aerosol. PNAS 112, 14168–14173. https://doi.org/10.1073/pnas.1517742112

Zhao, D.F., Buchholz, A., Tillmann, R., Kleist, E., Wu, C., Rubach, F., Kiendler-Scharr, A., Rudich, Y., Wildt, J., Mentel, T.F., 2017. Environmental conditions regulate the impact of plants on cloud formation. Nat Commun 8, 14067. https://doi.org/10.1038/ncomms14067

Zhao, R., Zhang, Q., Xu, X., Zhao, W., Yu, H., Wang, W., Zhang, Y., Zhang, W., 2021. Effect of experimental conditions on secondary organic aerosol formation in an oxidation flow reactor. Atmospheric Pollution Research 12, 205–213. https://doi.org/10.1016/j.apr.2021.01.011

Zhu, J.-K., 2002. Salt and Drought Stress Signal Transduction in Plants. Annual Review of Plant Biology 53, 247–273. https://doi.org/10.1146/annurev.arplant.53.091401.143329

Zobrist, B., Marcolli, C., Pedernera, D.A., Koop, T., 2008. Do atmospheric aerosols form glasses? Atmospheric Chemistry and Physics 8, 5221–5244. https://doi.org/10.5194/acp-8-5221-2008

Zu, P., Blanckenhorn, W.U., Schiestl, F.P., 2016. Heritability of floral volatiles and pleiotropic responses to artificial selection in Brassica rapa. New Phytologist 209, 1208–1219. https://doi.org/10.1111/nph.13652